

CRANFIELD UNIVERSITY

EVANGELOS D. GEORGAKOPOULOS

IRON AND STEEL SLAG VALORIZATION THROUGH CARBONATION  
AND SUPPLEMENTARY PROCESSES

SCHOOL OF WATER, ENERGY AND ENVIRONMENT

PhD

Academic Year: 2013 -2016

Supervisor: Professor Vasilije Manovic  
December 2016



CRANFIELD UNIVERSITY

SCHOOL OF WATER, ENERGY AND ENVIRONMENT

PhD

Academic Year: 2013 -2016

EVANGELOS D. GEORGAKOPOULOS

IRON AND STEEL SLAG VALORIZATION THROUGH CARBONATION  
AND SUPPLEMENTARY PROCESSES

Supervisor: Professor Vasilije Manovic  
December 2016

This Thesis is submitted in partial fulfilment of the requirements for the  
degree of PhD

© Cranfield University 2016. All rights reserved. No part of this  
publication may be reproduced without the written permission of the  
copyright owner.



## ABSTRACT

Alkaline industrial wastes are considered potential resources for the mitigation of CO<sub>2</sub> emissions by simultaneously capturing and sequestering CO<sub>2</sub> through mineralization. Mineralization safely and permanently stores CO<sub>2</sub> through its reaction with alkaline earth metals. Apart from natural formations, these elements can also be found in a variety of abundantly available industrial wastes that have high reactivity with CO<sub>2</sub>, and that are generated close to the emission point-sources.

Apparently, it is the applicability and marketability of the carbonated products that define to a great extent the efficiency and viability of the particular process as a point source CO<sub>2</sub> mitigation measure. This project investigates the valorization of iron- and steel-making slags through methods incorporating the carbonation of the material, in order to achieve the sequestration of sufficient amounts of CO<sub>2</sub> in parallel with the formation of valuable and marketable products. Iron- and steel-manufacturing slags were selected as the most suitable industrial byproducts for the purposes of this research, due to their high production amounts and notable carbonation capacities.

The same criteria (production amount and carbonation capacity) were also used for the selection of the iron- and steel-making slag types that are more suitable to the scope of this work. Specifically for the determination of the slag types with the most promising carbonation capacities, the maximum carbonation conversions resulting from recent publications related to the influence of process parameters on the conversion extent of iron- and steel-manufacturing slags, were directly compared to each other using a new index, the Carbonation Weathering Rate, which normalizes the results based on particle size and reaction duration. Among the several iron- and steel-manufacturing slags, basic oxygen furnace (BOF) and blast furnace (BF) slags were found to combine both high production volumes and significant affinity to carbonation.

In the context of this research, two different procedures aiming to the formation of value added materials with satisfactory CO<sub>2</sub> uptakes were investigated as potential BF and BOF slags valorization methods. In them, carbonation was combined either with granulation and alkali activation (BOF slag), or with hydrothermal conversion (BF slag). Both treatments seemed to be effective and returned encouraging results

by managing to store sufficient amounts of CO<sub>2</sub> and generating materials with promising qualities.

In particular, the performance of the granulation-carbonation of BOF slag as a method leading to the production of secondary aggregates and the sequestration of notable amounts of CO<sub>2</sub> in a solid and stable form, was evaluated in this work. For comparison purposes, the material was also subjected to single granulation tests under ambient conditions. In an effort to improve the mechanical properties of the finally synthesized products, apart from water, a mixture of sodium hydroxide and sodium silicate was also tested as a binding agent in both of the employed processes. According to the results, the granules produced after the alkali activation of the material were characterized by remarkably greater particle sizes (from 1 to 5 mm) compared to that of the as received material (0.2 mm), and by enhanced mechanical properties, which in some cases appeared to be adequate for their use as aggregates in construction applications. The maximum CO<sub>2</sub> uptake was 40 g CO<sub>2</sub>/kg of slag and it was achieved after 60 minutes of the combined treatment of alkali activated BOF slag. Regarding the environmental behavior of the synthesized granules, increased levels of Cr and V leaching were noticed from the granules generated by the combination of granulation-carbonation with alkali activation. Nevertheless, the combination of granulation with alkali activation or that of granulation with carbonation were found not to worsen, if not to improve, the leaching behaviour of the granules with regards to the untreated BOF slag.

The formation of a zeolitic material with notable heavy metal adsorption capacity, through the hydrothermal conversion of the solid residues resulting from the calcium-extraction stage of the indirect carbonation of BF slag, was also investigated in this project. To this end, calcium was selectively extracted from the slag by leaching, using acetic acid of specific concentration (2 M) as the extraction agent. The residual solids resulting from the filtration of the generated slurry were subsequently subjected to hydrothermal conversion in caustic solution of two different compositions (NaOH of 0.5 M and 2 M). Due to the presence of calcium acetate in the composition of the solid residues, as a result of their inadequate washing, only the hydrothermal conversion attempted using the sodium hydroxide solution of higher concentration (2 M) managed to turn the amorphous slag into a crystalline

material, mainly composed by a zeolitic mineral phase (detected by XRD), namely, analcime ( $\text{NaAlSi}_2\text{O}_6 \cdot \text{H}_2\text{O}$ ), and tobermorite ( $\text{Ca}_5(\text{OH})_2\text{Si}_6\text{O}_{16} \cdot 4\text{H}_2\text{O}$ ). Finally, the heavy metal adsorption capacity of the particular material was assessed using  $\text{Ni}^{2+}$  as the metal for investigation. Three different adsorption models were used for the characterization of the adsorption process, namely Langmuir, Freundlich and Temkin models. Langmuir and Temkin isotherms were found to better describe the process, compared to Freundlich model. Based on the ability of the particular material to adsorb  $\text{Ni}^{2+}$  as reported from batch adsorption experiments and ICP-OES analysis, and the maximum monolayer adsorption capacity ( $Q_0 = 11.51 \text{ mg/g}$ ) as determined by the Langmuir model, the finally synthesized product can potentially be used in wastewater treatment or environmental remediation applications.

**Keywords:**  $\text{CO}_2$  Sequestration, BOF steel slag, BF steel slag, carbonation, granulation, alkali activation, aggregates, hydrothermal conversion, zeolites, adsorption

## AKNOWLEDGEMENTS

This thesis would have never become a reality without the support of several individuals, to whom I would like to extend my gratitude.

I would like to express my immeasurable appreciation to my supervisor, Professor Vasilije Manovic for his support and guidance during the most crucial part of this research.

I also am obliged to my former supervisor, Professor Sai Gu, for having believed in me and given me the opportunity to pursue this PhD in Cranfield university.

I also feel the need to deeply thank Professor Renato Baciocchi for having given me the chance to join and work with the research group of Sanitary and Environmental Engineering (ISA) of University of Rome “Tor Vergata”, Italy. Special thanks should also be conveyed to Dr Giulia Costa, Dr Daniela Zingaretti and Dr Milena Morone for their patience and willingness to tutor me through this whole new experience for me in the labs of the group.

I am hugely indebted to Professor Rafael Santos, who, for the needs of my research, invited me to work in the labs of Sheridan College, Toronto, Canada, and guided me through the complicated scenarios that I encountered during my studies as a visiting researcher there. I am also grateful to all the technicians who covered all my needs while I was working in the facilities of the college. Furthermore, I would like to express my gratitude to Mr. Graham and Mrs. Johanne Howarth, for being there for me whenever I needed them and for making my staying in Canada comfortable.

I would also like to thank Ms Sofia Korre for her help and encouragement and for being a constant source of motivation throughout my studies. Without her support the completion of the particular project would not be possible.

Finally, I would like to thank my parents, Dimitrios and Stavroula Georgakopoulos, and all my family in general for their patience, support and understanding and for being a source of inspiration during the years of my studies.

**TABLE OF CONTENTS**

LIST OF FIGURES.....	x
LIST OF TABLES.....	xiii
LIST OF EQUATIONS.....	xv
LIST OF ABBREVIATIONS.....	xvi
LIST OF NOMENCLATURE.....	xvii
1. GENERAL INTRODUCTION.....	1
1.1. Context of research.....	1
1.2. Aim and Objectives .....	5
1.2.1. Aim .....	5
1.2.2. Research Objectives.....	5
1.3. Methodology outline.....	5
1.3.1. Synthesis of secondary aggregates from BOF slag.....	6
1.3.2. Synthesis of zeolitic material from BF slag .....	10
1.4. Issues analysis and contribution to knowledge .....	14
1.4.1. Introduction of Carbonation Weathering Rate (CWR).....	14
1.4.2. Synthesis of secondary aggregates from BOF slag.....	14
1.4.3. Synthesis of zeolites from BF slag and assessment of their adsorption capacity .....	15
1.5. Thesis structure .....	16
1.6. Studies breakdown and contributions .....	18
2. LITERATURE REVIEW.....	20
2.1. Introduction .....	20
2.1.1. Background.....	20
2.1.2. Mineral carbonation .....	21
2.1.3. Iron and Steel slags .....	24
2.1.3.1. Iron and steel production .....	24

2.1.3.2. Iron and steel slag types .....	27
2.1.3.2.1. Iron-making slag (BF slag) .....	27
2.1.3.2.2. Steel- making slags (BOF and EAF slags).....	28
2.1.3.2.3. Steel-refining process slags (AOD and CC slags) .....	30
2.2. Iron- and steel-making slag carbonation: A literature review of conversion extent and kinetics .....	32
2.2.1. BF slag.....	32
2.2.2. BOF slag.....	33
2.2.3. EAF and stainless steel slags .....	40
2.2.4. AOD and CC slags .....	42
2.2.5. Waelz slag .....	45
2.2.6. Conclusions .....	46
2.3. Carbonation Weathering Rate (CWR): Conceptualization and application ...	48
2.4. Selection of the most suitable types of slag for investigation .....	56
2.5. Literature review on the Valorization of carbonated BF and BOF slags .....	57
2.5.1. Valorization of carbonated BF slag .....	57
2.5.2. Valorization of carbonated BOF slag .....	63
2.5.3. Conclusions .....	72
2.6. Investigated processes for BF and BOF slag valorization.....	73
3. SYNTHESIS OF SECONDARY AGGREGATES THROUGH GRANULATION AND GRANULATION-CARBONATION OF ALKALI ACTIVATED BOF SLAG .....	76
3.1. Introduction .....	76
3.1.1. Accelerated mineral carbonation of BOF slag.....	77
3.1.2. Granulation .....	77
3.1.3. Alkali activation .....	81
3.2. Materials and Methods.....	83
3.2.1. Materials .....	83
3.2.2. Methodology .....	84

3.2.2.1. Granulation and granulation-carbonation tests .....	84
3.2.2.2. Batch carbonation tests .....	85
3.2.3. Analytical methods.....	87
3.3. Material characterization.....	90
3.3.1. Moisture level.....	90
3.3.2. Particle size distribution analysis .....	90
3.3.3. Elemental and mineralogical composition.....	92
3.3.4. Leaching behavior .....	93
3.4. Results and discussion .....	93
3.4.1. Particle size distribution (PSD) analysis .....	94
3.4.2. CO <sub>2</sub> uptake estimation.....	100
3.4.2.1. Assessment of the investigated treatment performance as a CO <sub>2</sub> emissions mitigation process.....	105
3.4.2.2. Batch carbonation tests and CWR estimation.....	110
3.4.3. Mechanical strength assessment.....	119
3.4.4. Leaching behavior .....	122
3.5. Preliminary economic feasibility assessment.....	131
3.6. Conclusions .....	132
4. SYNTHESIS OF ZEOLITIC HEAVY METAL ADSORBENT FROM BF SLAG ...	135
4.1. Introduction .....	135
4.1.1. Adsorption process .....	136
4.1.2. Zeolites as adsorbents.....	138
4.1.3. Formation of zeolites from BF slag .....	140
4.2. Materials and methods.....	144
4.2.1. Materials .....	144
4.2.2. Experimental methodology .....	144
4.2.3. Analytical methods.....	147

4.2.4. Material characterization.....	148
4.3. Results and discussion .....	153
4.3.1. Batch calcium extraction tests .....	153
4.3.2. Zeolitic materials characterization.....	156
4.3.2.1. Elemental composition.....	157
4.3.2.2. Mineralogical composition.....	159
4.3.2.3. SEM analysis .....	161
4.3.2.4. Particle size distribution analysis .....	163
4.3.2.5. Surface area, pore size and width .....	163
4.4. Adsorption capacity of the hydrothermally converted material.....	164
4.4.1. Effect of initial Ni <sup>2+</sup> concentration.....	166
4.4.2 Equilibrium adsorption isotherms.....	169
4.4.3. Adsorption process characterization.....	170
4.4.3.1. Langmuir adsorption model .....	170
4.4.3.2. Freundlich adsorption model.....	174
4.4.3.3. Temkin adsorption model.....	176
4.4.4 Results analysis.....	179
4.5. Conclusions .....	181
5. CONCLUSIONS AND FUTURE WORK.....	184
5.1. Valorization of BOF slag .....	184
5.1.1. Concluding remarks.....	184
5.1.2. Future work.....	186
5.2. Valorization of BF slag .....	188
5.2.1. Concluding remarks.....	188
5.2.2. Future Work.....	190
REFERENCES.....	196

APPENDIX A: LITERATURE REVIEW ON THE CARBONATION OF IRON- AND  
STEEL-MAKING SLAGS..... 233

APPENDIX B: ADSORPTION CAPACITY OF THE FORMED ZEOLITIC MATERIAL  
TOWARDS Ni<sup>2+</sup> ..... 247

**LIST OF FIGURES**

Figure 2-1: Theoretical illustration of a partially carbonated mineral particle....	50
Figure 2-2: Carbonation Weathering Rates as calculated for studies on BOF slag.....	54
Figure 2-3: Carbonation Weathering Rates as calculated for studies on AOD slag.....	54
Figure 2-4: Carbonation Weathering Rates as calculated for studies on CC slag. ....	55
Figure 2-5: Carbonation Weathering Rates as calculated for studies on SS, EAF, BF, and Waelz slags. ....	55
Figure 3-1: The equipment used for the a) granulation and (b,c) granulation-carbonation experiments.....	84
Figure 3-2: The equipment used for the batch carbonation tests .....	86
Figure 3-3: Particle size distribution diagram of the as received material.....	91
Figure 3-4: The generated granules: a) Untreated material b) G30'_W_W/S=0.12, c) G30'_SS_W/S=0.12, d) GC30'_W_W/S=0.12, e) GC60'_W_W/S=0.12, f) GC30'_SS_W/S=0.12, g) GC60'_SS_W/S=0.12, h) GC30'_SS_W/S=0.14, and i) GC60'_SS_W/S=0.14.....	96
Figure 3-5: PSD analysis diagrams for the untreated material and the granules produced by a) granulation and granulation-carbonation treatments at b) W/S = 0.12 L/kg and c) W/S = 0.14 L/kg .....	97
Figure 3-6: The effect of reaction time on the $d_{50}$ value of the samples generated from the combined treatment. ....	99
Figure 3-7: Comparative diagram displaying the effect of the different treatments and the different liquid binders at a stable L/S ratio equal to 0.12 L/kg, on the $d_{50}$ values of the treated samples .....	100
Figure 3-8: CO <sub>2</sub> Uptake of the granules produced by the different tested treatments .....	103
Figure 3-9: CO <sub>2</sub> uptake with curing time of the granules obtained after a) granulation and b) granulation-carbonation treatments.....	104
Figure 3-10: CO <sub>2</sub> uptake kinetics of BOF slag resulted from the batch carbonation tests under a) mild (T = 20 °C, pCO <sub>2</sub> = 1 bar and L/S = 0.3 L/kg) and b) enhanced (T = 50 °C, pCO <sub>2</sub> = 10 bar and L/S = 0.3 L/kg) conditions.....	113

Figure 3-11: Comparison between the CO <sub>2</sub> uptakes achieved by the batch carbonation tests (B30MA and B1HA) and the combined treatment (GC30'_W_W/S=0.12 and GC60'_W_W/S=0.12) of the as received BOF slag, as a function of reaction duration .....	116
Figure 3-12: ACV tests results .....	121
Figure 3-13: The pH values of eluates resulting from granules obtained after each of the tested treatments.....	129
Figure 3-14: Results of the EN 12457-2 test regarding the leaching of a) major constituents and b) regulated elements from granules (without grinding the material) obtained after the tested granulation and granulation-carbonation treatments. ....	130
Figure 4-1: X-ray diffractogram of the fresh PBF and GBF slag.....	150
Figure 4-2: SEM images of the fresh a) PBF slag and b) GBF slag, after their crushing to below 2 mm .....	150
Figure 4-3: Average particle size distribution of the original a) PBF slag b) GBF slag, after their crushing to below 2 mm.....	151
Figure 4-4: Content of Ca, Mg, Al and Si in the hydrothermally converted material (NaOH, 0.5 M), expressed in weight percentage per element normalized to 100% total .....	158
Figure 4-5: Content of Ca, Mg, Al and Si in the hydrothermally converted material (NaOH, 2 M), expressed in weight percentage per element normalized to 100% total .....	159
Figure 4-6: X-ray diffractogram of the hydrothermally converted material (NaOH, 0.5 M).....	160
Figure 4-7: XRD diagram of the hydrothermally converted material (NaOH, 2 M) .....	160
Figure 4-8: Morphology of PBF slag at its original state, after its treatment with CH <sub>3</sub> COOH (2 M), and of the finally produced material after the hydrothermal conversion of acetic acid residues by NaOH (2 M) with magnification: a) x500; b) x1000; c) x2000 and d) x5000.....	162
Figure 4-9: Average particle size distribution of the hydrothermally converted material .....	163
Figure 4-10: Correlation between the solutions initial Ni <sup>2+</sup> concentration and the percentage of Ni <sup>2+</sup> removal achieved .....	167

Figure 4-11: Correlation between the solutions initial Ni <sup>2+</sup> concentration and the achieved Ni <sup>2+</sup> sorption uptake .....	168
Figure 4-12: Adsorption isotherms of Ni <sup>2+</sup> on the hydrothermally converted material .....	169
Figure 4-13: Experimental data fitting with linearized Langmuir adsorption model .....	171
Figure 4-14: Comparison of experimental data and simulated adsorption isotherms of Ni <sup>2+</sup> onto the hydrothermally converted material according to Langmuir adsorption model.....	172
Figure 4-15: Variation of separation factor (R <sub>L</sub> ) as a function of initial Ni <sup>2+</sup> ion concentration (adsorbent dosage = 1g, shaking time = 24 hours, shaking speed = 160 rpm, T = 20 °C, pH = 5).....	174
Figure 4-16: Experimental data fitting with linearized Freundlich adsorption model .....	175
Figure 4-17: Comparison of experimental data and simulated adsorption isotherms of Ni <sup>2+</sup> onto the hydrothermally converted material according to Freundlich adsorption model.....	176
Figure 4-18: Experimental data fitting with linearized Temkin adsorption model .....	177
Figure 4-19: Comparison of experimental data and simulated adsorption isotherms of Ni <sup>2+</sup> onto the hydrothermally converted material according to Temkin adsorption model.....	178

**LIST OF TABLES**

Table 3-1: Particle size distribution analysis for the as received material.....	91
Table 3-2: Elemental composition of the untreated material expressed on a dry weight basis. ....	92
Table 3-3: IC analysis results of the as received material. ....	92
Table 3-4: The leaching behavior of the as received BOF slag.....	93
Table 3-5: The identity of granulation and granulation-carbonation experiments .....	94
Table 3-6: The $d_{50}$ values of the untreated material and the produced granules. ....	98
Table 3-7: IC analysis results of the granules formed after the granulation and granulation-carbonation of the BOF slag.....	102
Table 3-8: The identity of batch carbonation tests.....	111
Table 3-9: IC analysis results of the batch carbonation products. ....	112
Table 3-10: Carbonation conversions and CWRs achieved after the batch carbonation tests. ....	117
Table 3-11: Description and results of the ACV tests.....	120
Table 3-12: EN 12457-2 tests results for the untreated slag and the crushed granules obtained from the different tested treatments compared to the Italian limits for waste reuse (Italian Ministerial Decree 186/2006). ....	128
Table 4-1: Elemental composition of the fresh PBFS.....	150
Table 4-2: Elemental composition of the fresh GBFS. ....	150
Table 4-3: Specific surface area, pore volume and pore width of the fresh PBF and GBF slags. ....	152
Table 4-4: Attained calcium and alumina leaching from PBF and GBF slags after batch extraction tests .....	155
Table 4-5: Elemental composition of the hydrothermally converted material (NaOH, 0.5 M), expressed in weight percentage per element normalized to 100 % total.....	157
Table 4-6: Elemental composition of the hydrothermally converted material (NaOH, 2 M), expressed in weight percentage per element normalized to 100 % total .....	158

Table 4-7: Comparison between the specific surface area, pore volume and pore width of the fresh and the hydrothermally converted PBF slag .....	164
Table 4-8 Concentration of Ni <sup>2+</sup> in the solution at equilibrium, Ni <sup>2+</sup> removal percentage and actual amount of Ni <sup>2+</sup> adsorbed at equilibrium, prior and after pH adjustment.....	166
Table 4-9 Adsorption isotherm parameters for the Ni <sup>2+</sup> adsorption onto the zeolitic material .....	179
Table 4-10 Adsorption capacities, best fitting model and specific surface areas of different synthetic zeolites towards Ni <sup>2+</sup> .....	180

**LIST OF EQUATIONS**

Equation 1-1 .....	8
Equation 1-2 .....	8
Equation 1-3 .....	8
Equation 1-4 .....	13
Equation 2-1 .....	50
Equation 2-2 .....	50
Equation 2-3 .....	51
Equation 3-1 .....	88
Equation 3-2 .....	88
Equation 3-3 .....	89
Equation 3-4 .....	89
Equation 3-5 .....	90
Equation 4-1 .....	147
Equation 4-2 .....	166
Equation 4-3 .....	171
Equation 4-4 .....	173
Equation 4-5 .....	175
Equation 4-6 .....	177

**LIST OF ABBREVIATIONS**

<i>ACBF</i>	<i>Air-cooled Blast Furnace</i>
<i>ACBFS</i>	<i>Air-cooled Blast Furnace Slag</i>
<i>ACV</i>	<i>Aggregate Crushing Value</i>
<i>AOD</i>	<i>Argon Oxygen Decarburization</i>
<i>APC</i>	<i>Air Pollution Control</i>
<i>BF</i>	<i>Blast Furnace</i>
<i>BOF</i>	<i>Basic Oxygen Furnace</i>
<i>CC</i>	<i>Continuous Casting</i>
<i>CCS</i>	<i>Carbon Capture and Storage</i>
<i>CWR</i>	<i>Carbonation Weathering Rate</i>
<i>DI</i>	<i>De-Ionized</i>
<i>EDTA</i>	<i>Ethylenediaminetetraacetic acid</i>
<i>GBFS</i>	<i>Granulated Blast Furnace Slag</i>
<i>GDP</i>	<i>Gross Domestic Product</i>
<i>GHG</i>	<i>Greenhouse Gas</i>
<i>IC</i>	<i>Inorganic Carbon</i>
<i>ICP-OES</i>	<i>Inductively Couple Plasma-Optical Emission Spectroscopy</i>
<i>LDA</i>	<i>Laser Diffraction Analysis</i>
<i>MW</i>	<i>Molecular Weight</i>
<i>OHF</i>	<i>Open Hearth Furnace</i>
<i>PBFS</i>	<i>Pelletized Blast Furnace Slag</i>
<i>PC</i>	<i>Portland Cement</i>
<i>PCC</i>	<i>Precipitated Calcium Carbonate</i>
<i>PSD</i>	<i>Particle Size Distribution</i>
<i>RH</i>	<i>Relative Humidity</i>
<i>rpm</i>	<i>Rounds per minute</i>
<i>SEM</i>	<i>Scanning Electron Microscopy</i>
<i>SS</i>	<i>Stainless Steel</i>
<i>XRD</i>	<i>X-ray Diffraction</i>
<i>XRF</i>	<i>X-ray Fluorescence</i>

**LIST OF NOMENCLATURE**

$b$	<i>Langmuir isotherm constant</i>
$b_T$	<i>Temkin constant related to heat of sorption</i>
$C_e$	<i>Equilibrium concentration of the heavy metal ions in the solution</i>
$C_o$	<i>Initial concentration of the heavy metal ions in the solution</i>
$K_f$	<i>Freundlich constant corresponding to adsorption capacity</i>
$K_o$	<i>Temkin isotherm equilibrium binding constant</i>
$m$	<i>Mass of the dry adsorbent</i>
$M$	<i>Mass of pollutant at the equilibrium state of the adsorbent-adsorbate solution</i>
$M_o$	<i>Initial mass of pollutant</i>
$n$	<i>Freundlich constant corresponding to adsorption Intensity</i>
$P$	<i>Pressure</i>
$q_e$	<i>Amount of heavy metal adsorbed by the adsorbent at equilibrium</i>
$Q_m$	<i>Theoretical maximum monolayer coverage capacity</i>
$r^2$	<i>Regression coefficient</i>
$R$	<i>Universal gas constant</i>
$R_c$	<i>Average radius of the unreacted core of particle</i>
$R_L$	<i>Constant Separation Factor</i>
$r_x$	<i>Original average particle radius</i>
$T$	<i>Temperature</i>
$t_{carb}$	<i>Thickness of particle's carbonated shell</i>
$V$	<i>Volume</i>

**GREEK SYMBOLS**

$T_{react}$	<i>Reaction time</i>
-------------	----------------------



# 1. GENERAL INTRODUCTION

## 1.1. Context of research

The significance of the hazardous results coming from the greenhouse gas (GHG) emissions to both the atmosphere and our lives has already been urged and is nowadays well-known. Once they are released to the atmosphere these gases tend to absorb and emit radiation within the thermal infrared range. Today, the emissions of GHGs are considered to be the primary cause of the greenhouse effect. According to this effect, the thermal radiation from the surface of the Earth is absorbed by the GHGs and it is then radiated back to the Earth, in several directions. As a result, Earth's surface temperature gradually elevates and unless this phenomenon is efficiently confronted, it will reach levels that will be uncomfortable and eventually prohibitive for humans' lives.

CO<sub>2</sub> is a GHG whose concentration in the atmosphere is continuously elevating during the years that followed the industrial revolution, back in 1760. Since the beginning of atmospheric CO<sub>2</sub> measurements in Mauna Loa (Hawaii), in March 1958, the mean concentration of CO<sub>2</sub> per year has increased by approximately 27% [1]. In particular, over the last six decades, the presence of CO<sub>2</sub> in the atmosphere has escalated from  $315.97 \pm 0.12$  ppmv (in 1958) to about  $401.57 \pm 0.12$  ppmv (in 2016) [2]. In the same timeframe, the global and ocean surface temperature anomaly (defined with respect to the period 1901-2000) has increased by 1.1 °C, from an annual average of 0.11 °C to 1.22 °C [3]. Based on this correlation, and extensive climate studies, it could be inferred that there is a link between CO<sub>2</sub> emissions and global warming. In fact, it has been suggested by climate modeling, that if the anthropogenic CO<sub>2</sub> emissions continue to follow the current trends and the CO<sub>2</sub> concentration in the atmosphere doubles from pre-industrial levels, the Earth's mean surface temperature will rise by 2.1 to 4.6 °C [4].

Following these serious threats, at the United Nations Climate Change Conference that was held in Paris in December of 2015 (COP 21), 195 countries adopted the first-ever universal, legally binding global climate deal that will come into force in 2020 and calls for zero net anthropogenic GHG emissions during the second half of

the 21st century, or even earlier, in order to mitigate the global warming to well below 2 °C, and preferably below 1.5 °C [5].

To mitigate the anthropogenic CO<sub>2</sub> emissions several solutions have been suggested. Among them, carbon capture and storage (CCS) is considered as a promising technique, according to which, CO<sub>2</sub> is first separated from the rest of the emissions and subsequently captured. The captured CO<sub>2</sub> is then stored using different methods. Among all the mechanisms that have been investigated for the sequestration of CO<sub>2</sub>, the one that offers almost permanent storage is the mechanism of mineralization. According to it, CO<sub>2</sub> gets transformed into an insoluble carbonate (mainly calcite or magnesite) that is able to remain stable for geological timeframes.

The transformation of CO<sub>2</sub> into a stable mineral needs the reaction of itself with an alkaline earth metal bearing material. This process can occur either naturally (under ambient conditions, slow kinetics), or in laboratory (under controlled conditions, accelerated kinetics). Among the naturally occurring silicates containing alkaline earth metal oxides for carbonation, the most commonly used ones are olivine (Mg<sub>2</sub>SiO<sub>4</sub>), serpentine (Mg<sub>3</sub>Si<sub>2</sub>O<sub>5</sub>(OH)<sub>4</sub>) and wollastonite (CaSiO<sub>3</sub>) [6]. Industrial residues rich in alkaline earth metals can also be used for mineral carbonation purposes instead of natural minerals, which require energy-intensive mining and mineral processing for utilization. Several waste materials are qualified as efficient reactants for CO<sub>2</sub> mineralization due to their high alkaline earth metal content, as well as their proximity to CO<sub>2</sub> emission point sources. Based on the amount of available alkaline earth metals contained in these residues, worldwide, it can be inferred that they are capable of storing only a limited amount of CO<sub>2</sub> annually. According to the estimations of Kirchofer et al [7], the available industrial alkaline byproducts in USA, have the potential to mitigate approximately 7.6 Mt CO<sub>2</sub>/a (7.0 Mt/a by mineralization and 0.6 Mt/a by avoided emissions). By extrapolating this amount worldwide in proportion to the industrial fraction of the nominal gross domestic product (GDP) of each country (\$3.33T (19.1 % of 2014 GDP) for the U.S., \$22.8T (30.5 % of 2014 GDP) for the world) [8], the annual amount of CO<sub>2</sub> that could potentially be mineralized using industrial residues is estimated to about 52.0 Mt [1]. This represents a small fraction of of the annual global CO<sub>2</sub> emissions, which are

nearing 40 Gt CO<sub>2</sub>/a [9]. Although their contribution to the GHGs emissions reduction is small, attention should be paid to the carbonation of the particular types of industrial residues for the following reasons [1]:

- This process can substantially reduce the CO<sub>2</sub> emissions generated by specific industrial sectors, such as iron- and steel-making or cement manufacturing industries, where integration with mineral carbonation can be rather efficiently achieved.
- It is a way to make the disposal (landfilling) of such residues less hazardous, in an economical way [10, 11].
- The carbonates that are produced by this technology have the potential to be commercially used in several applications, for instance, as synthetic aggregates in construction applications with more favorable characteristics than the untreated raw material [12, 13].

Compared to the other industrial wastes, iron- and steel-making slags present the highest experimental CO<sub>2</sub> (ECO<sub>2</sub>) uptakes. The particular industry also appears to be the most significant industrial source of CO<sub>2</sub> emissions, mainly due to its energy intensive nature and the usage of coal as the primary fuel for the production of iron and steel [14,15]. Slags generated during steel production process amount to approximately 10 - 15 wt% of the steel produced [16]. These slags are classified based on on the different types and stages of the iron- and steel-making process; i.e., blast furnace (BF) slags from the iron-making process, basic oxygen furnace (BOF) slags or electric arc furnace (EAF) slags from the steel-making process, and argon-oxygen decarburization (AOD) slags and continuous casting (CC) slags from the refining process. The most of these residues have low commercial value due to their composition that is characterized by large amounts of mixed oxides such as CaO, SiO, MgO, Al<sub>2</sub>O<sub>3</sub> and MnO and only limited presence of metallic iron [17]. Furthermore, they also contain detectable amounts of toxic components such as As, Cd, Cr, Hg, Pb and Se [18], which is concerning for their reuse.

The large generation rate of iron- and steel-manufacturing slags, in combination with their limited commercial market, the rising landfill fees and the tightening environmental regulations have turned the management of the particular byproducts into a growing concern for the industry [1].

Carbonation of iron- and steel-making slags could be an efficient technology to store a significant percentage of CO<sub>2</sub> emitted from steel-making plants, while at the same time reducing their toxicity and generating new revenue streams. However, in order to achieve satisfactory levels of point source CO<sub>2</sub> mitigation, besides the high carbonation ability, the tested waste materials should also exhibit sufficient production amounts.

According to the particular criteria, among the several types of iron- and steel-manufacturing byproducts tested in literature, BF and BOF slags have been found to be the most suitable materials for such use. In fact, the particular types of slag manage to combine sufficient production amounts and satisfactory carbonation ability. BOF slag exhibits remarkable reactivity towards CO<sub>2</sub> [19-21], while presenting the highest production among the several types of steel waste materials. Respectful ECO<sub>2</sub> uptake values have also been achieved by BF slags [22, 23], whose production levels were found to be almost two times higher than those attributed to steel slags for the year 2015 [24].

With the satisfactory reactivity of the particular slags towards CO<sub>2</sub> having been proved, research should be focused on developing processes that would be able to also achieve the production of value-added materials. In fact, the only way for iron and steel-making mineral carbonation process to extend to industrial scale is apart from its satisfactory efficiency in sequestering CO<sub>2</sub> to also be proved an economically viable process. To achieve that, the materials retrieved after the mineral carbonation of the particular byproducts should be valorized by getting utilized in several sectors, increasing their marketability and thereupon decreasing the cost of the process.

BF and BOF slags in their original form, are characterized by remarkably different levels of applicability. In particular, BOF slag can be reused in low end applications or get recycled on site by being returned to the iron-making process [25]. Its use in road construction, civil and hydraulic engineering and cement industry is limited due to its high content in free CaO and MgO and a significant part of its production ends up in landfilling sites [25]. Apparently, due to the lack of applications, the rising landfill fees and its continuous production in high amounts, BOF slag is in great need for new valorization routes.

On the other hand, BF slag is already exploited in several valuable applications, especially in the construction sector where it is used either as aggregate or as partial replacement of traditional Portland cement (PC) for the production of blended cement [26-32]. The particular uses of BF slag create profit for the iron-manufacturing industry, while also achieving the reduction of the CO<sub>2</sub> footprint related to blended cement production, since by substituting PC, a part of CO<sub>2</sub> emissions linked to its production is avoided. Due to its successful usage in valuable applications in the construction business, BF slag is not in need for new valorization methods. Consequently, to attract the interest of the iron-making industry towards alternative valorization routes for BF slag, such as its mineral carbonation, apart from the CO<sub>2</sub> point-source emissions mitigation that could be attained through them, the new methodologies would also have to create extra value for the examined material.

## **1.2. Aim and Objectives**

### **1.2.1. Aim**

This thesis aims to the valorization of iron- and steel-making slags by coupling mineral carbonation with additional processes, through which the sequestration of sufficient amounts of CO<sub>2</sub> and the production of value added materials capable of being commercially exploited, would be achieved in parallel.

### **1.2.2. Research Objectives**

- Based on literature, distinguish the types of iron- and steel-making slags that combine high reactivity towards CO<sub>2</sub> with high production volumes.
- Assess, where applicable, the capability of the distinguished slags to store substantial amounts of CO<sub>2</sub> under the employed process conditions.
- Assess the usability of the formed products by subjecting them to the appropriate, in each case, tests.
- Make recommendations to upgrade the operational effectiveness of the proposed mechanisms, in order to maximize the amounts of stored CO<sub>2</sub> and/or to improve the qualities of the generated material.

## **1.3. Methodology outline**

In this study, a new process aiming to the valorization of BOF slag is presented and

analyzed, whereas a newly proposed technique aiming to the generation of higher value from BF slag is reproduced using a more porous type of it, in an effort to improve the efficiency of the technology. In both of the investigated methodologies, carbonation is coupled with supplementary processes, to achieve the sequestration of adequate amounts of CO<sub>2</sub> and the concurrent formation of value-added materials.

In particular, the carbonation of BOF slag is coupled with granulation and alkali activation of the material, in an effort to produce granules with sufficient CO<sub>2</sub> uptake, acceptable environmental behavior, and satisfactory mechanical performance, capable of being used as secondary aggregates in construction applications. Furthermore, the reproduction of zeolitic minerals through the hydrothermal conversion of the solid residues resulting from the indirect carbonation of BF slag, following the methodology proposed by Chiang et al. [43], is attempted and the heavy metal adsorption capacity of the generated materials towards Ni<sup>2+</sup> is assessed.

### **1.3.1. Synthesis of secondary aggregates from BOF slag**

In order to assess the effects of granulation, carbonation and alkali activation on the particle size, the finally achieved CO<sub>2</sub> uptake and the mechanical strength of the formed granules, the synthesis of secondary aggregates from BOF slag was attempted through granulation and granulation-carbonation, using either DI water or an alkaline solution as the liquid agent. The device used for both the granulation and granulation-carbonation experiments was a custom-made 180 W laboratory scale granulator.

Batch accelerated carbonation tests on both the as received BOF slag and a milled sample of it (<0.125 mm), using either DI water or an alkaline solution as the wetting agent were also conducted in order to characterize the material regarding its carbonation ability and to assess the effect of milling and alkali activation on the finally achieved CO<sub>2</sub> uptake. A stainless steel reactor equipped with a 150 ml internal Teflon jacket, a thermocouple, a pressure indicator and a gas feeding system, placed in a thermostatic bath for temperature control, was employed for the BOF slag batch carbonation tests.

The alkali-activation of the material was attempted where required, employing a 50:50 by weight mixture of a 2 M sodium hydroxide (NaOH) solution, prepared by dissolving pellets of NaOH (Fischer Scientific, 99.4 % purity) in deionized water, and a commercial sodium silicate ( $\text{Na}_2\text{SiO}_3$ ) solution.

### **1.3.1.1. Synthesizing granules through the granulation and granulation-carbonation of BOF slag**

For the formation of granules via granulation, 500 g of BOF slag were manually mixed with deionized water or sodium solution in a plastic bag at W/S ratio of 0.12 L/kg, for minimum 5 minutes. The resulting mixture was then pushed through a 2 mm sieve into the granulator, to secure the even distribution of the material in the device. The granulator was then set in operation at 24 rpm, applying a tilt of 50°. The granulation tests lasted for 30 minutes and were held under room temperature and pressure.

For the formation of granules via the combined treatment of granulation-carbonation, 500 g of BOF slag were manually mixed with deionized water or sodium solution in a plastic bag at varying W/S ratios (0.12 and 0.14 L/kg), for minimum 5 minutes. The resulting mixture was then pushed through a 2 mm sieve into the granulator. The granulator was then covered with a custom-made Perspex lid equipped with a gas feeding system that was placed right over the reactor. Then, 100%  $\text{CO}_2$  started flowing to the reactor through the gas feeding system, at 1 bar and the granulator was set in operation at 24 rpm, applying a tilt of 50°. The combined treatment experiments were held for 30 and 60 minutes.

The granules generated after both treatments were removed from the granulator and placed in containers. The containers were then moved to a controlled environment in which the granules were cured for 28 days, under room temperature and 100 % relative humidity.

In order to assess the effect of curing period on the  $\text{CO}_2$  uptake achieved by the granules formed after both treatments, part of the granules formed after each test, was separated from the rest of the material at different time intervals (0, 7 and 28 days of curing) and were subjected to manual crushing using mortar and pestle, in order to obtain a powder that was then sent for IC analysis. The results of the

particular analysis were used for the calculation of the achieved CO<sub>2</sub> uptakes by applying the following formulas:

$$\%CaCO_3 = \frac{\%IC \cdot MW(CaCO_3)}{MW(IC)} \quad (1-1)$$

where: %IC is the average %IC of the three measurements, MW (CaCO<sub>3</sub>) is the molecular weight of CaCO<sub>3</sub> that is equal to 100, and MW (IC) is the molecular weight of the “inorganic” carbon, that is equal to 12.

$$\%CO_2final = \frac{\%CaCO_3 \cdot MW(CO_2)}{MW(CaCO_3)} \quad (1-2)$$

where: MW (CO<sub>2</sub>) is the molecular weight of CO<sub>2</sub> that is equal to 44.

The finally achieved CO<sub>2</sub> uptake (%) was calculated by using the following formula:

$$CO_2 \text{ uptake}(\%) = \frac{CO_2 \text{ final}(\%) - CO_2 \text{ initial}(\%)}{100 - CO_2 \text{ final}(\%)} \cdot 100 \quad (1-3)$$

where CO<sub>2</sub>initial(%) is the content of CO<sub>2</sub> in the as received material, as it was determined by the IC analysis of the latter.

The average particle size, the leaching behavior and the mechanical strength of the formed granules were measured after the end of their curing period (28 days).

To appraise the influence of granulation and granulation-carbonation treatment on the particle size development of the tested material, the particle size distribution of the as received BOF slag and that of granulation and granulation-carbonation products were determined by applying the ASTM D422 standard procedure [33].

The leaching behavior of the granules formed after each test was evaluated following the EN 12457-2 standard compliance test [34], which involves the grinding of material with particle size greater than 4 mm. The leaching behavior of the agglomerated materials was also assessed by applying the EN 12457-2 procedure on unground granules, in order to assess their behavior under similar conditions to the expected application scenario. To determine the impact of the applied type of treatment on the material’s leaching behavior, the as received material was subjected to the EN 12457-2 standard procedure as well, and the obtained results were compared to those attributed to the granules formed after each test.

The mechanical strength of the synthesized granules was assessed by performing the Aggregate Crushing Value (ACV) test, following the British standard BS 812-110 [35].

To estimate if the formed granules are of sufficient strength to be used as secondary aggregates in civil engineering applications, the measured ACVs were compared to those attributed to mixed gravel or BF slag, which are widely used as such materials. If the measured ACV was lower than that of the reference materials, the tested granules were of sufficient strength for use as secondary aggregates. In the case that the measured ACV was higher than that of the reference materials, then the tested granules were of inadequate strength for such use.

### **1.3.1.2. BOF slag batch accelerated carbonation tests**

The batch accelerated carbonation tests were held in triplicates. For each test, three 1g slag samples were wetted with either DI water or sodium solution at L/S of 0.3 L/kg. During wetting, there was an effort to evenly cover the sample with the liquid. The moistened samples were then placed into the reactor. The reactor was then sealed and 100 % CO<sub>2</sub> was introduced to the system.

To assess the impact of milling on the finally achieved CO<sub>2</sub> uptake and to determine the influence of temperature and CO<sub>2</sub> pressure on the reactivity of the material towards CO<sub>2</sub>, two different particle size diameters (<2 mm and <0.125 mm) and two different sets of temperature-CO<sub>2</sub> pressure (20 °C - 1 bar and 50°C - 10 bar) were tested in these experiments. In particular, batch accelerated carbonation tests on the as received BOF slag were carried out at both temperature-CO<sub>2</sub> pressures combinations, whereas batch carbonation experiments on the milled BOF slag sample were held only at the higher set of temperature-CO<sub>2</sub> pressure. In order to evaluate the effect of reaction period on the achieved CO<sub>2</sub> uptake, for all sets of experiments the treatment period ranged between 30 minutes and 8 hours.

After the end of each test, the reactor was unsealed, the samples were removed and cured into the oven at 105 °C, overnight. After their curing, the samples were grinded using mortar and pestle, to create a powder of carbonated BOF steel slag that was then sent for Inorganic Carbon (IC) analysis. Based on the results of this analysis,

the  $\text{CaCO}_3$  content (%) and subsequently the  $\text{CO}_2$  content (%) of the carbonated product were calculated by applying the equations 1-1, 1-2, and 1-3.

By comparing the  $\text{CO}_2$  uptakes achieved by the combined treatment of BOF slag using DI water as the liquid agent, at  $\text{CO}_2$  pressure of 1 bar, after 30 and 60 minutes of reaction and zero days of curing, with those obtained after the batch carbonation tests on the as received material, conducted under similar conditions, the impact of the applied treatment (batch or granulation-carbonation) on the extent of BOF slag carbonation was evaluated.

### **1.3.2. Synthesis of zeolitic material from BF slag**

The particular methodology includes the extraction of calcium from pelletized BF slag, the subsequent hydrothermal conversion of the calcium-depleted residual solids and the assessment of the hydrothermally converted material as heavy metal sorbent in water. Batch calcium extraction tests on both granulated and pelletized BF slags were also performed, in order to assess the impact of materials porosity, acetic acid concentration and extraction duration on the extent of calcium leaching.

In all the experiments, analytical grade acetic acid ( $\text{CH}_3\text{COOH}$ ) solution was used as the calcium extraction agent and sodium hydroxide ( $\text{NaOH}$ ) solution was employed for the hydrothermal conversion process.

Both the calcium extraction and the hydrothermal conversion processes were held in the same autoclave reactor (Büchi, Type 3E), equipped with turbine impeller, baffle, electric heating jacket and a thermocouple.

For the batch extraction experiments, the mixing of the examined BF slag with the acetic acid solution was held in plastic capped bottles agitated by a lab orbital shaker (VWR Scientific Products).

Prior to experimentation, the BF slags were ground using mortar and pestle, and sieved to particle size below 2 mm.

#### **1.3.2.1. Batch calcium extraction experiments**

For each test, 20 grams of pelletized or granulated BF slag were mixed with 100 ml of analytical grade acetic acid solution (Caledon laboratories) of varying

concentrations (0.7, 1.4 and 2.8 M), at 160 rpm and ambient conditions, for different periods (1, 4, 24 hours).

After the end of each test, the slurry was subjected to vacuum filtration using filter paper with coarse pore size (Fischer Scientific, P8), to separate the residual solids from the leachate solution. The obtained solution was acidified using HNO<sub>3</sub> (Caledon Laboratories) (to 2 wt% nitric acid concentration), in order to reduce its pH to <2, and was subsequently analyzed for its content in calcium using inductively coupled plasma optical emission spectroscopy (ICP-OES, Perkin Elmer Optima 8300).

### **1.3.2.2. Calcium extraction from the pelletized BF slag**

Due to the detrimental effect of acidity on the leaching selectivity, the extraction of calcium from both of the tested types of BF slag took place in two steps using half the molarity of the acetic acid that otherwise would be used in one step. In the first step, 100g of the slag were mixed with 731 ml acetic acid (2 M) (Caledon Laboratories) in a sealed autoclave reactor, at 30 °C and 1000 rpm, for 60 minutes. Once acid extraction duration had elapsed, the reactor was unsealed and the slurry was poured into a beaker. To separate the leachate solution from the residual solids, the slurry was then vacuum filtered using filter paper with coarse pore size (Fischer Scientific, P8). The obtained solids were left to dry at ambient temperature, overnight. Once dried, the solid residues resulting from the first calcium-extraction step were mixed again with 731 ml of acetic acid (2 M) solution, in the same autoclave reactor and under the same operating conditions (30 °C and 1000 rpm, for 60 minutes). At the end of the second extraction step, the resulting slurry was poured into a beaker and it was subsequently vacuum filtered using filter paper with coarse pore size (Fischer Scientific, P8). After filtration, the retrieved solids were thoroughly washed with DI water under vacuum, in order to remove residual soluble acetates. The material was then allowed to dry under ambient conditions.

### **1.3.2.3. Hydrothermal conversion of the extraction solid residues**

After each extraction run (including both steps), less than 50 wt% of the initial mass was recovered (due to calcium extraction and partial loss of colloidal silica in filtration), hence multiple batches of extraction were required to generate the mass of solids used in the hydrothermal conversion step. In the particular step, 60 g of the

dry residual solids from the calcium extraction stage were mixed with 300 ml of a NaOH solution (Caledon Laboratories) of varying concentration (0.5 M and 2 M) in a sealed autoclave reactor at 150 °C and 300 rpm, for 24 hours. At the completion of the hydrothermal conversion, the reactor was unsealed and the converted slurry was poured into a beaker. To separate the converted solids from the solution, the slurry was vacuum filtered using a filter paper with coarse pore size (Fischer Scientific, P8). The solids were rinsed thoroughly with DI water under vacuum, to remove excess caustic. The filtered material was then oven-dried at 105 °C for 24 hours, to retrieve the hydrothermally converted material. The obtained material was granular and it was disaggregated using a mortar and pestle. The resulting material was sieved to particle size <0.85 mm.

To verify the production of zeolitic minerals and generally characterize the final product, its elemental composition and its mineral composition were determined by XRF and XRD analyses, respectively. The particle size distribution of the material was determined by laser diffraction analysis (LDA, Malvern Mastersizer 3000).

#### **1.3.2.4. Assessment of the heavy metal adsorption capacity of the hydrothermally converted material**

The efficiency of the generated material as a heavy metal sorbent in water was evaluated by using Ni<sup>2+</sup> as the heavy metal for investigation. For the preparation of the contaminated solutions for the equilibrium experiments, an appropriate amount of an analytical grade standard solution of Ni<sup>2+</sup> (Perkin Elmer, 1000 mg/1000 ml) was added into 1 L of ultra-pure water, in a volumetric flask, to produce solutions of the desired Ni<sup>2+</sup> concentration (2 mg/L, 10 mg/L, 20 mg/L, 100 mg/L and 200 mg/L). After their synthetic preparation, 100 ml of each contaminated solution was poured into capped plastic bottles and 1g of the hydrothermally converted material was subsequently dispersed into them. To, firstly, prevent dissolution of the material in the initial acidic environment of the synthetic solution, and, secondly, to adjust the pH to that typically found in heavy metal remediation conditions, the pH of the solution was controlled to 4-5 by adding concentrated NaOH (Caledon Laboratories) (2 M at first, and 0.5 M closer to end-point) dropwise. The addition of NaOH was carried out while the solution was continuously stirred, at low speed, using magnetic stirring bar on stirring plate, and the pH was continuously monitored by maintaining a pH

electrode soaked in the solution. The bottles were then placed in a shaker incubator (New Brunswick Scientific, I 24), where they were agitated at 160 rpm and 20 °C for 24 hours. After mixing, the pH of the solutions was found increased. Based on experimental studies and geochemical modeling of Santos et al. [228], at pH values over 5 nickel precipitates as Ni(OH)<sub>2</sub>. This type of heavy metal should not be accounted as actual adsorption capacity of the tested material. In an effort to avoid such biased measurements, the pH of the equilibrated adsorbent-adsorbate solution was re-adjusted to ~5.0 by adding drops of concentrated hydrochloric acid (HCl) (Caledon Laboratories) (2 M and 0.2 M closer to the end point). As in the case of NaOH addition, the addition of HCl was also carried out while the solution was continuously stirred, at low speed, using magnetic stirring bar on stirring plate, while the pH was continuously monitored by maintaining a pH electrode soaked in the solution.

To separate the solids from the solution, the slurry was then placed to centrifuge tubes and subjected to centrifugation using a laboratory centrifuge (Thermo Electron, IEC CL30) at 2500 rpm for minimum 5 minutes. After centrifugation, the supernatant solution was carefully poured to a new bottle while keeping the solids in the centrifuge tube. The solution was acidified with nitric acid (HNO<sub>3</sub>) (to 2 wt% HNO<sub>3</sub> concentration), in order to reduce its pH to <2, and was subsequently sent for ICP-OES analysis, to determine its Ni<sup>2+</sup> concentration.

By knowing the initial concentration of Ni<sup>2+</sup> in the synthetically prepared contaminated solution and the concentration of Ni<sup>2+</sup> at the equilibrium state of the adsorbent-adsorbate solution, the amount of the heavy metal adsorbed per gram of the adsorbent at equilibrium ( $q_e$ ) can be calculated by using the following formula:

$$q_e = \frac{(C_o - C_e) \cdot V}{m} \quad (1-4)$$

where:  $C_o$  is the initial concentration of the heavy metal ions in the solution ( $\mu\text{mol/ml}$ ),  $C_e$  is the equilibrium concentration of the heavy metal ions in the solution ( $\mu\text{mol/ml}$ ),  $V$  is the volume of the contaminated solution (ml), and  $m$  is the mass of the dry adsorbent (g).

Upon the  $q_e$  values, the ability of the produced materials to adsorb  $Ni^{2+}$  was appraised. Finally, three different isotherm models, namely Langmuir, Freundlich and Temkin were applied in order to characterize the adsorption processes.

## **1.4. Issues analysis and contribution to knowledge**

In this section, the specific issues addressed by this research are analyzed and the contributions of this study to knowledge are defined. To this end, the existing knowledge on the issues investigated in this study is briefly described. Any weaknesses, gaps or limitations observed in literature are highlighted, and the methods applied to address them are outlined.

### **1.4.1. Introduction of Carbonation Weathering Rate (CWR)**

*Issue:* Several studies on the accelerated mineral carbonation of iron- and steel-making slags have been conducted. However, due to the different particle sizes tested and the different reaction durations applied in each study, the comparison of the reported reaction rate and conversion extent results has been proved challenging.

*Contribution to existing knowledge:* In order to make direct comparisons among the results obtained by different studies, the CWR is conceptualized. The rate is expressed in units of  $\mu\text{m}/\text{min}$  and represents the weathering rate of the particle radius from the original outer radius to the final radius of the unreacted core of the carbonated particle. By taking into consideration the particle size of the treated material and the reaction period applied in each study, the CWR measure is able to deliver more accurate and insightful results than the  $\text{CO}_2$  uptake or conversion extent.

### **1.4.2. Synthesis of secondary aggregates from BOF slag**

*Issue:* The reuse of BOF slag as an aggregate in construction applications has been studied by several researchers. However, several of its characteristics like its high content in  $\text{Ca}(\text{OH})$  and  $\text{Mg}(\text{OH})$ , its high pH values [141], the high leaching levels of regulated elements (Cr and V) [15] and its low particle size, hinder its employment in such applications. Moreover, the elevated mechanical strength requested from aggregate materials is an additional issue.

Contribution to existing knowledge: According to literature and given the high alkaline earth metals content of the particular slag, the direct accelerated carbonation of the BOF slag can improve several of its undesired qualities. In fact, the direct carbonation of BOF slag has been found to lead to satisfactory levels of CO<sub>2</sub> sequestration [36-39] and therefore, to high consumption of Ca(OH) and Mg(OH). Furthermore, carbonation has also been found to enhance the strength of BOF slag [40] and notably alter its environmental behavior by decreasing its pH and the release levels of several regulated elements [38]. However, carbonation is not capable to significantly affect the average particle diameter of the slag. To face this issue, Morone et al. [41], studied the coupling of granulation with carbonation, as a process for BOF slag conversion towards secondary aggregates. The particular treatment of BOF slag resulted in the formation of granules with sufficient size, while substantial CO<sub>2</sub> uptakes were achieved despite the incorporation of granulation in the process. However, the mechanical performance of the generated products was not the desired one.

Alkali activation has been found to be effective in increasing the mechanical strength of materials that present high contents of calcium and silica [42], like BF slag or coal fly ash. Based on the work of Morone et al. [41] and the beneficial effects of alkali activation on the strength of materials with similar chemistry to that of BOF slag, in this study, a new method for the production of secondary aggregates from BOF slag is proposed. In particular, the combined granulation-carbonation of the BOF slag is coupled with the alkali activation of the material, to produce granules of satisfactory volumetric stability, acceptable particle size, sufficient CO<sub>2</sub> uptake, approved environmental behavior and adequate mechanical strength.

### **1.4.3. Synthesis of zeolites from BF slag and assessment of their adsorption capacity**

Issue: The use of BF slag as a carbon sink, capable of fixing sufficient amounts of CO<sub>2</sub>, requires the parallel generation of value added materials in order to secure the financial feasibility of the process and most importantly, to create new revenue streams for the industry, preferably of higher value than the already existing ones that result from the current use of the material.

The indirect carbonation of BF slag has been proved to be an efficient technique for the sequestration of notable amounts of CO<sub>2</sub> and the formation of high purity precipitated calcium carbonate (PCC), a material with various applications in several sectors. However, indirect carbonation generates solid residues from the material, which are not further processed or exploited after the calcium extraction stage, creating a disposal issue. Moreover, in order to create new and more profitable revenue streams and become appealing to the industry the proposed technique should aim to the synthesis of more than one products from BF slag.

*Contribution to existing knowledge:* An interesting study addressing both of the described issues is that of Chiang et al. [43] who combined the indirect carbonation of BF slag with the hydrothermal conversion of the residual solids resulting from the calcium extraction stage, in order to achieve the sequestration of respectful amounts of CO<sub>2</sub> and the production of PCC and zeolites.

The carbonation step of the proposed methodology has been successfully reproduced and optimized by De Crom et al. [44], who managed to synthesize a high purity PCC while storing satisfactory amounts of CO<sub>2</sub>. However, the reproducibility of zeolites through the hydrothermal conversion of the calcium-depleted solid residues and their efficiency as heavy metal sorbents in wastewater treatment applications remain to be assessed.

In this study, the reproduction of a zeolitic material via the hydrothermal conversion of the residual solids resulting from the calcium extraction step of the indirect carbonation of BF slag, as it was proposed by Chiang et al. [43], was attempted. In this project a different type of BF slag than the one originally used, was employed. In particular, pelletized BF slag that is characterized by higher porosity, in regards with the granulated BF slag that was used by Chiang et al. [43], was selected for investigation, to find out whether a more porous starting material would facilitate the formation of zeolites. Moreover, the heavy metal adsorption capacity of the produced material was evaluated for the first time, using Ni<sup>2+</sup> as the metal for investigation.

## **1.5. Thesis structure**

The first chapter contains the introduction to the project. The current situation is specified. The problems addressed in this project are outlined, and the methods with

which they are faced are explicitly described. In the particular section the aims and the objectives of the project as well as the contributions of this project to knowledge are also defined. It also contains a short description of each chapter.

The second chapter contains the literature study that was conducted for the needs of this project. In the first part of the chapter the theoretical framework on which the research was based is analytically discussed. Next, the recent publications related to the influence of accelerated mineral carbonation parameters on the carbonation rate and conversion extent of steelmaking slags, are reviewed, compared and analyzed, in order to define the state of the art. In the same section, a new index named CWR, with which the maximum conversions resulting from different studies are directly compared, is introduced. Finally, the recent literature on the valorization of BF and BOF slag, through both the direct and indirect carbonation of the material is also reviewed in this section.

In the third chapter, the performance of granulation and a combined granulation-carbonation treatment applied as a method leading to the transformation of BOF slag to synthetic aggregates and the sequestration of sufficient amounts of CO<sub>2</sub> in a stable and benign to the atmosphere mineral, is investigated. An alkaline solution of sodium hydroxide and sodium silicate is also used to improve the mechanical strength of the formed granules. The finally achieved particle sizes, CO<sub>2</sub> uptakes, mechanical strengths and leaching behaviors of the granules formed after each of the applied treatment, are evaluated and compared to each other, to distinguish the most effective processes. The mechanical strengths of the finally obtained granules are also compared to those attributed to materials regularly used as secondary aggregates in several civil engineering applications, in order to discover if the newly formed agglomerates are of adequate strength for such uses.

In the fourth chapter the reproduction of zeolites following the methodology proposed by Chiang et al. [43], is attempted. A more porous type of BF slag (pelletized BF slag) than the one used by Chiang et al. [43] (granulated BF slag) is used as the starting material. The particular slag is subjected firstly to a calcium extraction step and subsequently to hydrothermal activation. The finally formed materials are assessed regarding their elemental and mineralogical composition, whereas their heavy metal adsorption capacity in water is evaluated using Ni<sup>2+</sup> as the metal for

investigation. Finally, the characterization of the adsorption processes is performed by using three different isotherm models namely, Langmuir, Freundlich and Temkin.

The fifth chapter summarizes the conclusions drawn from this research and points out its deficiencies. Suggestions aiming to the future development of the particular research are made.

## **1.6. Studies breakdown and contributions**

The particular research is separated in three parts: the conduction of a literature review related to the carbonation and valorization of iron and steel-making slags, the formation of construction aggregates from BOF slag, and finally the synthesis of a zeolitic material with notable heavy metal adsorption capacity, from BF slag.

The conduction of the literature review was an ongoing process throughout my studies period. The literature review was conducted exclusively by me, mainly during the first year of my studies in Cranfield University, UK. More recent studies related to the subject of the review were added later on, in order for the literature review to be up to date. The Carbonation Weathering Rate was conceptualized in order to overcome the difficulties met with comparing the actual reactivity of different iron- and steel-making slags towards  $\text{CO}_2$ , based on the  $\text{CO}_2$  uptakes and carbonation conversions achieved after their subjection to carbonation. The idea came after discussions I had on the subject with Professor Rafael Santos. The mathematical formula for the Carbonation Weathering Rate was expressed by me.

The formation of secondary aggregates from BOF slag by combining granulation with carbonation and alkali activation was attempted in the University of Tor Vergata, Rome, Italy. My research in Tor Veragata University facilities lasted for a year. All the experiments related to this part of the project and described in this thesis were performed by me with the collaboration of Dr Milena Morone and under the supervision of Professor Renato Baciocchi and Dr. Giulia Costa.

Finally, the formation of zeolitic heavy metal adsorbent from BF slag after the extraction of calcium from the latter and the subsequent subjection of the resulting solid residues to hydrothermal conversion was performed in Sheridan College, Ontario, Canada. My research in Sheridan College facilities lasted for approximately

6 months. All the experiments related to this part of the project and described in this thesis were conducted by me under the supervision of Professor Rafael Santos.

## 2. LITERATURE REVIEW

### 2.1. Introduction

In this project, the valorization of BF and BOF slags through the coupling of carbonation with additional processes is pursued. The theoretical framework, on which the particular study was developed and the literature review on the key areas of related research are presented in this section. In particular, two topics are reviewed: a) the effects of different parameters on the carbonation extent and kinetics of different types of iron- and steel-making slags under various experimental conditions and b) the valorization of BF and BOF slag, through both the direct and indirect carbonation of the material.

Furthermore, the route through which the particular slags were selected as the most suitable for the aims of this study and the reasons for which the proposed processes were selected for examination, are presented and analyzed in this chapter.

#### 2.1.1. Background

CCS technology, though largely still under demonstration (e.g., IEAGHG Weyburn-Midale CO<sub>2</sub> Monitoring and Storage Project, concluded in 2012, has stored 22 Mt of CO<sub>2</sub>) [47], is considered an essential technology in the global climate change mitigation effort [44]. The particular technique could allow continued use of fossil fuels while reducing GHG emissions [46]. According to it, the post-combustion CO<sub>2</sub> is firstly, captured and subsequently sequestered in a secure and permanent way.

Carbon sequestration is the secure storage of CO<sub>2</sub> emitted by the global energy system. Carbon dioxide can be stored underground or in the ocean. There is also the alternative of the terrestrial biosphere sequestration which is more like natural carbon sinks, where carbon is mainly stored in vegetation and soils through the photosynthesis and the decomposition of organic matter.

Three different CO<sub>2</sub> sequestration fields have been identified for the underground storage: a) saline aquifers, b) depleted oil and gas reservoirs, and c) coal beds [56-59]. Trapping mechanisms for underground storage of CO<sub>2</sub> include the geological trapping that contains the structural and stratigraphic trapping, the geochemical trapping that includes the residual gas trapping, the solubility and ionic trapping and

the mineral trapping, and the hydrodynamic trapping that contains the migration trapping [48-50].

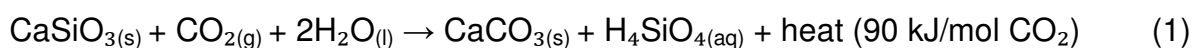
The structural and the stratigraphic trappings occur when the CO<sub>2</sub> is trapped below geological formations like anticlines, folds or fold blocks and seal rock units. Residual saturation is a trapping mechanism that is mainly caused by the capillary forces that force CO<sub>2</sub> to fill in the voids of the pores of a formation. Solubility and ionic trapping takes place when CO<sub>2</sub> is in its supercritical condition and migrates through the reservoir until it meets the seal cap rock and eventually dissolves into the formation's water. Mineral trapping is a mechanism that transforms the CO<sub>2</sub> into stable, newly formed secondary minerals after the CO<sub>2</sub> has reacted with host rocks, rich in alkaline metals. Finally, the migration trapping lets the CO<sub>2</sub> to migrate through the reservoir and beneath seal cap rock at extremely low velocities. Consequently, CO<sub>2</sub> will be able to reach the surface of the Earth after millions of years and only if no other mechanism has managed to trap it during its migration.

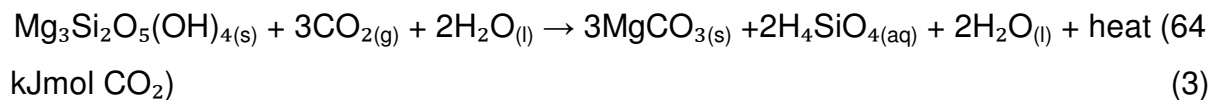
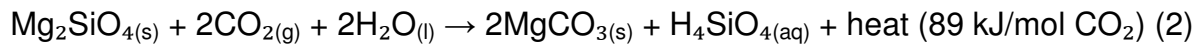
Among these trapping mechanisms, mineral carbonation is attractive as it manages to store CO<sub>2</sub> permanently by transforming it into a new carbonate mineral that is thermodynamically stable over geological timeframes [50].

### 2.1.2. Mineral carbonation

Mineral carbonation is the process by which CO<sub>2</sub> reacts with another organic matter rich in alkaline earth metals and produces new minerals that present significantly high stability. In this mechanism CO<sub>2</sub> gets transformed into an insoluble carbonate (mainly calcite or magnesite) that is able to remain stable for millions of years.

The transformation of CO<sub>2</sub> into a stable mineral needs the reaction of itself with a metal oxide bearing material. This process can take place either naturally or in laboratory/industrial settings, under controlled conditions. The natural occurring mineral carbonation is called "silica weathering". According to natural weathering, CO<sub>2</sub> reacts exothermically with alkaline elements that are present in natural metal oxide bearing silicates, forming thermodynamically stable and environmentally benign carbonates as exemplified by [51]:





The main drawback of the natural weathering process in terms of mineralization, is the very slow kinetics, which have been mainly attributed to the very low concentration of CO<sub>2</sub> in rainwater (approximately 1–2 mg/L) [52]. In the last two decades, many researchers have been experimenting on accelerating the reactions between CO<sub>2</sub> and alkaline minerals. Seifritz [53] was one of the first to propose the accelerated carbonation process according to which, the alkaline materials react with carbon dioxide of high pressure and high purity in the presence of moisture, in order to accelerate the reaction to a timescale of a few minutes or hours. A remarkable characteristic of the process is the exothermic nature of the occurring reactions (Reactions (1)–(3)). The heat released by the reaction could be recovered and used to compensate the significant amount of energy that is required as an input for industrial accelerated carbonation (due to required milling, pumping, compression, heating, sorbent regeneration, etc.) [54], lowering that way the costs of the process [55].

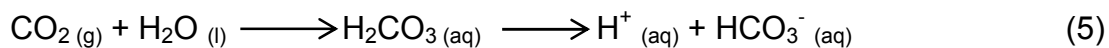
Accelerated carbonation can be classified into two types: a) direct carbonation, and b) indirect carbonation. According to the direct carbonation, CO<sub>2</sub> directly reacts with the tested material, in a single step (in one reactor). It can take place following two different procedures, namely gas-solid carbonation and aqueous carbonation.

Under the direct dry gas–solid carbonation, that was firstly studied by Lackner et al. [60], the alkaline earth metals present in silicate minerals are converted directly to carbonates using gaseous or supercritical CO<sub>2</sub>. The particular process requires high CO<sub>2</sub> pressures in order to obtain acceptable reaction rates [61]. A typical such reaction is exemplified by [21]:



Due to its very slow kinetics, the particular process has been proved inefficient for the fixation of substantial amounts of CO<sub>2</sub>, whereas its extension further than the research stage seems improbable.

Under the aqueous (wet/slurry) carbonation, operated at L/S ratio of more than 0.2 L/kg, the CO<sub>2</sub> firstly dissolves in water to form HCO<sub>3</sub><sup>-</sup>, then with the assistance of the formed protons, the metal (Ca or Mg) is leached from the solid matrix and eventually calcium or magnesium carbonates are formed. Typical reactions are exemplified by [21]:



The particular process is characterized by two major limitations that inhibit the achievement of high conversion rates and CO<sub>2</sub> uptakes: the limited mobility of the alkaline elements in the solids and the formation of a carbonate passivating layer within each solid particle which hinders its further carbonation, leaving its core unreacted. Both of these limitations have been proved sensitive to operating parameters alterations and additives use and depending on the tested material and the experimental set-up, the particular process can be optimized accordingly to achieve the sequestration of satisfactory amounts of CO<sub>2</sub>.

On the other hand, these restrictions do not apply to the indirect route of carbonation. According to it, the reactive alkaline elements of the tested material are first extracted from it (in one reactor) and subsequently subjected to carbonation, in a separate stage (in another reactor). By using strong acids to induce the leaching of the reactive ions from the material into the solution, the limitations characterizing the direct carbonation process are more easily surmounted, increasing the possibility of greater amounts of CO<sub>2</sub> to be stored, since clearly, the extracted ions in the leachate solution are free to move, whereas no passivating layer preventing the two reacting phases (CO<sub>2</sub> and Ca<sup>2+</sup>) from coming in contact, can be formed.

Apparently, under the right conditions, the efficiency of a material as a carbon sink can be maximized through its indirect carbonation. Nevertheless, the particular process is considerably more complicated and more expensive compared to direct mineral carbonation.

### 2.1.3. Iron and Steel slags

Apart from naturally occurring minerals, industrial solid wastes characterized by high alkaline earth metal content can also be used for mineral carbonation. Iron and steel slags, air pollution control (APC) residues, fly and bottom ash from municipal solid waste incineration processes, pulverized fuel ash produced by coal-fired power plants, paper pulping wastes, mining tailings, red mud, asbestos-containing residues, and oil-shale processing residues are some of the industrial residues that are suitable for mineral carbonation [10].

From them, iron- and steel-making slags exhibit the highest experimental CO<sub>2</sub> (ECO<sub>2</sub>) uptakes and have been proved to be of the most promising materials for such use.

#### 2.1.3.1. Iron and steel production

Earth is mainly composed by iron (32.1 % by mass) [67]. The same element is the fourth most abundant in the Earth's crust, making up almost 5.6 % of it [67]. It is naturally occurring in the form of iron ore, that basically consists of iron oxide and varying quantities of other metals such as sulfur, manganese, silicon and phosphorous. To extract the iron from the iron ore, the latter is subjected to heat treatment in BFs. Iron ore or pellets, coke and fluxes (dolomite, limestone or silica sand) melt together in the particular furnaces [69]. Coke is produced from coal and is the most common met fuel that is fed into the blast furnace. It is not only responsible for the heating of the ore and thereupon for its smelting but also helps the separation of iron from the oxides with which it is chemically bonded [68]. On the other hand, fluxes help with the removal of the impurities from the molten iron. In particular the mineral that is used as a flux in the process manages to combine with the impurities of the molten material and forms a slag that floats on the surface of the molten iron and which is afterwards separated from it [68]. The goal is to chemically reduce iron oxides and convert them into liquid iron. The resulting material is called pig iron and is an alloy of approximately 90 - 95 % of iron and 3 - 4 % of carbon [69]. Pig iron is used as the starting material for the production of steel.

Due to its notably high strength, its consistent quality and its low production cost, steel is one of the most versatile materials with applications in almost every aspect of

our everyday life. Among others, it is widely used in construction, as well as in automobile and shipbuilding industries, whereas numerous everyday life objects like table knives, tools or engines are made of it. Steel, is a mixture of iron and primarily carbon (up to 2.1 wt%). Mainly depending on the desired use of steel, the particular blend also comprises of several other elements such as manganese, phosphorous, sulfur, nickel, chromium and others, in smaller amounts.

Steel manufacturing can be accomplished by using two different types of furnaces: the BOF and the EAF. The basic differences between these two steel production routes is the type of raw materials used in each one and the manner according to which they are converted into steel.

For the production of BOF steel, pig iron along with steel scrap and coal are charged into the furnace, where they are heated and subjected to oxidation reactions to remove undesired impurities and produce liquid steel [70, 71]. For the oxidation process, pure oxygen (99 %) is introduced onto the surface of the mixture at supersonic speeds and a pressure of 100-150 psi, through lances [72]. As in the case of iron-making process, lime and dolomite can be used as fluxes in the furnace, to form a slag incorporating the impurities of the molten mixture [70, 71]. A pretreatment of the pig iron before its introduction to the furnace, according to which the quantities of sulfur, silicon, and phosphorus of the material are getting reduced, may also be included to the process, depending on the quality of the pig iron and the desired quality of the finally produced steel [70, 71].

The EAF produces steel using mainly steel scrap that is melted through high electric current [72]. In particular, steel scrap is melted through electric arcs, generated by graphite electrodes [72]. In several cases, mainly depending on the availability of steel scrap and the desired quality of the final product, direct reduced iron, iron carbide, and pig iron can also be used in the EAF route [73]. Oxygen or a mixture of oxygen-carbon is also injected to the material in order to purify the steel and improve the efficiency of the heat transfer from the arcs to the scrap [73]. Slag formers like lime and dolomite can be charged into the furnace with the scrap or later in the process. The slag synthesized in the EAF is a destination of the oxidized impurities initially located in the molten steel.

Stainless steel (SS) results from the further treatment of the molten metal, synthesized in the electric arc furnace. The particular term covers a wide range of steel alloys of varying quality and properties that make them useful in numerous fields of applications.

Approximately 75 % of SS is generated from a process known as argon oxygen decarburization [74]. AOD is a refining process mainly used to lower the level of carbon (C) in the composition of the metal. It comprises of three stages: decarburization, reduction and desulphurization [75]. In decarburization step the carbon content of steel is reduced by regular injection of oxygen and argon in different ratios [75]. However, the oxidizing effect is not only constrained to carbon. Instead, chromium gets oxidized as well. In order to drive the reaction to the formation of carbon monoxide and inhibit the loss of chromium into slag, other alloy elements with higher affinity to oxygen than chromium, like silicon or aluminum, are added to the mixture during the reduction step [75]. Consequently, the oxygen tends to combine with carbon to form CO and it only oxidizes a small fragment of the alloy and in particular Cr [75]. After the desired carbon has been removed, and the oxidized alloying elements have been recovered, the desulphurization step follows, in order to dilute the contained sulfur [75]. After the desired composition of steel is reached, it is separated from the slag.

Finally, there is the solidification process of molten steel. It is known as continuous casting. CC is the process during which molten steel from BOF or EAF is solidified into slabs or other shapes before being subjected to hot or cold rolling in the finishing mills and obtain its final thickness [76]. Its first implementation in steel manufacturing industry dates back in 1950's and it replaced the simple pouring of steel into stationary molds to form ingots [76]. Its adoption by the steel manufacturing industry and its gradual development resulted in significantly improved production yield, quality, productivity and cost efficiency.

Approximately 70 % of the global steel production results from BOF furnaces, whereas 29 % of it comes from the EAF route [77]. Another steel production technology known as open hearth (OH) furnace is responsible for the rest 1% of steel production [77]. The limited occurrence of this type of steel is basically owed to

the method's energy demanding nature that results in environmental and economic damages [77].

### **2.1.3.2. Iron and steel slag types**

As discussed, iron and steel produced by the aforementioned methods, are accompanied by byproducts known as iron and steel slags. Slag is a stony vitreous residue, comprising of metal oxides and silicates that result from the separation of molten iron or steel from impurities. Its presence in the furnace is of high significance since by floating on the surface of molten metal, it prevents excessive heat loss from the liquid iron or steel while inhibiting the erosion of the refractory lining of the furnace [72]. There are several different types of slags resulting from the different stages of iron- and steel-making process.

#### **2.1.3.2.1. Iron-making slag (BF slag)**

BF slag is a non-metallic by-product of iron-making process. BF slag contains CaO (34 - 43 %), Al<sub>2</sub>O<sub>3</sub> (7 - 12 %), SiO<sub>2</sub> (27 - 38 %), MgO (7 - 15 %), FeO or Fe<sub>2</sub>O<sub>3</sub> (0.2 - 1.6 %), MnO (0.15-0.76 %) and S (1 - 1.9 %) [78]. Its mineralogy is characterized by the occurrence of dicalcium ferrite (2CaO·Fe<sub>2</sub>O<sub>3</sub>), calcium alluminate (CaO·Al<sub>2</sub>O<sub>3</sub>) and wustite (FeO), whereas additional reactive phases such as C<sub>2</sub>S (2CaO·SiO<sub>2</sub>), C<sub>3</sub>S (3CaO·SiO<sub>2</sub>), free lime (CaO) and MgO are also present [79]. After its separation from the molten iron, the slag is cooled down in several ways. Based on the manner that it is cooled, BF slag exhibits significantly different physical characteristics that determine its potential future applications.

There are four different cooling methods of BF slag, leading to four different types of slag products. The air-cooled blast furnace slag (ACBFS), is formed when the molten slag is poured into beds and left to cool down slowly under ambient conditions. The particular type of BF slag has a crystalline structure and a vesicular texture with closed pores. It is hard and dense but once crushed and screened, it can be used as aggregate in construction business [79-82], as a material in road bases and surface and as raw material in clinker and in concrete products [83]. When the molten slag is cooled rapidly by being quenched in water, the granulated blast furnace slag (GBFS) is formed. GBFS actually consists of sand-sized particles of glass and is characterized by a disordered structure. When ground, the GBFS

presents moderate hydraulic cementitious properties that become significantly more pronounced if it accesses lime. That is the main reason why ground GBFS is widely used as a PC replacement in concrete mixes, reducing the cost of cement production [29-32, 79]. GBFS can also be efficiently used as aggregate in concrete mixtures and in several civil engineering applications, given its notable resistance to chemical attack and its significant long-term strength development [80]. The pelletized blast furnace slag (PBFS) is formed when the molten slag is cooled with a combination of water quenching in a spinning drum and air-cooling. The PBFS products can be either more crystalline or more vitrified, mainly depending on the quenching speed. Apparently, the crystalline structure is beneficial for the use of PBFS as a lightweight aggregate, whereas the glassy structure of the material promotes its use in cementitious applications as a PC replacement [32, 79, 80]. Finally, there is the expanded BF slag (EBFS) that is obtained after an accelerated processing of molten BF slag. For the production of the particular type of slag, several methods combining the BF slag with water or with water and air or steam have been developed. Depending on the applied process and the amount of water used, the final product can either be more crystalline or vitrified, resembling to ACBFS or PBFS, respectively. EBFS is characterized by a cellular structure, notable porosity and low bulk density.

BF slag presents remarkable reactivity with  $\text{CO}_2$ . In fact, BF slag has been reported to achieve  $\text{ECO}_2$  uptakes ranging between 75 – 294 g  $\text{CO}_2/\text{kg}$  slag [22,23].

Generally, 250 - 350 kg of BF slag are produced per ton of pig iron, mainly depending on the iron content of the iron ore [81]. It is estimated that the annual worldwide BF slag production for the year of 2015 was approximately 300 – 360 Mt based on typical ratios of slag to crude iron output [24].

#### **2.1.3.2.2. Steel- making slags (BOF and EAF slags)**

Depending on the process that is followed for the production of steel, different types of steel slag are produced.

BOF slag is formed during the conversion of pig iron into steel, in a basic oxygen furnace. The major components of the particular type of slag are CaO (30 - 60 %), FeO (3 - 38 %) and  $\text{SiO}_2$  (8 - 15 %). In less significant amounts, MgO (0.8 - 15 %),

$\text{Al}_2\text{O}_3$  (1 - 3.5 %),  $\text{P}_2\text{O}_5$  (0.2 - 3.5 %) and  $\text{MnO}$  (0.3 – 4 %) may also be present in the chemical composition of BOF slag [26, 82-85]. During the refining process of the liquid steel, oxides of Si, P, Mn and S are also formed. Its cooling is similar to that of ACBF slag, since it is simply poured into pits where it is air-cooled under controlled conditions. The final product is a crystalline slag that can be subsequently subjected to weathering, crushing or sieving to eventually obtain a material with the desired properties. This type of slag can be used as fertilizer, armourstone used in hydraulic engineering or even as aggregates in road construction [86].

The slag resulting from EAFs is known as EAF slag. The EAF steel production can lead to the formation of either carbon or high alloy steel. Depending on the desired steel quality two different types of the EAF slag can be generated; carbon steel EAF slag and stainless steel EAF slag. Typically, the EAF slags resulting from the stainless steel route have a notably lower content of iron than the slags coming from the carbon steel production. In general, the chemical composition of EAF slag resembles to that of BOF slag. The main constituents of EAF slag are  $\text{CaO}$ ,  $\text{FeO}$ ,  $\text{SiO}_2$ ,  $\text{Al}_2\text{O}_3$  and  $\text{MgO}$ . Regarding their quantitative presence in the slag,  $\text{CaO}$  is its main component (24 - 60 %), along with  $\text{FeO}$  (10 - 40 %),  $\text{SiO}_2$  (6 - 34 %),  $\text{MgO}$  (3 - 13 %) and  $\text{Al}_2\text{O}_3$  (3 - 14 %), whereas  $\text{MnO}$  (2 - 6 %) and  $\text{SO}_3$  (0.1 - 1 %) can be detected in lower amounts [87-90]. Trace amounts of Co, Ni and Cr may also be found within its composition [87-90]. After its separation from the molten steel, EAF slag is slowly air-cooled to form crystalline slag.

In the past, mainly because of the great volumes of BF slag that were available, the utilization of EAF slag was not attractive and its usage as fertilizer was the only possible route to avoid its disposal to landfill sites. However, basically due to the continuously increasing share of steel production coming from electric arc furnaces, the particular type of slag has found applications in numerous domains, such as in the civil engineering sector as a construction material [88, 91-93]. EAF slag has also been reported as an efficient low cost adsorbing agent, capable of being utilized in treatment applications of heavy metal laden streams (wastewater etc.) [94-96].

From mineralogical aspect, steel slags include the following phases: merwinite ( $3\text{CaO}\cdot\text{MgO}\cdot 2\text{SiO}_2$ ), olivine ( $2\text{MgO}\cdot 2\text{FeO}\cdot\text{SiO}_2$ ),  $\alpha\text{-C}_2\text{S}$  ( $2\text{CaO}\cdot\text{SiO}_2$ ),  $\beta\text{-C}_2\text{S}$ ,  $\text{C}_2\text{F}$  ( $2\text{CaO}\cdot\text{Fe}_2\text{O}_3$ ),  $\text{C}_4\text{AF}$  ( $4\text{CaO}\cdot\text{Al}_2\text{O}_3\cdot\text{FeO}_3$ ), free lime ( $\text{CaO}$ ),  $\text{MgO}$ ,  $\text{FeO}$ ,  $\text{C}_3\text{S}$

( $3\text{CaO}\cdot\text{SiO}_2$ ) and the RO phase (solid solution of  $\text{CaO}\text{-FeO}\text{-MnO}\text{-MgO}$ ) [97-99]. Due to the presence of unstable phases like free lime,  $\text{MgO}$  and  $\text{C}_2\text{S}$  in their mineralogy, steel slags are characterized by high volumetric instability when they come in contact with water, causing serious issues when they are used for construction applications. In presence of water,  $\text{CaO}$  and  $\text{MgO}$  hydrate causing the volumetric expansion of the slags [83, 100-103], whereas at temperatures below  $500\text{ }^\circ\text{C}$ ,  $\alpha\text{-C}_2\text{S}$  is transformed to  $\beta\text{-C}_2\text{S}$  also resulting in a notable volumetric increase of approximately 10 % [82]. Apparently, special treatment of BOF and EAF slags is required in order for them to be efficiently used in construction applications [80].

### **2.1.3.2.3. Steel-refining process slags (AOD and CC slags)**

Apart from the slags resulting from the different steel manufacturing methods, there are also steel residues coming from the refining processes of the produced steel, namely AOD and CC slags. Information on their chemical composition is limited since it is highly variable and dependent on the type of alloys employed to obtain steel of different grades. In general, the  $\text{FeO}$  content of the slags resulting from the refining processes is significantly lower ( $< 10\%$ ) than that of BOF and EAF slags. In the contrary, the contents of  $\text{CaO}$  and  $\text{Al}_2\text{O}_3$  appear to be remarkably higher for the slags coming from the refining of steel.

The slag resulting from the AOD process is known as AOD slag. It is separated from the treated steel, before the latter gets subjected to secondary metallurgical treatment to adjust its final chemical composition.

AOD slag comprises of silicates ( $\text{C}_2\text{S}$ ), oxides charged in the furnace and oxides of  $\text{Al}$  and  $\text{Si}$ , while metal particles of various sizes can also be present. The content of  $\text{Cr}$ -oxides varies significantly depending on the selected AOD operation techniques and the slag treatment after its tapping. Thus, AOD slag content in  $\text{Cr}$  can be different between different steel plants but also in the same plant for different AOD heats [102]. However,  $\text{Cr}$ -oxides in AOD slags are contained in rather low amounts which are bonded to other oxides forming stable slag phases, avoiding the danger of  $\text{Cr}$  leaching [104].

The slag produced during the CC phase of steelmaking process is the CC slag. This type of slag is the one remaining at the ladle after each casting process is finished

[105]. It is basically composed by lime. Its chemical composition varies depending on the secondary metallurgy process implemented to produce the desired steel grade.

Both AOD and CC slags are morphologically characterized as fine powders, something that makes their handling in steel industry difficult. This is mainly caused by the presence of dicalcium silicate in the slags that during the cooling period, gets transformed from  $\alpha$ -C<sub>2</sub>S to  $\beta$ -C<sub>2</sub>S and  $\gamma$ -C<sub>2</sub>S, inducing the expansion of the material and eventually the breakage of its crystalline matrix into powder [106]. To confront the particular issue and facilitate the utilization of the particular material, boron can be added to the molten slag [107]. That way, C<sub>2</sub>S can be stabilized at its  $\beta$ -C<sub>2</sub>S form and the pulverization of the slag can be avoided. The stabilized AOD and CC slags can be used as aggregates in low end applications, such as in road construction [108].

The ECO<sub>2</sub> uptakes ascribed to the several types of steel slags fluctuate within a broad range of values. In particular, BOF slag attributes an ECO<sub>2</sub> uptake of approximately 266 gCO<sub>2</sub>/kg slag [19-21]; EAF slag has demonstrated an ECO<sub>2</sub> uptake of 136 - 220 gCO<sub>2</sub>/kg slag [62,63]; AOD slag has presented ECO<sub>2</sub> uptakes of between 190 - 429 gCO<sub>2</sub>/kg slag [64,65]; and CC slag has realized an ECO<sub>2</sub> uptake of 312 g CO<sub>2</sub>/kg slag [66].

On average, 150 - 200 kg of BOF slag and 80 - 150 kg of EAF slag are generated per ton of steel produced [80, 109]. The annual worldwide steel slag production in 2015 was approximately 170 - 250 Mt, based on typical ratios of slag to steel output [24], whereas the global stainless steel production for the same year was approximately 41.5 Mt [110].

In the past, iron and steel manufacturing processes were exclusively aiming to the production of iron and steel of specific quality. Currently, the particular processes are designed to also generate slags of adequate environmental and technical value, in order to be efficiently utilized in several applications, while complying with the very strict international and national environmental regulations.

In spite of this effort, a great part of the produced slags remains of insufficient quality for commercial exploitation. As a result, further investigation regarding potential valorization routes for this type of residue should be conducted.

## 2.2. Iron- and steel-making slag carbonation: A literature review of conversion extent and kinetics

The target of this project is the sequestration of satisfactory amounts of CO<sub>2</sub> and the coincident formation of value added materials from iron and steel-making slags, through the coupling of carbonation with additional processes. In an effort to discover the level of reactivity of the particular materials towards CO<sub>2</sub> and to assess the effects of several operational parameters on it, a literature review on the carbonation extent and kinetics of iron- and steel-making slags under various experimental conditions was conducted.

In this section, literature on the carbonation of iron- and steel-making slags is reviewed. All relevant results from the cited studies are summarized in Tables A-1 and A-2 (Appendix A) to facilitate comparison. These results are discussed in the following subsections.

### 2.2.1. BF slag

Chang et al. [111] studied the slurry carbonation kinetics of this type of slag using an autoclave reactor and slag particles of less than 44 μm. The effect of reaction time, temperature, CO<sub>2</sub> partial pressure, and liquid-to-solid (L/S) ratio on the extent of carbonation was investigated.

*Reaction time:* according to Chang et al. [111], by increasing the duration of carbonation up to 60 minutes, the extent of carbonation increases with decreasing rate. Any further prolonging of the treatment period does not seem to affect the finally achieved extent of carbonation..

*Temperature and CO<sub>2</sub> pressure:* the manner that temperature affects the extent of BF slag carbonation is highly dependent on the applied CO<sub>2</sub> pressure. In particular, at a pressure of 48.3 bar, any temperature increase up to 100 °C leads to an increase of the conversion extent. By further increasing the reaction temperature over 100 °C, a decrease in the conversion extent is observed. This is not the case when CO<sub>2</sub> is inserted to the system at its supercritical condition (CO<sub>2</sub> pressure: 89.6 bar). In this case the extent of BF slag carbonation continues to increase even when reaction temperatures higher than 100 °C are applied. Chang et al. [112] explained

this behavior based on the manner that temperature increase influences the leaching of  $\text{Ca}^{2+}$  from the solid particles and the dissolution of  $\text{CO}_2$  in the solution. In fact, with increasing temperature,  $\text{Ca}^{2+}$  leaching increases, whereas  $\text{CO}_2$  dissolution decreases. Apparently, at 48.3 bar and within the 0 - 100 °C temperature range, the enhanced  $\text{Ca}^{2+}$  leaching caused by temperature increase, managed to overcome the  $\text{CO}_2$  dissolution attenuation, and led to increased extents of conversion. At temperatures over 100 °C and for the same  $\text{CO}_2$  pressure, the reduced  $\text{CO}_2$  dissolution becomes the limiting factor of the carbonation reaction, and the conversion decreases. On the other hand, when  $\text{CO}_2$  was introduced to the system at its supercritical condition, the higher  $\text{CO}_2$  solubility and lower dynamic viscosity permitted the  $\text{Ca}^{2+}$  leaching to remain the limiting factor of the carbonation reaction, even at elevated temperatures over 100 °C.

*Liquid-to-solid ratio:* among the liquid-to solid ratios tested by Chang et al. [111] the one that resulted to the higher carbonation extent was equal to 10 L/kg. For L/S values below or above this value the finally achieved carbonation extent was lower. As anticipated, in the absence of water (L/S ratio: 0 L/kg), the conversion extent was very low. For L/S ratios below the optimal, the the mixing of the slurry in the reactor was not good and the contact between the solid particles of the slag and the reaction fluid was poor.. For L/S ratios above the optimal one, the excessive presence of water decreased the ionic strength of the solution and created a mass transfer barrier that slowed both the leaching of  $\text{Ca}^{2+}$  and the mixing of  $\text{CO}_2$  with  $\text{Ca}^{2+}$  ions.

### **2.2.2. BOF slag**

The carbonation kinetics of this type of slag have been studied by several researchers using different types of reactors. More specifically, the kinetics of the slurry carbonation of BOF slag have been studied by Huijgen et al. [36] using a continuously-stirred autoclave reactor, by Chang et al. [37, 39, 112] using several types of reactors (column slurry reactor [37, 112], and high-gravity rotating packed bed [39]), by van Zomeren et al. [113] using column reactors, by Polettini et al. [114] and Baciocchi et al. [115] using a stirring pressurized stainless steel reactor, and by Tai et al. [20] using a continuously-stirred high-pressure batch reactor. The kinetics of the direct dry carbonation of BOF slag was tested by Santos et al. [38], who used

different experimental set-ups (thermogravimetric reactor, pressurized basket reactor, atmospheric furnace).

The impact of temperature, reaction time, CO<sub>2</sub> pressure, L/S ratio and particle size on carbonation conversion and kinetics was investigated in the aforementioned.

*Temperature:* up to a certain temperature, that is called optimal and was different in each study, the carbonation conversion extent and rate increased with increasing temperature. In the particular regime, the leaching of Ca<sup>2+</sup> from the solid BOF slag particles was the limiting factor of the carbonation conversion, with higher temperatures contributing to faster and more complete dissolution. Any further increase of temperature above the optimal value set in each study, resulted in a decrease in both the extent and rate of carbonation. At such temperatures, the reduced CO<sub>2</sub> solubility becomes the limiting factor of the carbonation process and leads to lower reaction rates and eventually to lower conversion extent. It also appears that at elevated temperatures conversion rate is not maintained at the same level throughout the process. This is mainly because carbonation occurs in two phases, in each of which different amounts of calcium are consumed for carbonation. In fact, under such conditions, the most of the calcium available in the solid particles of the slag is consumed during the initial stage of carbonation, when it rapidly dissolves into the solution and high rates of conversion are observed. However, this is not the case at the later stages of the reaction, during which, carbonation gets considerably slowed mainly due to the limited occurrence of calcium in the solids, the most of which has already been consumed in the first phase of carbonation.

Occasions where temperature does not have any particular effect on the BOF slags conversion extent or rate have also been reported in literature. For instance, Van Zomeren et al., [113] reports that under unsaturated conditions (L/S ratio = 0.01 - 0.1 L/kg), temperature increase did not result in any detectable effect on the carbonation of the tested BOF slag. This, however, can be due to the wet route of carbonation that was applied in this study and under such conditions temperature does not seem to significantly affect the conversion extent or rate of the reaction.

Several studies apply reaction temperatures that are below the point at which enhanced calcium leaching stops making up for lower CO<sub>2</sub> solubility (i.e., reaction

rate and conversion are still improving at the maximum temperature tested). Researchers do this in part to mitigate the energy demand of the process, which is important from the point of view of maximizing net CO<sub>2</sub> sequestration [1]. In such cases, the negative impact of increasing temperature above its optimal value is not reported. One such example is the recent study of Polettini et al. [114], where carbonation extent got continuously enhanced with increasing temperature (up to 100 °C). Huijgen et al. [36], using a similar experimental process, reported that the optimum temperature for the carbonation of BOF slags lies at approximately 175 °C.

*Reaction time:* the way that the extent and rate of BOF slag carbonation was affected by the treatment period was similar for every case studied. Initially, the carbonation extent increased with decreasing rate, and levelled off afterwards. The length of this initial period differed from study to study, ranging from 5 minutes [39] to 24 h [112], and it was mainly dependent on the experimental process and the other parameters of carbonation (temperature, CO<sub>2</sub> pressure, etc.). This behavior is mainly attributed to the pore blockage of the slag particles caused by the precipitation of the newly formed calcite. The precipitated CaCO<sub>3</sub> forms barriers that hinder the diffusion of the Ca<sup>2+</sup> ions from the solid slag particle to the solution [116]. In some cases, mineralogy also limits the ultimate reaction extent [117].

*Particle size:* one of the parameters that have been found to significantly affect the carbonation extent of BOF slag is its particle size. The impact of the BOF slag's particle size on the finally achieved conversion extent has been investigated by Huijgen et al. [36] and Santos et al. [38]. In both cases, the reduction of BOF slag's particle size led to the notable increase of the specific surface area of the treated material, which caused the significant enhancement of the finally achieved carbonation conversion.

In particular, Huijgen et al. [36] tested the influence of BOF slag's particle on the carbonation conversion achieved following the slurry route of carbonation. According to their findings, by reducing the particle size from <1 mm to <38 μm the conversion extent increased from 24 % to 74 %. Similar results were exerted by Santos et al. [38] who studied the direct dry carbonation of BOF slag using a pressurized basket reactor

As in the work of Huijgen et al. [36], they also identified a critical dependence of the carbonation conversion on the particle size of the treated BOF slag. In fact, they found that by reducing the particle size from <1.6 mm to <0.08 mm, the conversion of free lime to CaCO<sub>3</sub> conversion extent was increased from 8 % to 43 %.

*CO<sub>2</sub> pressure:* Huijgen et al. [36], Santos et al. [38], and Polettini et al. [114] investigated the effect of CO<sub>2</sub> pressure on the carbonation of BOF slag. According to Huijgen et al. [36] the impact of CO<sub>2</sub> partial pressure on the rate and extent of the conversion achieved by the slurry carbonation of BOF slag was highly dependent on the applied temperature. They reported that for temperatures below the optimal, stirring speed of more than 500 rpm and CO<sub>2</sub> pressure above 90 bar, the effect of CO<sub>2</sub> partial pressure on the finally achieved carbonation conversion was negligible. This further supports the previous findings of this review that present the Ca<sup>2+</sup> leaching as the limiting factor of carbonation at such temperatures. On the other hand, when lower CO<sub>2</sub> pressures and stirring speeds were tested, the conversion extent decreased, respectively, due to limited dissolution of CO<sub>2</sub> into the solution and low quality of mixing between the different phases.

The influence of CO<sub>2</sub> partial pressure on the CO<sub>2</sub> uptake as a function of temperature was investigated by Santos et al. [38], who worked on the direct dry carbonation of BOF slag. The authors found that the effect of increasing CO<sub>2</sub> pressure on the finally achieved carbonation conversion was highly dependent on the applied reaction temperature. According to their findings, CO<sub>2</sub> pressure increase resulted in significant CO<sub>2</sub> uptake enhancement (+176 % at 20 bar over 4 bar) only at lower temperatures (350 °C). At higher temperatures (500 °C) the CO<sub>2</sub> uptake improvement caused by the increased CO<sub>2</sub> pressure was remarkably lower (+7 % at 20 bar over 4 bar), whereas when even higher temperatures were applied to the system (650 °C) no improvement was detectable.

A different approach to the effect of CO<sub>2</sub> pressure on the carbonation extent of BOF slag was attempted by Polettini et al. [114]. They examined the influence of CO<sub>2</sub> pressure on the carbonation extent in correlation with the CO<sub>2</sub> concentration in the gas phase. In fact, three different CO<sub>2</sub> concentrations were studied in this work, namely 10 %, 40 % and 100 %. Based on the exerted results, for the two lower CO<sub>2</sub> concentrations tested, the impact of CO<sub>2</sub> partial pressure on the conversion was

most relevant for pressures up to 6 bar. For higher pressures, the CO<sub>2</sub> uptake levelled off. Furthermore, when pure CO<sub>2</sub> gas was tested, the influence of the CO<sub>2</sub> pressure on the carbonation yield was remarkably lower.

In general, by increasing the applied CO<sub>2</sub> partial pressure, the dissolution of CO<sub>2</sub> into the solution also gets increased. As it happens with other process parameters reviewed in this section, there is an optimum value of CO<sub>2</sub> pressure up to which any CO<sub>2</sub> pressure increase leads to carbonation conversion enhancement. However, for any further CO<sub>2</sub> pressure increase above this value the finally achieved carbonation extent of the treated material gets decreased. This should be mainly attributed to the fact that when CO<sub>2</sub> pressures higher than the optimum one are applied to the system, mechanisms of carbonation other than the CO<sub>2</sub> dissolution become the limiting ones. Such mechanisms could be the pH conditions that are created at such high pressures that may be unfavorable for further carbonation, or the faster formation of passivating layers around the particles, as a result of the accelerated precipitation of carbonates and silicates at higher CO<sub>2</sub> pressures, that hinders the further carbonation of the slag.

*Liquid-to-solid ratio:* the influence of L/S ratio on the carbonation conversion of BOF slag under slurry conditions was studied by Chang et al. [112], van Zomeren et al. [113] and Baciocchi et al. [115]. Chang et al. [112] investigated the effect of L/S ratio on the slurry carbonation of BOF slag and found the optimal value at 20 L/kg. For both lower and higher values than the optimal, the conversion extent decreased. For L/S ratios lower than 20 L/kg, the slurry did not mix well in the reactor and poor mass transfer was caused, whereas when L/S ratios above the optimal were tested, the excess liquid in the slurry resulted to a lower ionic strength of the solution. In both cases, the finally achieved carbonation conversion was lower than that achieved at the optimal L/S ratio.

In the works of van Zomeren et al. [113] and Baciocchi et al. [115] two different L/S ratio regimes were studied: one with lower L/S ratio (0.1 L/kg and 0.3 L/kg, respectively) and another with higher L/S ratio (2 L/kg and 5 L/kg, respectively). In both cases, the elevated L/S ratios led to increased CO<sub>2</sub> uptakes. By combining saturation conditions with mechanical mixing, the mass transfer between reacting

phases is assisted, with additional liquid allowing higher amounts of  $\text{CO}_2$  and  $\text{Ca}^{2+}$  to be in solution at a given time, accelerating the reaction.

*CO<sub>2</sub> Concentration:* the effect of  $\text{CO}_2$  concentration on the BOF slag carbonation extent was examined by Polettini et al. [114] and Baciocchi et al. [115]. In both works three different  $\text{CO}_2$  concentrations (10 %, 40 % and 100 %) were examined for their impact on the extent of BOF slag conversion. Polettini et al. [114] studied the slurry carbonation of the slag and concluded that compared to temperature and total pressure, the percentage of gaseous  $\text{CO}_2$  in the employed gas had a marginal effect on the carbonation conversion finally achieved. In particular, it was found that the diluted gas once pressurized (up to 10 bar tested) yielded results comparable to those achieved by pure  $\text{CO}_2$ . The influence of  $\text{CO}_2$  concentration on the finally achieved conversion of the slag was notable only at low total pressures (1 bar), where higher  $\text{CO}_2$  concentrations resulted in higher  $\text{CO}_2$  uptakes. Baciocchi et al. [115] tested both the wet and slurry routes of BOF slag carbonation. According to their findings, for both routes, the employment of gases with higher concentrations of  $\text{CO}_2$ , at fixed total pressure, resulted in remarkably greater  $\text{CO}_2$  uptakes, especially when comparing 10% to higher concentrations. The authors did not address the particularly low conversions achieved at 10%, which are at odds with the results of Polettini et al. [114].

*CO<sub>2</sub> flow rate:* Chang et al. [37, 112] worked on the slurry carbonation of BOF slag using a bubbling column where the slag circulated in the fluidized regime. Among other parameters, the authors of the particular studies also examined the influence of  $\text{CO}_2$  flow rate on the carbonation of the slag. Based on the results exerted by both of these works, it could be inferred that in both of the studies, there was a trend of conversion extent decrease with increasing flow rate. The authors attributed this behavior to the poor gas-liquid mass transfer caused by the channeling effects occurring in the slurry reactor at high gas flow rates. Therefore, it should be concluded that when such a reactor is used, the flow rate at which the  $\text{CO}_2$ -containing gas should be introduced to the system has to be limited to that which supports satisfactory fluidization, but no higher. This, however, is not the case when pressurized reactors are used. In pressurized reactors, the flow rate at which  $\text{CO}_2$  is

inserted to the reactor is not an issue, as long as CO<sub>2</sub> is continually supplied to maintain the required partial pressure.

*Slurry flow rate:* Chang et al. [39] studied the slurry carbonation of BOF slag using a rotating packed bed reactor. The slurry flow rate and its impact on the carbonation conversion of the slag was investigated in this work. According to the findings, there is an optimal value of slurry flow rate (1.2 L/min in this case) at which the maximum carbonation conversion is achieved. By increasing the flow rate at which the slurry was introduced to the reactor up to the particular value, the conversion rate and extent of the BOF slag was also increased, as a result of the increased radial velocity of the slurry particles and the subsequent improvement of both the slurry-gas phase mass transfer, and the micro-mixing within the slurry. On the other hand, at slurry flow rates above the optimal one the finally achieved carbonation extent was found to decrease, mainly due to the limited residence time of the slurry in the packed zone of the reactor.

*Stirring/rotation speed:* the way that stirring and rotation speed affect the slurry carbonation of BOF slag was respectively studied by Huijgen et al. [36] and Chang et al. [39]. It was found that by increasing the mixing/rotation speed, the mass transfer between the CO<sub>2</sub> and the slurry, as well as the diffusion of Ca<sup>2+</sup> ions from the slag particles into the solution were notably improved. As with the most parameters reviewed in this section, there was an optimum mixing speed (500 rpm for the reactor used by Huijgen et al. [36] and 1000 rpm for the reactor used by Chang et al. [39]), up to which any rotation speed enhancement led to a notable slag carbonation conversion increase. By further increasing the speed of mixing over the optimal values, the carbonation conversion got either decreased, due to the limited residence period of the mixing material in the packing zone of the reactor [39], or did not present any statistically appreciable improvement [36]. It should be noted, however, that above a certain mixing rate, particle abrasion may assist the carbonation rate and extent of the treated material [39], but the improvement of CO<sub>2</sub> sequestration resulting by that may not be worth the increased energy expenditure and processing cost [1].

*Slurry volume and steam addition:* in addition to the above parameters, the influence of slurry volume and steam addition on the carbonation conversion of BOF slag was

also tested. In particular Chang et al. [112] studied the effect of slurry volume on the carbonation of BOF slag using a bubbling fluidized column and Santos et al. [38] investigated the manner in which steam addition affected the direct dry carbonation of the same material. Chang et al. [112] discovered that by increasing the slurry volume up to an optimum value (350 mL) while keeping the L/S ratio and gas flow rate fixed, the conversion also got increased. The authors explained the particular behavior based on the increased retention time of CO<sub>2</sub> (which was continuously supplied and removed) in the reactor, caused by the higher volume of slurry employed to the process. However, at higher slurry volumes, the finally achieved BOF slag conversion was decreased. By keeping the gas flow rate of the system constant, the mixing of the liquid and the solid phase became poorer when the slurry volume was increased over the optimal value (i.e., fluidization was less effective) and normally lower conversions were achieved.

The addition of steam during the dry carbonation of BOF slag was found to positively affect the CO<sub>2</sub> uptake for all particle sizes tested by Santos et al. [38], with the larger sizes however, being less influenced by it. This positive effect of steam addition on the carbonation conversion of the slag could be related to a catalytic or mass transfer effect. However, the exact mechanism that leads to this behavior has not been fully understood. The most convincing theory is that the addition of steam to the process improves the solid state diffusion of the CO<sub>2</sub> into the solid particles. To enlighten the exact mechanism that leads to this CO<sub>2</sub> solid state diffusion improvement further research is required.

### **2.2.3. EAF and stainless steel slags**

On some occasions, stainless steel slag is considered as a mixture of EAF slag and AOD slag generated during the synthesis of alloy steel. Baciocchi et al. [63, 65] studied the wet and slurry carbonation of the EAF slag and the wet carbonation of SS slag. The effects of temperature, reaction time, CO<sub>2</sub> pressure, L/S ratio and particle size on the carbonation conversion of the particular types of slag were investigated in these studies and the results are reported next.

*Temperature:* Baciocchi et al. [65] studied the influence of temperature on the wet carbonation of EAF and SS slags. For both these types of slag, reaction temperature

increase was found leading to CO<sub>2</sub> uptake escalation that was attributed to the enhanced dissolution of the silicates. However, the highest temperature tested in the particular work was limited to 50 °C, and the carbonation behavior towards higher temperatures was not appraised.

*Particle size:* similarly to the cases of BF [111] and BOF slags [20, 36, 37, 38, 39, 112] the milling of EAF and SS slag particles led to significant improvement of the finally achieved carbonation conversion. This behavior was attributed to the increased specific surface area of the milled material that enhanced its ability for carbonation.

*Reaction time:* the way that carbonation duration affected the wet carbonation of both the tested slags was also studied by Baciocchi et al. [63, 65]. Based on the exerted results, it could be said that after an initial period during which the wet carbonation conversion of both the EAF and SS slags was increased with decreasing rate, it leveled off. This finding is in consistence with what has already been reported in previous studies regarding the effect of reaction period on the carbonation of BF and BOF slags. This behavior is mainly attributed to the precipitation of the newly formed CaCO<sub>3</sub> which blocks the pores of the slag particles and inhibits the diffusion of the silicates from them to the solution, hindering the further carbonation of the material.

*Liquid-to-solid ratio:* the effect of L/S ratio ratio on the wet carbonation conversion of the EAF and AOD slag mixture was investigated by Baciocchi et al. [65]. According to the results, the optimal L/S ratio was equal to 0.4 L/kg, whereas for both lower and higher ratios than that, the conversion decreased. The authors justified this notably high for a wet carbonation process, optimal L/S ratio by commenting on the low content of hydrated lime in the tested slag. They suggested that differences between this and other studies could be attributed to the slag's composition lacking hydrated lime, which would increase the water required for the hydration of the oxide and silicate phases and the dissolution of CO<sub>2</sub> and Ca<sup>2+</sup> ions. The study with which Baciocchi et al. [63, 65] made the comparison was that of Johnson et al. [117], who studied the wet carbonation of EAF slag, and found the optimal L/S ratio equal to 0.125 L/kg. However, it should be noted, that the goal of Johnson et al. [117] was the optimization of the compressive strength of the formed carbonated compacts.

Consequently, the L/S ratio was mainly optimized in view of the physical characteristics of the post-carbonation compacts and not their maximal carbonation conversion.

*CO<sub>2</sub> pressure:* Baciocchi et al. [63, 65] reported that for a CO<sub>2</sub> pressure range between 1 and 10 bar, the effect of increased partial CO<sub>2</sub> pressure on the wet carbonation conversion of both the EAF and SS slags, was insignificant. Only in the case of the EAF slag and for reaction duration of less than an hour, was it found that the increase of CO<sub>2</sub> pressure from 1 to 3 bar generated a 43 % enhancement of the CO<sub>2</sub> uptake.

#### **2.2.4. AOD and CC slags**

Carbonation of AOD and CC slags has been studied by Baciocchi et al. [65] using a pressurized stainless steel reactor, Vandeveld [118] using a CO<sub>2</sub> incubator, Santos et al. [64, 66] using an ultrasound-assisted beaker, a CO<sub>2</sub> incubator and an autoclave reactor, and Van Bouwel [120] using an autoclave reactor. The influence of temperature, reaction time, CO<sub>2</sub> pressure, L/S ratio, particle size and sonication on carbonation conversion rate and extent of AOD and CC slags was investigated in these studies and the findings are reported next.

*Temperature:* the effect of reaction temperature on the wet and slurry carbonation of AOD and CC slags was studied by Vandeveld [118] and Van Bouwel [120], respectively. Vandeveld [118] tested two different temperatures, namely 30 °C and 50 °C, and found that for the first hour of reaction, the application of the lower temperature led to higher CO<sub>2</sub> uptakes than the higher one; for carbonation periods exceeding 6 hours, however, the effect of temperature on the finally achieved carbonation conversion was insignificant. The author suggested that at low CO<sub>2</sub> pressures, the lower temperature favored the solubility of CO<sub>2</sub> in the liquid film and facilitated the transportation of CO<sub>2</sub> to the reaction zone within the paste, during the first stages of carbonation, before a passivating layer formed in the later stages, restricting access to the reaction front. Van Bouwel [120] tested a wider range of temperatures (between 30 °C and 180 °C), under pressurized conditions. The author discovered that the increased temperature affected the carbonation conversion of AOD and CC slags in a similar way to that observed during the carbonation of the

BF, BOF and EAF slags, except for different optimal temperature. The optimal temperature for both AOD and CC slags was 60 °C. For temperatures higher than the optimal, the reaction rate leveled off and the conversion extent remained the same (~60%). Mainly consisting of calcium silicates [66], AOD and CC slags are characterized by a more amenable mineralogy compared to BF, BOF and EAF slags, that appears to make them more susceptible to carbonation at more moderate processing conditions [1].

*Reaction Time:* the effect of reaction time on the carbonation conversion of AOD and CC slags was tested by Santos et al. [64, 66], Vandeveldel [118] and Van Bouwel [120]. All of them reported a similar influence of carbonation duration on the conversion of AOD and CC slags, regardless of the carbonation route followed in each case. In particular, the carbonation extent of both the tested slags was found to increase with time, until it leveled off before reaction completion (based on chemical composition). The carbonation rate on the other hand, after an initial rapid period, was found to decrease with time. This behavior is consistent with what has been already reported regarding the effect of carbonation duration on the finally achieved CO<sub>2</sub> uptakes of BF, BOF and EAF slags.

*CO<sub>2</sub> Pressure:* the way that CO<sub>2</sub> partial pressure affects the carbonation of AOD and CC slags was studied by Baciocchi et al. [65], Santos et al. [66], and Van Bouwel [120]. Based on the results exerted by these studies, AOD and CC slags were found to behave differently towards increasing CO<sub>2</sub> partial pressure. Van Bouwel [120] reported that up to 12 bar, CO<sub>2</sub> pressure increase did not have any significant influence on the carbonation of AOD slag. However, when CO<sub>2</sub> pressure was further increased (up to 30 bar) a steep increase of carbonation conversion was observed. The effect of CO<sub>2</sub> pressure on the conversion of CC slag was remarkably different. In fact, at lower CO<sub>2</sub> pressures, the carbonation conversion of CC slag was high. By increasing the pressure up to 20 bar, the conversion extent dropped and increased again when even higher CO<sub>2</sub> pressures (up to 30 bar) were applied to the system. Slightly different trends were reported by Santos et al. [66], who found that by increasing the CO<sub>2</sub> pressure, the carbonation conversion also got increased and peaked at 20 bar. Further increase of the pressure did not seem to notably affect the carbonation of the material. CC slag on the other hand, displayed a different

behavior towards CO<sub>2</sub> pressure increase. According to the findings of Sanos et al. [66], an increase of the partial CO<sub>2</sub> pressure up to 9 bar led to a conversion enhancement of CC slag. By further increasing the pressure to 13 bar, the conversion extent dropped and raised again when higher CO<sub>2</sub> pressures (up to 30 bar) were applied.

Baciocchi et al. [65], who studied the wet carbonation of AOD slag, examined the effect of CO<sub>2</sub> partial pressure on the carbonation conversion of AOD slag, as a function of reaction time. According to their findings, the influence of the increasing CO<sub>2</sub> partial pressure became more evident after the initial period of carbonation (2 h). This is in accordance with the findings discussed earlier regarding the other types of slag. The CO<sub>2</sub> pressure increase facilitates the diffusion of CO<sub>2</sub> through the passivating layers (precipitated carbonate and residual silica) that are formed and developed (thicken) during carbonation [64].

*L/S ratio:* Vandeveld [118] studied the effect of L/S ratio on the wet carbonation of AOD and CC slags, whereas Santos et al. [66] and Van Bouwel et al. [120] investigated the influence of the same parameter on the slurry carbonation of the particular slags. . For both the tested slags and regardless of the applied route of carbonation (wet or slurry), each of these studies concluded that there was an optimal value for the L/S ratio, up to which any increase of the liquid amount employed in the process resulted into carbonation conversion increase. For solids loading values below the optimal one (i.e., L/S ratio higher than the optimal), a mass transfer barrier was created in the wet (thin-film) systems and particle attrition was reduced in agitated slurry systems. For solids loading values above the optimal (i.e., L/S ratio lower than the optimal), the slurry did not mix well in the reactor, causing poor contact between the reacting particles and the carbonic acid solution. In both cases the resulting carbonation conversions were below the ones corresponding to the optimal L/S ratios, which were different in each study. This behavior is consistent with the findings of the previously reported works which also examined the effect of L/S ratio on the wet and slurry carbonation of BF, BOF and EAF slags.

*Sonication:* in the study of Santos et al. [64] ultrasound-assisted carbonation experiments were performed, in order to discover the manner in which it could

intensify the conversion of the slags. Based on the results exerted by this study, it is obvious that ultrasound usage significantly assisted the carbonation process and led to notably higher conversions of both AOD and CC slags. According to the authors, sonication employment in the carbonation experiments caused the enhanced solid-liquid-gas mixing and the better dissolution of  $\text{CO}_2$  into the solution, both resulting to notably enhanced carbonation conversions. Moreover, sonication also caused the removal of the passivating layers that are formed during carbonation and surround the unreacted inner part of the slag particles, further intensifying the reaction rate and sustaining the reaction until higher levels of carbonation conversions were achieved. In addition, sonication also induced the breakage of slag particles themselves, leading to higher specific surface area of the reacting material, and thus to improved reactivity with  $\text{CO}_2$ .

*Mineralogy:* by observing the results of all the studies reported in this section, it becomes clear that under similar conditions, the conversions achieved by CC slags were notably higher than those of AOD slags. This should be attributed to the mineralogy of the AOD and CC slags. CC slags present a more favorable mineralogy for carbonation than AOD slags [64]. In particular, CC slags contain considerably higher amounts of gamma-dicalcium-silicate ( $\gamma\text{-C}_2\text{S}$ ) than AOD slags, which in turn are richer in  $\beta\text{-C}_2\text{S}$ . Chang et al. [121] recently proposed, based on nuclear magnetic resonance studies, that the structural environment of silicon in  $\gamma\text{-C}_2\text{S}$  leads to easier protonation of  $\text{SiO}_4^{4-}$  groups (and thus easier decalcification), based on the predominant monomeric structure ( $\text{Q}_0$ ) of silica in the carbonated mineral.

### **2.2.5. Waelz slag**

Waelz process is a steel refining process, according to which, zinc is recovered, mainly from EAF slag, by using a rotary kiln. The byproduct that is left after the recovery of zinc is called Waelz slag. Cappai et al. [122] studied the effect of three parameters, namely reaction time,  $\text{CO}_2$  partial pressure, and L/S ratio on the carbonation conversion extent and rate of Waelz slags,

under constant temperature (25 °C). The results of this study are reported below.

*Reaction time:* as reported for the other types of slag reviewed in this section, the carbonation conversion extent of Waelz slag was found to increase with decreasing rate, as the reaction duration increased. In particular, the maximum conversion was achieved after the longer treatment period tested in the study (240 h) [122].

*CO<sub>2</sub> pressure:* Cappai et al. [122] showed that in general, carbonation conversion was enhanced with increasing CO<sub>2</sub> pressure. This carbonation conversion extent improvement was more evident after the initial stages of carbonation and in particular, after the first 24 hours of reaction. For shorter reaction times, the employment of higher CO<sub>2</sub> pressures to the system was not found to appreciably affect the conversion of the tested slag. Conversely, the influence of CO<sub>2</sub> pressure on finally achieved carbonation conversion became more evident after the initial stages of carbonation during which the passivating layers were formed around the reacting particles. Higher CO<sub>2</sub> pressures have been found to substantially facilitate the diffusion of alkaline elements through these layers and their reaction with the dissolved CO<sub>2</sub>.

*L/S ratio:* the L/S ratio applied in the carbonation of Waelz slag strongly influenced its kinetics [122]. As expected, at L/S = 0, the kinetics were very slow, due to the absence of water (only the moisture of the solid particles was available for the reaction). As already mentioned, hydration aids in the mobility, and thus reactivity of ions within the solid minerals. The gradual increase of the L/S ratio up to 1 L/kg, however, led to remarkably faster carbonation rates and notably higher carbonation conversions, indicating a positive effect of increasing L/S ratio on the carbonation rate and extent of Waelz slags.

## 2.2.6. Conclusions

Iron- and steel-manufacturing slags are characterized by a remarkable ability to fix CO<sub>2</sub> by forming carbonate minerals that can permanently remain stable,

from a thermodynamic aspect. Although they are incapable of sequestering a notable fraction of anthropogenic CO<sub>2</sub> emissions (due to relatively limited availability of the material), iron- and steel-making slags have the ability to store substantial quantities of CO<sub>2</sub> emitted by the iron- and steel-manufacturing industries. The way that several operational parameters affect the carbonation conversion rate and extent of iron- and steel-making slags has been thoroughly examined in this section. Despite the variation in the slag types examined, and consequently composition and morphology, and the carbonation process employed in different studies, general trends regarding the influence of each operational parameter on the carbonation of these types of slags were obtained, and seen to be largely in agreement among the various studies reviewed.

The influence of the four main experimental parameters on the carbonation of iron- and steel-making slags can be outlined as follows [1]:

Temperature: three different mechanisms compose the carbonation process: the dissolution of CO<sub>2</sub> into the aqueous solution, the diffusion of Ca<sup>2+</sup> from the solid particle, and the carbonate nucleation. Each mechanism exhibits a different behavior towards temperature alterations. Temperature increase enhances Ca<sup>2+</sup> leaching from the solid matrix, but decreases CO<sub>2</sub> dissolution. Consequently, there are two main regimes that describe the influence of temperature on carbonation conversion of iron- and steel-making slags. Up to an optimal value, temperature increase leads to a conversion rate and extent improvement, whereas any further increase of the reaction temperature over the particular value ultimately hinders the conversion.

Particle size: since direct mineral carbonation is a surface based reaction, any decrease in the slag's particle size leads to carbonation conversion enhancement.

Reaction time: the increase of the reaction time affects the carbonation rate and extent in different ways. As time passes, the conversion extent improves but the reaction rate decreases, due to particle passivation. Consequently, after a certain period, the carbonation conversion levels off as the formed

passivation layer covering the slag particles becomes impenetrable, or poorly reactive alkaline minerals do not respond to carbonation at the utilized process conditions.

Liquid-to-solid ratio: accelerated mineral carbonation is highly dependent on the applied L/S ratio, with too high or too low values of it being detrimental to its efficiency; dry-out conditions inhibit reactivity, while dilute conditions diminish abrasion among particles in mixed systems, and enlarge diffusion boundary layers in stationary systems. The optimization of L/S ratio must be based on the type of the material that is subjected to carbonation and the type of carbonation process that is followed in each case.

### **2.3. Carbonation Weathering Rate (CWR): Conceptualization and application**

Although the accelerated mineral carbonation of iron- and steel-making slags has been thoroughly studied in literature, the comparison of the carbonation conversion rate and extent reported by different studies has been proven challenging. This is mainly due to the nature of the carbonation process which, under most conditions, is a solid-state-diffusion-limited process and the fact that different researchers use slags of different particle sizes, and thus different specific surface areas. Apparently, the maximal achievable conversion, as well as the carbonation rate are both significantly affected by the specific surface area of the slag used. In order to directly compare the results obtained from different studies, the CWR is conceptualized. “The rate is expressed in units of  $\mu\text{m}\cdot\text{min}^{-1}$ , and represents the weathering rate of the particle radius from the original outer radius to the final radius of the unreacted core of the carbonated particle” [1].

The CWR only tracks the location of the reacted/unreacted interface within the particle, and does not account for the changing size of particles due to the accumulation of precipitated carbonates on the particle. This implies that the outer edge of the particle is not tracked and the length unit of CWR relates to the original average radius of the particle. CWR also assumes that all particles are spherical and that all reactive minerals carbonate at similar rates. The first assumption is supported by research: the study of Bodor et al. [123],

who after synthesizing several alkaline minerals that can be found in the composition of iron- and steel-making slags, they carbonated them and found out that for the most of them, the carbonation kinetics and extent differ but not substantially. The second assumption is in principle not as accurate, since the aspect ratio of iron- and steel-making slag particles is sometimes relatively high [64]. However, since the average particle size is typically determined by laser diffraction, a method that does not distinguish particle shapes [124], the values used in the calculation of the CWR are already assumed to represent spherical particles.

One limitation of the CWR that has to be noted is that it does not differentiate for particle size or porosity changes, meaning that if, for instance, a material is mechanically activated to improve carbonation, CWR will not be capable of describing this carbonation enhancement, since it does not respond to either particle size reduction or particle porosity enhancement [1]. Another aspect to bear in mind is that the CWR can either represent the average carbonation weathering rate over the duration of carbonation, or it can be taken as an instantaneous snapshot at any point in time during the carbonation process. Due to the nature of the shrinking core model on which the conceptualization of CWR was based, it would be expected that the CWR would be greater initially, and reduce as time passes. If a carbonation process mainly aims to CO<sub>2</sub> storage and mineral acquisition and handling costs are low, it can, in principle, operate near peak-CWR. On the other hand, if the valorization of the treated material is also a goal of the process, the carbonation process should be designed to operate at lower overall CWR by prolonging the processing duration, to achieve the production of a material with the required final properties for commercialization or safe disposal.

The first step towards CWR calculation is to obtain the average radius of the unreacted core of mineral particles ( $R$ ). This is achieved by using Equation (2-1) that describes the average particle conversion degree ( $C\%$ ), for  $C\% \leq 100\%$  [1]. The value of  $C\%$  is typically experimentally obtained by researchers via thermogravimetric analysis or quantitative X-ray crystallography.

$$C\% = \frac{\frac{4}{3}\pi r_x^3 - \frac{4}{3}\pi R^3}{\frac{4}{3}\pi r_x^3} \cdot 100\% = \frac{r_x^3 - R^3}{r_x^3} \cdot 100\% \quad (2-1)$$

Based on the aforementioned assumptions, Figure 2-1 depicts a partially carbonated mineral particle. Based on this theoretical illustration,  $r_x$  is the original average particle radius,  $R$  is the average radius of the unreacted core of the particle, and  $t_{carb}$  is the thickness of the carbonated shell of the particle.. It should be noted that in case that the particle size distribution of a sample is known, it is possible to apply this equation to each particle size fraction and solve for a single value of  $R$ ; the particle with a radius ( $r_x$ ) equal to  $R$  ( $r_x = R$ ) would be the largest particle that carbonates fully (within the bounds of the assumptions made) [125].

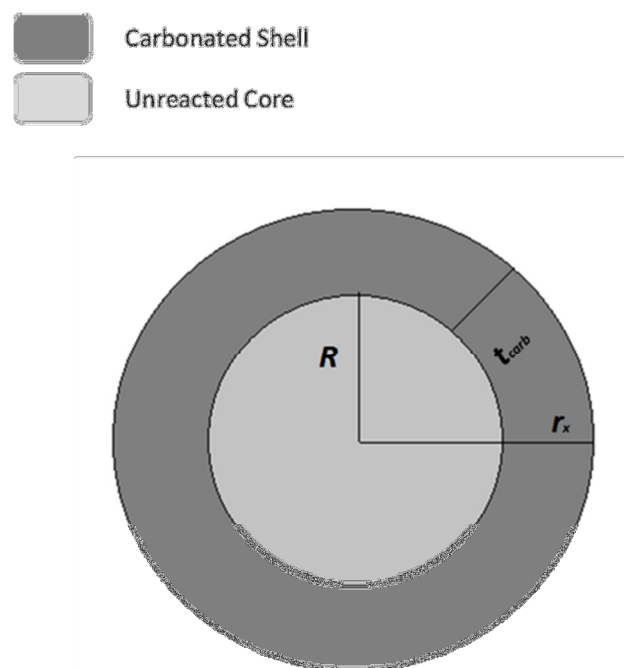


**Figure 2-1. Theoretical illustration of a partially carbonated mineral particle [1].**

From the illustration in Figure 2-1 it is clear that  $R = (r_x - t_{carb})$ . Based on this and the Equation (2-1), it is possible to calculate the value of  $t_{carb}$  by using the following solution [1]:

$$t_{carb} = r_x \cdot \left(1 - \sqrt[3]{1 - C\%/100\%}\right) \quad (2-2)$$

According to Equation (2-2), if the conversion is complete ( $C\% = 100\%$ ), then  $t_{carb}$  will be equal to  $r_x$ , as the whole particle becomes a carbonate sphere. If the conversion is half ( $C\% = 50\%$ ), then  $t_{carb}$  will be 20.6% of  $r_x$ , since the radius of a sphere half the volume of a larger sphere is 79.4% of the larger sphere's radius [1]. By knowing the  $t_{carb}$  for a given  $C\%$ , and the reaction time ( $\tau_{react}$ ) required to achieve the particular  $C\%$ , it is possible to calculate the CWR (Equation (2-3)), which is essentially the  $t_{carb}$  normalized per unit time [1]:

$$CWR = \frac{t_{carb}}{\tau_{react}} = \frac{r_x \cdot \left(1 - \sqrt[3]{1 - C\%/100\%}\right)}{\tau_{react}} \quad (2-3)$$

By applying Equation (2-3) to the conversions achieved by the studies that have been reviewed in this paper, Table A-3 (Appendix A) was created. In several of the reviewed studies the size of the slag particles is referred to as a range instead of a specific average mean diameter. In those cases, an arithmetic average of the range was taken as the mean diameter. The calculated CWRs of the reported studies on BOF, AOD, and CC slags are reported in Figures 2, 3, and 4, respectively, in chronological order, whereas Figure 5 depicts the CWRs of studies on SS, EAF, BF, and Waelz slags.

Apparently, the highest carbonation conversions do not necessarily correspond to the highest CWRs. In fact, the distribution of CWR values among the different studies is remarkably different to that of the corresponding conversions. The highest CWR (0.618  $\mu\text{m}/\text{min}$ ) originates from the study of Chang et al. [39], who studied the carbonation of the BOF slag under mild conditions ( $T = 65\text{ }^\circ\text{C}$ ,  $p\text{CO}_2 = 1\text{ bar}$ , L/S ratio of 20 L/kg,  $\text{CO}_2$  flow rate equal to 1.2 L/min, and an average particle diameter of 62  $\mu\text{m}$ ). The particular work also achieved the highest reported iron- and steel-manufacturing slag carbonation conversion (93.5%). However, this is not the case for the rest of the studies. According to the calculated CWR values, the next most effective experimental studies are those of Huijgen et al. [36], followed by Tai et al. [20], who carbonated BOF and BF steelmaking slag, respectively. In particular, the setups used in these works resulted in CWR values equal to 0.229  $\mu\text{m}/\text{min}$  and 0.188  $\mu\text{m}/\text{min}$ , respectively. However, the

conversion extents achieved by these studies were remarkably lower in comparison with others reported in this section. This should be mainly attributed to either the too large particles that may have been used during experimentation and were incapable of inducing high levels of conversion, or to the short carbonation durations that may have been applied in these works and were insufficient to allow high conversions to be reached. In addition, the carbonation kinetics, and thus the level of conversion achieved by different slags is also affected by differences in their mineralogy (some minerals are more reactive than others) or their morphology (some slags are more or less porous, or become more or less porous during reaction).

CWR values are most applicable when results obtained for the same type of iron- or steel-making slag are compared. In this case, the only barrier to the effective comparison among conversions resulting from different studies, are the particle size and the reaction time. For the BOF slags (Figure 2-2), it is shown that the CWR achieved by Chang et al. [39] is clearly the highest, followed by Huijgen et al. [36] (0.229  $\mu\text{m}/\text{min}$ ) and Santos et al. [64] (0.184  $\mu\text{m}/\text{min}$ ). In the case of AOD and CC slags (Figures 2-3 and 2-4), the CWRs resulting from the work of Van Bouwel [120] are the highest for both of these types of slag, with 0.108 and 0.124  $\mu\text{m}/\text{min}$ , respectively. As in the carbonation conversion of the particular types of slag, the CWR values for CC are higher than those of AOD slag. Santos [125] points out that apart from mineralogy, the particle size difference between the two slags, which are naturally comminuted, can also explain the differences in carbonation rate and conversion. With the CWR value, these differences are innately considered.

It is worth to mention the EAF slag study conducted by Baciocchi et al. [63]. It is one of the few cases in literature where wet (thin-film) carbonation of a particular slag appears leading to higher conversion extent than the slurry route of the same material. However, after applying the CWR to the conversions resulting from both of the carbonation routes investigated in this work, it becomes clear that the weathering rate at which carbonation proceeds to the interior of the slag particles following the wet route of carbonation is remarkably lower than that corresponding to the slurry route (0.010  $\mu\text{m}/\text{min}$  for

wet carbonation, versus 0.046  $\mu\text{m}/\text{min}$  for slurry carbonation). This finding implies that the slurry route was the more time-efficient way for carbonation (Figure 2-5). In fact, the higher conversion that was achieved by the wet carbonation of EAF slag should be attributed to the longer period of carbonation (6 days vs. 6 hours) [1]. The particular example confirms “the usefulness of the CWR measure in delivering more accurate and insightful results as opposed to simple  $\text{CO}_2$  uptake or conversion extent, since the CWR takes the reaction period into consideration, in addition to the particle size” [1].

The average CWR of iron- and steel-making slags, as it was estimated based on the 17 studies covered in this review, was 0.08  $\mu\text{m}/\text{min}$ . This means that a slag particle 10  $\mu\text{m}$  in diameter requires, on average, roughly one hour to achieve full carbonation carbonate, whereas a slag particle 100  $\mu\text{m}$  in diameter fully carbonates in approximately 10 hours, disregarding mineralogical or morphological impediments and any intensification technique used (e.g., sonication [64] or mechanical attrition [39]) [1]. The particular estimation is useful for the industrialization of mineral carbonation as a means of  $\text{CO}_2$  sequestration. Based on that, process designers can have a reasonable idea of the sort of reactor scale required and logistics involved in storing  $\text{CO}_2$  from flue gas emissions, depending on the rate of emissions and sequestration target, and the level of comminution required to turn iron- or steel-making slag into a suitable carbon sink [1]. To accelerate mineral carbonation, process intensification techniques may be applied to it [64]. However, the extra processing costs and higher energy demand accompanying these techniques may not justify their application when the sole purpose of carbonation is  $\text{CO}_2$  sequestration [125], which requires a low-carbon-intensity process. Process intensification strategies become useful if the resulting CWR is augmented by one or more orders of magnitude [1]. In comparison with the aforementioned CWR average for iron and steel-making slags, only Chang et al. [39] managed to nearly achieve this, with a CWR of 0.62  $\mu\text{m}/\text{min}$  for BOF slag carbonation in a high-gravity rotating packed bed.

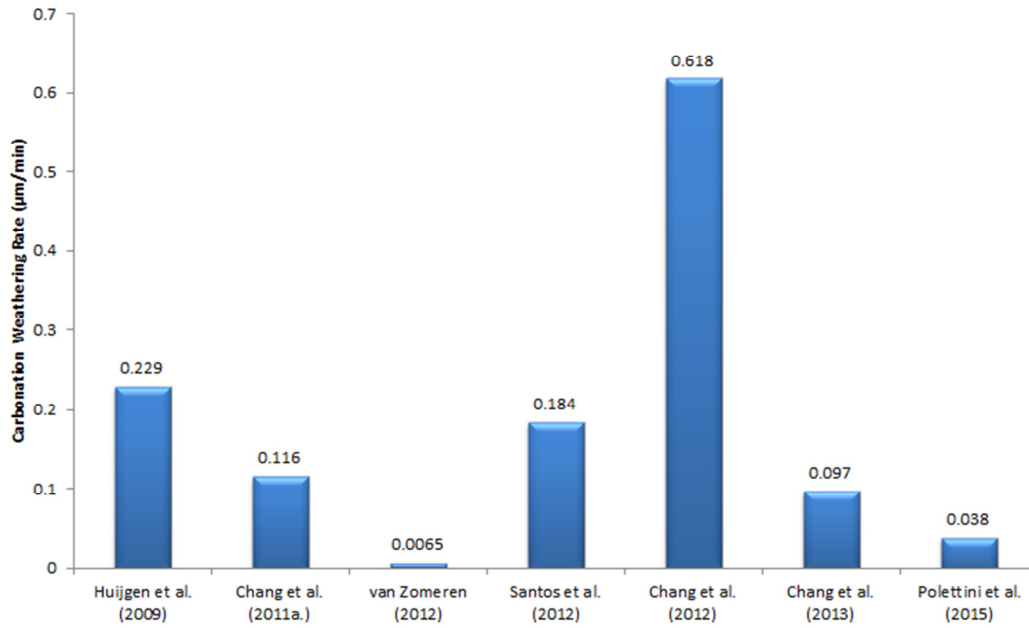


**Figure 2-2. Carbonation Weathering Rates as calculated for studies on BOF slag [1].**

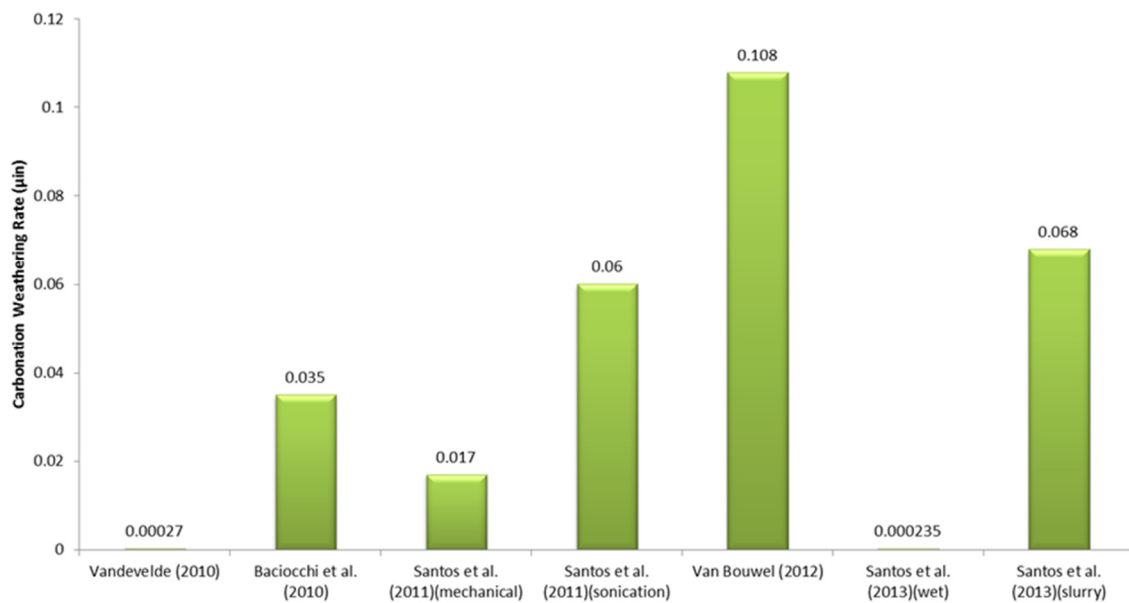


**Figure 2-3. Carbonation Weathering Rates as calculated for studies on AOD slag [1].**

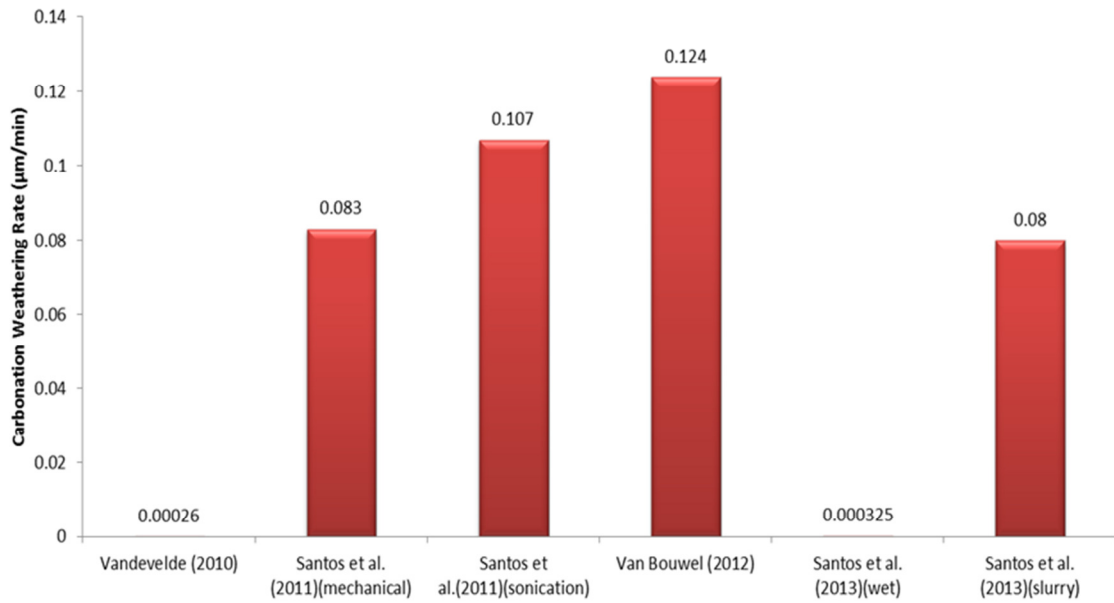


Figure 2-4. Carbonation Weathering Rates as calculated for studies on CC slag [1].

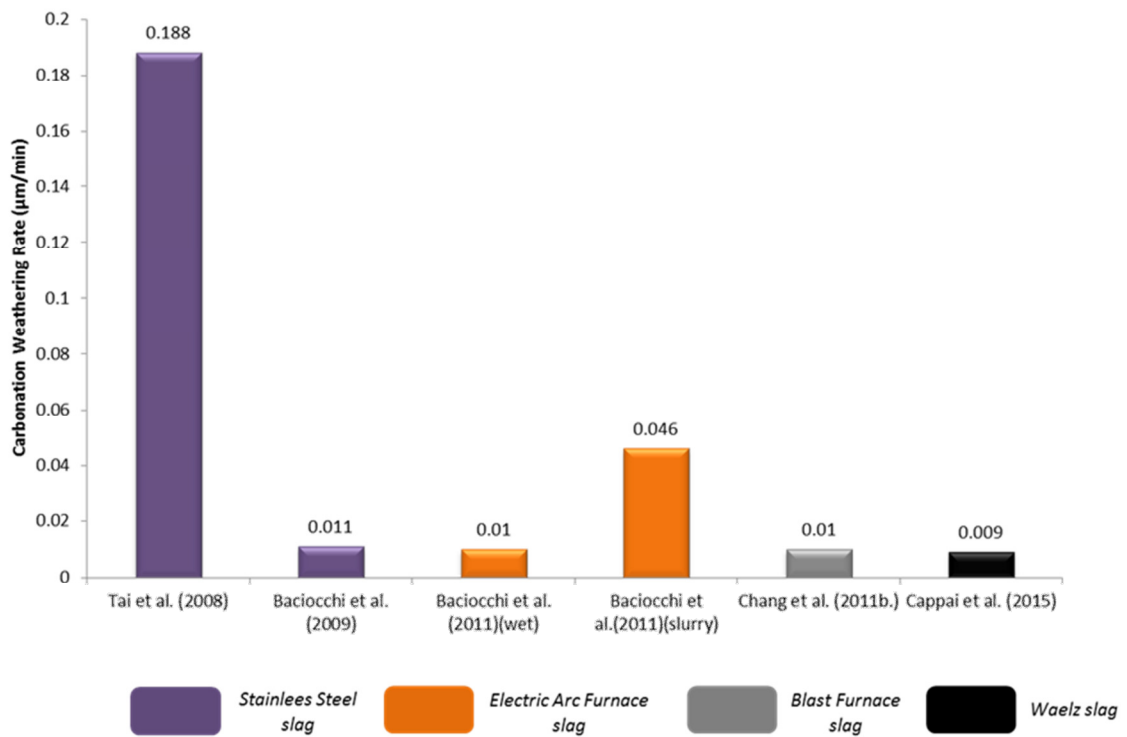


Figure 2-5. Carbonation Weathering Rates as calculated for studies on SS, EAF, BF, and Waelz slags [1].

## 2.4. Selection of the most suitable types of slag for investigation

Literature review findings, confirm that slags resulting from iron and steel-manufacturing processes are characterized by a remarkable ability to react with CO<sub>2</sub> and store it in a permanent way by converting it into a stable carbonate mineral. Therefore, it could be assumed that the accelerated carbonation of the particular types of industrial wastes could be an efficient method to considerably limit the CO<sub>2</sub> emissions generated by the corresponding industrial sectors. However, aside from the capability of the material to react with CO<sub>2</sub>, the production amount of each type of iron- and steel-making byproduct is also a significant factor affecting the extent of the finally achieved CO<sub>2</sub> sequestration and thereupon the mitigation level of the emitted CO<sub>2</sub>. Apparently, high experimental CO<sub>2</sub> uptakes combined with significant amounts of waste material production would result in larger amounts of sequestered CO<sub>2</sub>.

By comparing the production amounts of the different types of iron and steel slags as they were reported in section 2.1.5., it becomes clear that the two types with the higher productivity are BF and BOF slags.

As already discussed, BOF slag was found to present both the highest carbonation conversion and CWR value among the different types of slags tested in literature. A conversion comparable to those attributed to BOF slag was also achieved by the BF slag tested by Chang et al. [111]. However, the CWR value calculated for the particular experimental set up was not encouraging regarding the reactivity of the material. This should be mainly attributed to the remarkably long treatment duration of the material, which reached its maximum conversion (68.3 %) after 12 hours of reaction. However, by carefully observing the curve describing the effect of reaction time on the carbonation conversion of the slag in the particular study, it appeared that the greatest part of conversion (60 %) was achieved only after 2 hours of treatment. For the particular duration, the calculated CWR increased from 0.01 µm/min to 0.048 µm/min, indicating a higher reactivity of

the material towards CO<sub>2</sub>, however, still remarkably lower than that of BOF slag (0.618 μm/min)

Overall, among the several types of iron- and steel-manufacturing byproducts tested in literature, only BF and BOF slags manage to combine sufficient production amounts with promising carbonation capacities. The particular slags were selected to be investigated regarding their ability to store sufficient amounts of CO<sub>2</sub> by producing carbonates and/or other materials of commercial applicability, through carbonation and supplementary processes.

## **2.5. Literature review on the Valorization of carbonated BF and BOF slags**

Although carbonation of BF and BOF slags can be an efficient manner to reduce the CO<sub>2</sub> emissions generated by iron- and steel-making industries, the usefulness of the produced minerals is another challenge that has to be addressed. In fact, the possible commercial usability of the produced carbonates is of decisive importance for the economic feasibility of mineral carbonation and thereupon for the potential of the particular process to attract the interest of the industry and get efficiently scaled-up from lab and pilot scale to industrial-sized plants.

In this section literature on the valorization of BF and BOF slags through their mineral carbonation is reviewed. Only studies assessing the characteristics or the performance of the finally formed carbonates are included.

### **2.5.1. Valorization of carbonated BF slag**

Nowadays, a significantly large part of BF slag production is utilized either as natural aggregates in concrete mixtures [28, 80] or in cement industry, partially replacing traditional PC for the production of blended cement [29-32, 79]. Due to its proven technical efficiency in the particular uses and its stable value-add market, BF slag is not in need for new valorization methods. However, due to its high calcium content and respectful amounts of production, several researchers have subjected BF slag to mineral carbonation in order to evaluate their performance as carbon sinks but also to create products of profitable marketability.

Only limited work on the direct carbonation of BF slag has been done. In the few studies that have been found in literature investigating the direct mineral carbonation of BF slag, the potential of the produced carbonates for valorization was not assessed.

On the other hand, the indirect carbonation of BF slag as a manner to efficiently store sufficient amounts of CO<sub>2</sub> while synthesizing PCC of possibly high marketability has been investigated in several studies. In fact, Eloneva et al. [22], Mun and Cho [127], Chiang et al. [43], De Crom et al. [44] and Santos et al. [128] tested the effects of several experimental parameters on both the extent and selectivity of calcium extraction and assessed the qualities of the produced PCC.

Eloneva et al. [22], performed indirect carbonation experiments using BF slag as the starting material. The aim of the particular study was the sequestration of CO<sub>2</sub> and the concurrent formation of commercial grade PCC. The BF slag was dissolved in an acetic acid solution (20 vol%) employing an L/S ratio of 20 mL/g, at 70 °C and with 1 L N<sub>2</sub>/min (±0.2 l/min) bubbling through it, for 2 hours. After separating the leachate solution from the post-extraction BF slag, it was heated at 150 - 160 °C, in order for solid acetate salt to precipitate. To assess the effect of solution pH on the precipitation of calcium carbonate, the obtained solid acetate salt was dissolved in DI water at an L/S ratio of 20 mL/g and a stirring speed around 600 - 700 rpm. Nitrogen was introduced to the solution at a flow rate of 1L/min until the temperature of the solution was stabilized at 30 °C. After that, the nitrogen flow was switched off and that of CO<sub>2</sub> was switched on. After the stabilization of solution's pH and temperature, different amounts (0, 2, 5 and 20 ml) of NaOH (50 wt%) was added to it. The pH of the solution was allowed to stabilize and after that the flow of CO<sub>2</sub> was switched off. The resulting solution was filtered and the obtained solids were washed thoroughly to remove water-soluble compounds. Finally, the precipitate was dried at 120 °C, overnight. The effect of temperature on calcium carbonate precipitation was assessed by conducting similar experiments and adjusting the temperature of the solution at 50 and 70 °C. The particular tests were carried out with and without the addition of NaOH to

the solution. The impact of the elevated CO<sub>2</sub> pressure on the precipitation efficiency was assessed using a different experimental process. According to it, the solid acetate salt was mixed with distilled water at L/S of 10 mL/g and stirring speed of 1000 rpm. In the first experiment 5 ml of NaOH were added to the solution, whereas the second was performed without adding NaOH. The temperature of the solution was stabilized at 50 °C and then pure CO<sub>2</sub> was introduced to the reactor at 30 bar for 2 hours. After this period, the CO<sub>2</sub> pressure was lowered to 1 bar before its flow was switched off and the solution was filtered to retrieve the precipitates. According to the results, the use of NaOH was of instrumental importance for the precipitation of calcium carbonates. For all the experiments conducted without adjusting the pH of the solution to higher levels, the precipitation of calcium carbonates was insignificant. Temperature and CO<sub>2</sub> pressure were not found to substantially affect the precipitates yield. Impurities of magnesium, silica, aluminum and iron were detected in the precipitates and their calcium carbonate content was found to range between 63 wt% and 89 wt%. Apparently, the finally formed calcium carbonate was of low purity and could not be used as PCC. Finally, according to the authors' preliminary calculations, for the sequestration of 1 kg of CO<sub>2</sub>, 4.4 kg of blast furnace slag, 3.6 L of acetic acid (100 wt%), and 3.5 kg of sodium hydroxide would be required, while 2.5 kg of 90 % calcium carbonate would be synthesized.

Mun and Cho [127] also examined the possibility of sequestering CO<sub>2</sub> while, concurrently, creating PCC of high purity by subjecting BF slag to indirect carbonation. In this study the efficiency of six different solutions as calcium extraction agents was investigated. In fact, hydrochloric acid (0.1 M), acetic acid (0.1 M), EDTA (0.1 wt%), a mixture of hydrochloric acid (0.1 M) and EDTA (0.1 wt%) and a mixture of acetic acid (0.1 M) and EDTA (0.1 wt%) were tested. Calcium extraction experiments were held at L/S of 10 mL/g, ambient temperature and pressure. Each leachate solution obtained after the extraction step was subsequently subjected to carbonation by bubbling CO<sub>2</sub> without pressure through it. Among the several extraction agents tested, the mixture of acetic acid and EDTA proved to be the most efficient one, managing to extract 4.017 g of Ca/L of solution, from the slag. Apparently, the

carbonation of the particular leachate solution also led to the highest achieved CO<sub>2</sub> sequestration in the study (90g of CO<sub>2</sub>/kg slag). However, the material generated was of low purity PCC (83.35 %), characterized by heterogenous particles.

Recently, Chiang et al. [43] investigated the indirect carbonation of BF slag as a method leading to the sequestration of sufficient amounts of CO<sub>2</sub>, while producing value-added materials (PCC and zeolites) and eliminating potential solid residues. To this end, BF slag was first subjected to calcium extraction. In an effort to optimize the calcium extraction step, the authors proposed the implementation of a two-step extraction procedure. According to it, the slag was subjected to two rounds of calcium extraction. In each round half the molarity of the acetic acid solution that otherwise would be used in one step, is used. That way the negative effect of acidity on leaching selectivity would be avoided, while a sufficient amount of calcium fixed on the slag would be extracted to the solution. In each step, BF slag was mixed with 731 ml of acetic acid solution of several concentrations (0.5, 1 and 2M) at 30 °C and 1000 rpm, for 60 min. To separate the leachate solution from the solids, after each step the slurry was vacuum filtered. The leachate solutions resulting from both steps were then mixed together, whereas the residual solids resulting after the second step were oven dried at 105 °C, overnight. The resulting leachate solution was then subjected to carbonation using industrial quality CO<sub>2</sub> (> 99.5%). Carbonation tests were held at two different temperature-CO<sub>2</sub> pressure combinations (90 °C - 6bar and 120 °C - 40bar) for 60 minutes, using two different neutralization additives, namely NaOH and NaHCO<sub>3</sub>. In parallel, the residual solids resulting from the extraction stage were subjected to hydrothermal conversion to produce a zeolitic material. The alkaline solution used for the conversion was NaOH of varying concentrations (0.5, 1 and 3 M). Based on the results, although the lower concentration of acetic acid in the solution was proved to be beneficial for the selectivity of leaching, it also led to lower amounts of calcium being extracted from the material. In fact, higher amounts of calcium were extracted after using solutions with higher concentration of acetic acid, whereas Mg, Al and Si leaching was also found to grow with increasing acetic acid concentrations.

Regarding the quality of the formed carbonates, carbonation intensity did not significantly affect the precipitation of calcium which was almost complete (96 - 99 %) at all tested conditions. On the other hand, magnesium precipitation was highly affected by the carbonation conditions, getting remarkably increased at the higher combination of temperature and CO<sub>2</sub> pressure. Al and Si were found in the composition of PCCs at contents ranging between 0.5 and 3.2 % and 0.9 and 3.5 %, respectively. The concentration of calcium in the carbonated precipitates was found to range between 69 and 90 %. Finally, the hydrothermal conversion of the solid residues led to the formation of four different zeolitic phases, namely tobermorite, sodalite, lazurite and analcime. The extent of calcium extraction from the slag as well as the concentration of the alkaline solution used in the hydrothermal conversion stage were found to define in great extent the type of the zeolitic material to be formed. In fact, tobermorite was created when the calcium content of the residue was high. At lower calcium contents, sodalite or lazurite were formed, whereas by decreasing the concentration of NaOH solution from 3 to 1 and 0.5 M, the formation of analcime was promoted.

De Crom et al. [44] attempted the indirect carbonation of BF slag for the formation of a carbonate that could be used as paper filler. The particular PCC should be of high purity (> 98% Ca) and characterized by a homogenous mineralogical structure, a small average particle size and a narrow size distribution. After implementing the calcium extraction process proposed by Chiang et al. [41], the authors tried to improve the purity of the resulting leachate solution. To achieve that, instead of using vacuum filtration for the separation of the solution from the solids, the subjection of the resulting slurry to centrifugation was preferred. In an effort to further purify the resulting supernatant from the contained soluble or colloidal impurities, like silica, magnesium and aluminum, two different procedures were tested. In particular, to achieve the removal of magnesium and aluminum impurities from the supernatant, the authors adjusted its pH to higher levels (up to 8.43) by adding NaOH to it, whereas to cause the extra precipitation of silica the supernatant was placed in a refrigerator and cooled down at 1°C. The resulting solutions from both of these treatments were subjected to

microfiltration, in order to separate the further purified leachates from silica and the precipitated impurities of magnesium and aluminum. Finally, the purified leachates were subjected to carbonation. The carbonation process was also optimized by conducting the carbonation step applying three different reaction temperature-CO<sub>2</sub> pressure combinations (30 °C - 2 bar, 60 °C - 2.5 bar and 90 °C - 6 bar). To evaluate the effects of the proposed processes on the purity and the other tested characteristics of the produced PCC, a reference PCC sample was synthesized using the same conditions of Chiang et al. [41]. Based on the results, the optimal post-extraction solid/liquid separation process was the centrifugation of the leachate solution and the subsequent microfiltration of the resulting supernatant. That way, the content of silica in the obtained filtrate was reduced from 14 wt% using the standard process to 1 wt%. Furthermore, both the purification methods tested, proved to be beneficial for the removal of silica. In fact, silica removal of around 62 % was achieved by either cooling down the supernatant at 1 °C or increasing its pH to approximately 8.4. The addition of NaOH to the supernatant was also found to efficiently decrease the solubility of magnesium and aluminum. In particular, a pH adjustment at 8.4 resulted in a magnesium and aluminum removal of 65 % and 92 %, respectively. Finally, the less intensive carbonation process (30 °C - 2 bar) led to the production of purer and more homogenous precipitates. The PCC produced following the optimized indirect carbonation process proposed by the authors, was characterized by high chemical purity (98.1 wt%), homogenous mineralogy (> 88 % calcite), uniform morphology (scalenohedral), small particle size ( $d_{50} = 1.1 \mu\text{m}$ ) and narrow particle size distribution (1.09 uniformity).

Finally, Santos et al. [128] investigated the indirect carbonation of BF slag for the production of PCC using two different acids as calcium extraction agents, namely succinic acid and acetic acid. As in the case of Chiang et al. [43], calcium extraction was performed in two steps to restrain the acidity and thus promote leaching selectivity. In the first step, 100 g of BF slag were mixed with 731 ml of succinic or acetic acid solution of 0.5 M, at 80 °C, and 1000 rpm under air atmosphere in a Büchi ecoclave reactor for 60 minutes. The resulting slurry was then vacuum filtered and the obtained solids were

subjected to a second extraction step under the same conditions. The leachate solutions resulting from both steps were then mixed together and subsequently subjected to carbonation in the same reactor at different temperatures (60 and 120 °C) and varying CO<sub>2</sub> pressures (2, 6 and 40 bar), for 60 minutes. NaOH or NaHCO<sub>3</sub> in equimolar amounts to the organic acid concentration used in the extraction stage for each leachate, were included in some of the experiments, to buffer the pH and induce precipitation from both leachate solutions. According to the results, succinic acid proved to be more effective in extracting calcium and magnesium, compared to acetic acid. In fact, the total extent of calcium extraction achieved by using the succinic acid (31 %) was notably higher than that achieved by acetic acid (21 %). For both of the leachate solutions, pH buffering was necessary for precipitation to take place. The precipitation extent attained after the subjecting of the leachate solutions to carbonation, was remarkably higher from acetic acid than from the succinic acid leachates. In particular, from the total amount of calcium contained in the acetic acid leachates, 98 - 99 % of it precipitated, whereas from succinic acid leachate only 74 % of its calcium content was found in the precipitates. However, the precipitates resulting from the carbonation of succinic acid leachates were recognized as calcium succinates and not as calcium carbonates. In the contrary the carbonation of acetic acid leachate solution resulted in the precipitation of calcium carbonates, characterized by a notable level of magnesium, aluminum and silicon impurities.

### **2.5.2. Valorization of carbonated BOF slag**

In its original form BOF slag is either used in low-end applications (as fertilizer, armourstone in hydraulic engineering or even as aggregates in road construction). As a result, the particular steel-manufacturing waste is in need for new valorization routes.

One of the major concerns limiting the reuse of the particular type of slag, especially in construction applications, is its significant content in free calcium and magnesium (hydro)oxides which causes the poor volumetric stability of the material and thereupon its low technical performance. The reuse of BOF slag in several applications may also be restricted by the requirement from the

material to comply with several environmental criteria as they have been set by national legislations. Their fine particle size may be an additional issue for its employment, especially in construction applications, since natural aggregates replacement requires a specific particle size from the substitute material, surely greater than the one exhibited by BOF slag after its grinding for metal separation.

As shown in literature, accelerated carbonation has been proven to efficiently improve the leaching of certain metals from the slag, reduce its content of CaO and MgO and strength, while only slightly improving its particle size.

The direct carbonation of BOF slag as a method for CO<sub>2</sub> sequestration leading to the formation of value added materials has been studied by Monkman et al. [129], Santos et al. [38], Morone et al. [41], Morone et al., [130], Bodor et al. [12] and Quaghebour et al. [131].

Monkman et al. [129] investigated BOF slag as a potential replacement of natural aggregates in concrete. The main objective of the study was to reduce the CaO content of the slag, in order to enhance the volumetric stability of the material. Carbonation experiments were held at two different CO<sub>2</sub> pressures, namely 500 kPa and atmospheric pressure for 2 hours and 56 days, respectively. As expected, slag particles of lower diameters (75 µm) managed to store remarkably higher amounts of CO<sub>2</sub> (15.2 % compared to 4.2 % of their mass) than particles of greater size (300 - 600 µm). The carbonated product was then used as a fine aggregate in zero-slump press-formed compact mortar samples. Similar mortars using river sand as fine aggregate were also prepared in order to be used as controls. After 28 days of curing, the strength of the mortars formed using the carbonated BOF slag exhibited comparable strength to that achieved by the control mortars. Based on these results, it was concluded that carbonated BOF slag could be efficiently used as fine aggregate in concrete.

Santos et al. [38], examined the carbonation of BOF slag utilizing the hot-stage carbonation treatment. By testing three different methodologies (in-situ thermogravimetric analyzer carbonation, pressurized basket reactor

carbonation and atmospheric furnace carbonation) they also found a correlation between the particle size of the tested slag and the finally achieved CO<sub>2</sub> uptake, with slag samples of lower diameters exhibiting higher CO<sub>2</sub> uptakes than the samples of greater size. Furthermore, they detected a marginal improvement of CO<sub>2</sub> sequestration when implementing higher CO<sub>2</sub> pressures or adding steam to the process. In this study the basicity and the leaching behavior of the samples were addressed. According to the findings, carbonation led to the reduction of material's basicity while managing to significantly reduce the release levels of several regulated elements (Ba, Co, Ni). On the other hand V and Cr solubility appeared to increase after carbonation, complicating the reuse of the material. To confront that, the authors suggested an alternative way of using the particular product in construction applications. In case that the targeted use of the carbonated slag was as aggregate in cement mortars or concrete, authors proposed the use of additives like zeolitic sorbents in the matrix as a way to contain the release of the regulated elements. However, the efficiency of the particular solution was not experimentally evaluated in the study, whereas the use of additional materials (zeolitic sorbents) would also increase the cost of the process. Furthermore, according to the authors mineral carbonation of BOF slag could also be seen as a method to achieve the easier recovery of V and Cr from the slag, compared to the traditional energy intensive methods currently used. Since the main focus of this work was to assess the effects of several experimental parameters on the extent of the achieved carbonation and the leaching behavior of the produced material, the mechanical characteristics of the formed carbonates were not evaluated.

Morone et al. [41], investigated the potential of a combined wet granulation-carbonation treatment of BOF slag to produce secondary aggregates for construction applications, while managing to transform sufficient amounts of CO<sub>2</sub> in a thermodynamically stable and benign to the atmosphere material. To this end, BOF slag ( $d_{50} = 0.45$  mm) was mixed with deionized water at an L/S ratio of 0.12 L/kg. The humidified slag was then placed in a custom made granulator, equipped with a lid and a CO<sub>2</sub> feeding system. The material was treated for different periods (30, 60, 90, and 120 min) under either

atmospheric air or a 100% CO<sub>2</sub> environment. The particle size of the treated material presented a significant enlargement with time under both conditions, reaching a diameter of 4 mm after 10 minutes and 10 mm after 120 minutes of reaction. As expected, the CO<sub>2</sub> uptakes achieved after the combined treatment under 100 % CO<sub>2</sub> were remarkably higher than those achieved under atmospheric air. The highest CO<sub>2</sub> uptake achieved by BOF slag in this project was equal to 14 % after 90 minutes of treatment under 100 % CO<sub>2</sub> environment. The apparent particle density of the granules formed after granulation (t = 90 minutes) and granulation-carbonation (t = 30 and 120 minutes) was evaluated and compared with that of the untreated slag and natural gravel. Both of the treatments resulted in lower densities compared to that of untreated slag and greater than that of natural gravel. Carbonation appeared to improve the density of the produced material, whereas the combined treatment duration did not seem to have any impact on it, since similar values of particle density were obtained after 30 and 120 minutes of reaction. The leaching behavior of both crushed and uncrushed granules was also assessed. The uncrushed granules obtained after the agglomeration process exhibited an increased leaching of Cr and Zn, whereas as in the case of Santos et al. [38], the granules resulting from the combined treatment of the material presented an increased V leaching. The increase noted in the release of the Cr and V may be correlated to the pH reduction as both of these metals exhibit higher solubility with decreased basicity. To address the differentiations observed in pH, and in Ca, Ba and V leaching, between the crushed and the uncrushed granules obtained after the combined treatment of the slag, the authors compared the level of carbonation achieved at the surface of the finally formed granules with that of their core. The carbonation achieved at the surface of the uncrushed granules was found to be higher than that of their inner space which was found to be remarkably less affected by carbonation, explaining the difference in the basicity and the leaching behavior of the crushed and uncrushed granules. The mechanical performance of the produced granules was not tested in this project. Overall, the combined granulation-carbonation treatment of BOF slag could be evaluated as a technique with promising results for the transformation of the material into secondary aggregates, especially in terms of particle size

enlargement and volumetric stability improvement. However, the mechanical performance of the synthesized granules, one of the most significant qualities for their use as aggregates in civil engineering applications, remains to be assessed.

Morone et al. [130], investigated the combined carbonation-alkali activation of BOF slag and assessed the efficiency of the process as a treatment aiming to the sequestration of sufficient amounts of CO<sub>2</sub> while improving the hydraulic reactivity of the material. Two different alkaline solutions were tested as the activating agents: NaOH (2 M) + Na<sub>2</sub>SiO<sub>3</sub> (50:50 % by wt.) and NaOH (4 M) + Na<sub>2</sub>CO<sub>3</sub> (2 M) (75:25 % by wt.). The slag was mixed with each of the solutions and mortars were formed out of the particular mixtures. The mortars were then placed in either a humidity chamber (RH = 90 % and T = 20 °C) or a carbonation chamber (RH = 75 %, CO<sub>2</sub> = 5 %) and treated for 3, 7 and 28 days under ambient or enhanced (T = 50 °C) conditions. According to the results, the highest CO<sub>2</sub> uptake (6 wt%) was achieved by the slag that was mixed with the sodium solution incorporating sodium carbonate (NaOH/Na<sub>2</sub>CO<sub>3</sub>) and treated for 28 days in the carbonation chamber. The slag mixed with the NaOH/Na<sub>2</sub>SiO<sub>3</sub> solution and cured at 50 °C, for 7 days in the carbonation chamber exhibited the highest compressive strength (2 MPa).

Bodor et al. [12], tested the direct carbonation of BOF slag and assessed the efficiency of the produced carbonates as natural aggregates substitutes in construction applications. For the needs of the experiments, three different particle size classes of BOF slag were tested, namely < 0.08 mm, 0,08 - 0.5 mm and 0.5 - 1.6 mm. Each one of them was individually carbonated in a stirred batch autoclave reactor at 90 °C, 20 bar CO<sub>2</sub> pressure and L/S ratio of 4 mL/g, for 2 hours. The carbonated slurry was vacuum filtered and the retrieved solids were oven dried at 105 °C for 24 hours. In order to test the possibility of the carbonated materials to be used as aggregates in civil engineering applications, a reference mortar specimen, using standard quartz sand as aggregate and cement as the binder, was prepared following the standard EN 196-1:1994. Using the same mix ratios, mortar specimens incorporating uncarbonated and carbonated BOF slag as quartz sand

replacements were also created. According to the results, carbonation remarkably reduced the free lime content of the slag, whereas greater CO<sub>2</sub> uptakes were achieved by finer particles. In fact, the highest Ca-conversion observed was equal to 58.3 % and was achieved by the finest sample. Furthermore, compared to the reference mortar mixture, the mortar specimens prepared with uncarbonated BOF slag and carbonated BOF slag of < 0.5 mm particle size exhibited higher compressive strengths, with the latter one also presenting satisfactory results regarding its consistency, soundness and toxic elements leaching. Overall, the methodology proposed by Bodor et al. resulted in encouraging results for both the utilization of BOF slag in construction business as partial replacement of natural aggregates and the level of CO<sub>2</sub> sequestration that can be achieved.

Quanghebeur et al. [131], examined the accelerated carbonation of BOF slag as a method to produce a construction material with technical properties equivalent to those of conventional concrete products without adding any hydraulic or pozzolanic binder. According to the examined method, the BOF slag was first mixed with the appropriate amount of water (10 wt%) and then shaped into building blocks by hydraulic compaction. The formed blocks were placed in an autoclave reactor and subjected to accelerated carbonation at different temperatures (20 - 140 °C), CO<sub>2</sub> pressures (0.5, 2 and 4 MPa) and CO<sub>2</sub> concentrations (20, 50, 77 and 100 %), for up to 16 hours. Temperature elevation was found to cause the attenuation of the CO<sub>2</sub> uptake achieved by the slag, whereas the enhancement of both CO<sub>2</sub> pressure and CO<sub>2</sub> concentration of the feed gas led to a remarkable improvement of both the finally achieved CO<sub>2</sub> uptakes (up to 180 g/kg) and strength development (approximately 55 MPa) of the material. Results on the environmental behavior of the blocks formed by the carbonation of BOF slag were not reported in this study.

Quite a few studies on the indirect carbonation of BOF slag as a method for CO<sub>2</sub> sequestration have been published. However, only a few of them focused on the valorization potential of the produced material and characterized the synthesized PCC. Among the studies assessing the

qualities of the carbonates formed by the indirect carbonation of BOF slag are the ones conducted by Eloneva et al. [132], Eloneva et al. [126] Sun et al. [133], Mattila et al [134] and Chang et al. [135].

Eloneva et al., [132] explored the possibility of producing PCC of high purity through the indirect carbonation of BOF slag. In the particular study, acetic acid of varying concentrations was used as the calcium extraction agent. After its separation from the residual solids, the leachate solution was subjected to carbonation. The addition of NaOH solution was found to be necessary for the induction of calcium carbonate precipitation. As in the case of BF slag, acetic acid solutions of higher concentrations were found to extract higher amounts of calcium from the slag, whereas weaker acetic acid solutions appeared to improve the selectivity of leaching. The conversion of calcium from the solution into the precipitate was equal to 86 %, whereas the purity of the formed carbonates was over 99 %. The formed PCC also exhibited a rhombohedral morphology, a remarkably high brightness (98.7 %) and small particle size (mean value of 0.6  $\mu\text{m}$ ).

Eloneva et al. [126] further experimented with the indirect carbonation of BOF slag for the formation of PCC. The extraction agents tested in this research were ammonium nitrate (2 M) and ammonium chloride (2 M). The slag was mixed with the particular salts at L/S of 10 mL/g, for 2 hours. The leachate solution was separated from the solids and carbonated in a glass reactor vessel at 30 °C, employing different CO<sub>2</sub> concentrations (10, 25, 50 and 100 vol%) and gas (N<sub>2</sub>+CO<sub>2</sub>) flow rates (0.2, 0.5, 1 and 2 L/min) while stirred at around 600-700 rpm. The end point of each test was the point at which the solution pH was stabilized. Calcium concentration in the leachate solutions of both ammonium nitrate and ammonium chloride was around 13 g/L. Notably high levels of magnesium extraction were accomplished by ammonium chloride, whereas ammonium nitrate was found to extract significant amounts of silica from the slag. Unlike CO<sub>2</sub> concentration, which did not affect the yield of the finally precipitated carbonates, the type of the extraction agent appeared to have a slight impact on it, with the experiments using ammonium chloride resulting in slightly higher precipitate yields than the experiments with

ammonium nitrate. The formed precipitates were in form of calcite, except for the cases where the concentration of CO<sub>2</sub> was 50 vol% which led to the formation of aragonite along with calcite. The rest of the experiments resulted in the formation of high quality CaCO<sub>3</sub>, with bright white colour, powdery texture and fine particle size.

The formation of PCC through the indirect carbonation of BOF slag was also studied by Sun et al. [133]. In this study the extraction of calcium from the tested material was attempted using NH<sub>4</sub>Cl of a certain concentration (2 M) as the leaching agent, at 60 °C, for 120 minutes. The resulting leachate solution was subsequently carbonated in an autoclave reactor at varying temperatures (room temperature, 40, 60 and 80 °C), CO<sub>2</sub> pressures (10, 20, 30 and 40 bar) and stirring speeds (0, 400, 600 and 800 rpm). The concentrations of calcium and magnesium in the leachate solution after the extraction step were 15 g/L and 4 g/L respectively, whereas the rest of the assessed metals were found in contents below 0.5 g/L. As expected, the raise of temperature led to the improvement of carbonation kinetics and the increase of the weight of precipitate. The maximum mass of precipitate was obtained at 60 °C, whereas at higher temperatures the decrease of CO<sub>2</sub> and Ca(OH)<sub>2</sub> solubility started controlling the carbonation process. The CO<sub>2</sub> pressure increase did not significantly affect the mass of precipitate obtained after 60 minutes of reaction. Although stirring notably improved the amount of precipitate yield achieved after 60 minutes at room temperature, stirring speed enhancement only slightly affected it. Finally, the PCC produced by the carbonation of BOF slag under the optimized carbonation conditions (T = 60 °C, CO<sub>2</sub> pressure of 10 bar and stirring speed of 400 rpm) after 60 minutes of reaction was characterized as of quite high purity (96±2 wt%). Magnesium carbonate crystallite was also detected in the precipitate with composition percentage below 1 wt%, whereas the sum of the other impurities amounted to below 1 wt%.

Mattila et al. [134], attempted to produce PCC for paper-making use through the indirect carbonation of BOF slag. According, to the procedure employed in this study, the extraction of calcium from the slag was conducted at 30 °C

using  $\text{NH}_4\text{Cl}$  of varying concentrations (1.8, 3.5 and 4.9 mol/L) as the liquid agent and employing different solid-to-liquid ratios (100, 200 and 300 g/L). The resulting slurry was filtered and the obtained leachate solution was carbonated for 1 hour. The precipitates were separated from the solution by microfiltration and oven dried at 105 °C. Based on the results, calcium extraction efficiency was found to increase with increasing solids amount, while it was only slightly affected by the concentration of  $\text{NH}_4\text{Cl}$ . Magnesium extraction increased with increasing  $\text{NH}_4\text{Cl}$  concentration and with increasing solid/liquid ratio, whereas silica extraction levels were found to be remarkably low, especially compared to those of calcium. In all of the formed precipitates, apart from calcium, carbon and oxygen, an amount of chlorine was also detected. The particular amount was notable (5 - 8 wt%) even in the experiments where lower concentrations of  $\text{NH}_4\text{Cl}$  were used. The particular finding was attributed by the authors to the fact that the precipitates were not thoroughly washed after their formation. The particle morphology of the formed carbonates was also assessed. According to the results, instead of cubical calcite particles, unsuitable for paper-making spherical vaterite particles of small size (2 - 5  $\mu\text{m}$ ) were formed.

Chang et al. [135] investigated the indirect carbonation of BOF slag using deionized water and a highly alkaline liquid waste resulting from the steel-making industry (cold rolling water (CRW)), as the calcium extraction agents. Five different particle sizes of the slag were tested, namely < 0.125 mm, 0.125 - 0.35 mm, 0.35 - 0.5 mm, 0.5 - 0.84 mm and 0.84 - 1.19 mm. BOF slag was mixed with both of the tested liquids at L/S ratio of 20 mL/g and 800 rpm for 90 minutes. After the end of mixing, the leachate solution was separated by the residual solids and subjected to carbonation in a rotating packed bed reactor at a rotation speed of 750 rpm, gas flow rate of 3.5 L/min and a  $\text{CO}_2$  concentration of 30 vol%, for 20 minutes. The carbonated slurry was then circulated for further carbonation to be achieved. The maximum  $\text{CO}_2$  capture capacity observed was equal to approximately 0.175 g of  $\text{CO}_2$ /g BOF slag, with a particle size of less than 0.125 mm and after mixing with CRW. Although no results on the purity of the formed PCC are presented in the study, based on the concentration of elements in the leachate solution before

and after its carbonation, the leaching selectivity of the process should be characterized as low, with notable amounts of elements other than calcium (aluminum, magnesium and others) also found to precipitate, contaminating the composition of the formed PCC.

### **2.5.3. Conclusions**

Generally, two types of products can be synthesized after the mineral carbonation of any rich in calcium material. Depending on the applied method of carbonation (direct or indirect), the resulting product can either be PCC or a material rich in carbonates and of low quantity in free oxides. The former is produced after indirect carbonation and, based on its purity and other qualities, can be utilized in several industrial sectors, whereas the latter is formed after direct carbonation and can be used in the construction sector, mainly as an aggregate.

The direct carbonation of BOF slag resulted in the formation of carbonates with improved regulated elements leachability and reduced basicity. As expected, the level of free lime in the composition of the slag was significantly decreased after carbonation and the volumetric stability of the material was improved. On the other hand, the coupling of carbonation with additional techniques like granulation or alkali activation was found to improve other qualities of the synthesized materials, important for their utilization in the construction business, like their compressive strength or their average particle size.

The indirect carbonation of both types of slag resulted in the formation of PCC, the purity of which was mainly dependent on the selectivity of the calcium extraction process. The marketability of PCC was found to be highly related to its content in calcium, with the most valuable of its applications requiring high levels of purity (> 98 %). The type of the employed calcium extraction technique, the type of the extraction agent, its concentration and the intensity of the carbonation process were the variables that were found to affect the purity of the PCC obtained after the indirect carbonation of both BF and BOF slags. Among the several researches reviewed in this section, the

PCC synthesized by the indirect carbonation of BOF slag following the process proposed by Eloneva et al. [132] was the one with the highest purity (> 99 %), followed by that produced from BF slag (98.1 %), according to the methodology originally suggested by Chiang et al. [43] and optimized by De Crom et al. [44].

Opposite to direct carbonation which requires additional processes to form commercially exploitable products out of BOF slag, the indirect carbonation of either of the slags was found to be an efficient technique for the formation of high purity PCC. However, the most comprehensive indirect carbonation methodology proposed, was that of Chiang et al. [43], who combined the indirect carbonation of BF slag with the hydrothermal conversion of the residual solids resulting from the calcium extraction stage, in order to achieve the sequestration of respectful amounts of CO<sub>2</sub> and the parallel generation of PCC and zeolites, while leaving no wastes behind.

In general, it could be concluded that mineral carbonation of BF and BOF slags is a promising CO<sub>2</sub> sequestration process that after being coupled with supplementary processes can also become an efficient valorization option for both of the slags.

## **2.6. Investigated processes for BF and BOF slag valorization**

BF and BOF slags were qualified as the most suitable types of iron- and steel-manufacturing slags to be investigated as starting materials whose subjection to mineral carbonation could lead to the sequestration of sufficient amounts of CO<sub>2</sub> and the synthesis of marketable products.

According to literature review findings, the direct carbonation of BOF slag was found capable of fixing satisfactory amounts of CO<sub>2</sub>, while managing to generate carbonates with improved environmental behavior and remarkably decreased content of calcium and magnesium (hydro)oxides. In addition, the coupling of carbonation with supplementary processes was found to improve both the average diameter of the material (carbonation-granulation) and its mechanical strength (carbonation-alkali activation), qualities that are required

for the exploitation of the produced material as aggregate in construction applications.

On the other hand, BF slag is an iron-manufacturing byproduct already utilized in several valuable applications, mainly in the construction sector. Apparently, alternative valorization routes, apart from the sequestration of substantial amounts of CO<sub>2</sub>, should also manage to achieve the value-upgrading of BF slag through the formation of marketable products.

Compared to BOF slag, the direct carbonation of BF slag was found to result in considerably lower CWR values. In fact, the CWR values calculated based on the carbonation conversions obtained by the direct carbonation of BOF slags, were up to 12 times higher than that of BF slag, as studied by Chang et al. [111]. To improve the level of carbon sequestration achieved from the reaction of iron-making slags with CO<sub>2</sub>, the indirect carbonation of the particular byproduct should be investigated.

According to literature, the indirect carbonation of rich in calcium materials is capable of maximizing its CO<sub>2</sub> sequestration capacity, while also managing to form PCC of high purity. Nevertheless, the generation of solid wastes from the particular technique is a characteristic that damages its efficiency as a waste management process. The indirect BF slag carbonation technique proposed by Chiang et al. [43], and optimized for its carbonation step by De Crom et al. [44] was found to generate higher value material from BF slag while also addressing the residual solids issue. The particular methodology managed to sequester sufficient amounts of CO<sub>2</sub>, while producing PCC of adequate quality for use as paper filler (98.1 % purity) and zeolites, potentially capable of being used as heavy metal sorbents in wastewater treatment applications.

Based on the findings of this literature review, in this study, alkali activated BOF slag is subjected to a combined granulation-carbonation treatment, to produce secondary aggregates for civil engineering applications. Moreover, in an effort to further improve the efficiency of the proposed by Chiang et al. [43] and optimized by De Crom et al. [44] process, as an alternative route for BF slag valorization, the reproduction of zeolites through the hydrothermal

conversion of the solid residues resulting from the calcium extraction step of the indirect carbonation of a more porous type of BF slag is attempted. Additionally, the performance of the produced material as a heavy metal adsorbent in water is assessed, using  $\text{Ni}^{2+}$  as the metal for investigation.

### **3. SYNTHESIS OF SECONDARY AGGREGATES THROUGH GRANULATION AND GRANULATION-CARBONATION OF ALKALI ACTIVATED BOF SLAG**

#### **3.1. Introduction**

The recycling or reuse of the large amounts of steel slag that are formed during steel production is not always feasible, mainly due to the variability of the material characteristics but also due to the limited availability of low-cost technologies capable of producing valuable secondary products from it. Consequently, despite the growing awareness on the environmental impacts related to final disposal, for a relevant fraction of these residues no well-established management strategies apart from landfilling have been developed yet [136].

Among the several types of steel slag generated during the different routes of steel production, BOF slag is the most abundant one, amounting for 46% of the total European steel slag production in 2012 [137]. After its subjection to grinding for metal recovery, BOF slag is limitedly reused for low-end applications, whereas a significant part of it, approximately 25 %, ends up in landfilling sites [25]. In view of the EU's ambitious circular economy strategy, according to which the percentage of the final landfill disposal should be mitigated to a maximum of 10 % of all waste by 2030 [138], the management practices for the particular type of slag should be significantly improved.

The possibility of using BOF slag as a replacement of natural aggregates in construction applications has been studied by several researchers [84,139,140]. In order to be used as secondary aggregates in construction, the residues should exhibit a specific grain size distribution, certain free lime content (preferably below 4 % [141]) and adequate mechanical strength. Furthermore, the leaching behavior of the slag should also be of specific standards, as dictated by the regulations imposed by several EU countries, setting specific limits regarding the reuse of wastes and the release of potential contaminants, such as metals, metalloids and salts.

Apparently, some of the BOF slag's characteristics constrain its potential use in the particular sector. Its fine particle size, which is the result of BOF slag subsection to grinding in the plant for metal recovery, the notable mobility of certain elements, such as Ba, Cr, V and Mo as it has been reported in literature [143], as well as the fact that the pH value of alkaline industrial residues such as steel slags, is typically above 12 [144], are the BOF slag's properties that have a considerably negative impact on both its mechanical performance and its environmental behavior.

The significant improvement of its technical and environmental behavior is the key to achieve the further valorization of the BOF slag as an aggregate in civil engineering applications.

### **3.1.1. Accelerated mineral carbonation of BOF slag**

According to literature, accelerated carbonation can be an effective treatment for improving both the leaching behavior and the mechanical characteristics of BOF slag, while managing to permanently store the reacted CO<sub>2</sub> in a solid and thermodynamically stable form [117, 144-147]. In particular, the carbonation of BOF slag has been proved to increase the density of the material, producing carbonates of notable strength, whereas it has also been found leading to the reduction of the slags lime content, which, as already marked, should be present in low amounts in the slag in order to promote the volumetric stability of the material. Finally, the carbonation of BOF slag has been reported to also affect the pH of the leaching eluates, substantially decreasing it [38].

Although carbonation seems to influence several qualities of the BOF slag, it does not have any significant impact on the particle size distribution of the material. The latter could be significantly affected by the granulation process.

### **3.1.2. Granulation**

Granulation is a particle size enlargement process achieved through the agglomeration of smaller grains to greater ones. There are two different types of granulation [148, 149]: a) dry granulation, where compaction techniques take over the production of granules and b) wet granulation, during which a

volatile liquid agent is introduced to the dry primary particles mixture to form the desired granules.

Dry granulation is a simple process. It is used to create granules out of smaller particles without the incorporation of any liquid agent. Such an agglomeration technique implies the subjection of the primary powder particles to high pressure compaction [150-152]. This can be achieved by either using a compaction press or a roller compactor (both widely used in the pharmaceutical sector) [150, 151]. The compaction products are subsequently milled to finally obtain the granules with the desired size.

On the other hand, wet granulation can be as simple or much more sophisticated particle enlargement technique, mainly depending on the available equipment, the type of the primary material and the final objective of granulation. Due to its characteristics, wet granulation is a process with great applicability in several sectors such as in the fertilizers, agrochemicals, pharmaceutical, ceramics, plastic and detergent industries.

In its plain version, wet granulation is simply the damping of the dry particles mixture that is then forced through a sieve of a particular diameter. The wet agglomerates generated that way are subsequently dried to obtain the final granules. In its more sophisticated form, wet granulation is characterized by the mixing of dry powder with a liquid agent in a disc granulator, a rotating drum or other dynamic devices [152, 153]. The granulation liquid has to be volatile in order to be easily removed by drying. Due to the continuous rolling of the moistened particles and their collisions with each other, granules of greater sizes are formed [152]. The particular agglomerates grow until the binding forces are no longer capable of holding them together due to either their large size or drying out.

According to literature the wet granulation process of this type can be analyzed into three main stages, [150, 153-157]: 1) nucleation, 2) consolidation and growth and 3) attrition and breakage. Each stage of the process, as well as their impact on the amount and mass of both the primary particles and the formed granules are described below.

- 1) Nucleation: this is the first phase of wet granulation. After the drops of the liquid agent are added to the particles mix, the bonding mechanisms that are generated between the liquid and the particles lead to the creation of nuclei with different sizes. The particular stage of granulation results in the reduction of both the amount and mass of the primary particles and the increase of the amount and mass of granules [157].
- 2) Consolidation and growth: this is the phase during which collisions between granules and equipment take place. The granules collisions lead to their compaction and finally to their enlargement. Consolidation occurs through three different mechanisms, namely layering, coalescence and abrasion transfer. During layering, extra particles that have remained unaffected or have been slightly influenced by the first phase of granulation, are bound to the surface of the generated nuclei, increasing the mass of the created granules but holding their number stable, while further decreasing the amount and mass of the primary particles [157]. The layering mechanism is also the one dominating the integration of fragments resulting from smaller granules breakage to the surface of the bigger ones. Due to the continuous agitation of granules in a granulator, they experience numerous collisions with other granules and parts of the equipment. As a result, the small granules break into smaller pieces that are subsequently adhered to the surface of the bigger granules which have not experienced severe size changes from the collisions. In this case, layering results in a decrease of the number of granules, whereas it preserves their total mass at the same levels [157]. Coalescence is the type of consolidation during which a granule of greater size is formed from the collision and integration of two smaller granules. The binding forces of the newly formed granules must be sufficient to hold it together. Coalescence reduces the total number of granules but increases their mass [157]. Finally, according to abrasion transfer, material from the surface of one granule is transferred to the surface of another. The particular consolidation mechanism does not affect either the amount

or the mass of the formed granules and its impact on the granules size alterations is considered to be negligible [157]. In general, the consolidation step seems to be the most decisive step of wet granulation process since this stage determines in great degree the extent of particles enlargement but also other properties of the produced granules, like their porosity and strength. It is a complex process that is mainly controlled by three different forces: the inter-particle friction, the capillary force and the viscous force. As a mechanism based on inter-particle collisions, its complexity lies to the fact that consolidation is actually a balance between the tendency of the granules to either dilate or compact as a result of the impacts to which they are subjected [158].

- 3) Attrition: this is the last phase of wet granulation process. The mechanical stresses and the size of the granules keep on increasing during granulation. At a particular time, they reach a point at which the bonding forces are unable to continue holding the granule together due to either their large size or their drying. This is the point when the stresses overcome the bonding forces and the attrition of the formed granule takes place.

The granules formed by the wet granulation process result from the combination of the aforementioned steps. The described mechanisms have been found to take place during every granulation process, to some extent [157]. The process is mainly controlled by those mechanisms. Apparently, granulation does not only dictate the rate and extent of growth development. It also determines in great degree other qualities of the final product like its porosity, strength and leaching behavior. The type of granulator, the type of the feed material (particle size distribution and chemical properties) and that of binders and additives (viscosity, surface tension and contact angle), as well as the operating conditions (level of moisture, rotation speed etc.) are the basic parameters that determine the level of influence of each one of the above mentioned mechanisms over the final product properties.

Recently proposed by Gunning et al. [159], the combination of granulation with accelerated carbonation, as a solid residues treatment, has been reported to result in the production of artificial aggregates with improved strength and leaching behavior. During this process, granulation takes place normally while CO<sub>2</sub> is introduced to the system. By combining these two mechanisms, apart from the formation of aggregates with potential commercial applicability in civil engineering business, the reduction of point-source CO<sub>2</sub> emissions is also achieved. Morone et al. [41] investigated the combination of carbonation with wet granulation as a potential treatment for BOF slag with the aim to use the produced material as secondary aggregate in construction applications. In the particular study, a fine sample of BOF steel slag ( $d_{50} = 0.4$  mm) was subjected to a combined granulation-carbonation treatment using water as the liquid binder. According to the results, already after 30 min of reaction, the formation of coarse aggregates ( $d_{50} = 4$  mm) and significant CO<sub>2</sub> uptakes (120 - 144 gCO<sub>2</sub>/kg) were achieved [41]. Furthermore, the pH, as well as the Ca and Ba concentrations measured in the leachates of the uncrushed granules exhibited a noteworthy decrease compared to those resulting from the untreated slag, while conversely a slight increase of V leaching was observed [41]. However, the apparent particle density of the formed granules appeared to be quite poor and below the one attributed to the untreated BOF slag.

### **3.1.3. Alkali activation**

To further improve the mechanical properties of the produced agglomerates, apart from carbonation, granulation can also be combined with other supplementary processes, such as alkali activation.

Among the treatments that have been found to be effective in increasing the mechanical performance of a material, alkali activation stands as one of the most widely investigated methods. Alkali activation is a chemical process according to which a usually amorphous and/or metastable raw material, characterized by high contents of Ca and Si or Al and Si, is mixed with a solution containing sodium or potassium hydroxides, carbonates and/or silicates, in order to favor the dissolution of the reacting species and enhance

hydration reactions leading to the formation of a compact and strong product [160, 161]. According to literature, all caustic alkalis or alkali compounds with anions that after reacting with  $\text{Ca}^{2+}$  produce Ca compounds that are less soluble than  $\text{Ca}(\text{OH})_2$  are able to act as slags' activators [162-164]. However, the most commonly employed alkali activators are mixtures of sodium or potassium hydroxides (NaOH or KOH) with sodium silicate or potassium silicate ( $n\text{Na}_2\text{SiO}_3$  or  $n\text{K}_2\text{SiO}_3$ ) [165].

The final product of the alkali activation process depends on the composition of the activator, the type of the raw material and the curing conditions. Generally, in case that the raw material is rich in calcium and silica, then the reactions lead to the formation of binding phases such as a calcium silicate hydrate (C-S-H) gel, that yields a compact and strong product [165, 166]. In the case that the initial material is rich in aluminum and silica, then an aluminosilicate gel (N-A-S-H gel) also known as 'zeolite precursor' is created. The particular phase also returns products of enhanced strength [167].

Alkali solution can be used either as the main binding phase during granulation or as an extra granulation liquid which can act as an extra binding agent and create granules with extra strength.

Alkali activation has been proved to be a rather efficient method for the improvement of hardening mechanisms of BF slags and of several other amorphous residues, rich in calcium and silicon [160]. As for residues characterized by similar chemical composition but high crystallinity, alkali activation has been less applied. However, recent studies examined the application of alkali activation on other steelmaking slags rich in calcium and silicon to produce a final product with suitable mechanical properties [167, 168]. In particular the work of Salman et al. [167] showed that treating a crystalline and non-hydraulic slag by alkali activation with an initial period of steam curing at high temperature led to the formation of a dense and strong solid, consisting of C-S-H matrix.

The objective of this project was to assess if the application of a process combining the three above described mechanisms (i.e. carbonation, granulation and alkali activation) on a BOF slag, could lead to the formation of

products with satisfactory environmental and mechanical characteristics, in order to be used as aggregates in the construction sector. Based on the work of Morone et al. [130], who worked on the alkali-activation of BOF slag applying different alkali activators on BOF slag mortars and pastes, a mixture of sodium hydroxide (NaOH) and sodium silicate ( $\text{Na}_2\text{SiO}_3$ ) was selected for the alkali activation experiments. The results of lab-scale granulation and combined granulation-carbonation tests using only water as the liquid binder, as well as the results obtained after granulation and granulation-carbonation tests using the particular alkali solution as the binder are reported in the following sections. The effects of the treatments were assessed in terms of the particle size distribution,  $\text{CO}_2$  uptake, mechanical strength (as ACV) and leaching behavior at native pH of the produced granules. The reactivity of the BOF slag sample towards  $\text{CO}_2$  was investigated performing batch wet carbonation tests applying different operating conditions. Furthermore, key operating parameters like the reaction time and the amount of liquid agent were varied and tested for the combined process in order to evaluate their effect on the final properties of the granules and to assess the conditions that may lead to the achievement of the best technical and environmental performance.

## **3.2. Materials and Methods**

### **3.2.1. Materials**

The steel slag sample used in this research was collected just downstream of two different BOF units of an integrated cycle steelmaking plant. Before collection, it was subjected to crushing and magnetic separation for iron and steel recovery.

The activating solution employed in some of the experiments of this study was a 50:50 by weight mixture of a 2 M sodium hydroxide (NaOH) solution, prepared by dissolving pellets of NaOH (Fischer Scientific, 99.4 % purity) in deionized water, and a commercial sodium silicate ( $\text{Na}_2\text{SiO}_3$ ) solution (Sigma-Aldrich) in water, whose concentration of silicates was determined by ICP-OES analysis and was equal to 36 %.

### 3.2.2. Methodology

#### 3.2.2.1. Granulation and granulation-carbonation tests

Granulation and granulation-carbonation experiments were carried out using a 180W lab scale disc granulator reactor (Figure 3-1), characterized by a diameter of 0.3 m and height of 0.23 m. The granulator operated at 24 rpm and a tilt of 50 ° during all experiments. A blade assisting the even allocation of the sample into the reactor during its rotation was also available.

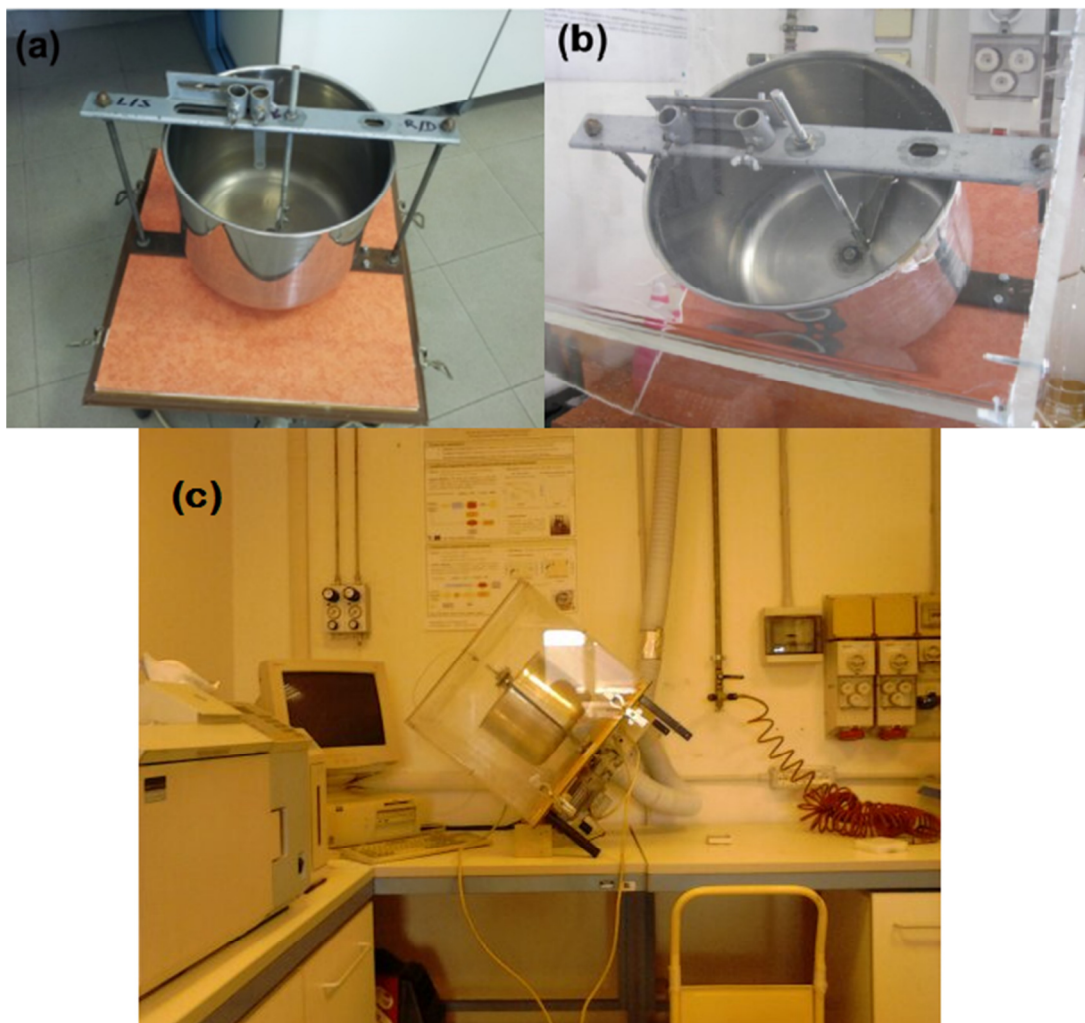


**Figure 3-1**The equipment used for the a) granulation and (b, c) granulation-carbonation experiments.

Especially for the needs of the combined granulation-carbonation tests, a custom-made Perspex lid equipped with a gas feeding system was placed right over the reactor.

In both types of experiments, approximately 500 g of BOF steel slag were pre-mixed in a plastic bag with either deionized water or sodium solution at set W/S ratios. In fact, the W/S ratio applied in the most of the experiments was equal to 0.12 L/kg, which was experimentally proved to be the optimal value for the granulation of the BOF slag sample. The highest water-to-solid (W/S) ratio used in the experiments was that of 0.14 L/kg which was applied in combined treatment tests carried out on alkali activated slag. The employed ratios of alkali activation solution to slag (AA/S) were equal to 0.16 L/kg (baseline condition) and 0.18 L/kg (for W/S = 0.14 L/kg).

The mixed samples were then pushed through a 2 mm sieve into the granulator, and left to react for a set time. The granulation tests were held under ambient temperature and pressure and lasted for 30 minutes. The granulation-carbonation tests were performed under 100 % CO<sub>2</sub> that was introduced to the system at a pressure of 1 bar, for the entire duration of the experiment (30 or 60 minutes).

The materials formed after both treatments were collected in containers and moved to a controlled environment where they were cured for 28 days, at room temperature and 100 % relative humidity, in order to allow the completion of hydration reactions. At different time intervals (0, 7 and 28 days of curing), a small part of the material was withdrawn from the containers and after being ground to powder, it was analyzed for its content in CO<sub>2</sub>. Based on the obtained results, the achieved CO<sub>2</sub> uptakes were determined.

### **3.2.2.2. Batch carbonation tests**

For the batch carbonation experiments, a stainless steel reactor equipped with a 150 ml internal Teflon jacket was used. To control the reaction temperature, the reactor was placed in a thermostatic bath (Figure 3-2). The reactor was also equipped with a thermo-couple that was used to indicate the temperature within it, a pressure indicator displaying the internal pressure and a gas feeding system, through which the CO<sub>2</sub> was introduced to it.



**Figure 3-2 The equipment used for the batch carbonation tests.**

The tests were performed in triplicates. Each one of the three 1 g slag samples was evenly wetted with the tested liquid (DI water or alkali solution) applying a liquid-to-solid (L/S) ratio of 0.3 L/kg. The moistened samples were then placed into the reactor, where they were subjected to carbonation under a 100% CO<sub>2</sub> flow at varying temperatures (20 and 50 °C) and pressures (1 or 10 bar). The moisture of the gas was maintained at 75 % during the whole process by using a saturated NaCl solution, placed at the bottom of the reactor.

In particular, batch carbonation tests were carried out on the as received BOF slag at mild operating conditions ( $T = 20\text{ °C}$ ,  $p\text{CO}_2 = 1\text{ bar}$ ,  $L/S = 0.3\text{ L/kg}$ ), using DI water as the liquid agent. The particular experiments under the specific conditions, which were similar to those applied in the granulation-carbonation tests, were conducted in order to assess the influence of the different reaction modes applied (batch or granulation-carbonation) on the finally achieved CO<sub>2</sub> uptakes. In addition, carbonation tests on the as received BOF slag applying the same reaction conditions but using the sodium solution

that was used in the granulation-carbonation experiments, as the wetting agent, were also performed, in order to evaluate the effect of the alkali solution on the CO<sub>2</sub> uptake of the residues.

Finally, carbonation tests on the as received BOF slag and a milled sample (0.038 mm <math>d < 0.125\text{ mm}</math>) of it, at enhanced conditions ( $T = 50\text{ }^{\circ}\text{C}$ ,  $p = 10\text{ bar}$ ,  $L/S = 0.3\text{ L/kg}$ ) were also conducted in this study. Based on previous works on carbonation of steel-making slags, the particular conditions have been found leading to remarkable CO<sub>2</sub> uptakes when applying the wet carbonation route. The aim of the particular tests was to assess the maximum reactivity of the investigated material towards CO<sub>2</sub>, in order to compare it with those exerted by previous works and with the CO<sub>2</sub> uptakes obtained from the granulation-carbonation tests.

After the end of each test, the samples were removed from the reactor and cured into the oven at 105 °C, overnight. After their curing, the samples were crushed to create a powder of carbonated BOF steel slag that was then analyzed for its CO<sub>2</sub> content, based on which the achieved CO<sub>2</sub> uptake was calculated.

### **3.2.3. Analytical methods**

The moisture level of the fresh material was determined by placing 15 grams of fresh BOF slag in the oven (at 105 °C) for a day. The difference between the weight of the sample after its curing and its initial one would indicate the percentage of water within it. The particular test was performed in duplicates.

The particle size distribution of the as received material as well as that of granulation and granulation-carbonation products was determined by applying the ASTM D422 standard procedure [33]. The selection of the particular standard procedure was made based on the available equipment of the lab.

The elemental composition of the as received material was determined by alkaline fusion of the dried material using lithium metaborate (Li<sub>2</sub>B<sub>4</sub>O<sub>7</sub>) in platinum melting pots at 1050 °C, followed by dissolution of the molten material using 4 % HNO<sub>3</sub> and a subsequent ICP-OES analysis of the obtained

solution, using an Agilent 710-ES spectrometer. This analysis was carried out in triplicates.

The mineralogical analysis of the untreated material was performed by powder X-ray diffraction (XRD) with Cu K $\alpha$  radiation using a Philips Expert Pro diffractometer equipped with a copper tube operated at 40 kV and 40 mA.

The CO<sub>2</sub> uptake of the batch carbonation tests resulting materials and that of the formed granules after varying curing periods (0, 7 and 28 days), as well as the CO<sub>2</sub> content of the as received BOF slag, were assessed on the basis of the results of inorganic carbon (IC) analysis as it was performed by a Shimadzu TOC VCPH analyzer equipped with the SSM-5000A solid sampler. IC measurements were performed in triplicates. Based on the IC values obtained by the particular analysis, the calculation of the CaCO<sub>3</sub> content (%) as well as that of the final CO<sub>2</sub> content (%) and thereupon the calculation of the achieved CO<sub>2</sub> uptake (%) was achieved by applying the following equations.

The %CaCO<sub>3</sub> in each case was calculated by using the following formula:

$$\%CaCO_3 = \frac{\%IC * MW(CaCO_3)}{MW(IC)} \quad (3-1)$$

where %IC is the average %IC of the three measurements, MW (CaCO<sub>3</sub>) is the molecular weight of CaCO<sub>3</sub> that is equal to 100, and MW (IC) is the molecular weight of the “inorganic” carbon that is equal to 12.

For the calculation of the %CO<sub>2</sub>(final) in each case, the following formula was used:

$$\%CO_2 final = \frac{\%CaCO_3 * MW(CO_2)}{MW(CaCO_3)} \quad (3-2)$$

where MW (CO<sub>2</sub>) is the molecular weight of CO<sub>2</sub> that is equal to 44.

The CO<sub>2</sub> (uptake) in each case was calculated by using the formula:

$$CO_2 \text{ uptake}(\%) = \frac{CO_2 \text{ final}(\%) - CO_2 \text{ initial}(\%)}{100 - CO_2 \text{ final}(\%)} 100 \quad (3-3)$$

where  $CO_2 \text{ initial}(\%)$  is the content of  $CO_2$  in the as received material, as it is determined by the IC analysis of the latter.

In order to obtain the CWR values achieved after the batch carbonation tests, the calcium conversion yields (the ratio between the measured  $CO_2$  uptake and the amount of potentially reactive calcium phases) resulting from the carbonation treatment of the investigated material was calculated by applying the following formula [58, 60]:

$$C\% = \frac{CO_2 \text{ uptake}(\%) * MW(Ca)/MW(CO_2)}{Ca \text{ initial}(\%) - CaCO_3 \text{ initial}(\%) * MW(Ca)/MW(CaCO_3)} * 100 \quad (3-4)$$

where  $MW(Ca)$  is the molecular weight of Ca that is equal to 40 and  $CaCO_3 \text{ initial}(\%)$  is the content of  $CaCO_3$  in the as received material.

Apparently, magnesium phases were not taken into consideration in the particular calculations, since compared to calcium phases, they were found in considerably lower amounts in the composition of the slag. Furthermore, relevant  $CO_2$  uptakes by magnesium oxides or silicates have not been reported in prior carbonation studies on steel slag, regardless of the intensity of the applied treatment (mild or enhanced operating conditions).

The mechanical strength of the granulation and granulation-carbonation products was assessed in the civil engineering labs of Tor Vergata University. The instrument available for compressive strength measurements was preset to perform the ACV test, following the British standard BS 812-110 [35]. The particular test gives a relative measure of an aggregate's resistance against crushing under a gradually applied compressive load. The ACV is expressed as the ratio between the amount of fines formed as the result of the compressive load, and the total mass of the tested specimen, as it is expressed in equation 4, where  $M_2$  is the mass (grams) of the fine material

passing a standard sieve and  $M_1$  is the total mass (grams) of the tested specimen.

$$ACV(\%) = \frac{M_2}{M_1} 100 \quad (3-5)$$

Finally, the leaching behavior of the as received BOF slag and that of the formed granules was evaluated following the EN 12457-2 standard compliance test [34], which involves the grinding of material with particle size greater than 4 mm. The particular standard procedure was selected based on the equipment that was available in the labs. The leaching behavior of the agglomerated materials was also assessed by applying the EN 12457-2 procedure on unground granules, in order to appraise their behavior under similar conditions to the expected application scenario. The eluates obtained by each test were subsequently analyzed by ICP-OES analysis, employing an Agilent 710-ES spectrometer. Leaching tests were performed in duplicates. Since the particular part of research was conducted in Rome, Italy, in this study, the pH and heavy metal leaching regulatory limits were set based on Italian legislation. In Italy, these limits have been issued by Ministerial Decree 186 (2006) [142].

### **3.3. Material characterization**

Several features of the as received BOF slag were analysed during its characterization process. The results of this analysis are presented in the following subsections.

#### **3.3.1. Moisture level**

The content of water within the fresh BOF slag was estimated to be approximately equal to 2 %.

#### **3.3.2. Particle size distribution analysis**

As shown in Table 3-1, nine different sieve diameters were used.

**Table 3-1 Particle size distribution analysis for the as received material**

<b>As Received Material</b>			
<b>D (mm)</b>	<b>Weight (g)</b>	<b>Weight (%)</b>	<b>Passing (%)</b>
<b>2.36</b>	0	0	100
<b>1.18</b>	1.5	0.09	99.91
<b>0.84</b>	100.8	6.34	93.66
<b>0.425</b>	588.3	36.99	63.01
<b>0.25</b>	768	48.29	51.71
<b>0.177</b>	851.9	53.57	46.43
<b>0.125</b>	960.4	60.39	39.61
<b>0.105</b>	1042.5	65.55	34.45
<b>0.038</b>	1373	86.33	13.67
<b>0</b>	1590.4	100	0
<b>Final Weight</b>	1590.4		

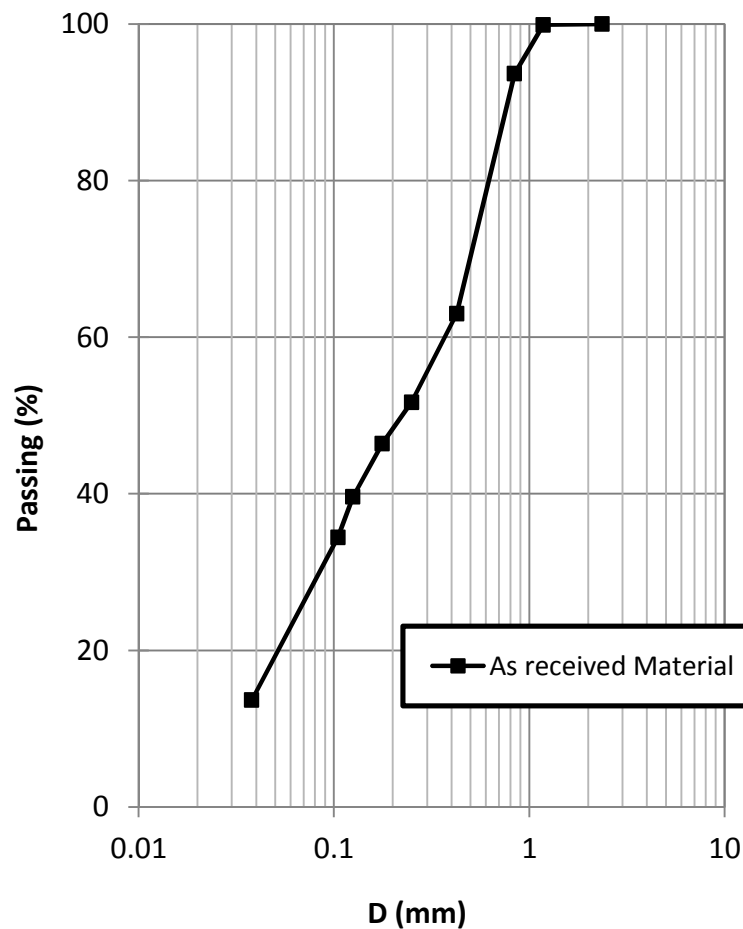


**Figure 3-3 Particle size distribution diagram of the as received material.**

The particle size of the untreated material (20 kg) was below 1mm (negligible part of the material presented sizes over 1.18 mm), whereas its mean diameter was found to be equal to 0.2 mm. The particle size distribution of the investigated BOF slag is graphically presented in Figure 3-3.

### 3.3.3. Elemental and mineralogical composition

The elemental composition of the fresh BOF slag is presented in Table 3-2. The basic chemical constituents of the sample were Ca (268 g/kg) and Fe (222.67 g/kg), followed by Mg (42.55 g/kg), Mn (31.97 g/kg) and Si (15.77 g/kg). The presence of Al was approximately equal to 8 g/kg, whereas noteworthy concentrations of Cr (0.73 g/kg), Ba (0.7 g/kg) and V (0.47 g/kg) were also detected.

**Table 3-2 Elemental composition of the untreated material expressed on a dry weight basis [138]**

Elemental Composition (g/kg)					
Al	Ba	Ca	Cd	Cr	Cu
8.02	0.7	268.12	0.17	0.73	0.14
Fe	Mg	Mn	Si	V	Zn
222.71	42.55	31.31	15.77	0.47	0.15

The main phases detected after the mineralogical analysis of the untreated material, were silicates, i.e. larnite ( $\text{Ca}_2\text{SiO}_4$ ) and hatrurite ( $\text{Ca}_3\text{SiO}_5$ ) and oxides, such as magnesium oxide (MgO), a mixed Ca-Al-Fe oxide ( $\text{Ca}_2\text{Fe}_{1.4}\text{Al}_{0.6}\text{O}_5$ ), a mixed Ca-Cr-Fe oxide ( $\text{Ca}_2\text{Cr}_{0.5}\text{Fe}_{1.5}\text{O}_5$ ), wüstite (FeO) and magnetite ( $\text{Fe}_2\text{O}_3$ ).

**Table 3-3 IC analysis results of the as received material**

Sample Name	%IC (#1)	%IC (#2)	%IC(#3)	%IC (average)	%CaCO <sub>3</sub> (initial)	%CO <sub>2</sub> (initial)
Fresh BOF slag	0.02534	0.02935	0.03204	0.027	0.0225	0.098

The  $\text{CaCO}_3$  and thereupon the  $\text{CO}_2$  content of the fresh BOF slag (expressed in percentage) was also determined by subjecting the material to IC analysis. The results of this analysis are presented in Table 3-3.

### 3.3.4. Leaching behavior

The leaching behavior of the fresh BOF slag is discussed in this section. The eluate concentrations of major constituents (Al, Ca, Na, Si) and regulated elements that proved higher than instrumental quantification limits (Ba, Cr, V, Zn) are presented in Table 3-4.

**Table 3-4 The leaching behavior of the as received BOF slag**

<b>Eluate Concentrations of Major Constituents (mg/L)</b>			
<b>Al</b>	<b>Ca</b>	<b>Na</b>	<b>Si</b>
0.11	915.3	1.67	0.13
<b>Eluate Concentrations of Regulated Elements (mg/L)</b>			
<b>Ba</b>	<b>Cr</b>	<b>V</b>	<b>Zn</b>
0.37	0.013	0.003	0.032

None of the regulated elements contained in the fresh slag appeared to exceed the Italian regulatory limits for waste reuse.

The pH of the as received material was found equal to 13.13.

## 3.4. Results and discussion

The operating conditions applied during each granulation and granulation-carbonation experiment carried out for the needs of this study are presented in Table 3-5.

As already mentioned, the products of each test were cured under a controlled atmosphere (room temperature, 100% relative humidity) for 28 days. After that period the granules presented in Figure 3-4 were obtained.

The particular granules were assessed regarding their particle size,  $\text{CO}_2$  uptake, mechanical strength and leaching behavior.

**Table 3-5 The identity of granulation and granulation-carbonation experiments**

Sample Name	Type	Liquid Agent	Duration	W/S ratio
G30'_W_W/S=0.12	Granulation	DI water	30 mins	0.12
G30'_SS_W/S=0.12	Granulation	Na-solution	30 mins	0.12
GC30'_W_W/S=0.12	Gran.-Carb.	DI water	30 mins	0.12
GC60'_W_W/S=0.12	Gran.-Carb.	DI water	60 mins	0.12
GC30'_SS_W/S=0.12	Gran.-Carb.	Na-solution	30 mins	0.12
GC60'_SS_W/S=0.12	Gran.-Carb.	Na-solution	60 mins	0.12
GC30'_SS_W/S=0.14	Gran.-Carb.	Na-solution	30 mins	0.14
GC60'_SS_W/S=0.14	Gran.-Carb.	Na-solution	60 mins	0.14

### 3.4.1. Particle size distribution (PSD) analysis

The particle size distribution diagrams of the produced granules are presented in Figure 3-5.

The  $d_{50}$  values for the products of each test are presented in Table 3-6.

From the obtained data the diagrams in Figures 3-6 and 3-7 describing the effects of different operating conditions on the size of the finally formed granules, are created.

According to the results, the type of treatment significantly affected the size of the created granules. In agreement with the findings of Morone et al. [41], who also investigated the granulation of BOF slag under atmospheric air and in a 100% CO<sub>2</sub> environment, the granules generated by the combined treatment were characterized by smaller diameters compared to the ones obtained after granulation under atmospheric air, using either water or sodium solution as the liquid binder (Figure 3-7). In particular, depending on the employed binding solution and the applied W/S ratio, granules generated by the combined treatment presented a mean diameter that was 5 to 20 times greater than that of the untreated slag (Figure 3-6), whereas by following the granulation process under ambient conditions, granules with sizes 50 or 60 times greater than that of the as received material were formed. The particular effect should be ascribed to the different conditions established in

the reactor (e.g temperature and moisture level) under the continuous flux of CO<sub>2</sub> [136]. Apparently, the presence of CO<sub>2</sub> during granulation seemed to slow down the growth rate of the produced granules.

As observed in Figure 3-5a. and 3-7, granules produced by granulation using either water or the alkali activator as the liquid agent, were characterized by comparable particle size distributions, exhibiting mean diameters of 10mm and 13mm, respectively, with the granules obtained after granulation using sodium solution as the liquid binder, characterized by a slightly increased amount of coarser particles.

The influence of the applied liquid binder type on the mean diameter of the granules formed after the combined granulation-carbonation treatment of the BOF slag was investigated for W/S = 0.12 L/kg (Figure 3-7). After both tested periods, the use of sodium solution resulted in the production of granules with remarkably lower size than that of the granules created using DI water. This should be mainly attributed to the higher viscosity of the alkali solution compared to DI water. In general the use of a more viscous binder leads to the formation of stronger granules that deform less during the granulation process. The particular behavior leads to lower consolidation rates and therefore to lower growth rates [136].

The amount of the employed liquid binder was also found to exert a notable effect on the size of the granules synthesized after the combined treatment of BOF slag (Figure 3-5c. and 3-6). According to the results, for both the tested reaction times, by increasing the amount of sodium solution in the mixture (W/S ratio: from 0.12 to 0.14 L/kg), granules with greater diameters were generated. According to literature, the effect of liquid binder amount on the final size of the granules is highly affected by the granulating material particles size distribution, with smaller primary grains requiring higher amounts of granulating solution in order to take part in the agglomeration process [170-176]. Apparently, by increasing the amount of liquid binder up to a particular value, greater proportion of the granulating mass participated in the formation of agglomerates and subsequently granules of greater sizes were formed.

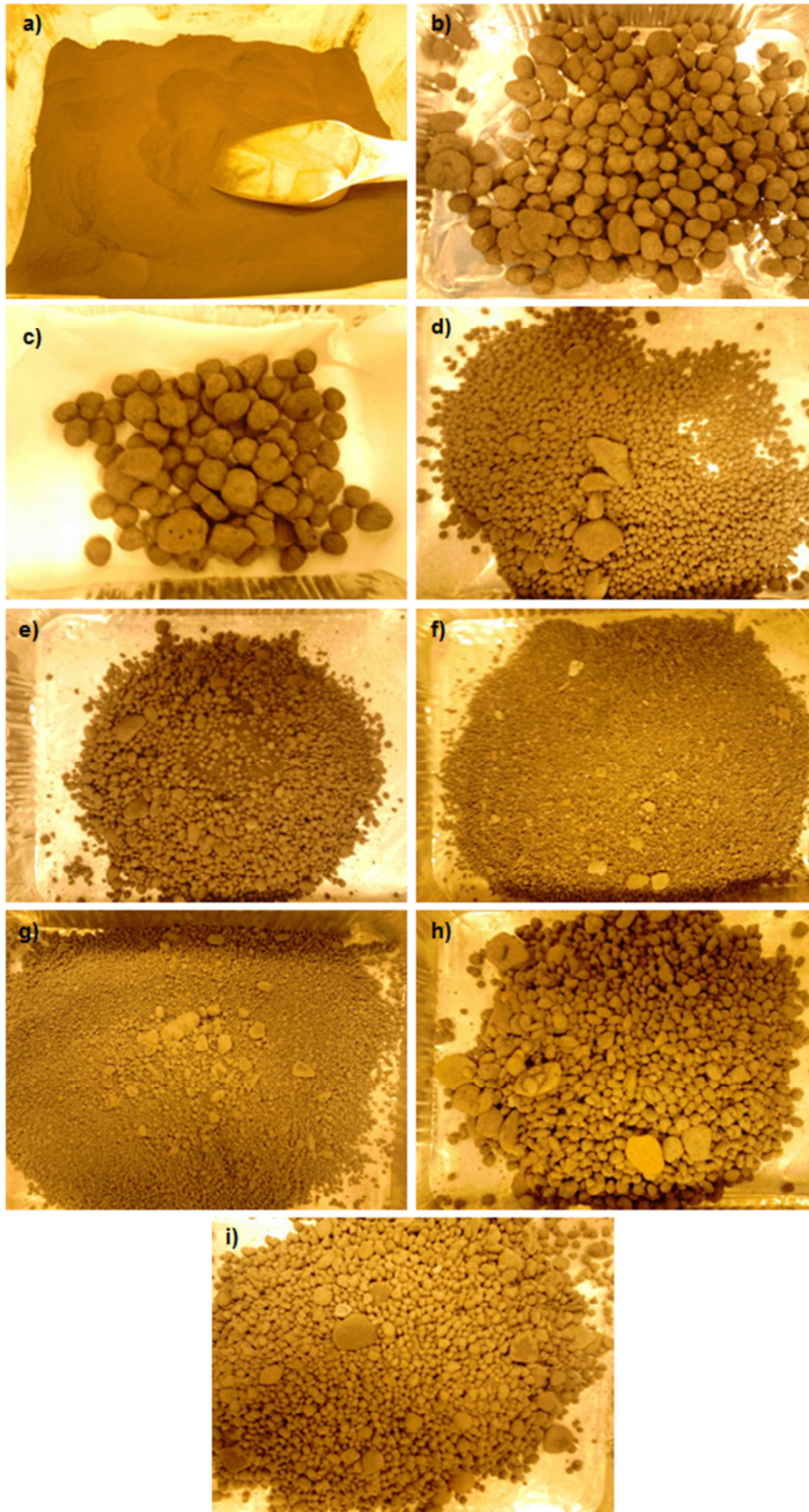


**Figure 3-4** The generated granules: a) Untreated material b)  $G30'_{W} W/S=0.12$ , c)  $G30'_{SS} W/S=0.12$ , d)  $GC30'_{W} W/S=0.12$ , e)  $GC60'_{W} W/S=0.12$ , f)  $GC30'_{SS} W/S=0.12$ , g)  $GC60'_{SS} W/S=0.12$ , h)  $GC30'_{SS} W/S=0.14$ , and i)  $GC60'_{SS} W/S=0.14$ .

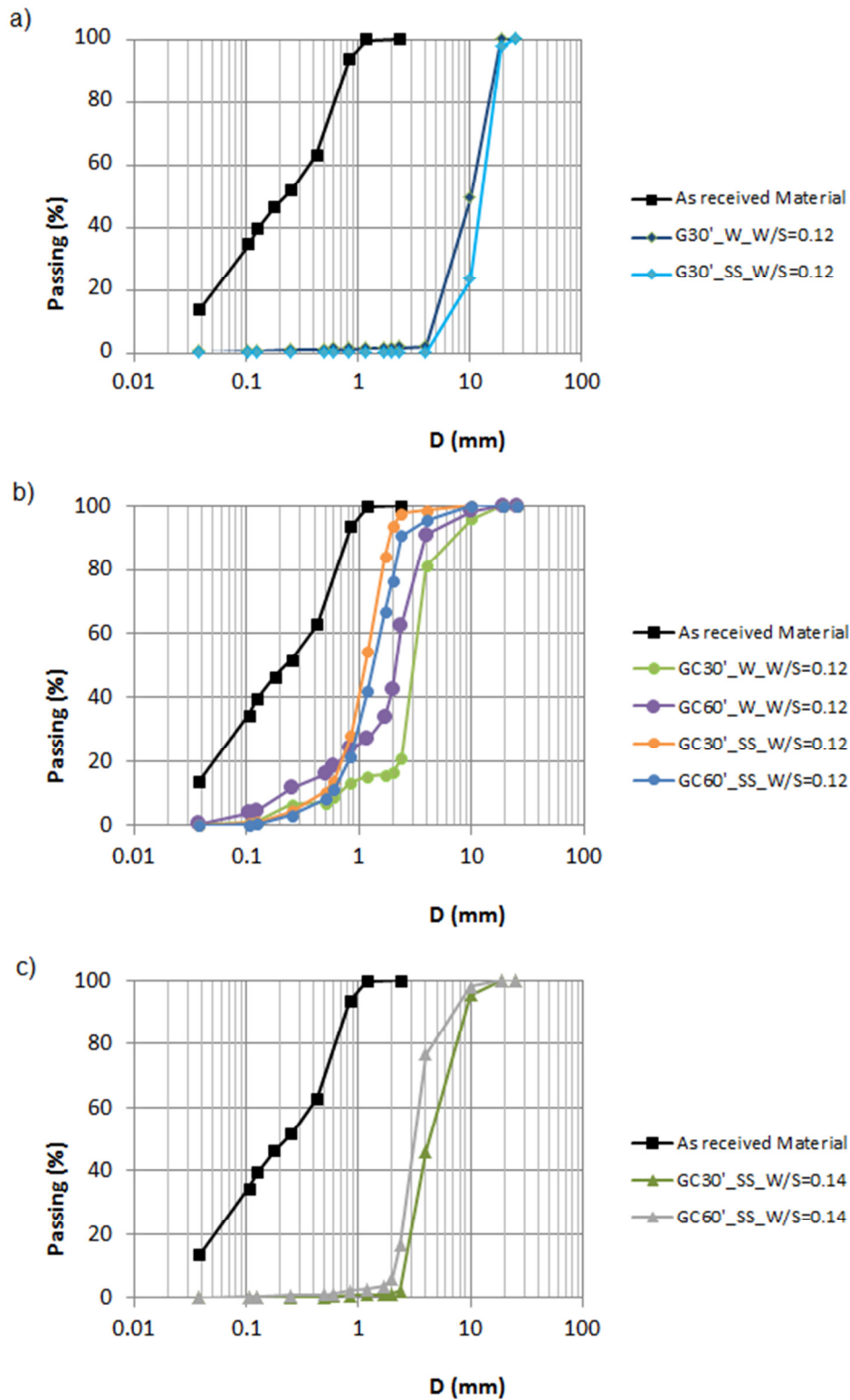


**Figure 3-5 PSD analysis diagrams for the untreated material and the granules produced by a) granulation and granulation-carbonation treatments at b) W/S = 0.12 L/kg and c) W/S = 0.14 L/kg [136].**

**Table 3-6 The  $d_{50}$  values of the untreated material and the produced granules**

Test	$d_{50}$ (mm)
Untreated BOF	0.2
G30' _W_ W/S=0.12	10.2
G30' _SS_ W/S=0.12	13.3
GC30' _W_ W/S=0.12	3.2
GC60' _W_ W/S=0.12	2.1
GC30' _SS_ W/S=0.12	1.1
GC60' _SS_ W/S=0.12	1.3
GC30' _SS_ W/S=0.14	4.5
GC60' _SS_ W/S=0.14	3.3

The impact of reaction time on the size of the produced granules as a function of the applied liquid binder type was investigated for the combined treatment of the slag and W/S ratio of 0.12 L/kg (Figure 3-7). According to the results, treatment duration had only a negligible effect on the size of the granules formed using the alkaline activator. In fact, by increasing the duration of the combined treatment from 30 to 60 minutes, the mean diameter of the synthesized granules got only slightly increased (from 1.1 to 1.3 mm). On the other hand, when DI water was employed as the wetting agent, granules of lower diameters were formed after the longer treatment period. More specifically, by increasing the treatment duration from 30 to 60 minutes, the mean diameter of the produced granules decreased from 3 to 2 mm. According to literature, generally, prolonged granulation periods have a positive impact on the size of the finally formed granules, as long as the breakage stage of the agglomeration process is not reached [174, 177-181].

Apparently, in the case of water-based granules, the point at which water-based bonds could no longer hold the enlarged granules together was reached sooner than in the case of the alkali activated process and breakage phenomena occurred before the end of its prolonged treatment, creating granules of lower sizes than those obtained after the shorter tested period.

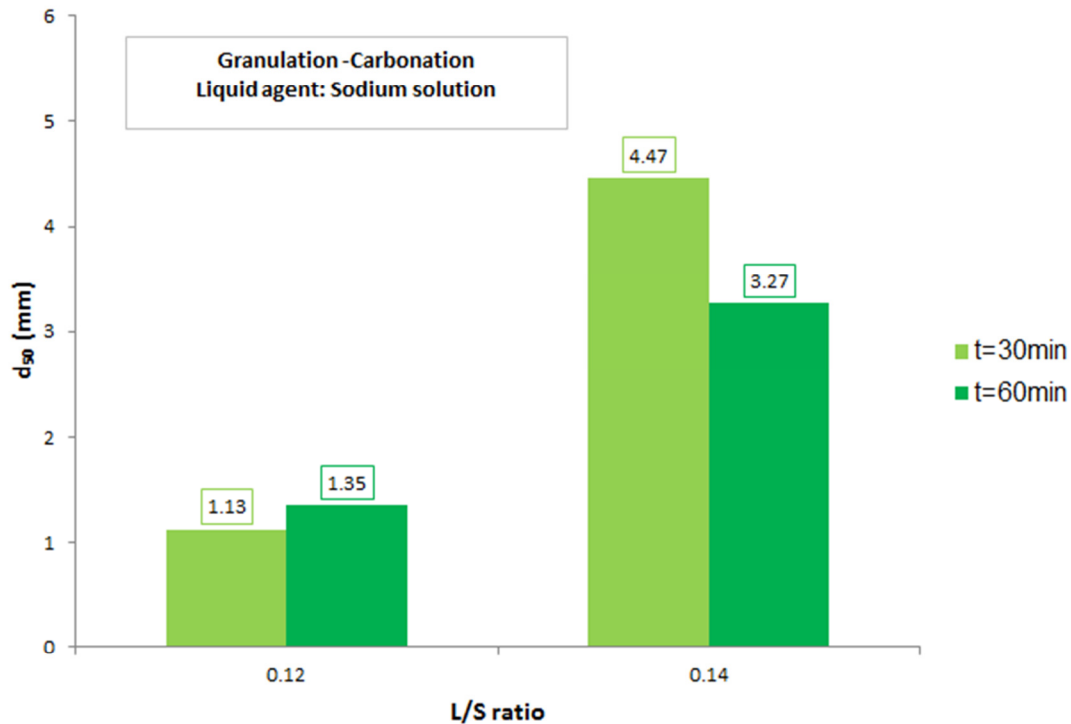


**Figure 3-6 The effect of reaction time on the  $d_{50}$  value of the samples generated from the combined treatment.**

The effect of reaction time on the size of the granules formed after the combined treatment of the alkali activated material, was also assessed employing higher amounts of alkali solution ( $W/S = 0.14$  L/kg) (Figure 3-6). Contrarily to the case of the lower  $W/S$  ratio, for  $W/S$  of 0.14 L/kg, increased treatment duration led to the formation of granules with lower size. The particular behavior should also be ascribed to breakage phenomena occurring during granulation.

The increased amount of binder resulted in the production of granules with greater sizes within shorter periods of time, reaching the breaking point earlier than when lower  $W/S$  ratio (0.12 L/kg) was used, and surely before 60 minutes. In any case, after both treatment periods (30 and 60 minutes), the mean diameters of the granules obtained by the combined granulation-carbonation of the BOF slag applying the higher  $W/S$  ratio (0.14 L/kg), were remarkably greater (4 times after 30 minutes and 2.5 times after 60 minutes of reaction) than those resulting from the combined treatment of the slag using the lower  $W/S$  ratio (0.12 L/kg).

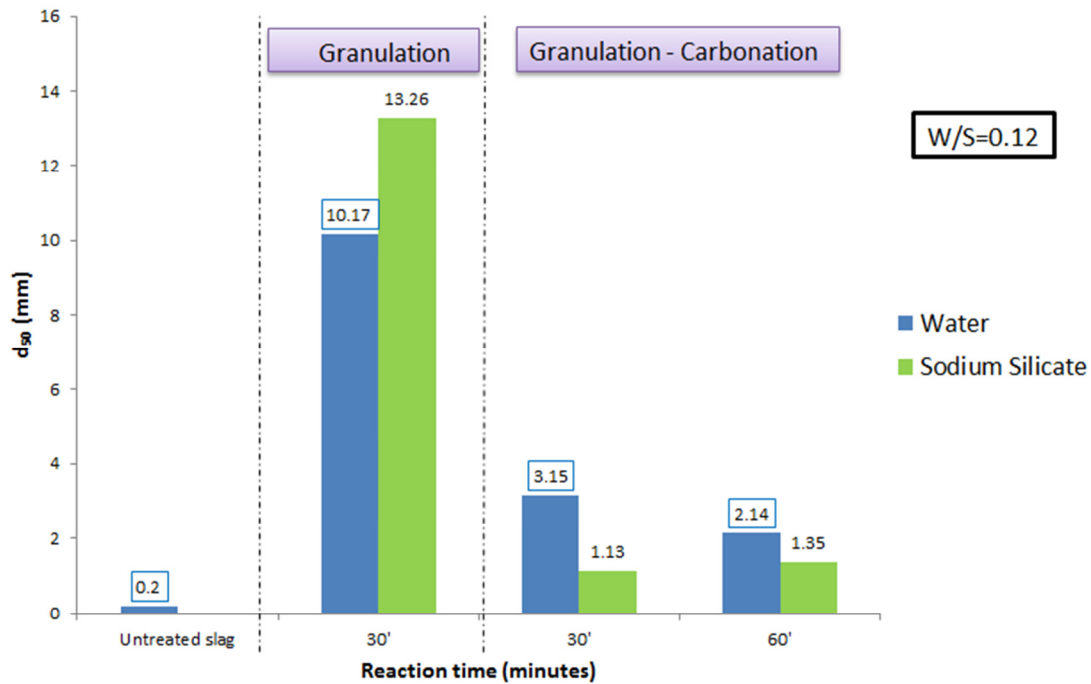


**Figure 3-7 Comparative diagram displaying the effect of the different treatments and the different liquid binders at a stable L/S ratio equal to 0.12 L/kg, on the  $d_{50}$  values of the treated samples.**

### 3.4.2. CO<sub>2</sub> uptake estimation

As already discussed, the materials resulting from the granulation and granulation-carbonation tests were subjected to IC analysis in triplicates. This implies that for each treated material, three different %IC measurements were available. The calculation of %CaCO<sub>3</sub>, %CO<sub>2</sub> (final) and %CO<sub>2</sub> uptake (final) values was made based upon the average of these measurements. In particular, %CO<sub>2</sub> uptake was calculated based on the final CO<sub>2</sub> content of the sample and the amount of CO<sub>2</sub> that was initially present in it. This implies that potential uncertainties in the calculated values of %CO<sub>2</sub> uptake have their source either in the preparation of the material for analysis or in the IC measurements conduction process.

A potential source of error during the preparation of the material may be its improper weighing prior to its subsection to IC analysis. The IC instrument calculates the tested material's IC content based, among others, on its weight, and a potential inaccurate weighing of the sample would cause a measurement error. Inaccurate material weighing may have been caused by a potential improper calibration of the used balance or by the operator's

misjudgement. According to the manufacturer, to minimize such errors, but also to secure the even distribution of the slag carbon content within the tested material, its amount should be below 1 gram. In this study, the IC analyses were conducted using each time, 0.2 grams of the examined material and its weighing was made with high accuracy (+0.0001 g) using recently calibrated balances.

Errors owed to a potential uncalibrated IC analysis instrument or a malfunction of it may also have an impact on the conducted measurements accuracy. To avoid such errors, the instrument used in this work was regularly calibrated and it was daily checked for its precision by using standard materials of known IC content.

The %IC, %CaCO<sub>3</sub> and %CO<sub>2</sub> content of the treated material, as well as the average %CO<sub>2</sub> uptakes achieved after all the tested treatments and curing periods are presented in Table 3-7.

The %IC values are reported along with their standard errors of the mean, as an indication of the measurements repeatability, whereas the values of %CaCO<sub>3</sub>, %CO<sub>2</sub> final and %CO<sub>2</sub> uptake are accompanied by their uncertainties caused by the aforementioned experimental or instrumental errors. Especially in the case of %CO<sub>2</sub> uptakes, the herein reported uncertainties have been calculated following the error propagation method [182]. The particular method is used when a value is a function of other parameters with certain uncertainties, which apparently propagate to the uncertainty of the value. According to the particular method, the manner in which the error of such a value is calculated depends on the type of the equation that describes it and more specifically, on whether the parameters of known uncertainties are multiplied, divided, summed or deducted.

According to the results, each treatment affected the carbonation of the material in a different manner. The CO<sub>2</sub> uptakes achieved after all the tested treatments and zero days of curing are depicted in Figure 3-8. As expected, the combined granulation-carbonation treatment produced granules of BOF slag with significantly higher carbonate content than those generated from the granulation process.

**Table 3-7 IC analysis results of the granules formed after the granulation and granulation-carbonation of the BOD slag**

Sample Name	%IC	%CaCO <sub>3</sub>	%CO <sub>2</sub> (final)	%CO <sub>2</sub> (uptake)
<b>Granulation and Granulation-Carbonation experiments (0 days)</b>				
<b>G30_W_W/S=0.12</b>	0.095±0.007	0.79±0.04	0.35±0.02	<b>0.25±0.01</b>
<b>G30_SS_W/S=0.12</b>	0.158±0.004	1.32±0.07	0.58±0.03	<b>0.48±0.02</b>
<b>GC30_W_W/S=0.12</b>	0.660±0.014	5.50±0.28	2.42±0.12	<b>2.38±0.09</b>
<b>GC60_W_W/S=0.12</b>	0.771±0.006	6.42±0.32	2.83±0.14	<b>2.80±0.11</b>
<b>GC30_SS_W/S=0.12</b>	0.811±0.012	6.76±0.34	2.97±0.15	<b>2.96±0.12</b>
<b>GC60_SS_W/S=0.12</b>	0.903±0.008	7.53±0.38	3.31±0.17	<b>3.32±0.13</b>
<b>GC30_SS_W/S=0.14</b>	0.492±0.004	4.10±0.20	1.80±0.09	<b>1.73±0.07</b>
<b>GC60_SS_W/S=0.14</b>	0.779±0.005	6.49±0.32	2.86±0.14	<b>2.84±0.11</b>
<b>Granulation and Granulation-Carbonation experiments (7 days)</b>				
<b>G30_W_W/S=0.12</b>	0.147±0.006	1.23±0.06	0.54±0.03	<b>0.54±0.02</b>
<b>G30_SS_W/S=0.12</b>	0.188±0.002	1.57±0.08	0.69±0.03	<b>0.69±0.03</b>
<b>GC30_W_W/S=0.12</b>	0.686±0.018	5.72±0.29	2.52±0.13	<b>2.52±0.10</b>
<b>GC60_W_W/S=0.12</b>	0.802±0.010	6.68±0.33	2.94±0.15	<b>2.94±0.12</b>
<b>GC30_SS_W/S=0.12</b>	0.851±0.014	7.10±0.35	3.12±0.16	<b>3.12±0.12</b>
<b>GC60_SS_W/S=0.12</b>	1.090±0.014	9.08±0.45	4.00±0.20	<b>4.00±0.16</b>
<b>GC30_SS_W/S=0.14</b>	0.581±0.007	4.84±0.24	2.13±0.11	<b>2.13±0.08</b>
<b>GC60_SS_W/S=0.14</b>	0.771±0.009	6.43±0.32	2.83±0.14	<b>2.83±0.11</b>
<b>Granulation and Granulation-Carbonation experiments (28 days)</b>				
<b>G30_W_W/S=0.12</b>	0.191±0.010	1.59±0.08	0.70±0.03	<b>0.70±0.03</b>
<b>G30_SS_W/S=0.12</b>	0.138±0.008	1.15±0.06	0.51±0.03	<b>0.51±0.02</b>
<b>GC30_W_W/S=0.12</b>	0.629±0.006	5.25±0.26	2.31±0.12	<b>2.31±0.09</b>
<b>GC60_W_W/S=0.12</b>	0.689±0.010	5.74±0.29	2.52±0.13	<b>2.52±0.10</b>
<b>GC30_SS_W/S=0.12</b>	0.808±0.003	6.73±0.34	2.96±0.15	<b>2.96±0.12</b>
<b>GC60_SS_W/S=0.12</b>	1.075±0.047	8.96±0.45	3.94±0.20	<b>3.94±0.15</b>
<b>GC30_SS_W/S=0.14</b>	0.569±0.019	4.74±0.24	2.09±0.10	<b>2.09±0.08</b>
<b>GC60_SS_W/S=0.14</b>	0.779±0.002	6.49±0.32	2.85±0.14	<b>2.85±0.11</b>

Generally, the CO<sub>2</sub> uptakes achieved by the granules formed right after the granulation treatment were very low (< 0.5%), irrespectively to the applied type of liquid binder. In the contrary, granules obtained right after the combined treatment of the slag exhibited CO<sub>2</sub> uptakes ranging between 1.73

and 3.32 %, with the higher values attributed to the granules containing the alkaline solution.

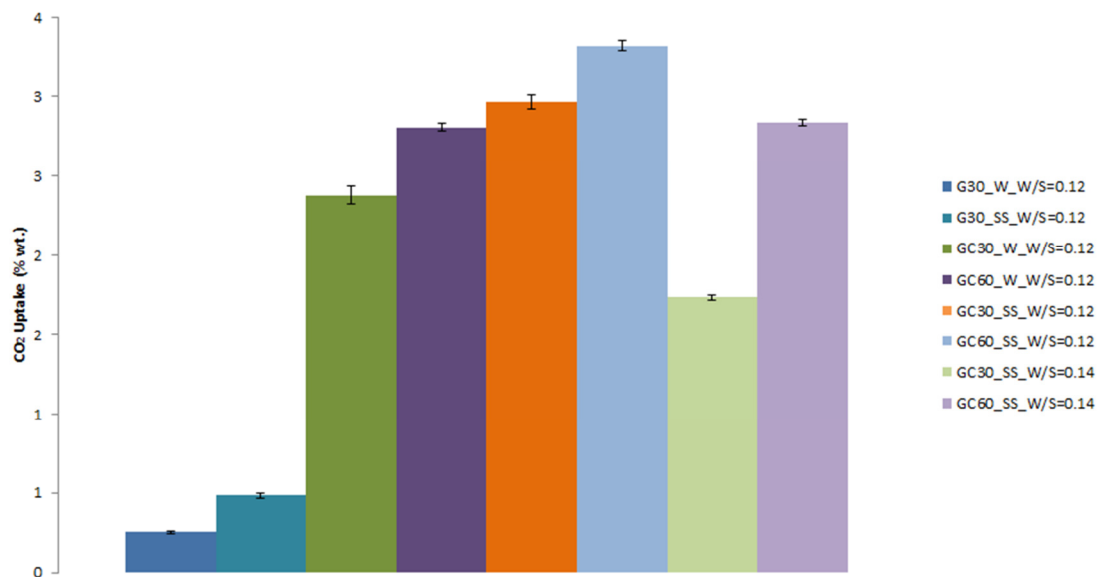


**Figure 3-8 CO<sub>2</sub> Uptake of the granules produced by the different tested treatments [136].**

The effect of reaction time on the achieved CO<sub>2</sub> uptake was studied in the case of the combined treatment. According to the results, longer carbonation periods positively affected the carbonation extent of the formed granules, regardless of the employed liquid agent (DI water or sodium solution). By increasing the reaction time from 30 to 60 minutes, using water as the binding solution and for W/S ratio of 0.12, the achieved CO<sub>2</sub> uptakes were increased from 2.38 to 2.8 %. Similar were the effects of increasing treatment period on the CO<sub>2</sub> uptakes achieved by granules containing alkaline solution. In the particular case, for the same reaction time extension (from 30 to 60 minutes) the obtained CO<sub>2</sub> uptakes increased from 2.96 to 3.32 %.

The amount of the alkaline activator also appeared to affect the CO<sub>2</sub> uptake achieved by the combined granulation-carbonation treatment of the slag. According to the results, by increasing the amount of sodium solution in the system (from W/S = 0.12 L/kg to W/S = 0.14 L/kg), the finally achieved CO<sub>2</sub> uptake was decreased. The particular behavior was more pronounced for the 30 min tests, where by increasing the W/S ratio of the granulating system, the achieved CO<sub>2</sub> uptake decreased from 2.96 % to 1.73 %. The higher amount

of liquid binder must have had an impact on the attained CO<sub>2</sub> uptake. As aforementioned, in case that the W/S ratio of a carbonating system exceeds an optimum value, its ionic strength gets decreased and thereupon the finally achieved carbonation extent attenuates.

The curing period of the formed granules is another factor that was found affecting the extent of carbonation. In order to assess the influence of curing period on the finally achieved CO<sub>2</sub> uptake, granules obtained after each of the performed tests were collected after 7 and 28 days of curing and subjected to IC analysis.

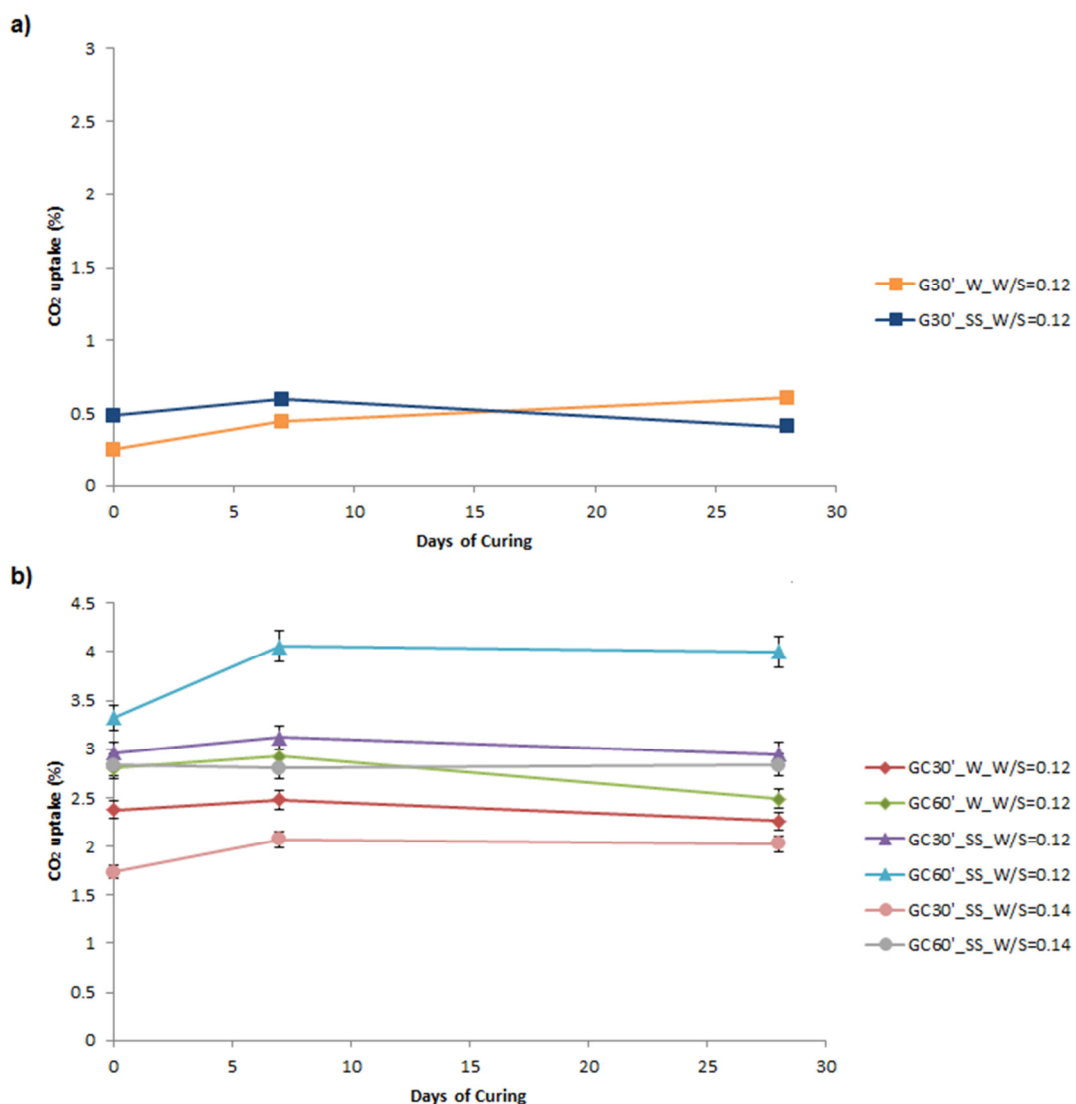


**Figure 3-9 CO<sub>2</sub> uptake with curing time of the granules obtained after a) granulation and b) granulation-carbonation treatments [136].**

According to the results, the effect of curing period on the CO<sub>2</sub> uptake was dependent on the type of treatment and its duration (Figure 3-9).

It was found that for granules obtained after 30 minutes of granulation or combined granulation-carbonation, and regardless of the employed type of liquid binder, the CO<sub>2</sub> uptake was slightly increased after 7 days of curing and remained stable thereafter. On the other hand, granules formed after 60 minutes of the combined treatment did not present any CO<sub>2</sub> uptake increase after 7 or 28 days. It could be concluded that every phase of the tested BOF slag that can be carbonated under ambient conditions reacts completely after 60 minutes of combined granulation-carbonation or after 30 minutes of either of the treatments (granulation or granulation-carbonation) and a small period of curing (equal to or less than 7 days).

In any case, compared to the CO<sub>2</sub> uptakes achieved by Morone et al. [41], the ones achieved by the combined granulation-carbonation treatment of the BOF slag in the present study were remarkably lower. This should be basically ascribed to the different mineralogy characterizing the two types of slags; as already mentioned, the slag used in this study was characterized by high amounts of calcium-silicate based phases, while the one investigated in the work of Morone et al. [41], contained relevant amounts of portlandite, that is well known for its reactivity with CO<sub>2</sub> even under mild conditions [138]. The presence of the particular phase in the composition of the slag used in the study of Morone et al. [41] should be responsible for the higher amounts of CO<sub>2</sub> stored by it.

#### **3.4.2.1. Assessment of the investigated treatment performance as a CO<sub>2</sub> emissions mitigation process**

In 2015 the total production of steel worldwide was 1617.3 Mt, from which 1203.3 Mt was generated through the BOF process [185]. Based on the fact that the BOF slag formed per ton of BOF steel is equal to 150-200 kg [76], it could be inferred that on average, 180.5 - 240.65 Mt of BOF slag were produced in the same year.

According to literature, the highest CO<sub>2</sub> capture capacity of BOF slag was reported by Chang et al. [39] and it was equal to 290 g CO<sub>2</sub>/kg of BOF slag. By applying this value to the annual production of BOF slag for the year of 2015, the potential mitigation of CO<sub>2</sub> emissions to the atmosphere was found to be on average, 52.35 – 69.8 Mt/a, a range of values well below the total annual global CO<sub>2</sub> emissions (approximately 40 Gt CO<sub>2</sub>/a [9]). This is why, in general, any carbonation treatment of the particular material should only be considered as a method to substantially reduce the CO<sub>2</sub> emissions of the specific industrial sector (BOF steel making industry) and not as a solution for the global CO<sub>2</sub> emissions issue.

In this study, the maximum CO<sub>2</sub> uptake achieved was equal to 40g CO<sub>2</sub>/kg of BOF slag, and the corresponding potential CO<sub>2</sub> mitigation was calculated to be on average, 7.22 – 9.63 Mt of CO<sub>2</sub>/a. However, the agglomerates to which the particular amount of stored CO<sub>2</sub> should be attributed are granules that mainly due to their low compressive strength, were reported as unsuitable for secondary aggregates use. The agglomerates that were found to be the most suitable for construction aggregates use were the ones resulting from the GC30'\_SS\_W/S=0.14 treatment. The potential CO<sub>2</sub> emissions mitigation corresponding to these granules was calculated based on the CO<sub>2</sub> uptake achieved by them (40g CO<sub>2</sub>/kg of BOF slag) and was found ranging between 3.61 – 4.81 Mt.

Apparently, none of the herein investigated treatments was capable of significantly contributing to the global CO<sub>2</sub> emissions mitigation effort. In fact, based on the current results, the subjection of BOF slag to the proposed technology has a negligible contribution to the goal set at the Paris climate conference (COP21) that calls for zero anthropogenic greenhouse gas emissions during the second half of 21<sup>st</sup> century [5]. In addition, the fact that the CO<sub>2</sub> uptakes achieved in this work were remarkably lower compared to the highest reported ones for BOF slags [39], puts in question the ability of the process to substantially reduce the CO<sub>2</sub> emissions resulting from the particular industrial sector. In order for the proposed technique to be considered as a process capable of substantially reducing the CO<sub>2</sub> emissions correlated to the production of steel through the BOF route and thereupon, to

increase its potential to get commercialized, the CO<sub>2</sub> capture capacity of the granules formed by the GC30'\_SS\_W/S=0.14 test should get remarkably improved. This could be attained by adding a pretreating stage of the material (grinding) and by applying different experimental conditions that have been reported to improve the finally achieved CO<sub>2</sub> uptake of the treated material.

In any case, it has to be noted that the goal of this part of the research was the sequestration of sufficient amounts of CO<sub>2</sub> through the transformation of BOF slag into granules with satisfactory strength, sufficient size, volume stability and limited leaching, in order to be used as aggregates in construction applications. As a result, the requirement to find out the way that each of the proposed mechanisms affects the other characteristics of the granules should be highlighted. It is of critical importance to achieve CO<sub>2</sub> uptake enhancement without damaging any of the other qualities of the granules that are vital for their use as aggregates. In any other case, the CO<sub>2</sub> uptake improvement would be of no meaning for the purposes of this study.

The difference between the highest reported CO<sub>2</sub> uptake achieved by BOF slag (290 g CO<sub>2</sub>/kg of BOF slag [39]) and the amount of CO<sub>2</sub> sequestered by the granules formed in this work and have been found to be of sufficient quality for construction aggregates use (20g CO<sub>2</sub>/kg of BOF slag), should be mainly attributed to the different carbonation mechanisms applied in each case. In particular, the CO<sub>2</sub> uptake reported by Chang et al. [39] was achieved after the slurry carbonation (L/S ratio: 20 L/kg) of BOF slag, whereas the limited CO<sub>2</sub> conversion reported in this study was achieved after the wet carbonation (L/S ratio: 0.14 L/kg) of the material.

The increase of the amount of sodium solution employed in the test could be an option towards bridging the significant difference between these two CO<sub>2</sub> uptake values. However, in the proposed technique, carbonation is coupled with granulation and it has been experimentally found that at W/S ratios higher than 0.14 L/kg the process is incapable of turning the mixture into granules and, instead, a muddy material is formed. Consequently, although the addition of higher amounts of sodium solution to the system could lead to carbonation conversion escalation, the particular solution cannot be applied to

the specific technique due to its detrimental impact on the granulation process.

On the other hand, the grinding of BOF slag prior to its subsection to the combined granulation-carbonation treatment is very likely to cause a significant enhancement of the finally achieved CO<sub>2</sub> uptake. According to literature but also based on the results of the batch carbonation tests performed in this study, by decreasing the particle size of the treated material, its specific surface area gets increased and the carbonation conversion gets remarkably enhanced [36, 38]. In this work, the BOF slag used in the granulation-carbonation experiments presented a d<sub>50</sub> value of 0.2 mm and was not subjected to milling prior to experimentation. The grinding of the material to lower diameters, while keeping the rest of the experimental parameters steady, would certainly lead to higher conversion values. However, in order for the granulation-carbonation process to be successful, in case that milled BOF slag was employed to the process, additional alterations to other parameters of the proposed technology should have been applied. For instance, it is well known that by decreasing the particle size of the granulated material, additional amount of liquid binder is required in order for the smaller particles to get efficiently granulated. Clearly, the way that BOF slag milling may influence the whole process has to be carefully examined in order to make sure that increased carbonation conversion will be achieved with the other qualities of the formed granules remaining unaffected, if not improved.

The experiments held in this study were performed using a disc granulator and applying a rotating speed of 24 rpm. According to literature, higher mixing speeds have been proved to facilitate the carbonation of slurry systems by improving the mass transfer between the CO<sub>2</sub> and the slurry and the diffusion of Ca<sup>2+</sup> from the slag particles to the solution [36, 39]. However, as already mentioned, in the investigated process, the wet route of carbonation was followed and consequently, higher mixing speeds would not improve the carbonation rate or extent the way it has been found to do in slurry reactors. Nonetheless, the particle abrasion that should take place at mixing speeds

significantly higher than that applied in the particular experiment could improve the carbonation conversion of the slag.

The increase of treatment duration up to a point has also been found to have a positive effect on the level of the finally sequestered CO<sub>2</sub> by BOF slag [36, 37, 39, 112, 113]. Indeed, by prolonging the treatment period of the particular test from 30 to 60 minutes, the extent of carbonation was found to get increased. Based on this finding, but also on the results of the batch carbonation tests applied on the same material under similar conditions but using a static reactor, which show the carbonation conversion to continuously increase with increased reaction period up to 8 hours, it could be inferred that a treatment duration increase could aid the improvement of carbonation conversion extent. However, the prolonged treatment period should be carefully selected in order to avoid any negative impact on the size of the finally formed agglomerates. As already discussed, if granulation period is long enough to allow the breaking stage of granulation to occur, granules of lower diameters are formed [150, 153-157] and aggregates size issues may arise.

CO<sub>2</sub> pressure could also affect the finally achieved CO<sub>2</sub> uptake. However, its influence on the BOF slag carbonation extent has been found to be dependent on several other parameters, such as the applied temperature or the stirring speed [36, 38, 115]. The CO<sub>2</sub> pressure applied in the tests of this research was selected to be equal to 1 bar. The increased CO<sub>2</sub> pressure may be found to improve the sequestration of CO<sub>2</sub> in the formed granules. However, as in the cases of mixing speed and treatment duration, the increased cost of the process may not be worth the improvement from a CO<sub>2</sub> sequestration point of view.

Finally, temperature has also been found to affect the carbonation conversion of BOF slag. In particular, it has been reported that by increasing the temperature up to an optimum value, both the carbonation rate and extent also get increased [36, 37, 38, 39, 112-114]. Due to the lack of a system to adjust the temperature in the granulator, the influence of temperature on the finally achieved CO<sub>2</sub> uptake was not studied in this work. However, based on

results reported in literature, it is unlikely for temperature alterations to significantly affect the carbonation conversion achieved. The positive effect of temperature on the carbonation extent of the treated material has only been reported for slurry reactors. In the case of wet carbonation, temperature enhancement has been found to only have a negligible effect on the finally achieved CO<sub>2</sub> uptake [113, 131].

### 3.4.2.2. Batch carbonation tests and CWR estimation

In an effort to discover the way that different operating conditions may influence the extent of BOF slag carbonation, but also to determine the manner with which the employed type of treatment (granulation-carbonation) affected the carbonation extent of the produced granules, batch carbonation tests were also carried out. The identity of the experiments is presented in Table 3-8.

As can be observed, three different types of batch carbonation tests were performed. In every one of them, 100% CO<sub>2</sub> was employed on the as received and milled (ranging between 0.038mm and 0.125 mm) BOF slag, at a mild (T = 20 °C, pCO<sub>2</sub> = 1 bar, L/S = 0.3 L/kg) or enhanced (T = 50 °C, pCO<sub>2</sub> = 10bar, L/S = 0.3 L/kg) set of operating conditions.

Batch carbonation tests on the milled material under mild operating conditions employing the alkaline solution as the wetting agent, were also conducted. All types of experiments were carried out for different reaction times (30, 60, 120, 240 and 480 minutes).

The average %IC, as well as the %CaCO<sub>3</sub>, %CO<sub>2</sub>(final) and %CO<sub>2</sub> uptake values achieved after all the batch carbonation tests are reported in Table 3-9. These results are also depicted in Figure 3-10. The %IC values are reported with their standard errors of the mean, whereas the %CaCO<sub>3</sub>, %CO<sub>2</sub> and %CO<sub>2</sub> uptake are accompanied by their uncertainties. The sources of these uncertainties are the same as the ones discussed in the case of the granulation and granulation-carbonation experiments (section 3.4.2.), and have been calculated according to the error propagation method [182].

Table 3-8 The identity of batch carbonation tests

Sample Name	Sample Type	Liquid Agent	Duration	Temperature	CO <sub>2</sub> Pressure
<b>B30MA</b>	As received	DI Water	30 mins	20 °C	1 bar
<b>B1HA</b>	As received	DI Water	60 mins	20 °C	1 bar
<b>B2HA</b>	As received	DI Water	120 mins	20 °C	1 bar
<b>B4HA</b>	As received	DI Water	240 mins	20 °C	1 bar
<b>B8HA</b>	As received	DI Water	480 mins	20 °C	1 bar
<b>M30MA</b>	Milled	DI Water	30 mins	20 °C	1 bar
<b>M1HA</b>	Milled	DI Water	60 mins	20 °C	1 bar
<b>M2HA</b>	Milled	DI Water	120 mins	20 °C	1 bar
<b>M4HA</b>	Milled	DI Water	240 mins	20 °C	1 bar
<b>M8HA</b>	Milled	DI Water	480 mins	20 °C	1 bar
<b>SSM30MA</b>	Milled	Na-solution	30 mins	20 °C	1 bar
<b>SSM1HA</b>	Milled	Na-solution	60 mins	20 °C	1 bar
<b>SSM2HA</b>	Milled	Na-solution	120 mins	20 °C	1 bar
<b>SSM4HA</b>	Milled	Na-solution	240 mins	20 °C	1 bar
<b>SSM8HA</b>	Milled	Na-solution	480 mins	20 °C	1 bar
<b>B30ME</b>	As received	DI Water	30 mins	50 °C	10 bar
<b>B1HE</b>	As received	DI Water	60 mins	50 °C	10 bar
<b>B2HE</b>	As received	DI Water	120 mins	50 °C	10 bar
<b>B4HE</b>	As received	DI Water	240 mins	50 °C	10 bar
<b>B8HE</b>	As received	DI Water	480 mins	50 °C	10 bar
<b>M30ME</b>	Milled	DI Water	30 mins	50 °C	10 bar
<b>M1HE</b>	Milled	DI Water	60 mins	50 °C	10 bar
<b>M2HE</b>	Milled	DI Water	120 mins	50 °C	10 bar
<b>M4HE</b>	Milled	DI Water	240 mins	50 °C	10 bar
<b>M8HE</b>	Milled	DI Water	480 mins	50 °C	10 bar

According to the results of the batch carbonation tests, the different operating conditions (mild and enhanced) applied during the carbonation of both the as received and milled material did not result in significantly different carbonation yields.

Table 3-9 IC analysis results of the batch carbonation products

Sample Name	%IC	%CaCO <sub>3</sub>	%CO <sub>2</sub> (final)	%CO <sub>2</sub> (uptake)
<b>As received Material, Mild Conditions (T = 25 °C, pCO<sub>2</sub> = 1 bar)</b>				
B30MA	0.432±0.017	3.60±0.18	1.59±0.08	1.51±0.06
B1HA	0.409±0.014	3.41±0.17	1.50±0.07	1.42±0.06
B2HA	0.800±0.014	6.67±0.33	2.93±0.15	2.92±0.12
B4HA	0.948±0.014	7.90±0.39	3.48±0.17	3.50±0.14
B8HA	1.357±0.006	11.31±0.57	4.98±0.25	5.13±0.20
<b>Milled Material, Mild Conditions (T = 25 °C, pCO<sub>2</sub> = 1bar)</b>				
M30MA	1.259±0.006	10.49±0.52	4.62±0.23	4.73±0.19
M1HA	1.363±0.017	11.36±0.57	5.00±0.25	5.16±0.20
M2HA	2.373±0.122	19.78±0.99	8.70±0.44	9.43±0.37
M4HA	2.768±0.057	23.07±1.15	10.15±0.51	11.19±0.44
M8HA	3.057±0.021	25.47±1.27	11.21±0.56	12.51±0.49
<b>Milled Material, Mild Conditions (T = 25 °C, pCO<sub>2</sub> = 1bar), Sodium Solution</b>				
SSM30MA	1.622±0.003	13.52±0.68	5.95±0.30	6.22±0.24
SSM1HA	1.898±0.005	15.81±0.79	6.96±0.35	7.37±0.29
SSM2HA	2.104±0.038	17.54±0.88	7.72±0.39	8.25±0.32
SSM4HA	2.090±0.003	17.42±0.87	7.66±0.38	8.19±0.32
SSM8HA	2.427±0.052	20.23±1.01	8.90±0.44	9.66±0.38
<b>As received Material, Enhanced Conditions (T = 50 °C, pCO<sub>2</sub> = 10 bar)</b>				
B30ME	1.207±0.017	10.06±0.50	4.43±0.22	4.53±0.18
B1HE	1.276±0.005	10.63±0.53	4.68±0.23	4.80±0.19
B2HE	1.375±0.028	11.46±0.57	5.04±0.25	5.20±0.20
B4HE	1.598±0.026	13.32±0.67	5.86±0.29	6.12±0.24
B8HE	2.215±0.045	18.46±0.92	8.12±0.41	8.73±0.34
<b>Milled Material, Enhanced Conditions (T = 50 °C, pCO<sub>2</sub> = 10 bar)</b>				
M30ME	1.577±0.026	13.14±0.66	5.78±0.29	6.03±0.24
M1HE	1.978±0.042	16.48±0.82	7.25±0.36	7.71±0.30
M2HE	3.426±0.084	28.55±1.43	12.56±0.63	14.26±0.56
M4HE	3.722±0.014	31.01±1.55	13.65±0.68	15.69±0.62
M8HE	3.796±0.021	31.64±1.58	13.92±0.70	16.05±0.63

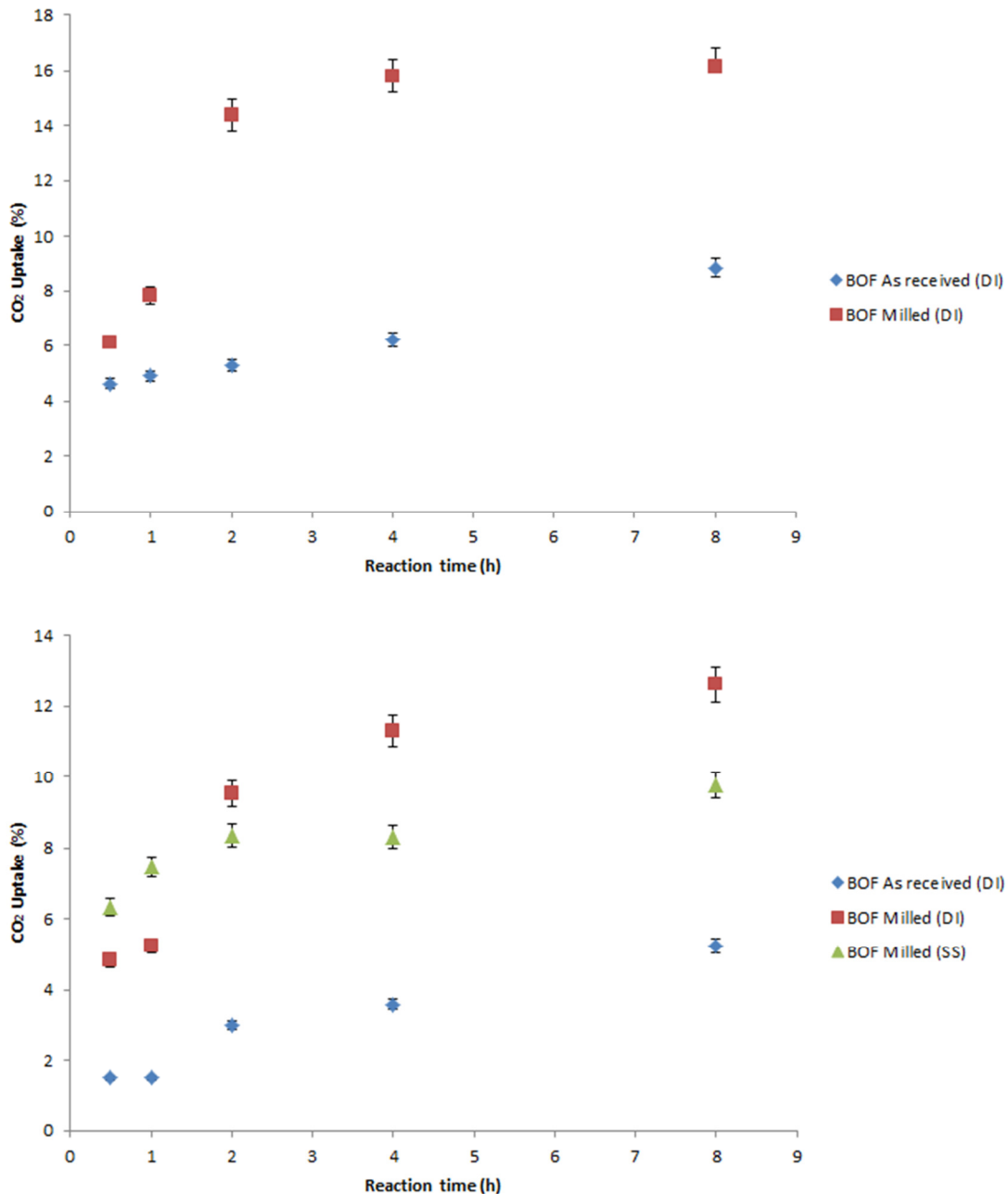


**Figure 3-10 CO<sub>2</sub> uptake kinetics of BOF slag resulted from the batch carbonation tests under a) enhanced (T = 50 °C, pCO<sub>2</sub> = 10 bar and L/S = 0.3 L/kg) conditions and b) mild (T = 20 °C, pCO<sub>2</sub> = 1 bar and L/S = 0.3 L/kg) [136].**

More specifically, the CO<sub>2</sub> uptakes achieved by the carbonation of the as received material at mild and enhanced operating conditions, after 8 hours of treatment were very close to each other (5.13 % vs 8.73 %). Similar results were exerted from the carbonation of the milled material at mild and enhanced conditions. In fact, after 8 hours of carbonation at enhanced conditions, the CO<sub>2</sub> uptake achieved by the milled material was just above 16 %, whereas at

mild conditions and after the same treatment period, this value got decreased to approximately 12.51 %.

On the other hand, the material's particle size and reaction duration were found to significantly affect the final CO<sub>2</sub> uptake achieved by the investigated BOF slag. In fact, the particle size of the treated material appeared to be one of the most decisive factors affecting its carbonation capacity. According to the results, for the same operating conditions, the milled sample exhibited considerably higher CO<sub>2</sub> uptakes than the as received material, after every tested carbonation period. The particular results agree with the literature review findings, according to which by decreasing the particle size of the tested material, its specific surface and thereupon the finally achieved CO<sub>2</sub> uptake, increases [31, 36].

The effect of carbonation duration on the finally achieved CO<sub>2</sub> uptake is presented in Figures 3-10a. and 3-10b. According to literature, for every carbonation system, there is a specific reaction duration, up to which the extent of carbonation increases with time. For reaction periods over the particular duration, the extent of carbonation remains unaffected, basically as a result of the slag particles' pore clogging caused by the precipitation of newly formed carbonates. This behavior was clearly exhibited by the milled material carbonated under enhanced conditions. In the particular case, the CO<sub>2</sub> uptake was increased with time for the first 4 hours of carbonation, and remained stable thereafter.

However, for carbonation tests carried out under mild conditions, CO<sub>2</sub> uptakes appeared to get continuously enhanced with time during the whole duration of the process (8 hours) and the plateau characterizing the materials that have reached their highest conversion point after a particular period of reaction, did not appear within the investigated reaction duration.

Apparently, in these cases the carbonation rate was notably lower compared to the one observed during the carbonation of BOF slag under enhanced conditions. As a result, longer reaction periods were required for the carbonation conversion to reach its maximum point and stabilize.

The influence of the different liquid agent types on the extent of BOF slag carbonation was assessed for the milled samples under mild conditions. The CO<sub>2</sub> uptake values obtained by the carbonation of milled samples under mild conditions, using the alkaline solution as a wetting agent are similar to the ones obtained for the milled samples treated under the same conditions without the alkaline additives. During the initial stages of treatment (up to 60 minutes), alkali activation appeared to have a positive influence on the extent of reactivity between the milled BOF slag and CO<sub>2</sub>, exhibiting CO<sub>2</sub> uptake values slightly higher than those achieved after using DI water. The particular results are consistent with those of the granulation-carbonation experiments.

However, alkali activation appeared to limit the extent of carbonation after longer carbonation periods (2, 4 and 8 hours), presenting CO<sub>2</sub> uptake values lower than those achieved after employing DI water as the wetting agent. Based on the particular findings, it could be inferred that the use of the alkaline activator instead of DI water as the liquid agent in the carbonation tests, hindered the long term reactivity of the material towards CO<sub>2</sub>.

Overall, the highest CO<sub>2</sub> uptake (16.17 %) was achieved by the carbonation of milled material, under enhanced operating conditions, and after 8 hours of reaction, using DI water as the liquid agent.

In Figure 3-11, a comparison between the CO<sub>2</sub> uptakes achieved by the combined treatment and those obtained by the batch carbonation tests is attempted. According to the results, for similar operating conditions ( $p_{CO_2} = 1$  bar and no temperature enhancement), the CO<sub>2</sub> uptakes achieved by the batch carbonation tests were almost two times lower than those achieved by the granulation-carbonation ones (around 1.5% compared to 2.23 and 2.85 % after 30 and 60 minutes of reaction, respectively). The particular finding is impressive, since in the case of the combined granulation-carbonation treatment a considerably higher amount of material (approximately 500 g) was tested compared to the 1 g of BOF slag treated in the batch reactor.

The dynamic device (disc granulator) employed in the combined granulation-carbonation tests must have improved the CO<sub>2</sub> diffusion kinetics and thereupon the carbonation reactions, remarkably increasing the achieved CO<sub>2</sub>

uptake after both the tested reaction periods (30 and 60 minutes), with respect to the static conditions applied during the batch carbonation tests.

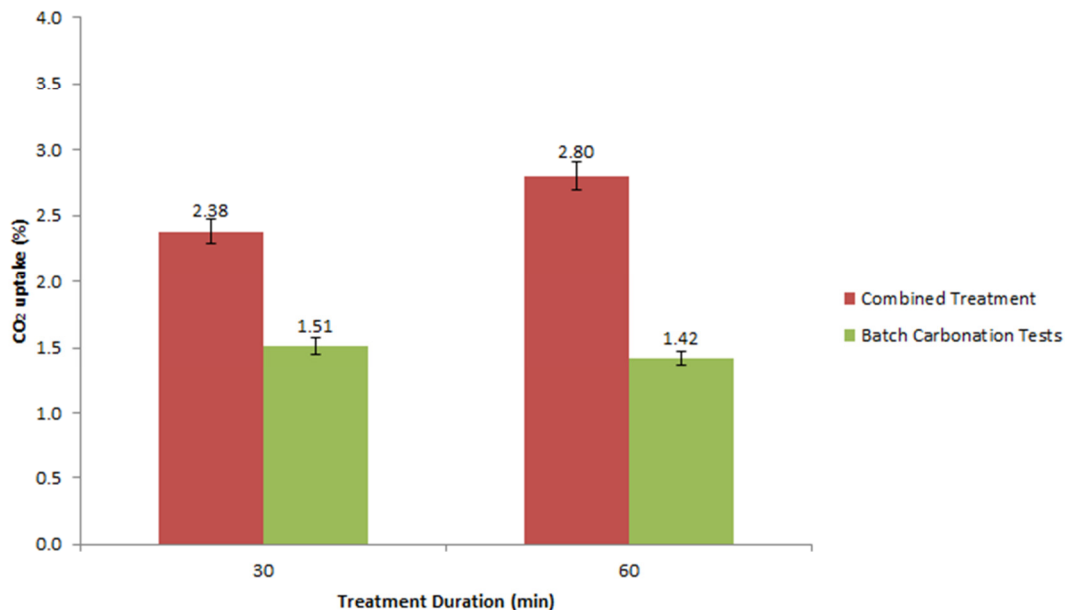


**Figure 3-11 Comparison between the CO<sub>2</sub> uptakes achieved by the batch carbonation tests (B30MA and B1HA) and the combined treatment (GC30'\_W\_W/S=0.12 and GC60'\_W\_W/S=0.12) of the as received BOF slag, as a function of reaction duration.**

To compare the reactivity of the BOF slag employed in this study, towards CO<sub>2</sub> with that of other slags of the same type that have been carbonated following the wet route in other studies in literature, the CWRs attained by each of the batch tests were calculated by applying Equation (2-3) to the results.

Based on the exerted CO<sub>2</sub> uptakes and the Ca and CaCO<sub>3</sub> content of the untreated BOF slag, the calcium conversion percentages of the carbonated materials were estimated using Equation (3-4). The particular values are required for the calculation of the CWRs achieved by the carbonation tests. The CO<sub>2</sub> uptakes, the carbonation conversions, as well as the CWRs of all the batch carbonation experiments are reported in Table 3-10. For reasons of simplicity, the CO<sub>2</sub> uptakes, the carbonation conversions achieved and the CWR values are reported without their uncertainties.

**Table 3-10 Carbonation conversions and CWRs achieved after the batch carbonation tests**

<b>Samples Name</b>	<b>CO<sub>2</sub> Uptake (%)</b>	<b>Conversion (%)</b>	<b>CWR (µm/min)</b>
<b>Fresh Material, Mild Conditions (T = 20 °C, pCO<sub>2</sub> = 1 bar)</b>			
<b>B30MA</b>	1.51	5.14	0.058
<b>B1HA</b>	1.42	4.84	0.027
<b>B2HA</b>	2.92	9.94	0.029
<b>B4HA</b>	3.50	11.90	0.017
<b>B8HA</b>	5.13	17.47	0.013
<b>Milled Material, Mild Conditions (T = 20 °C, pCO<sub>2</sub> = 1 bar)</b>			
<b>M30MA</b>	4.73	16.47	0.077
<b>M1HA</b>	5.16	17.90	0.042
<b>M2HA</b>	9.43	32.44	0.041
<b>M4HA</b>	11.19	38.46	0.025
<b>M8HA</b>	12.51	42.95	0.014
<b>Milled Material, Mild Conditions (T = 20 °C, p CO<sub>2</sub> = 1 bar), Sodium Solution</b>			
<b>SSM30MA</b>	6.22	21.16	0.104
<b>SSM1HA</b>	7.37	25.09	0.062
<b>SSM2HA</b>	8.25	28.09	0.035
<b>SSM4HA</b>	8.19	27.88	0.018
<b>SSM8HA</b>	9.66	32.88	0.011
<b>Fresh Material, Enhanced Conditions (T = 50 °C, pCO<sub>2</sub> = 10 bar)</b>			
<b>B30ME</b>	4.53	15.41	0.181
<b>B1HE</b>	4.80	16.34	0.096
<b>B2HE</b>	5.20	17.71	0.052
<b>B4HE</b>	6.12	20.83	0.031
<b>B8HE</b>	8.73	29.71	0.023
<b>Milled Material, Enhanced Conditions (T = 50 °C, p CO<sub>2</sub> = 10 bar)</b>			
<b>M30ME</b>	6.03	20.53	0.100
<b>M1HE</b>	7.71	26.25	0.066
<b>M2HE</b>	14.26	48.52	0.067
<b>M4HE</b>	15.69	53.39	0.038
<b>M8HE</b>	16.05	54.64	0.020

As expected, due to the newly formed carbonated phases, that inhibit the diffusion of  $\text{Ca}^{2+}$  from the slag particle to the solution, and the less amount of reactive phases available after the initial stages of carbonation, during which a great part of them was consumed, CWR appeared to decrease with reaction time for all the applied treatments.

As already discussed, the highest carbonation conversions do not necessarily correspond to the highest CWRs. In fact, carbonation conversions and CWR values exhibit totally different distributions among the different carbonation tests.

Although conversions achieved after the carbonation of milled material under both mild and enhanced conditions were higher than those attributed to the carbonation of the as received material under enhanced conditions, the CWR values of the two materials were comparable. This could be attributed to the fact that particles of the as received material were too large for the applied operating conditions to enable high levels of conversion. By calculating the CWR values for the particular tests, the effect of particle size was also taken into consideration and the actual reactivity of the material towards  $\text{CO}_2$  under the same conditions was found to be similar.

As anticipated, the intensity of the applied operating conditions was also proved to significantly affect the rate of carbonation weathering. After each reaction period and regardless of the type of the tested material (as received or milled), the employment of the enhanced operating conditions resulted in notably higher CWR values compared to the ones exhibited after the employment of mild conditions.

Compared to  $\text{CO}_2$  uptakes, CWR values appeared to be similarly influenced by the different types of employed liquid agents. The employment of sodium solution instead of water as the wetting liquid in experiments testing the reactivity of milled material towards  $\text{CO}_2$  under mild conditions was proved to be beneficial for the CWR value only during the first stages of carbonation.

For experimental durations over 60 minutes the use of the alkaline activator instead of water resulted in a remarkable attenuation of CWR. Nevertheless,

for reaction durations up to 60 minutes, the use of sodium solution in experiments testing the carbonation of milled material under mild conditions proved to be the second most time-efficient treatment for the investigated material.

Compared to other researches in literature which also investigate the carbonation of BOF slag, the batch carbonation experiments conducted in this study resulted in rather low CWR values. In fact, the highest CWR value obtained in this study is remarkably lower than those achieved by the studies investigating the carbonation of BOF slag and are included in the literature review section of this work [36, 37, 38, 39, 112]. Since, the effects of different slag's particle size and varying reaction time from study to study have been taken into consideration by calculating the CWR for each of these researches, the different operating conditions applied in each case should be the main reason for these differentiations. Indeed, the higher CWRs observed in literature, were achieved by studies applying considerably more enhanced temperatures and CO<sub>2</sub> pressures, or greater amounts of the wetting agent, compared to those applied in this research.

### **3.4.3. Mechanical strength assessment**

The results of the ACV tests are shown in Table 3-11 and depicted in Figure 3-12, along with the average ACV typically reported for mixed gravel (21 %) and blast furnace slag (35 %) [35]. It has to be noted that the granules with the higher strength are those exhibiting the lower ACV.

According to the results, the type of treatment and of the employed liquid binder affected the mechanical resistance of the formed granules. As observed, the granulation of alkali activated material resulted in the production of granules with enhanced strength. More specifically, granules with the highest mechanical strength were formed after the combination of granulation with alkali activation, exhibiting an ACV of 15.96 %. The particular value is remarkably lower than the one attributed to granules formed after granulation using water as the binding solution (44.72 %) and those exhibited by BF slag and mixed gravel.

In the contrary, the combined granulation-carbonation treatment of the BOF slag, applying a W/S ratio of 0.12 L/kg, appeared to be less effective in the production of granules with elevated mechanical strength. Although under the particular conditions, the use of sodium solution instead of DI water resulted in granules with better mechanical performance, the ACVs exhibited by the granules produced after using either of the liquid agents were notably high (ACVs above 35%). Nevertheless, by increasing the amount of alkaline activator in the system from 0.12 L/kg to 0.14 L/kg, the ACVs of the obtained granules significantly decreased to about 17.64 % and 29.02 %, after 30 and 60 minutes of reaction, respectively. Both of these values were below the one attributed to BF slag, whereas the ACV obtained from granules produced after 30 minutes of the particular treatment, was half the value exhibited by the granules formed with W/S of 0.12 L/kg after the same period, and below the ACV attributed to mixed gravel.

**Table 3-11 Description and results of the ACV tests**

Test	Diameter (mm)	M1 (g)	M2 (g)	ACValue (%)
G30' _W_ W/S=0.12	2.36	411.2	183.9	44.72
G30' _SS_ W/S=0.12	2.36	466.8	74.5	15.96
GC30' _W_ W/S=0.12	1.18	327.5	153.4	46.84
GC60' _W_ W/S=0.12	1.18	343.6	176.74	51.44
GC30' _SS_ W/S=0.12	1.18	356.7	141.63	39.71
GC60' _SS_ W/S=0.12	1.18	415.9	188.24	45.26
GC30' _SS_ W/S=0.14	1.7	410.9	72.5	17.64
GC60' _SS_ W/S=0.14	1.18	410	119	29.02

Furthermore, reaction time also had an impact on the mechanical strength of the granules formed after the combined granulation-carbonation treatment of the BOF slag. Normally, by prolonging the granulation time, agglomerates of higher strength should be formed as a result of the greater compaction achieved and consequently the greater consolidation extent accomplished [181, 184, 185].

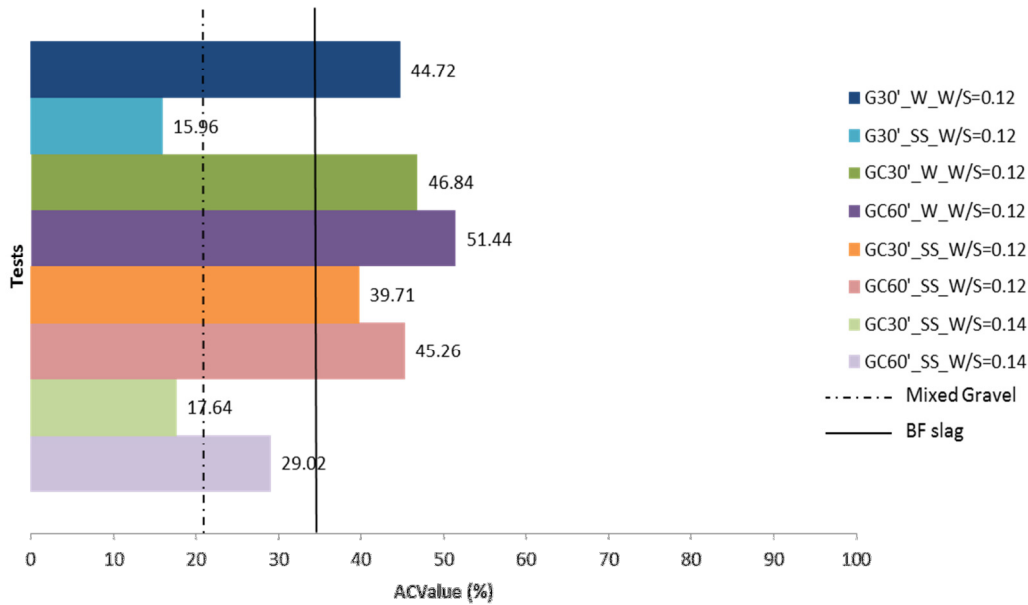


**Figure 3-12 ACV tests results [136].**

However, in this study, by increasing the reaction period from 30 to 60 minutes, the mechanical strength of the granules got decreased, irrespectively to the type of the employed liquid binder or its amount in the system. The particular behavior further explains the lower particle size of granules obtained after 60 minutes of reaction time compared to that of the granules obtained after 30 minutes, since due to their lower strength, they are more vulnerable to breakage due to collisions and friction.

Overall, based on the obtained results, it could be inferred that alkali activation significantly improved the mechanical performance of the granules obtained after granulation and remarkably increased the strength of the granules formed after the combined granulation-carbonation treatment when employed at a W/S ratio of 0.14 L/kg and for treatment durations of 30 minutes. In fact, the granules produced by these treatments exhibited adequate mechanical strength for use as aggregates, since compared to mixed gravel or BF slag, that are widely used as secondary aggregates in several civil engineering applications, they present higher mechanical strength.

### 3.4.4. Leaching behavior

The leaching behavior of the granules generated after the different treatments tested, was assessed applying the EN 12457-2 standard compliance test. As mentioned in section 3.2.3., the particular test was applied to both crushed and uncrushed granules.

The leaching behavior of the crushed granules generated after the different treatments tested are demonstrated in Table 3-12. In particular, the concentrations of major constituents and regulated elements that proved higher than the instrumental quantification limits, along with the pH values of the eluates and the Italian limits for waste reuse are presented in this table. The leaching behavior of the uncrushed granules is depicted in Figure 3-14. The concentrations of the major constituents and those of the regulated elements that were higher than the instrumental quantification limits are clearly displayed in this figure.

Each sample was subjected to three different measurements regarding their content in the investigated major and regulated elements. The concentrations reported in Table 3-12 and Figure 3-14 are the average values of those measurements and are accompanied by their standard errors of the mean. Relatively high standard errors were reported only in the cases of Ba (GC30'\_SS\_W/S=0.12 and GC30'\_SS\_W/S=0.14) and Zn (Untreated slag, GC30'\_SS\_W/S=0.12 and GC60'\_SS\_W/S=0.12) measurements.

The pH of the untreated slag was alkaline. The native pH value of the material was found to exceed the Italian limits for waste reuse, whereas its heavy metals release levels were well below those limits.

To assess the effect of treatment type (granulation or granulation-carbonation), the influence of the employed liquid binder (water or sodium solution) and the impact of the combined treatment duration on the leaching behavior of the tested slag, the environmental behavior of granules obtained after specific tests was evaluated.

Granules obtained after the granulation of BOF slag using water (G30'\_W\_W/S=0.12) or sodium solution (G30'\_SS\_W/S=0.12) as the liquid

binder were analyzed, in order to determine the influence of the particular treatment and that of the employed binding solution on the leaching behavior of the tested material. According to the results, the products of BOF slag granulation using water as the liquid binder exhibited a similar behavior to that of the as received material. On the other hand, the employment of sodium solution in the process resulted in granules exhibiting a slight decrease of pH (from 13.13 to 12.85) and a rational increase of Na mobility, as a result of the chemistry of the employed binding solution. The leaching of Ca got decreased to half, compared to its release levels from the untreated material, justifying the observed pH attenuation. The release levels of Al remained stable, whereas Si leaching remarkably increased. Finally, Cr, Zn and especially Ba leaching levels were decreased.

The effect of carbonation treatment without the assistance of alkali activation on the leaching behavior of the formed granules was determined by analyzing the agglomerates produced after 30 minutes of the combined treatment of BOF slag, using water as the liquid binder (GC30'\_W\_W/S=0.12). Apart from a decrease of the pH value, the particular treatment also led to an increase of Al and Si leaching, for which hydration reactions must be responsible, and a notable decrease of Ba, Cr and Zn mobility. The release levels of V remained below the quantification limits of the instrument.

Granules produced after 30 minutes of combined granulation-carbonation treatment using sodium solution as the liquid binder, at W/S = 0.14 L/kg (GC30'\_SS\_W/S=0.14), were also analyzed regarding their leaching behavior, since they exhibited the best mechanical performance among the granules formed after the combined treatment of the alkali activated BOF slag. Due to the incorporation of carbonation in the process, the concentration of Ca in the eluates was remarkably decreased. The pH was also decreased from 13.13 to 12.89, whereas the leaching of Al and Cr increased. As expected, the levels of Na release also got raised, since sodium solution was used as the binding agent. The leaching of V and Zn did not seem to be remarkably affected by the process. By prolonging the treatment period from 30 to 60 minutes, significant differentiations on the leaching behavior of the products were observed. Although still over the Italian limits, the pH further decreased to

12.29, whereas the release of Cr and V significantly increased over the regulatory limits to 0.11 and 1.26 mg/L, respectively. The amount of Ca found in the eluates of the granules produced by this treatment was the lowest among the investigated products, supporting the remarkable drop of pH from 13.13 to 12.29.

Overall, these results indicate a general tendency, especially of the combined treatment to create granules containing phases of high Al and Si solubility, probably as a result of hydration reactions occurring in the material. Na release was significantly increased only after experiments incorporating the employment of sodium solution, whereas all the regulated elements were kept well below the Italian waste reuse limits after every tested treatment except for the one which combined granulation with carbonation and alkali activation and was carried out for 60 minutes, which resulted in the formation of granules with undesired Cr and V leaching behavior.

In order to evaluate the effect of the different tested treatments on the release of major and regulated components from the formed agglomerates at their final particle size, and also to determine whether the calcite layer formed on the granules synthesized after the combined treatment of the material, affected the release of the investigated elements from the unground granules in a more appreciable way than from the crushed ones, granules obtained after all the conducted experiments were subjected to the same leaching test, without being ground. The outcomes of these tests are shown in Figures 3-13 and 3-14.

In terms of pH values, the results are similar to those exerted by the crushed granules (Figure 3-13). Only in the case of the combined granulation-carbonation treatment of the slag using water as the liquid binder, carried out for 60 minutes, there was a remarkable drop of pH from 13.13 to 11.87, i.e. over one unit lower than the pH of the as received BOF slag and within the acceptable range of pH values for waste reuse (5.5 - 12), as it has been set by the Italian legislation.

Regarding the leaching of major constituents (Figure 3-14a.), the uncrushed granules displayed a different behavior compared to the crushed ones. The

release of Al was found to increase after all the tested treatments with respect to the as received slag, probably due to the formation of more soluble phases like Al-containing hydroxide, as a result of hydration reactions [133]. Specifically for the granulation-carbonation treatments, the level of aluminum release was found to be dependent on reaction time. In fact, the release of Al decreased with increasing treatment duration, regardless of the type of the liquid binder employed.

As far as the leaching of Ca, the granules produced after all the tested treatments exhibited lower levels of Ca release than the untreated material. This is in accordance with the lower pH values obtained after all the investigated processes, compared to that of the as received material. The use of alkaline activator instead of water as the binding solution was proved to further decrease the Ca release, after both granulation and granulation-carbonation experiments. The effects of reaction time and alkali activator amount on Ca leaching were investigated for the combined treatment. Based on the exerted results, it could be inferred that calcium leaching decreased with increasing treatment duration, irrespectively to the type of the employed liquid binder, and with increasing amounts of sodium solution after both of the investigated reaction times.

As in the case of uncrushed granules, the release of Na was highly affected by alkali activation. More specifically, granules prepared with the assistance of alkali activation resulted in eluates with remarkably higher concentrations of Na (two orders of magnitude higher) than those resulting from the water-based granules, regardless if carbonation was applied or not. The amount of the alkali activating solution, on the other hand, did not present any significant influence on the release of Na, since eluates with similar Na concentrations were obtained from granules formed after the combined treatment of the material applying either of the tested W/S ratios (0.12 or 0.14 L/kg).

Carbonation significantly increased the release of Si, especially from the alkali activated granules. This behavior is the opposite of the one that calcium had towards carbonation. Similar findings were reported by Huijgen and Commans [144], Baciocchi et al. [143] and Morone et al. [41], who also analysed the

leaching behavior of steel slag by geochemical modeling and concluded that carbonation remarkably decreased the leaching of Ca and increased the release levels of Si. According to their explanation, the carbonation of Ca-containing slag caused the formation of calcite, a phase characterized by notably less solubility than the initial Ca-solubility controlling phases of the material, decreasing the concentration of Ca in the leachates. On the other hand, carbonation also transformed a part of Ca-silicates into more soluble amorphous SiO<sub>2</sub>, with the latter controlling the solubility of Si from the material. Based on these suggestions, it could be assumed that the coupling of the combined granulation-carbonation with the alkaline activation of the investigated BOF slag resulted in the formation of a layer covering the granule, mainly constituted by a less soluble Ca-containing phase, like calcite, and more soluble Si-phases, as amorphous SiO<sub>2</sub>, with these two phases being the ones controlling the solubility and hence the release of Ca and Si from the carbonated steel slag [145, 146]. This could explain the increased amounts of Si and the low concentration of Ca in the eluates of granules formed by the particular process. However, in the particular case, solubility control by hydrated phases, such as C-H-S cannot be ruled out [147]. The effect of alkaline activator amount on the leaching of Si from the granules formed after the combined treatment of the slag was also evaluated. According to the results, by increasing the amount of sodium solution in the granulating system, Si mobility decreased.

The effect of the applied treatment on the leaching of the regulated elements from the uncrushed granules was also assessed (Figure 3-14b.). As can be observed, the release of Ba from the alkali activated granules obtained from both granulation and granulation-carbonation of BOF slag, was more than one order of magnitude lower than that from granules synthesized at the same conditions by mixing the material with water. The particular effect was more remarkable after the longer treatment periods (60 minutes).

As far as Cr leaching, granulation, granulation with alkali activation and granulation-carbonation appeared to reduce its release from the slag. In the contrary, the combination of alkali activation with granulation-carbonation

resulted in a remarkable increase of Cr release levels, well over the Italian regulatory limits (0.05 L/kg).

**Table 3-12 EN 12457-2 tests results for the untreated slag and the crushed granules obtained from the different tested treatments compared to the Italian limits for waste reuse (Italian Ministerial Decree 186/2006) [136]**

	<b>Leaching Behaviour</b>							
<b>Sample name</b>	<b>Al (mg/L)</b>	<b>Ca (mg/L)</b>	<b>Na (mg/L)</b>	<b>Si (mg/L)</b>	<b>Ba (mg/L)</b>	<b>Cr (mg/L)</b>	<b>V (mg/L)</b>	<b>Zn (mg/L)</b>
<b><i>Untreated Slag</i></b>								
<b>As received Material</b>	0.11±0.01	915.2±9.7	1.67±0.04	0.13±0.01	0.36±0.003	0.01±0.0003	<0.003	0.03±0.019
<b><i>Granulation</i></b>								
<b>G30'_W_W/S=0.12</b>	0.57±0.05	444.35±4.4	2.4±0.1	0.57±0.01	0.163±0.002	0.003±0.0001	<0.003	0.014±0.0003
<b>G30'_SS_W/S=0.12</b>	0.58±0.11	42.39±4.3	429.2±9.3	3.86±0.36	0.012±0.002	0.005±0.00004	0.01±0.0013	0.023±0.002
<b><i>Granulation-Carbonation</i></b>								
<b>GC30'_W_W/S=0.12</b>	0.57±0.02	318.9±15.4	1.25±0.06	2.62±0.27	0.113±0.002	0.005±0.001	0.01±0.0015	0.014±0.001
<b>GC60'_W_W/S=0.12</b>	0.3±0.004	112.04±4.8	1.53±0.01	11.3±0.06	0.03±0.001	0.008±0.0004	0.08±0.004	0.02±0.0021
<b>GC30'_SS_W/S=0.12</b>	0.7±0.14	29.4±12.3	445±16.72	91.1±4.8	0.007±0.005	0.083±0.0145	1.186±0.11	0.12±0.0863
<b>GC60'_SS_W/S=0.12</b>	0.4±0.007	13.22±0.16	443±26	112.8±6.9	<0.002	0.093±0.0227	1.142±0.01	0.019±0.011
<b>GC30'_SS_W/S=0.14</b>	1.58±0.12	17.83±3.4	512±38.7	13.51±0.8	0.004±0.002	0.129±0.0167	0.087±0.01	0.026±0.0002
<b>GC60'_SS_W/S=0.14</b>	0.8±0.007	9.67±0.58	439±1.63	69.4±2.7	<0.002	0.124±0.0015	1.159±0.07	0.012±0.0008
<b><i>Limit for Reuse (It. DM 186/2006)</i></b>								
	-	-	-	-	1	0.05	0.25	3

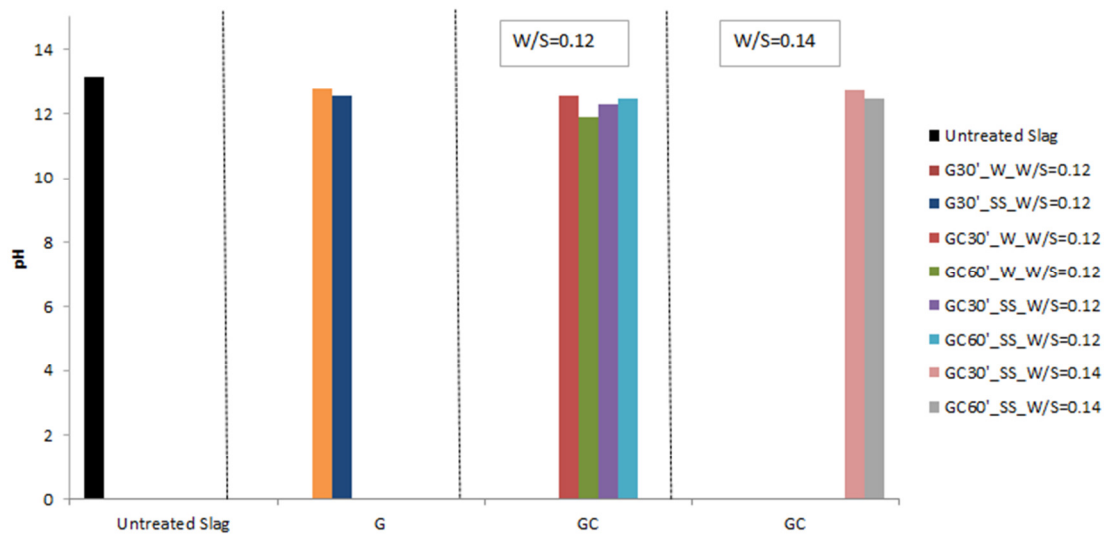


**Figure 3-13 The pH values of eluates resulting from granules obtained after each of the tested treatments [136].**

On the other hand, the release of vanadium from the slag got increased after all the tested treatments. Particularly for the granules produced after the combination of granulation-carbonation with alkali activation, this increase was remarkable, with the levels of V mobility exceeding the Italian limits for waste reuse (0.25 mg/L). From this set of experiments, only the granules produced after 30 minutes of combined treatment using sodium solution at  $W/S = 0.14$  L/kg resulted in leaching values which, although remarkably increased, remained below the regulatory limits. This should be attributed to the lower pH reduction achieved after the particular treatment, since V solubility has been found to decrease with increasing basicity [108, 186].

It is also noteworthy to point out that the leaching pattern of V as it is created by its release levels from the granules formed after all the carbonation tests, is very similar to that of Si. Based on the findings of a previous study on BOF slag carbonation [113], it could be assumed that V was incorporated in a dicalcium silicate phase, such as larnite, whose dissolution in the fresh slag was limited and became significantly enhanced by carbonation, and in particular, granulation-carbonation with alkali activation, causing the enhanced release levels of both V and Si.

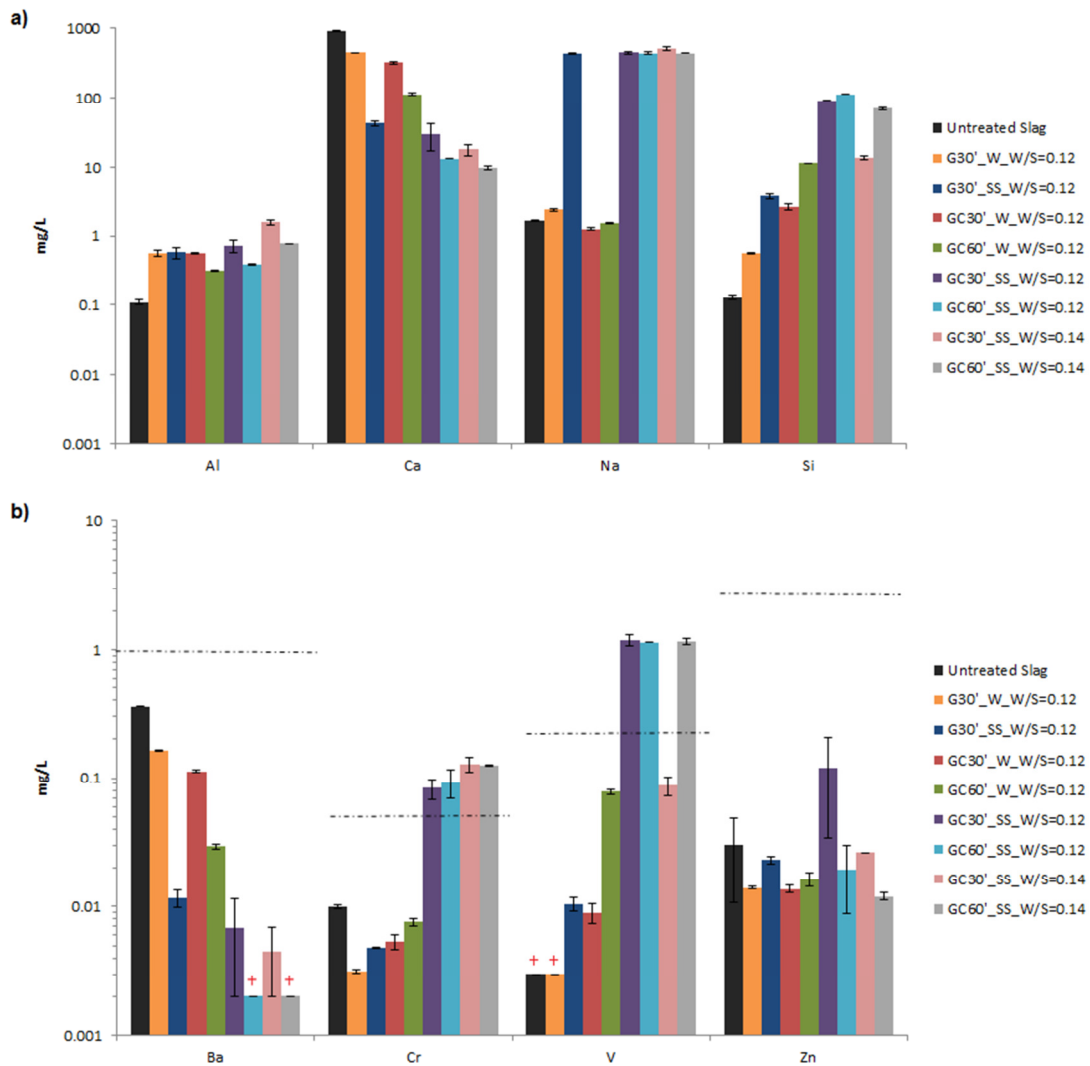


**Figure 3-14 Results of the EN 12457-2 test regarding the leaching of a) major constituents and b) regulated elements from granules (without grinding the material) obtained after the tested granulation and granulation-carbonation treatments. The leaching results of the untreated material are also presented in the graphs for comparison. The dotted line reports the Italian limits for waste reuse and the cross indicates that the concentration is below the quantification limits of the instrument [136].**

Finally, the leaching behavior of Zn appeared to be influenced by the type of liquid agent and the treatment duration. In particular, the alkali activation of the slag was found to notably increase the leaching levels of Zn, regardless of the type of the applied process. For the alkali activated material, the release of Zn appeared to decrease with increased treatment duration. Only when DI water was used the increased reaction duration caused the enhancement of Zn leaching. From all the applied treatments, only the alkali activation of the slag at  $W/S = 0.12$  L/kg, for 30 minutes led to the formation of granules

displaying Zn release levels notably above those ascribed to the untreated material. However, after every treatment, Zn leaching was maintained well below the regulatory limits.

### 3.5. Preliminary economic feasibility assessment

In this section, an effort to conduct a preliminary assessment of the economic viability of the process is made.

As already discussed, among the several treatments tested in this work, the one that resulted in the formation of granules with the most suitable characteristics for use as aggregates was the GC\_SS\_W/S=0.14. The particular treatment lasted for 30 minutes, and incorporated the alkali activation of the BOF slag using the alkaline solution at an L/S ratio of 0.18 L/kg.

A rough estimation of the process cost would include the expenditures related to the energy required for the conduction of each test and the alkali activation of the material. Since this is only a preliminary economic feasibility study, costs like those of operating labor, granulator maintenance, laboratory operating costs and insurance or local taxes, were not taken into consideration.

By having in mind that the experiments in this study were performed using a 180 W granulator and knowing the exact duration of the investigated treatment (30 minutes), the cost of energy required for it, can be easily calculated. In particular, the electricity consumed during each of those treatments was equal to:  $180 \text{ W} \times 0.5 \text{ hours} = 0.09 \text{ kWh}$ . Based on the electricity cost in Italy (0.1954 €/kWh [187]), which was the place where the granulation-carbonation tests took place, the cost of the energy required for the treatment was:  $0.09 \text{ kWh} \times 0.1954 \text{ €/kWh} = 0.0176 \text{ €/treatment}$ .

As already mentioned, in this work, the solution used for the alkaline activation of the BOF slag was a 50:50 by weight mixture of a 2 M NaOH solution prepared by dissolving NaOH pellets in deionized water, and a commercial sodium silicate solution. Based on the retail prices of each one of the sodium solution constituents (NaOH pellets: 151.6 €/2.5 kg [188], sodium

silicate solution: 60.40 €/2.5 L [189]) and their amount in the process, the cost of the alkaline solution was calculated at 1.305 € per treatment.

Based on these calculations, it can be inferred that the cost of each treatment was 1.323 €. Based on the fact that after each treatment approximately 500 g of secondary aggregates were generated and 10 g of CO<sub>2</sub> were stored, it could be inferred that the production of a ton of aggregates and the sequestration of approximately 20 kg of CO<sub>2</sub> by subjecting BOF slag to the proposed technique, would cost a total of 2,646 €. By comparing this value with the cost (8-20 € [23, 190]) of a ton of other suitable materials for aggregates use (e.g. BF slag, natural gravel, crushed stone), it is clear that the proposed process is economically infeasible. Moreover, based on the limited ability of the investigated methodology to achieve the sequestration of a significant amount of CO<sub>2</sub> by the BOF slag, a substantial mitigation of the process cost due to CO<sub>2</sub> storage is not likely.

Nonetheless, there are ways to improve the economic feasibility of the process. By the analysis made above, it is clear that alkali activation is the part of the process that increases its cost. If the process was scaled up and higher amounts of sodium solution were required, the cost of the solution and thereupon, the cost of the whole process would probably be decreased. However, the level at which this would be achieved cannot be estimated at this stage. Furthermore, a dramatical reduction of the process cost would be achieved, if instead of using synthetic alkaline activating solutions for the activation of the slag, waste solutions of suitable chemistry were used. Finally, if the CO<sub>2</sub> storage capacity of the formed granules was somehow improved, the total cost of the process would also be notably mitigated.

### **3.6. Conclusions**

The main goal of this project was to evaluate the performance of the combined granulation-carbonation process, as efficient treatment for the production of secondary aggregates out of BOF slag. For comparison reasons, single granulation of BOF slag was also performed. To this end, two different types of liquid binders, namely DI water and sodium hydroxide and silicates solution were used. Particularly, in the case of the combined

treatments, two different W/S ratios (0.12 and 0.14 L/kg) and two different treatment durations (30 and 60 minutes) were tested.

None of the applied treatments managed to produce granules that met all the 4 targeted requirements for use as aggregates (particle size enlargement, eluates pH ranging between 5.5 and 12 and limited leaching of regulated elements, as dictated by Italian legislation for waste reuse, and mechanical strength enhancement), while achieving satisfactory CO<sub>2</sub> sequestration, in order to also contribute to the greenhouse gas emissions reduction.

In fact, while all the tested treatments appeared to remarkably increase the material's particle size, only experiments incorporating alkaline activation managed to produce granules with sufficient mechanical strength for their use as aggregates. As expected, carbonation was proved to significantly improve the attained CO<sub>2</sub> uptakes, whereas it also turned out to be an efficient treatment for the reduction of the eluates pH. Finally, the combination of the three treatments (granulation, carbonation and alkali activation) positively affected all the investigated parameters of the produced granules, except for the leaching of Cr and V which got remarkably increased.

Apparently, the granulation-carbonation treatment of BOF slag, using sodium solution as the liquid agent, under varying experimental parameters, gave birth to granules exhibiting satisfactory characteristics for use as secondary aggregates in the construction business, while achieving decent CO<sub>2</sub> uptakes. In fact, the particle size enlargement achieved after 30 minutes of the particular treatment of BOF slag at W/S = 0.14 L/kg, stands among the best achieved in this study, with the formed granules exhibiting a mean diameter of more than 20 times greater than that of the as received material (4.5 mm compared to 0.2 mm). In addition, granules with remarkable compressive strength were also created after the coupling of alkaline activation with the combined granulation-carbonation treatment. In particular, agglomerates with ACV of 17.64 %, a value below the one attributed to gravels and therefore sufficient for use as aggregates, were formed by the granulation-carbonation experiment performed using the alkaline solution as the wetting agent, at W/S = 0.14 L/kg and after 30 minutes of reaction. The same type of treatment, at

W/S = 0.12 L/kg, also led to the formation of granules displaying the maximum achieved CO<sub>2</sub> uptake of approximately 40 g/kg of steel slag, after 60 minutes of treatment and 7 days of curing.

The only requirement that granules synthesized after the granulation-carbonation treatment of the alkali activated BOF slag could not meet, was that of their satisfactory environmental behavior. In fact, the coupling of granulation-carbonation with alkaline activation resulted in a significant increase of Cr and V release, over the Italian regulatory limits.

Considering only the requirements for use as secondary aggregates and assuming that the requirement of eluates pH below 12, as established by Italian legislation, is not in force in other countries, the most effective treatment of the tested BOF slag was that of coupled granulation-alkali activation [138]. In fact, the granules produced after the particular treatment presented remarkable particle size enlargement ( $d_{50}$  increased from 0.2 to 13.3 mm), limited release of all the investigated regulated elements (well below the Italian limits for waste reuse) and significant compressive strength enhancement, exhibiting the lowest ACV (15.96 %) of all the formed agglomerates.

Overall, the results of these preliminary experiments were rather encouraging regarding the feasibility of applying the proposed combined treatments on BOF slag in order to obtain granules with enhanced mechanical performance. Nevertheless, special attention should be paid on the varying parameters of the experiments conducted in this study, like the amount of the liquid binder and treatment duration, which appeared to significantly affect both the mechanical characteristics and the environmental behavior of the finally produced granules [136].

## 4. SYNTHESIS OF ZEOLITIC HEAVY METAL ADSORBENT FROM BF SLAG

### 4.1. Introduction

Heavy metals are an integral part of Earth's crust. Due to the continuously increasing human activities that interfere with their geochemical cycle, these metals are released into the natural environment and are accumulated in water, air and soil [191, 192].

Several schemes have been proposed for the designation of heavy metals, with the most of them being based upon atomic number, density, atomic weight and toxicity of metals [193]. Although a widely accepted definition for heavy metals has not yet been agreed, the particular term is usually used to describe metals and metalloids that are linked with contamination and are characterized as toxic or poisonous. Some of the most characteristic examples of these metals and metalloids include zinc (Zn), mercury (Hg), arsenic (As), chromium (Cr), copper (Cu), nickel (Ni), lead (Pb), thallium (Tl) and cadmium (Cd).

Although some of them have been proved to be beneficial or even essential for certain functions of living organisms, in concentrations higher than the appropriate ones, they have detrimental impacts upon plants, animals and human beings [194, 195].

Nowadays, heavy metals have been recognized as one of the most significant environmental pollutants. They can be found in several types of industries such as mining, metal and wood processing, finishing, petroleum refining and plating. Wastewater streams with different contents of heavy metals are produced by such industries. Wastewater regulations set limits on both the type and the concentration of heavy metals that can be found in discharged waters. As a result, it is often required from the industries to remove heavy metals before the release of such effluents.

In an effort to adapt to the demanding legislation, industries are eager to implement methods and technologies that will manage to remove the toxic heavy metal ions from their wastes before discharging them. Some of the

methods that are applied for that purpose include chemical precipitation, ion exchange, reverse osmosis, electrodialysis, ultra- and nano-filtration, flocculation, membrane filtration etc. However, these techniques present several drawbacks such as high reagent requirements or generation of toxic sludge.

Adsorption, on the other hand, is an efficient and economic technique that due to its simplicity and versatility has become the most widely used method for the removal of heavy metal ions from wastewaters.

#### **4.1.1. Adsorption process**

Adsorption is essentially a surface phenomenon. It is the process in which a molecule, atom or ion of a fluid (gas or liquid) adhere to a solid surface. The substance on the surface of which adsorption occurs is called adsorbent, whereas the substance that is adsorbed by the surface of the adsorbent is the adsorbate. Between the adsorbent and the adsorbate attraction forces are developed. Depending on the nature of these forces, the adsorption process can be classified as physical or chemical. In the case that the process is governed by the weak Vanderwaal forces, the adsorption is considered to be physical. In the alternative scenario that the attraction forces are chemical forces generated from the reaction between the adsorbate and the surface of the adsorbent, then chemical adsorption or chemisorption occurs.

The extent of the achieved adsorption in aquatic environments has been found to depend on several factors. The temperature at which the process takes place, the pH of the contaminated solution, the contact time between the adsorbent and the adsorbate, the particle size and the surface area of the adsorbent, the amount of metal ions available, as well as the amount of the adsorbent used, have been found to determine to a great extent, the efficiency of the adsorption process.

The way that temperature affects adsorption depends on the nature of the process. More specifically, an exothermic adsorption is favored at low temperature conditions [196, 197], whereas, an endothermic adsorption benefits from increased temperatures [198, 199].

The solution pH is another determining parameter in the adsorption process. The pH value has been found to affect the surface charge of the adsorbent and the ionization and speciation of the adsorbate during the adsorption process. For any adsorbent-adsorbate solution there is an optimum pH value up to which metal adsorption increases with increasing pH [197, 199-204]. At the optimum pH value, maximum adsorption occurs. In general, it could be inferred that at low pH values the  $H^+$  ions occupy the greatest part of the adsorption sites, positively charging the adsorbent's surface and hindering the retention of substantial amounts of positively charged metals, due to electric repulsion forces. By increasing the pH of the adsorbent-adsorbate solution, the adsorption sites of zeolites get more negatively charged, the competition between the protons and the metal ions of the solution for activated adsorption sites gets remarkably decreased and consequently, the metal adsorption gets increased and reaches equilibrium at the optimum pH value. At higher pH values than the optimum one, hydroxylated complexes of the metal are formed and therefore the adsorption of metal ions gets decreased [199, 200, 202].

The contact time between the adsorbent and the adsorbate has also been found to significantly affect the adsorption process. In fact, up to a particular duration at which the adsorbent-adsorbate solution reaches its equilibrium, adsorption increases with increased contact time [197, 199-204]. After the particular period, no further adsorption takes place [197, 199-204].

As a surface phenomenon, adsorption is also highly dependent on the surface area of the adsorbing material. Apparently, any increase of the adsorbent's surface area leads to the adsorption increase.

Finally, the initial concentration of the adsorbate in the solution, as well as the adsorbent dosage are also crucial parameters determining the heavy metal adsorption efficiency and the adsorption capacity of the sorbent. In fact, by increasing the initial concentration of the metal in the contaminated solution, the percentage of metal removal decreases probably due to the saturation of the available active sites on the adsorbent's surface [197, 201, 205]. On the other hand, an increase of the adsorbate concentration in the solution has

also been found to cause an increase of the adsorption capacity of the sorbent [197, 199, 200, 203, 205]. The particular finding should be mainly ascribed to the utilization of all the available active sites of the sorbent and the higher adsorption rate, both resulting from the higher concentration of the adsorbate in the solution.

In the contrary, by increasing the dosage of sorbent in the solution up to an optimum amount, the percentage of the metal removed increases as a result of the increased available active sites [197, 199-204], whereas the adsorption capacity of the adsorbent decreases [200, 203], mainly due the lower utilization of the sorbent's adsorption capacity.

#### **4.1.2. Zeolites as adsorbents**

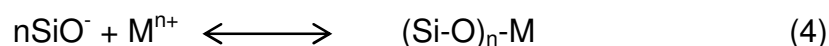
Several materials have been used as adsorbents in numerous applications. Activated carbon [206, 207] and alumina [208, 209], natural or synthetic zeolites [210, 211] and silica gel [212] are some of the most important commercial adsorbents. In particular for the removal of toxic contaminants from wastewaters, agricultural waste, industrial by-products and numerous natural components have been tested as potential low cost sorbents. From them, zeolites appear to be very promising such materials [213-216], mainly due to their large specific surface area and their cation exchange capacity, which is actually an exchange process between the metal cation in the aqueous solution and the metal cation present in the zeolitic framework [210, 217-219].

Zeolites are crystalline, micro-porous alumino-silicate minerals. Several unique zeolite frameworks have been identified. They are broadly distributed in nature but they can also be synthetically produced on a large scale. The maximum cation exchange capacity of a zeolite depends on [242]: 1) the exchangeable sites on the zeolitic surface, 2) the pore size of the zeolitic framework, 3) the equilibrium temperature and 4) the charge density of the metal cations. According to this process, the positively charged cations are approached by water molecules that surround them and create a shell around the cation. These cations are then moving in the zeolitic framework through its pores, in order to find the suitable sites and replace the exchangeable cations.

The ion exchange mechanism can be described as [242]:



An alternative mechanism that is also commonly met in literature describing the uptake of heavy metal cations on the surface of zeolites is a reaction that leads to the combination of metals with different charge. This is a surface reaction occurring between the positively charged metal cations in solution and the negatively charged sites on the surface of the zeolite. This adsorption mechanism can be described as [242]:



Based on Reaction (1), if the adsorption process follows the ion exchange mechanism, the pH of the solution during the adsorption will be continuously increased, since  $\text{OH}^-$  groups will be generated. On the other hand, according to Reactions (2-4), a continuous decrease of the solution's pH indicates the surface reaction mechanism as the one dominating the adsorption process.

Apart from heavy metal sorbents, zeolites can also be used as catalysts in several industrial sectors [220, 221], they are found in detergents and in the construction materials, as an additive in asphalt, concrete [222, 223] and Portland cement [224, 225], and they also have applications in the medical [226-228] and agricultural [229-231] domains.

Nowadays, synthetic zeolites are used in a greater extent than the naturally occurring ones due to the purity of crystalline products and the uniformity of particle sizes. Moreover, the synthetic zeolites can be engineered with the preferable chemical properties and pore sizes, whereas they have been found to present notably greater thermal stability. The production of zeolites using chemical sources of alumina and silica is expensive. However, several cheaper raw materials like fly and bottom ashes from coal combustion [232, 233] or municipal solid waste incineration [223, 234], natural clinker [235] and clay minerals [237-239] have also been successfully utilized as the starting

materials for the synthesis of zeolitic minerals. Although the hydrothermal conversion of several cheap alumina- and silica-rich raw materials for the formation of zeolites has been widely researched, the literature on the hydrothermal conversion of industrial slags for the same purpose is still limited [239-241].

#### **4.1.3. Formation of zeolites from BF slag**

BF slag is a by-product of iron-making process, wherein impurities from iron ore are removed in a pyrometallurgical process. As already discussed, based on the way it is cooled down after its separation from the molten iron, four different types of the particular slag are generated: (i) air-cooled (i.e. crystalline), (ii) granulated (i.e. vitrified), (iii) expanded (otherwise known as foamed), and (iv) pelletized.

The attractiveness of BF slag for waste valorization lies in its qualities (chemical, mineral and morphological properties) and the potential applications of the material [43]. In its original form, the particular type of slag is already widely used in cement industry, partially replacing PC for the production of blended cement. The particular use of BF slag creates profit for the iron-manufacturing industry, while contributing to the mitigation of the CO<sub>2</sub> footprint related to blended cement production, since a part of CO<sub>2</sub> emissions linked to the production of PC is avoided.

Therefore, BF slag is not in pressing need for new valorization routes and only alternative valorization methodologies generating higher value than the already existing one would be able to attract the interest of iron-manufacturing industry. Such a method could be the indirect carbonation of the material.

In general, the indirect carbonation of industrial residues rich in alkaline metals has been widely researched as part of CCS technology. According to the particular process, an amount of CO<sub>2</sub> is efficiently stored in a permanent and benign-to-the-atmosphere way, while valuable materials (PCC) are formed. However, there is a part of the particular technique that remains inadequately explored. Indirect carbonation consists of two different processes: the selective extraction of calcium from the material and the

subsequent carbonation of the obtained leachate solution, under controlled conditions. Apparently, the particular waste valorization process generates solid residues from the material, which are not further processed or exploited after the calcium extraction stage. Processing routes that reduce the production of such residues, or even to eliminate them, should be found.

In order to achieve that but also to generate products of higher value than that of BF slag in its original form, while managing to sequester sufficient amounts of CO<sub>2</sub>, lately, there has been an effort to build up and optimize a technology which combines the indirect carbonation of BF slag with the hydrothermal conversion of the calcium depleted residual solids resulting from the calcium extraction stage of the process [43]. According to it, CO<sub>2</sub> is stored in the calcium extracted by acid leaching from the slag, producing PCC via mineral carbonation reaction, while, in parallel, zeolitic minerals are formed through the hydrothermal conversion of the solid residues in alkali solution [43].

Although the production of PCC using the indirect carbonation of BF slag is a process that has managed to attract a lot of attention [22, 243], the hydrothermal conversion of the particular slag for the production of zeolitic minerals is a technology that has been studied and developed only during the recent years [244-246]. However, in none of the cases it has been considered as a technique that could be used in combination with the indirect carbonation of BF slag in order to achieve the common formation of PCC and zeolites.

Chiang et al. [43] originally proposed the particular methodology, as an alternative “zero-waste” method for BF slag valorization. The generation of high purity PCC and the synthesis of zeolites with notable heavy metal adsorption capacity in water were their main objectives.

To this end, an extraction agent amiable to both the PCC and zeolites formation should be used. Thus the selection of a suitable extractant was critical. Among the several leaching agents applied in prior researches on both indirect carbonation [22, 243] and hydrothermal conversion [239, 240] of BF slag, acetic acid was selected as the most promising one. Hydrochloric acid exhibits detrimental effects on both the generation of PCC and the leaching selectivity, losing significant quantities of Si and Al in the leachate

solution [239]. On the other hand, formic acid has proved to be efficient, since it manages to efficiently remove Ca and Mg from the slag while presenting remarkable leaching selectivity, leaving undisturbed both the Si and Al [240]. However, it presents lower acid dissociation constant than acetic acid [246], suggesting that the precipitation of calcium carbonate should be more readily achievable after employment of acetate solutions as the extraction agent. It has also been shown that in some cases, such as with the use of succinates [128] and oxalates [247], non-carbonate precipitates form in place of PCC. Furthermore, Eloneva et al. [248] compared sixteen extractants for calcium removal from steelmaking slags, and found acetic acid to be the most efficient (best performance between 0.5 M and 2 M extractant concentrations) and most successful (highest calcium recovery at ~ 100 %).

The PCC produced by Chiang et al. [43], was of intermediate purity ranging between 68 and 90 %, whereas depending on the intensity of the calcium extraction stage and the concentration of the sodium hydroxide (NaOH) solution employed during the hydrothermal conversion of the calcium depleted residues, tobermorite and three different types of zeolitic products were synthesized, namely lazurite, sodalite and analcime.

The indirect carbonation part of the proposed process was reproduced and optimized by De Crom et al. [44], who by applying two additional leachate solution purification steps and by optimizing the carbonation conditions, managed to produce PCC of high purity (> 98 %), homogenous mineralogy (88 % calcite), uniform morphology, small particle size and narrow particle size distribution, suitable for use as filler in papermaking. On the other hand, the reproducibility of zeolites through the hydrothermal conversion of the calcium-depleted solid residues has not been assessed yet. Moreover, the efficiency of the produced zeolitic minerals as heavy metal sorbents in wastewater treatment applications also remains to be evaluated.

From the mineral phases formed by Chiang et al. [43], tobermorite was the least desirable one. The formation of tobermorite requires the participation of calcium which according to the proposed methodology, should only be present in negligible amounts in the composition of the calcium extraction

residues. Furthermore, its layered crystal structure leads to reduced specific surface area [241], a trait important for sorbents, though it has been reported that tobermorite can act as a sorbent through ion exchange mechanism [244]. On the other hand, the formation of analcime, a product that is only rarely found in nature, presented the highest valorization potential among the synthesized phases.

According to Chiang et al. [43], the level of calcium extraction and thereupon the concentration of the applied acetic acid solution, determined in great extent the type of the finally produced mineral. Based on their findings, the use of lower concentrations of acetic acid led to limited leaching of calcium and therefore to the formation of high amounts of the less desirable phase of tobermorite. By employing acid solutions of higher concentrations, higher levels of calcium extraction were achieved and lower amounts of tobermorite were found in the synthesized products. The type of the finally formed material was also found to be dependent on the concentration of the employed alkaline (NaOH) solution. The use of higher NaOH concentrations was found to promote the formation of tobermorite, probably as a result of the increased basicity that induces the precipitation of calcium. The extraction of calcium from the slag using acetic acid of high concentration (2 M) and the hydrothermal conversion of the resulting calcium depleted residues employing a NaOH solution of low concentration (0.5 or 1 M), led to the formation of high amounts of analcime and only limited occurrence of tobermorite.

In this chapter the reproducibility of zeolites via the hydrothermal conversion of the residual solids obtained after the extraction of calcium from BF slag as proposed by Chiang et al. [43], was investigated and the heavy metal adsorption capacity of the formed material was assessed. The novelty of this work is the usage of a more porous BF slag as the starting material. In the original study, a GBFS was used. In this research, a different type of BF slag, namely PBFS was selected for investigation. Generated by the rapid cooling of BF slag, following different processes, both of these types of BF slag are amorphous (glassy) and characterized by similar chemical and mineralogical compositions. However, the different processes employed for their formation resulted in materials with different levels of porosity. Compared to GBFS,

PBFS is of higher porosity. This extra porosity of PBFS should considerably facilitate the extraction of calcium from the material and secure the synthesis of high amounts of analcime and the limited formation of the undesired tobermorite.

## **4.2. Materials and methods**

### **4.2.1. Materials**

The steel slag samples used in this research were GBFS and PBFS acquired by two different steelworks, located in Belgium and Canada, respectively.

The agent used for the calcium-extraction process was acetic acid ( $\text{CH}_3\text{COOH}$ ) (Caledon Laboratories) of 2 M. Two different concentrations (0.5 and 2 M) of sodium hydroxide (NaOH) solution (Caledon Laboratories) were employed for the synthesis of zeolites via the hydrothermal conversion of the residual solids resulting from the calcium extraction of PBF slag.

For the preparation of the contaminated solutions for the heavy metal adsorption tests, a standard solution of  $\text{Ni}^{2+}$  (Perkin Elmer, 1000mg/1000ml) was used. Sodium hydroxide (NaOH) (Caledon Laboratories) and hydrochloric acid (HCl) (Caledon Laboratories) were used to buffer the pH of the adsorbent-adsorbate solutions to 4-5, before and after their equilibration. Nitric acid ( $\text{HNO}_3$ ) (Caledon Laboratories) was added to the supernatant resulting from the centrifussion of the adsorbent-adsorbate solution, prior to its  $\text{Ni}^{2+}$  content analysis.

The vacuum filtering required in several stages of the process was performed using filter paper with coarse pore size (Fischer Scientific, P8).

### **4.2.2. Experimental methodology**

Prior to experimentation, both types of BF slag were ground to particle size < 2 mm, using mortar and pestle.

In an effort to discover the way that the starting material properties affected the extent of calcium leaching, PBFS and GBFS were initially subjected to

batch calcium extraction tests, applying different acetic acid concentrations and varying reaction durations.

The formation of zeolites from PBFS was also attempted by firstly, subjecting the tested material to an extraction stage, where calcium was leached out from the slag to an acetic acid solution of certain concentration and by subsequently activating the resulting calcium depleted solids via heat treatment in a highly caustic environment. Finally, the obtained materials were analyzed for their elemental and mineralogical composition and assessed for their heavy metal adsorption capacity, using  $\text{Ni}^{2+}$  as the metal for investigation.

In the following sections a more detailed description of the employed processes is presented.

#### **4.2.2.1. Batch calcium extraction tests**

During the first phase of experimentation, batch calcium extraction tests on PBFS and GBFS were performed. In all the tests analytical grade acetic acid of varying concentrations (0.7 M, 1.4 M, and 2.8 M) was used as the leaching agent. For each extraction test, 20 g of BF slag were mixed with 100 ml of acetic acid solution in capped plastic bottles, at 160 rpm and ambient temperature, for different extraction durations (1, 4 and 24 hours). After the end of mixing, the slurry was vacuum filtered to separate the solids from the leachate solution. Finally, the leachate solution was analyzed for its content in calcium.

#### **4.2.2.2. Synthesis of zeolites**

For the second phase of experimentation the formation of zeolites through the hydrothermal conversion of calcium depleted PBFS was attempted.

As suggested by Chiang et al. [43], due to the sensitivity of the extraction process to the acidity and the detrimental impact of the latter on leaching selectivity, the calcium extraction took place in two steps, using each time half the molarity of the acetic acid that otherwise would be used in a single step.

For the first step, 100 g of the tested slag were mixed with 731 ml of acetic acid solution (2 M), in an autoclave reactor (Büchi, Type 3E) at 300 rpm and 30 °C, for 60 minutes. The resulting slurry was vacuum filtered in order to separate the solids from the leachate solution. The obtained solid residues were left to dry overnight, under ambient conditions. The dried solids were subjected to a second cycle of calcium extraction, according to which they were, again, mixed with 731 ml of acetic acid solution (2 M) in the same autoclave reactor, under the same conditions (30 °C, 300 rpm) and for the same period (60 minutes). After the end of mixing, the slurry was vacuum filtered to retrieve the filter cake which was subsequently washed under vacuum using ultra-pure water, to remove any potential residual leaching solution from it. Finally, the solid residues were oven-dried at 105 °C for 24 hours.

For the hydrothermal conversion phase, two different concentrations of NaOH solution, namely 0.5 and 2 M were used. For each conversion experiment, 60 grams of the residual solids obtained from the calcium-extraction stage were mixed with 300 ml of NaOH solution (L/S = 5 L/kg), in an autoclave reactor at 300 rpm and 150 °C, for 24 hours. The resulting slurry was vacuum filtered to retrieve the activated solids, which in turn, were thoroughly washed under vacuum, using ultra-pure water, in order to remove excess caustic. The obtained solids were then oven-dried at 105 °C for 24 hours. Finally, the converted material was disaggregated using mortar and pestle.

#### **4.2.2.3. Heavy metal adsorption tests**

The adequacy of the produced materials as heavy metal adsorbents was evaluated by applying adsorption equilibrium experiments. For the requirements of these tests, Ni<sup>2+</sup> was selected as model for investigation.

To determine the equilibrium Ni<sup>2+</sup> concentration, the synthesized sorbents were placed in synthetic aqueous solutions with varying initial concentrations (2, 10, 20, 100, 200 mg/l) of the particular metal. A standard solution of Ni<sup>2+</sup> was used for the synthesis of the contaminated solutions. For each test, 1 g of the activated material was dispersed in 100 ml of the solution. In order to prevent dissolution of the material in the initial acidic environment of the

synthetic solution and to adjust the pH to that typically found in heavy metal remediation conditions [250], the pH of the mixture was adjusted to 4-5 by adding concentrated NaOH (2 M at first, and 0.5 M closer to end-point) dropwise. The slurry was placed in an incubator and subjected to mixing at 160 rpm and 20°C (293 K), for 24 hours. During the adsorption reactions occurring in the solution until its equilibrium was reached, the pH was raised to values over 5. As reported by experimental studies and geochemical modeling conducted by Santos et al. [11], at the particular pH conditions, nickel precipitates as Ni(OH)<sub>2</sub>. This type of heavy metal removal should not be accounted as actual adsorption capacity of the tested material. In an effort to avoid such biased measurements, the pH of the equilibrated adsorbent-adsorbate solution was re-adjusted to ~ 5.0 by adding drops of concentrated hydrochloric acid (2 M at first and 0.2 M closer to the end-point) dropwise. The mixture was then subjected to centrifugation (Thermo Electron, IEC CL30) at 2500 rpm for minimum 5 minutes, in order to separate the solution from the residual solids. Finally, drops of HNO<sub>3</sub> were added to the resulting supernatant (to 2 wt % nitric acid concentration), which was then analyzed for its content in Ni<sup>2+</sup>.

By knowing the initial concentration of Ni<sup>2+</sup> in the synthetically prepared contaminated solution (C<sub>0</sub>) (μmol/ml) and the concentration of Ni<sup>2+</sup> at the equilibrium state of the solution (C<sub>e</sub>) (μmol/ml), the amount of heavy metal adsorbed per gram of the adsorbent at equilibrium (q<sub>e</sub>) can be calculated by using the following formula:

$$q_e = \frac{(C_0 - C_e) \cdot V}{m} \quad (4-1)$$

where V is the volume of the contaminated solution (ml), and m is the mass of the dry adsorbent (g).

### 4.2.3. Analytical methods

The particle size distributions of the as received GBFS and PBFS and that of the zeolitic material created after the hydrothermal conversion of the solid

residues resulting from the calcium-extraction step were determined by laser diffraction analysis (LDA, Malvern Mastersizer 3000).

The chemical compositions of the as received GBFS and PBFS and these of the hydrothermally converted materials were determined by wavelength dispersive X-ray fluorescence (WDXRF, PANalytical Zetium).

The mineralogical compositions of the as received materials and these of the synthetic adsorbents were determined by X-ray diffraction (XRD, Rigaku MiniFlex 600).

The surface area, pore volume and width of the fresh GBFS, PBFS and of the formed adsorbents were discovered using the nitrogen adsorption method (NOVAtouch). In particular, the surface area of the materials was calculated using the BET method with multi-point calibration, whereas their pore size and width were measured employing the DFT method for silica with cylindrical pores.

To determine the concentration of calcium in the post extraction leachates resulting from the batch extraction tests, as well as that of  $\text{Ni}^{2+}$  in the post-centrifuged equilibrated adsorbent-adsorbate solutions, inductively coupled plasma optical emission spectroscopy (ICP-OES, Perkin Elmer Optima 8300) was employed.

#### **4.2.4. Material characterization**

##### **4.2.4.1. Elemental composition**

The elemental composition analyses of the fresh PBFS and GBFS are presented in Tables 4-1 and 4-2. According to the results, the investigated materials were characterized by similar chemistry.

In particular, the composition of PBFS was mainly characterized by the presence of Ca (285.93 g/kg), Si (161.2 g/kg), Mg (68.85 g/kg) and Al (51.01 g/kg). Minor metallic components were Ti (7.9 g/kg), K (4.097 g/kg), Fe (3.25 g/kg), P (2.18 g/kg) and Mn (2.3 g/kg). Sulfur content was 12.2 g/kg.

**Table 4-1 Elemental composition of the fresh PBFS**

<i>Elements</i>							
	<b>Mn</b>	<b>Mg</b>	<b>Al</b>	<b>Si</b>	<b>P</b>	<b>S</b>	<b>Cl</b>
<b>g/kg</b>	2.296	68.85	51.01	161.19	2.18	12.2	2.1
<i>Elements</i>							
	<b>K</b>	<b>Ca</b>	<b>Na</b>	<b>Ti</b>	<b>Ba</b>	<b>Fe</b>	<b>Zn</b>
<b>g/kg</b>	4.097	285.93	3.15	7.896	0.833	3.25	0.048
<i>Elements</i>							
	<b>Rb</b>	<b>Sr</b>	<b>Y</b>	<b>Zr</b>	<b>Nb</b>	<b>Cr</b>	<b>Br</b>
<b>g/kg</b>	0.0274	0.592	0.102	0.489	0.028	0.099	0.02

GBFS was found to mainly contain Ca (324.63 g/kg), Si (149.67 g/kg), Al (52.26 g/kg) and Mg (33.14 g/kg). Minor metallic components were Ti (5.6 g/kg), Fe (2.84 g/kg), Mn (1.913 g/kg) and Ba (1.39 g/kg). Sulfur content was 15.01 g/kg.

**Table 4-2 Elemental composition of the fresh GBFS**

<i>Elements</i>								
	<b>Mn</b>	<b>Mg</b>	<b>Al</b>	<b>Si</b>	<b>P</b>	<b>S</b>	<b>Cl</b>	<b>K</b>
<b>g/kg</b>	1.913	33.14	52.26	149.27	2.566	15.01	0.59	4.81
<i>Elements</i>								
	<b>Ca</b>	<b>Na</b>	<b>Ti</b>	<b>Ba</b>	<b>Fe</b>	<b>Zn</b>	<b>Rb</b>	<b>Sr</b>
<b>g/kg</b>	324.63	2.6	5.66	1.39	2.84	0.16	0.0366	0.812
<i>Elements</i>								
	<b>Y</b>	<b>Zr</b>	<b>Cu</b>					
<b>g/kg</b>	0.063	0.392	0.08					

#### 4.2.4.2. Mineralogical composition

The XRD diagrams of the investigated materials are presented in Figure 4-1.

Both PBF and GBF slags consist essentially of an amorphous silica structure and only PBF slag also exhibited some calcite peaks.

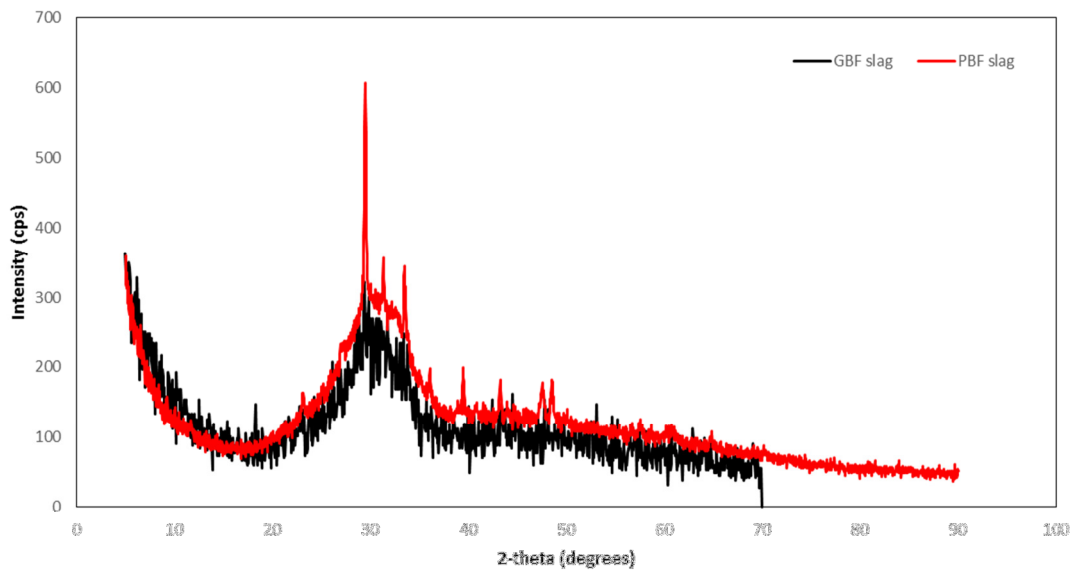


Figure 4-1 X-ray diffractogram of the fresh PBF and GBF slag.

#### 4.2.4.3. SEM analysis

The SEM analysis of the fresh PBFS and GBFS was performed after their grinding to < 2mm.

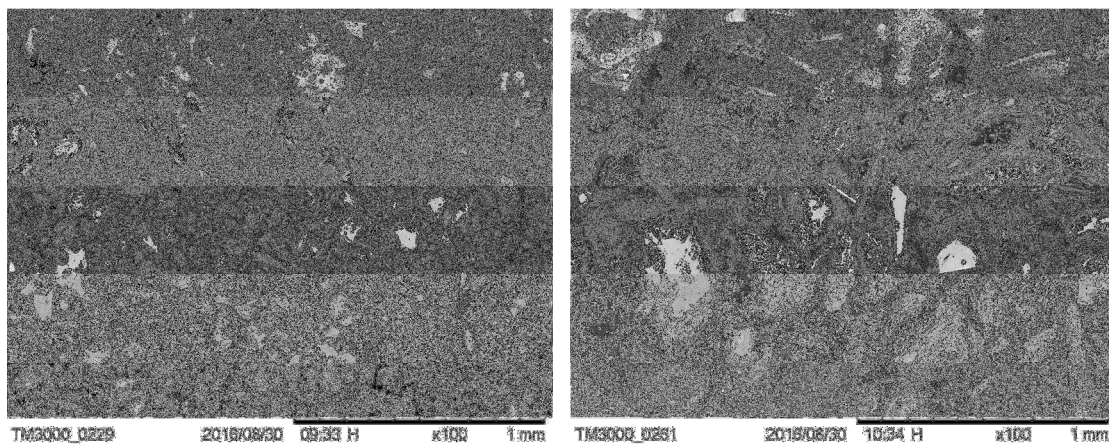


Figure 4-2 SEM images of the fresh a) PBFS and b) GBFS, after their crushing to below 2mm.

By looking at the SEM images of the fresh PBFS and GBFS in Figure 4-2, no significant differences in the porosity of the materials could be observed, whereas PBFS was characterized by smaller particle size compared to GBFS.

#### 4.2.4.4. Particle size distribution (PSD) analysis

The SEM analysis results regarding the particle size of the ground PBFS and GBFS were reaffirmed by the PSD analysis of the materials.

According to it, the volume moment (De Brouckere) mean particle diameter ( $D[4,3]$ ) of the ground PBF slag was 446  $\mu\text{m}$ , whereas the size distribution ranged from 2.13  $\mu\text{m}$  to 2.39 mm. Despite the crushing and sieving of the material to particle size below 2 mm, a negligible amount (0.12 vol.%) of material over 2 mm remained in the sample.

On the other hand, the mean particle diameter ( $D[4,3]$ ) of the ground GBF slag was found equal to 728  $\mu\text{m}$  and the size distribution ranged between 3.12  $\mu\text{m}$  and 1.63 mm.

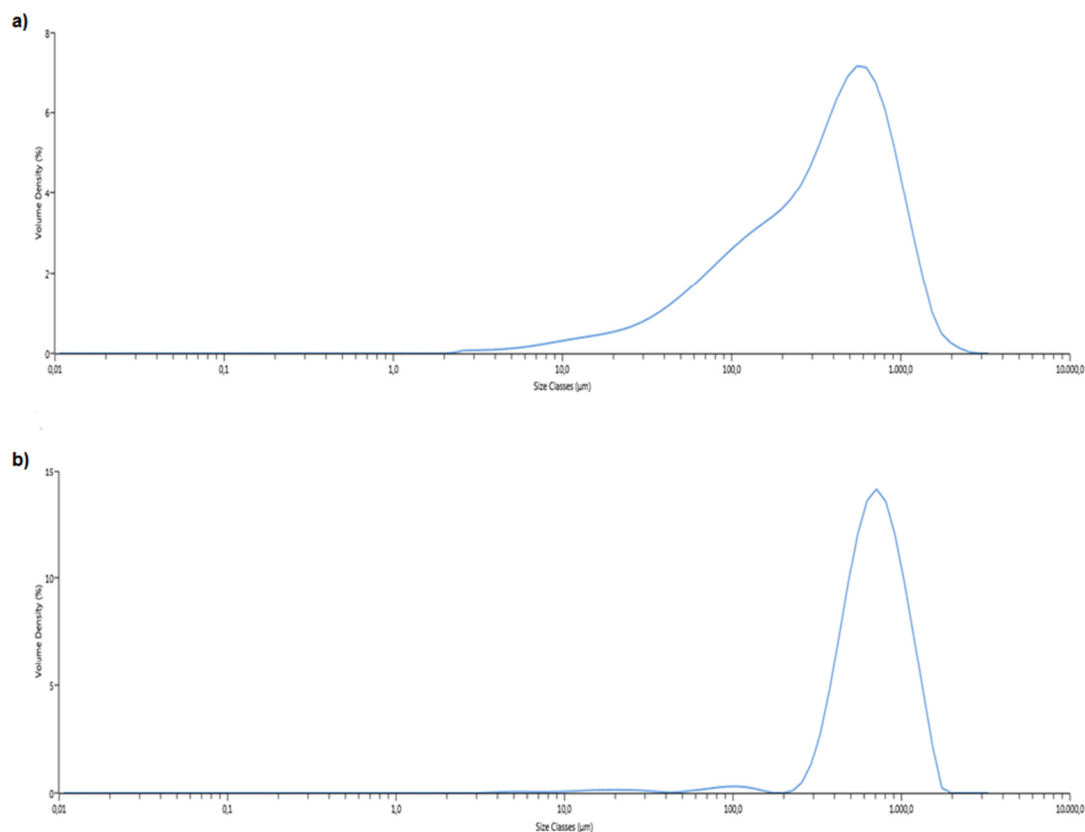


**Figure 4-3 Average particle size distribution of the original a) PBF slag b) GBF slag, after their crushing to below 2 mm.**

The average PSD distributions of both the materials are depicted in Figure 4-3.

Apparently, the mean particle size of the ground GBFS was larger than that of the ground PBFS. This should be attributed to the larger pores of the fresh PBFS which caused the easier fracturing of the material during its manual crushing and led to the formation of smaller particles than those of the ground GBFS.

#### 4.2.4.5. Surface area, pore size and width

The specific surface area, pore volume and width of the original PBFS and GBFS after their grinding, are presented in Table 4-3.

In contrast to the anticipated scenario, the porosities of PBFS and GBFS were comparable, reaffirming the observations made analyzing the SEM images of both the tested materials (Figure 4-2), which also did not display any remarkable difference in their porosity.

**Table 4-3 Specific surface area, pore volume and pore width of the fresh PBF and GBF slags**

Type of Material	Surface area (m <sup>2</sup> /g)	Pore volume (ml/g)	Pore width (nm)
GBF slag	4.28	0.021	26.4
PBF slag	4.89	0.014	22.9

As already discussed, due to the different processes adapted for the formation of these iron-making byproducts, PBFS and GBFS are characterized by different structural properties. In fact, PBFS generally exhibits a notably higher macro-porosity, compared to GBFS.

However, according to the measurements conducted for the determination of the materials porosity, GBFS exhibited higher pore volume and width compared to PBFS. The particular discrepancy should be mainly ascribed to the subjection of the fresh slags to grinding prior to experimentation. The grinding of the slags must have destroyed the larger macro-pores of the PBFS that was eventually turned into a less porous material than GBFS.

### 4.3. Results and discussion

To discover the extent of calcium leaching that can be achieved from both of the tested samples, batch extraction tests were performed

#### 4.3.1. Batch calcium extraction tests

According to the results of Chiang et al. [43], the greatest extent of calcium extraction from the tested BF slag was achieved after applying in each extraction step an acetic acid-to-calcium molar ratio of 2:1. In the calcium extraction experiments held by them, in each of the two rounds of calcium extraction, 100 grams of the tested slag were mixed with 731 ml of acetic acid (2 M).

In the particular set of experiments, the extraction of calcium from the tested material was performed in one step, using however, the same acetic acid-to-calcium molar ratio (2:1) used in each extraction step by Chiang et al. [43]. Based on the volume of acetic acid solution (100 ml), the amount of slag that was used in each test (20 g) and the calcium content of the slags, the particular molar ratio would be achieved by using an acetic acid solution of 2.8 M. It has to be noted that since the elemental compositions of the investigated materials were very similar to each other and the particular batch tests were only held for qualitative comparison reasons, the calcium content of both of the slags was considered to be the same (that of PBFS: 27.8 wt%).

Different acetic-acid to calcium molar ratios (1:1 and 1:2) and reaction durations (1, 4 and 24 hours) were also tested, to discover the way that the particular parameters affected the extent of calcium leaching from the treated material.

The percentage of calcium extracted from the slag was calculated based on the amount of calcium initially present in the tested material and its amount in the acetic acid solution at the end of each test. Each of the solutions resulting from these tests were analysed for their content in calcium in triplicates and the calcium leaching percentages were calculated based on the average concentrations of calcium in the solutions.

Apparently, a potential error during the weighing of the amount of slag used in each test may have led to inaccurate calcium extraction estimations and thereupon, to faulty conclusions regarding the ability of different concentrations of acid to leach calcium from the investigated types of slag. To minimize such errors, in this work, the weighing of the slag was conducted with high accuracy ( $\pm 0.001$  g) by using recently calibrated, high accuracy balances.

Moreover, since the percentage of calcium extracted from the slag was calculated via ICP-OES analyses of the finally obtained acidic solutions, all the potential errors related to the particular analysis may also have affected the accuracy of the conducted measurements.

Such sources of potential uncertainties can be calibration errors. Calibration errors may be caused by the improper preparation of the blanks or the poor preparation of the standard solutions required for the conduction of the ICP-OES measurements. In particular, a potential contamination of the blanks or the preparation of the standard solutions with wrong concentrations could lead to incorrect results regarding the concentration of metals in the tested solution. To minimize such errors, the blanks and the standard solutions were carefully prepared using clean and recently calibrated equipment (e.g. pipettes etc.) and under the close supervision of experienced technicians of the lab. The estimation of such errors in this work was based on the difference between the standards and the standards run as samples.

The calcium leaching percentages achieved after each tested treatment are reported in Table 4-4, along with their absolute uncertainties, which have been calculated based on the aforementioned potential experimental errors and following the experimental error propagation method [182].

According to the exerted results the reaction duration had a negligible effect on the extent of calcium extraction from both of the tested materials. In the contrary, acetic acid concentration had a critical impact on the extent of calcium leaching. In the case of GBFS, the calcium extraction achieved using acetic acid of 2.8 M was almost double the extraction achieved using 1.4 M and three times higher than that using acetic acid of 0.7 M, after every tested

period. The concentration of the acetic acid solution was also found to influence the extent of calcium leaching from PBF slag but not as profoundly as in the case of GBFS. Specifically, by using acetic acid of 2.8 M the calcium extraction achieved was 24.79 %, for 1.4 M it was 21.21 % and for 0.7 M it was 13.73 %.

**Table 4-4 Attained calcium leaching from PBFS and GBFS after batch extraction tests**

Test	Slag type	Particle size (mm)	Acetic acid conc. (M)	Duraton (min)	Ca leaching (%)
1	PBFS	<2 mm	2.8	60	24.79±1.94
2	PBFS	<2 mm	2.8	240	26.08±2.04
3	PBFS	<2 mm	2.8	1440	29.43±2.30
4	GBFS	<2 mm	2.8	60	42.63±3.34
5	GBFS	<2 mm	2.8	240	45.03±3.52
6	GBFS	<2 mm	2.8	1440	46.54±3.64
7	PBFS	<2 mm	1.4	60	21.21±1.66
8	PBFS	<2 mm	1.4	240	23.23±1.82
9	PBFS	<2 mm	1.4	1440	23.21±1.82
10	GBFS	<2 mm	1.4	60	22.45±1.76
11	GBFS	<2 mm	1.4	240	23.96±1.87
12	GBFS	<2 mm	1.4	1440	24.55±1.92
13	PBFS	<2 mm	0.7	60	13.73±1.07
14	PBFS	<2 mm	0.7	240	15.41±1.21
15	PBFS	<2 mm	0.7	1440	15.62±1.22
16	GBFS	<2 mm	0.7	60	15.29±1.20
17	GBFS	<2 mm	0.7	240	15.17±1.19
18	GBFS	<2 mm	0.7	1440	16.48±1.29

Although for low acid concentrations (0.7 and 1.4 M) the extraction of calcium from both of the slags ranged within comparable levels, at the highest tested concentration (2.8 M), the extent of calcium extraction from GBFS was remarkably higher than that of PBFS. In particular, after only 60 minutes of

reaction between the slag and the acetic acid solution, almost 43 % of the calcium contained in the GBFS was extracted, a percentage considerably higher than the one achieved by PBFS (24.8 %) using the same acetic acid concentration and after the same period.

In general, based on these findings, it could be inferred that for lower acetic acid-to-calcium molar ratios it was the concentration of the extracting solution that determined to a great extent the level of the achieved calcium extraction from both of the slags, whereas at higher acetic acid concentrations, the structure and the elemental composition of the material defined the extent of calcium removal.

Qualities like the particle size, the specific surface, the elemental composition and the porosity of the tested material have been found to affect the extent of calcium extraction. According to the exerted results, although PBFS appeared to have higher specific surface than GBFS, the extent of calcium extraction from the latter was significantly higher. This should be mainly attributed to the higher porosity of GBFS and the higher content of calcium in its composition, compared to PBFS.

The extent of calcium extraction achieved after 60 minutes of reaction between the GBFS and the acetic acid solution of 2.8 M (~ 43 %) was found to be comparable to that attained after the first step of the extraction process performed by Chiang et al. [43] (~ 58 %) under similar conditions, using the same acetic acid-to-calcium molar ratio (acetic acid solution of 2 M). The relative proximity of these two values verifies the validity of the exerted results.

The higher level of calcium leaching obtained by Chiang et al. [43], should be attributed to the smaller mean diameter of the GBFS particles ( $D_{[4,3]}$ : 138  $\mu\text{m}$  vs 728  $\mu\text{m}$ ) and the slightly higher acetic acid-to-calcium molar ratio used in the particular research, compared to that employed in the present study.

#### **4.3.2. Zeolitic materials characterization**

In this project, the production of zeolitic material through the hydrothermal conversion of the solid residues resulting from the subsection of BF slag to a

calcium extraction process, as proposed by Chiang et al. [43], was attempted. The efficiency of the particular process using PBFS as the starting material and applying two different concentrations of NaOH (0.5 and 2 M) as the alkaline solution was investigated. The selection of the lower concentration of NaOH was made based on the findings of Chiang et al. [43], according to which at 0.5 M of NaOH the formation of analcime in the finally synthesized material was promoted and the occurrence of tobermorite was limited to only negligible levels. The higher concentration of the alkaline solution examined in this study was not tested in the study of Chiang et al. [43] and was chosen for investigative purposes.

The characteristics of the obtained materials, as well as their adsorption capacity towards  $\text{Ni}^{2+}$  from synthetically contaminated solutions, are reported in this section.

#### 4.3.2.1. Elemental composition

The elemental compositions of the hydrothermally converted materials expressed as the % oxides of the elements are presented in Tables 4-5 and 4-6. The contents of the primary elements in the hydrothermally converted materials expressed in weight percentage per element normalized to 100 % total are shown in Figures 4-4 and 4-5.

**Table 4-5 Elemental composition of the hydrothermally converted material (NaOH, 0.5 M), expressed in weight percentage per element normalized to 100% total**

<i>Elements</i>								
	NiO	MgO	Al <sub>2</sub> O <sub>3</sub>	SiO <sub>2</sub>	P <sub>2</sub> O <sub>5</sub>	SO <sub>3</sub>	Cl	K <sub>2</sub> O
<b>wt%</b>	0.264	3.821	11.469	57.573	0.571	0.33	0.09	0.464
<i>Elements</i>								
	CaO	TiO <sub>2</sub>	Cr <sub>2</sub> O <sub>3</sub>	Na <sub>2</sub> O	Fe <sub>2</sub> O <sub>3</sub>	WO <sub>3</sub>	CuO	ZnO
<b>wt%</b>	14.603	2.485	0.099	7.645	0.202	0.012	0.021	0.016
<i>Elements</i>								
	SeO <sub>2</sub>	SrO	Y <sub>2</sub> O <sub>3</sub>	ZrO <sub>2</sub>	Nb <sub>2</sub> O <sub>5</sub>	MoO <sub>3</sub>	BaO	MnO
<b>wt%</b>	0.002	0.029	0.003	0.066	0.004	0.068	0.049	0.11

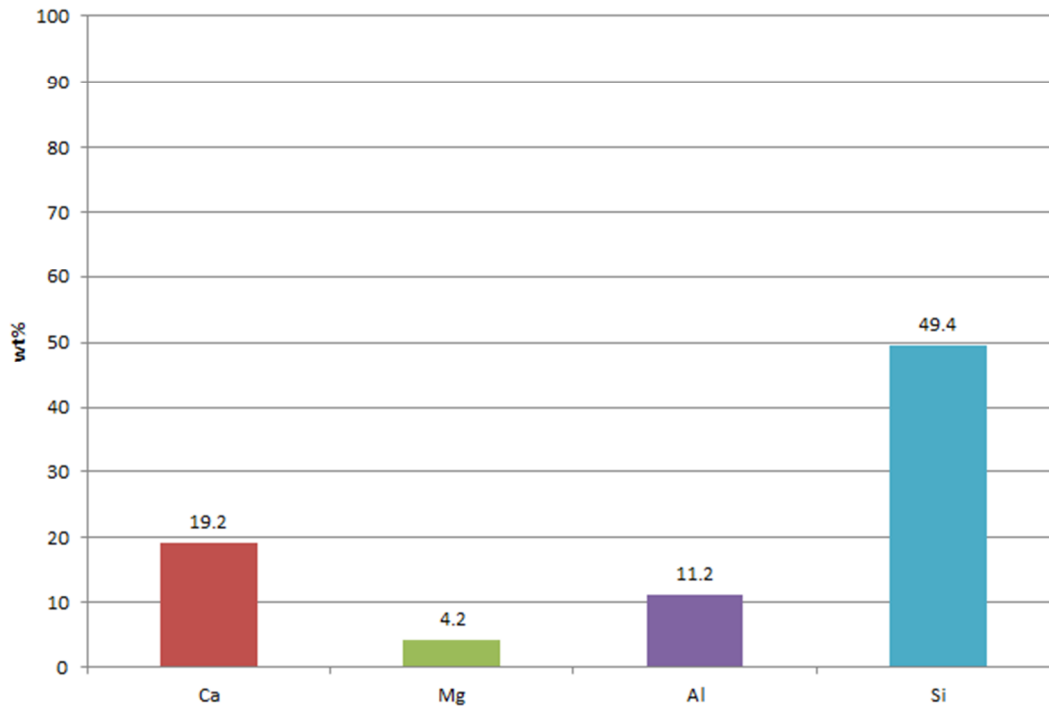


**Figure 4-4 Content of Ca, Mg, Al and Si in the hydrothermally converted material (NaOH, 0.5 M), expressed in weight percentage per element normalized to 100% total.**

**Table 4-6 Elemental composition of the hydrothermally converted material (NaOH, 2 M), expressed in weight percentage per element normalized to 100% total**

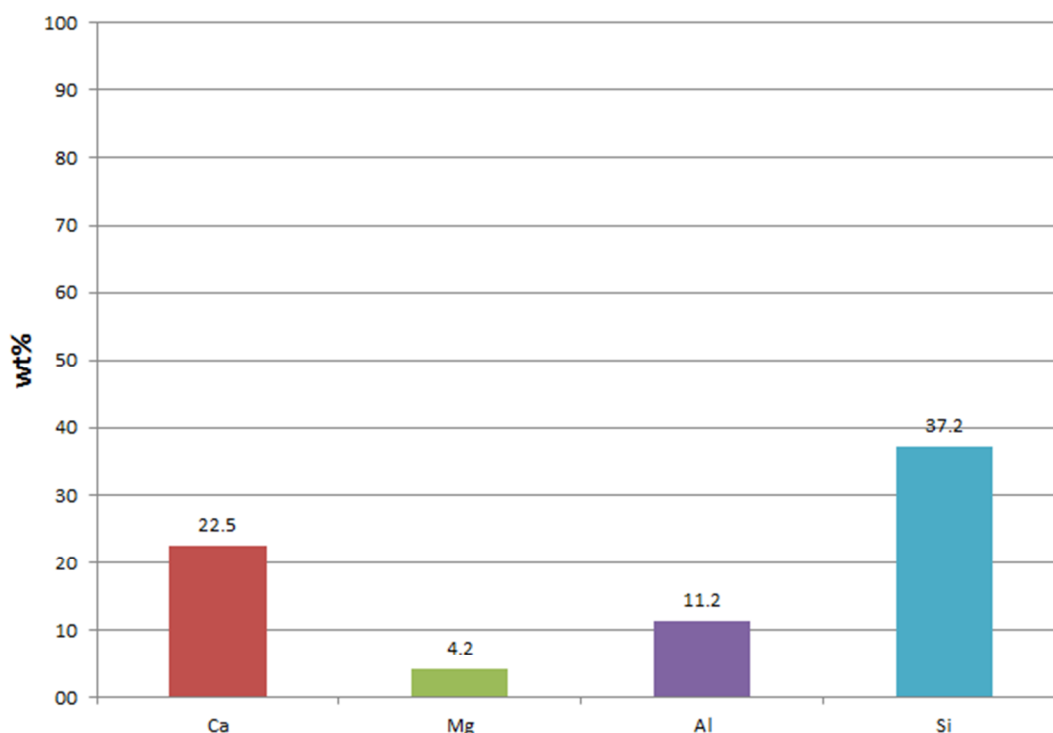
<i>Elements</i>								
	$\text{Fe}_2\text{O}_3$	$\text{MgO}$	$\text{Al}_2\text{O}_3$	$\text{SiO}_2$	$\text{P}_2\text{O}_5$	$\text{SO}_3$	$\text{Cl}$	$\text{K}_2\text{O}$
<b>wt%</b>	0.25	4.0	12.1	45.4	0.59	0.36	0.13	0.24

<i>Elements</i>								
	$\text{CaO}$	$\text{TiO}_2$	$\text{Na}_2\text{O}$	$\text{MnO}$	$\text{CeO}_2$	$\text{NiO}$	$\text{CuO}$	$\text{ZnO}$
<b>wt%</b>	17.97	2.62	15.8	0.12	0.07	0.07	0.025	0.02

<i>Elements</i>								
	$\text{Rb}_2\text{O}$	$\text{SrO}$	$\text{Y}_2\text{O}_3$	$\text{ZrO}_2$	$\text{Nb}_2\text{O}_5$	$\text{MoO}_3$	$\text{BaO}$	$\text{Cr}_2\text{O}_3$
<b>wt%</b>	0.002	0.04	0.004	0.085	0.005	0.017	0.07	0.023



**Figure 4-5 Content of Ca, Mg, Al and Si in the hydrothermally converted material (NaOH, 2 M), expressed in weight percentage per element normalized to 100% total [249].**

Calcium, aluminum and magnesium were present at comparable amounts in the composition of the materials formed at both NaOH concentrations, whereas the silica content of the material synthesized at lower concentrations of NaOH (0.5 M) was notably higher.

#### **4.3.2.2. Mineralogical composition**

The XRD diagrams determining the mineralogical composition of the hydrothermally converted materials are presented in Figures 4-6 and 4-7.

The material activated using the NaOH solution with the lower concentration (0.5 M) was unexpectedly found to be totally amorphous.

On the other hand, the hydrothermally converted material using a higher concentration of NaOH solution (2 M) was characterized by high crystallinity. In particular, two main phases were detected in the mineralogical composition of the specific material: analcime ( $\text{NaAlSi}_2\text{O}_6 \cdot \text{H}_2\text{O}$ ) and tobermorite ( $\text{Ca}_5(\text{OH})_2\text{Si}_6\text{O}_{16} \cdot 4\text{H}_2\text{O}$ ).

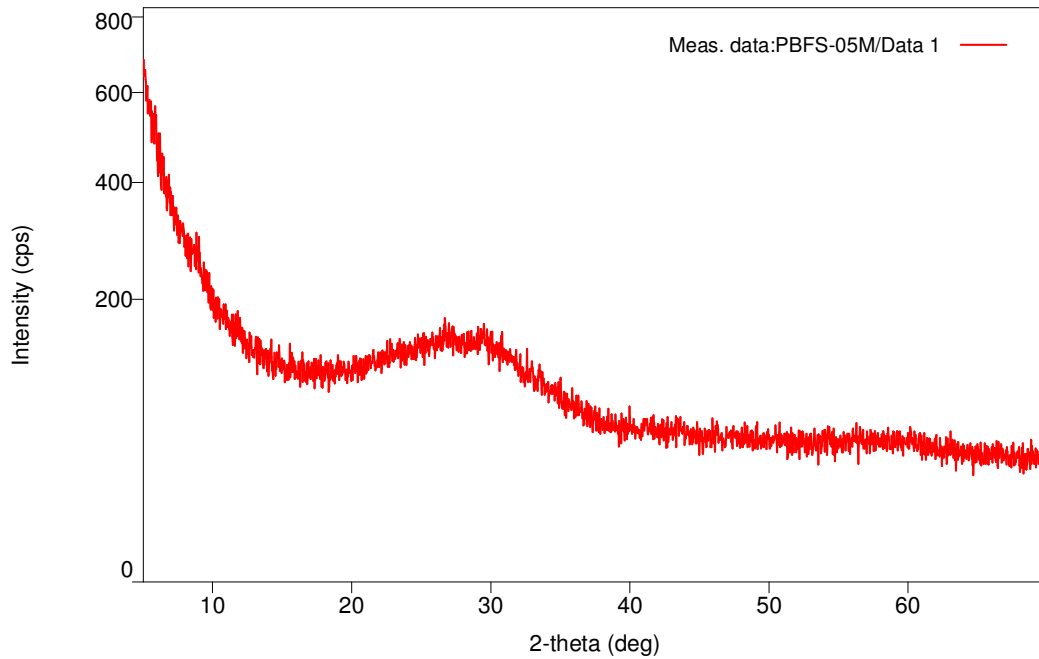


**Figure 4-6 X-ray diffractogram of the hydrothermally converted material (NaOH, 0.5 M).**

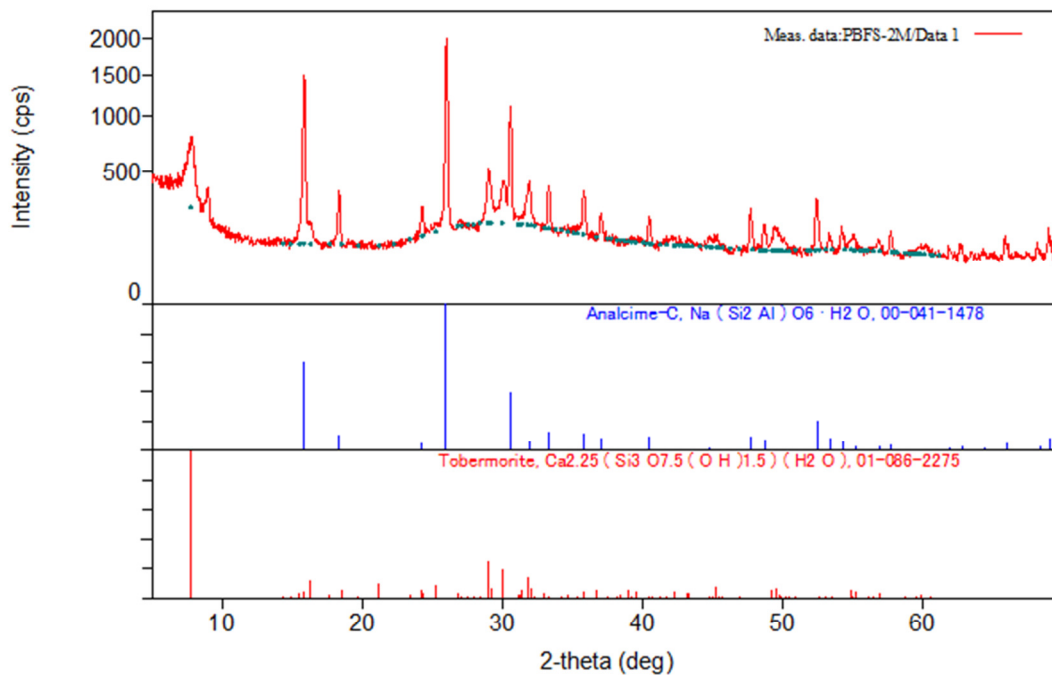


**Figure 4-7 X- ray diffractogram of the hydrothermally converted material (NaOH, 2 M) [249].**

Quantitatively, tobermorite was the predominant phase accounting 70 wt% of the formed material, whereas analcime was present at amounts close to 30 wt%. The existence of tobermorite in the converted material justifies the

notable content of calcium that was detected in the elemental composition of the extraction residues.

#### **4.3.2.3. SEM analysis**

By looking at the SEM images of PBFS after its treatment with  $\text{CH}_3\text{COOH}$  (2 M) (Figure 4-8), the occurrence of several needle-like crystals can be observed. The presence of these particles most likely, indicates the existence of calcium acetate in the sample to be hydrothermally activated. The particular finding implies inadequate washing of the obtained solids after their separation from the acetic acid leachate solution and reasonably explains the behavior of the material that was hydrothermally activated using the NaOH solution with the lower concentration (0.5 M). Probably, since the samples were contaminated with calcium acetate, the applied concentration of NaOH was too low to raise the pH of the slurry at levels that would have caused the generation of minerals and hence, the material remained amorphous. However, by increasing the concentration of the applied alkaline solution to 2 M, the pH of the solution also increased and managed to reach levels where the formation of minerals was enabled.

Actually, the roughness observed on the surface of PBFS after its subsection to hydrothermal conversion (NaOH, 2 M) should be attributed to the formation of tobermorite and analcime during the process.

Compared to the material formed by Chiang et al. [43], the occurrence of tobermorite in the composition of the product synthesized in the present study was remarkably higher. In particular, among the several products formed in the study of Chiang et al. [43], the most intensive presence of tobermorite (33 wt%) was detected in the one obtained after the extraction of calcium from the GBF slag employing an acetic acid solution of 2 M, and the subsequent hydrothermal conversion of the resulting residues using a NaOH solution of 3 M. Apparently, the highest occurrence of tobermorite in the study of Chiang et al. [43] is approximately the half of the one describing the presence of tobermorite in the finally produced material of the present study, even though a lower concentration of NaOH solution (2 M) was used.

This could be partially ascribed to the lower extent of calcium leaching that was generally achieved using PBFS instead of GBFS, as shown by the batch calcium extraction tests. However, the most important reason should be the inadequate washing of the residues derived from the calcium extraction process. Due to that, significant amounts of calcium in the form of calcium acetates were present in the composition of the material that was subjected to hydrothermal conversion and therefore remarkable amounts of the undesirable phase of tobermorite were formed.

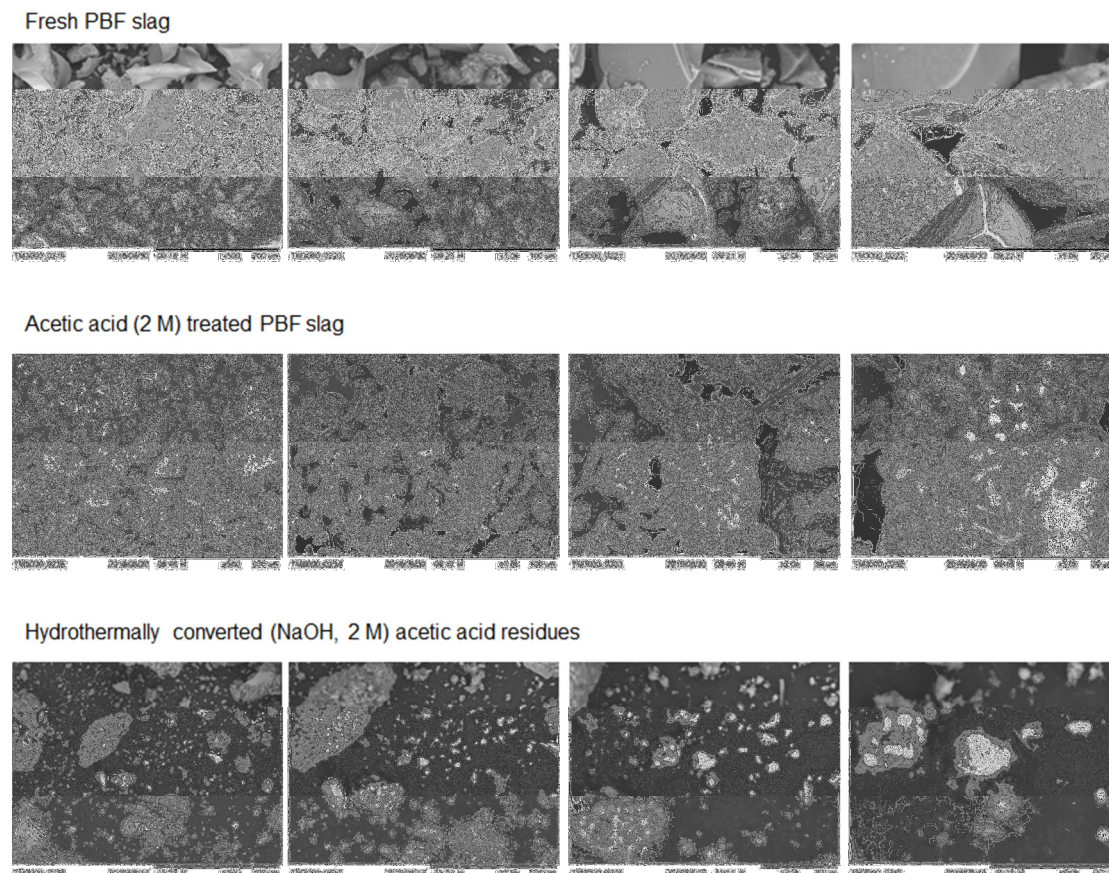


**Figure 4-8 Morphology of PBF slag at its original state, after its treatment with  $\text{CH}_3\text{COOH}$  (2 M), and of the finally produced material after the hydrothermal conversion of acetic acid residues by NaOH (2 M) with magnification: a) x500; b) x1000; c) x2000 and d) x5000.**

According to the findings of Chiang et al. [43] who observed an effect of the applied NaOH concentrations on the extent of analcime and tobermorite formation, and based on the concentrations of Na(OH) solution used in this study, it could be assumed that there is a range of concentrations, probably lower than 2 M, within which, products with higher contents of analcime would

be obtained. However, this is just a speculation whose credibility can only be reaffirmed by further experimentation. The possibility of the particular NaOH concentration (2 M) being the lowest at which mineralization occurred should also be considered.

#### 4.3.2.4. Particle size distribution analysis

The average particle size distribution of the material that was hydrothermally converted using the solution with the higher tested NaOH concentration (2 M) is presented in Figure 4-9.

Based on the PSD analysis, the mean particle diameter ( $D[4,3]$ ) of the converted material was 86.6  $\mu\text{m}$ , whereas the size distribution ranged from 0.594  $\mu\text{m}$  to 1.11 mm.

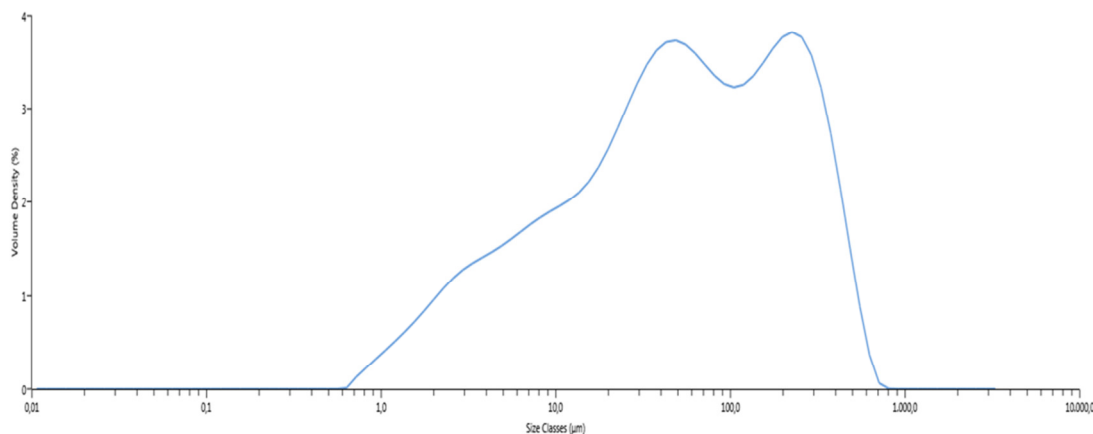


**Figure 4-9 Average particle size distribution of the hydrothermally converted material [249].**

#### 4.3.2.5. Surface area, pore size and width

Nitrogen adsorption analysis confirmed the formation of mesoporous material (46.0 nm mean pore diameter), with the specific surface area and pore volume of the hydrothermally converted material increasing, respectively, from 4.89  $\text{m}^2/\text{g}$  to 95.23  $\text{m}^2/\text{g}$  and from 0.014  $\text{ml}/\text{g}$  to 0.610  $\text{ml}/\text{g}$ , over the original slag (Table 4-7).

**Table 4-7 Comparison between the specific surface area, pore volume and pore width of the fresh and the hydrothermally converted PBF slag**

Type of Material	Surface area (m <sup>2</sup> /g)	Pore volume (ml/g)	Pore width (nm)
Fresh PBF slag	4.89	0.014	22.9
Hydrothermally activated PBF slag	95.23	0.61	46

#### 4.4. Adsorption capacity of the hydrothermally converted material

The efficiency of the material obtained by the hydrothermal activation (NaOH 2 M) of the Ca-depleted PBFS, as sorbent for Ni<sup>2+</sup> removal from synthetically contaminated water was assessed.

As already described, five synthetically contaminated solutions characterized by different initial concentrations of Ni<sup>2+</sup> were used for the conduction of the adsorption experiments. According to literature, pH has been found to significantly affect the efficiency of Ni<sup>2+</sup> removal, with increased values of solution pH enhancing the retention of the metal due to either adsorption or precipitation. However, in real remediation applications the sorbent will not be capable to permanently buffer the pH of the medium to a level higher than the natural pH that is usually low. In addition, nickel has been found to precipitate as Ni(OH)<sub>2</sub> at pH values higher than 5 [11].

In an effort to avoid accounting the removal of Ni<sup>2+</sup> by precipitation as actual adsorption capacity of the tested material and to assess the functionality of the material as a Ni<sup>2+</sup> sorbent at pH conditions typically characterizing real heavy metal remediation applications, in this study the pH of the synthetically prepared contaminated solutions of Ni<sup>2+</sup> was controlled to 4-5, prior and after their equilibration.

After the end of each experiment the equilibrated adsorbent-adsorbate solutions were subjected to ICP-OES analysis for their content in Ni<sup>2+</sup>. Upon this value,  $q_e$  was calculated.

It has to be noted that each equilibrated sample was subjected to ICP-OES analysis for five times. The values of  $C_e$  that were used for the determination of  $q_e$  were the average of these measurements. The repeatability of these measurements was assessed by calculating the standard error of the mean for each value, whereas the accuracy of  $q_e$  values was assessed by determining their absolute uncertainties.

The absolute uncertainties were calculated following the experimental error propagation method [182], based on the mathematical expression of  $q_e$  and by defining the potential errors that may have occurred during the experimental process.

According to the Equation (4-1), the calculation of  $q_e$  is based on  $C_0$  and  $C_e$  of  $Ni^{2+}$  in the contaminated solution, the volume of the contaminated solution and the mass of adsorbent used in the adsorption experiments. Apparently, apart from the errors related to ICP-OES measurements that have already been discussed in section 4.3.1 and are related to the  $C_e$  measurements, potential errors during the weighing or measurements of the particular parameters could also lead to the calculation of inaccurate values for  $q_e$ .

To minimize such errors, the volumes of  $Ni^{2+}$  standard solution required for the formation of contaminated solutions with different initial  $Ni^{2+}$  concentration, as well as the volumes of these solutions used in each adsorption test were carefully measured with high accuracy volumetric flasks, the mass of adsorbent used in the experiments was weighed with accuracy of four decimal places, using a calibrated high accuracy balance, whereas the ICP-OES measurements were conducted after the proper calibration of the instrument, as described in section 4.3.1.

The measured  $C_e$  and the corresponding  $q_e$  values are presented in Table 4.8. The  $q_e$  values are reported along with their absolute uncertainties, whereas  $C_e$  values are accompanied by their standard errors of the mean, as an indication of the measurements repeatability.

**Table 4-8 Concentration of Ni<sup>2+</sup> in the solution, Ni<sup>2+</sup> removal percentage and actual amount of Ni<sup>2+</sup> adsorbed at equilibrium, prior and after pH adjustment**

Initial Ni <sup>2+</sup> concentration (mg/L)	Equilibrium Ni <sup>2+</sup> Concentration (C <sub>e</sub> ) (μmol/100ml)	Adsorption of Ni <sup>2+</sup> by adsorbent at equilibrium (q <sub>e</sub> ) (μmol/g)
	pH Unadjusted	
2	0.12±0.06	4.51±0.33
10	0.21±0.1	22.92±1.7
20	0.82±0.11	45.45±3.37
100	72.39±0.34	158.98±11.8
200	269.5±2.92	193.19±14.33
pH Adjusted		
2	0.2±0.06	4.43±0.33
10	1.24±0.04	21.9±1.62
20	1.52±0.1	44.75±3.32
100	85.6±0.41	145.77±10.81
200	272.59±0.92	190.15±14.10

The equilibrium adsorption isotherms of Ni<sup>2+</sup> onto the hydrothermally converted material, prior and after the pH adjustment of the equilibrated adsorbent-adsorbate solutions, as well as the fitting of the experimental data to the linearized Langmuir, Freundlich and Temkin adsorption models for the further characterization of the adsorption process are presented in the following sections.

#### 4.4.1. Effect of initial Ni<sup>2+</sup> concentration

The removal of Ni<sup>2+</sup> from the solution to the surface of the adsorbent is expressed in percentage and is calculated by using the following formula:

$$R\% = \frac{M_0 - M}{M_0} \cdot 100 \quad (4-2)$$

where M<sub>0</sub> is the initial mass of pollutant (Ni<sup>2+</sup>) and M is the mass of pollutant at the equilibrium state of the adsorbent-adsorbate solution.

In general, the removal of  $\text{Ni}^{2+}$  to the surface of the hydrothermally converted material as a function of its initial concentration in the solution is depicted in Figure 4-10. Based on the exerted results, the removal of  $\text{Ni}^{2+}$  was found to attenuate with increasing initial  $\text{Ni}^{2+}$  concentration. In particular, nickel removal was close to complete for initial metal concentrations up to 20 mg/L, whereas at higher concentrations, it was significantly decreased.

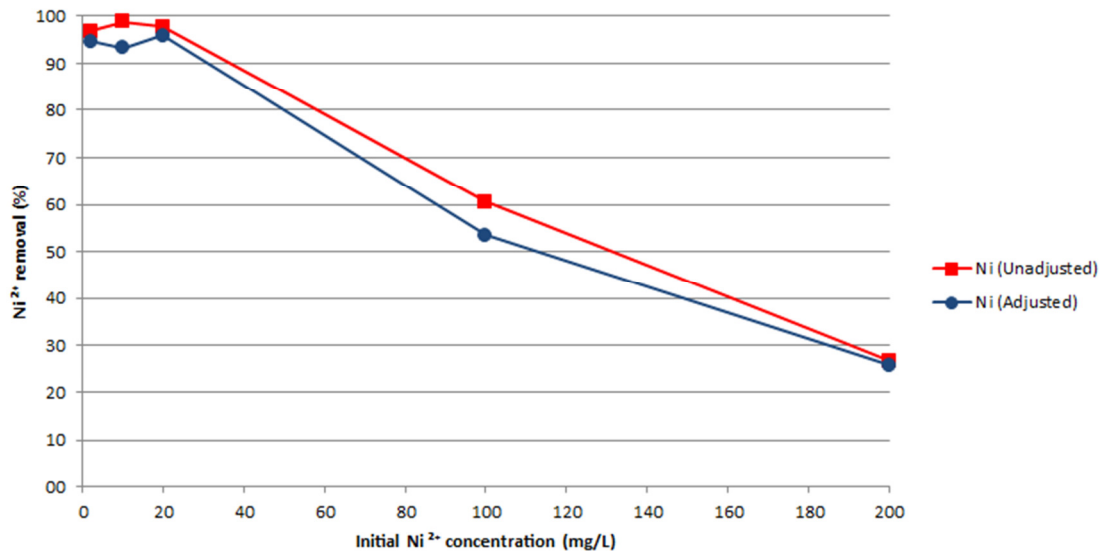


**Figure 4-10 Correlation between the solutions initial  $\text{Ni}^{2+}$  concentration and the percentage of  $\text{Ni}^{2+}$  removal achieved.**

The decrease in the percentage of  $\text{Ni}^{2+}$  removal with increasing initial concentration of the metal can be explained by the saturation of the available adsorption sites on the surface of the adsorbent due to the high metal concentration.

The influence of the solutions initial metal concentration on the achieved  $\text{Ni}^{2+}$  removal before and after pH readjustment, can also be observed in Figure 4-10. The pH readjustment of the equilibrated solutions slightly affected the removal of  $\text{Ni}^{2+}$  from them. In fact, the  $\text{Ni}^{2+}$  removal achieved by the equilibrated solutions prior to their pH modification was found to be somewhat higher than the one measured after it.

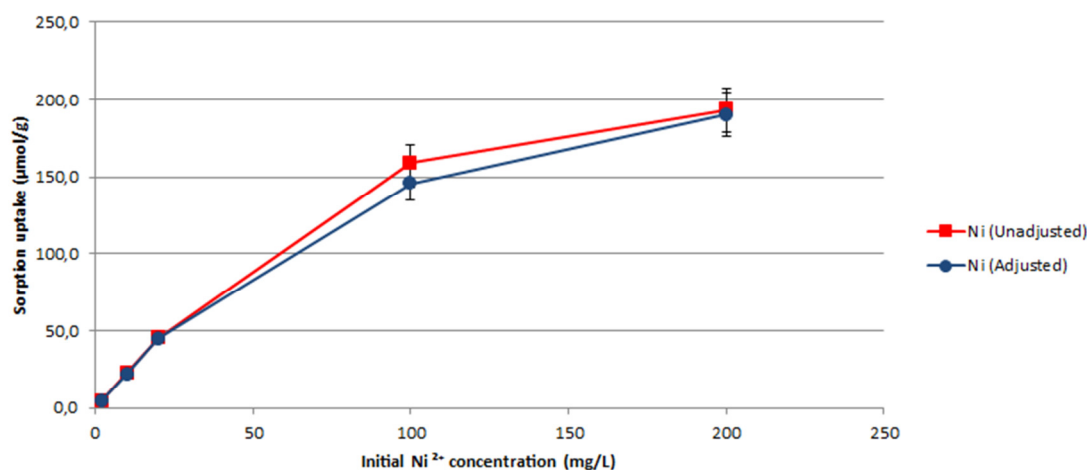


**Figure 4-11 Correlation between the solutions initial Ni<sup>2+</sup> concentration and the achieved Ni<sup>2+</sup> sorption uptake.**

On the other hand, Ni<sup>2+</sup> sorption uptake was found to increase with increasing initial concentration of the metal in the tested solutions. The particular correlation is clearly demonstrated in the graph of Figure 4-11. The  $q_e$  measurements uncertainties are reported in Figure 4-12 in the form of error bars. By increasing the initial amount of Ni<sup>2+</sup> in the solution from 10 to 200 mg/L, the sorption uptake increased from 4.5 to 193.2 µmol/g. The increased Ni<sup>2+</sup> uptakes observed at higher initial concentrations of the metal could be the result of increased adsorption rate and activation of greater number of adsorption sites on the surface of the adsorbent due to the higher amount of metal available. As expected, the sorption uptakes characterizing the pH adjusted solutions were somewhat lower than those achieved at higher basicity levels.

Another noteworthy characteristic of the investigated adsorption process that can be exerted from the diagram depicting the influence of the initial Ni<sup>2+</sup> concentration on the achieved sorption uptake is the tendency of the latter to stabilize at higher initial metal concentrations. According to the results, for Ni<sup>2+</sup> concentrations below 100 mg/L, the metal adsorption uptake sharply increased with increasing initial concentration of Ni<sup>2+</sup> in the contaminated solution. For Ni<sup>2+</sup> concentrations over 100 mg/L the particular effect was less intense and the sorption uptake achieved at 200 mg/L was comparable to that attained at 100 mg/L. Based on the particular observations and the plot of the graph, it could be assumed that there is a specific initial Ni<sup>2+</sup> concentration at

which the maximum sorption uptake would be achieved. Any increase of the initial metal concentration over the particular value would not result in further increase of the sorption uptake. This behavior can be explained by the tested material's finite number of adsorption sites, after the coverage of which no further adsorption can take place.

#### 4.4.2 Equilibrium adsorption isotherms

Based on the equilibrium concentrations of  $\text{Ni}^{2+}$  in the tested solutions and the achieved  $\text{Ni}^{2+}$  sorption uptakes, the adsorption isotherms of  $\text{Ni}^{2+}$  on the hydrothermally converted material, before and after pH readjustment, were plotted (Figure 4-12).

As in Figure 4-11, the calculated  $q_e$  absolute uncertainties are reported in the diagram of Figure 4-12, as error bars.

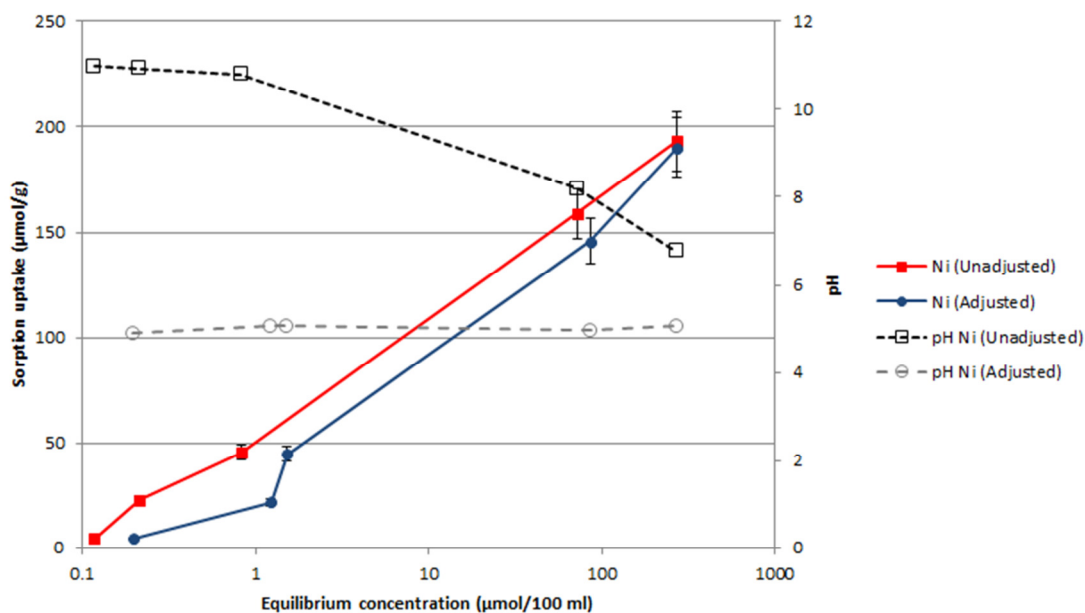


**Figure 4-12 Adsorption isotherms of  $\text{Ni}^{2+}$  on the hydrothermally converted material [249].**

The concentrations of  $\text{Ni}^{2+}$  in each of the tested solutions after their equilibration and the subsequent pH adjustment, was found to be higher than that of the equilibrated samples prior to pH buffering, with the particular deviation becoming less acute at higher initial  $\text{Ni}^{2+}$  concentrations. The equilibrium sorption uptakes characterizing the pH adjusted samples were

only slightly lower than the ones calculated for the same samples before their pH buffering.

Furthermore, the pH of the equilibrated solutions was found to be higher than that of the adsorbent-adsorbate solutions prior to their equilibration. According to theory, this finding implies that the primary mechanism that led to the removal of  $\text{Ni}^{2+}$  from the solution to the synthetic adsorbent was probably that of cation exchange.

### **4.4.3. Adsorption process characterization**

Adsorption isotherms are significant tools that help analyzing the adsorption processes. Three different adsorption models were used for the characterization of the particular adsorption process, namely Langmuir, Freundlich and Temkin. For the determination of the coefficients of each model, the fitting of the experimental data to the linearized adsorption isotherms was attempted. In an effort to discover the efficiency level at which each model describes the investigated adsorption process, the experimental data were also fitted to the simulated adsorption isotherms. Finally, the impact of experimental errors on the modeling fits of each isotherm was also assessed, by applying the calculated for each model, uncertainties, to the simulated adsorption isotherms, in the form of error bars. These error bars were calculated as dictated by the error propagation method, based on the nonlinear types that describe each model and the uncertainties that characterize each one of their parameters.

#### **4.4.3.1. Langmuir adsorption model**

Langmuir model is based on some reasonable assumptions, characterizing the chemisorption process. According to them, the surface of the adsorbent only offers a fixed number of adsorption sites, with identical shapes and sizes, characterized by the same adsorption capacity. The maximum adsorption occurs when the adsorbed material forms only one layer (thickness of one molecule) on the surface of the adsorbent, the energy of the adsorption is constant and there is no migration of adsorbate molecules in the surface

plane. Mathematically, Langmuir model is expressed by the following equation:

$$q_e = \frac{Q_m \cdot b \cdot C_e}{1 + b \cdot C_e} \quad (4-3)$$

where  $C_e$  is the equilibrium concentration of adsorbate ( $\mu\text{mol}/100\text{ml}$ ),  $q_e$  is the amount of metal adsorbed per gram of the adsorbent at equilibrium ( $\mu\text{mol}/\text{g}$ ),  $Q_m$  is the theoretical maximum monolayer coverage capacity ( $\mu\text{mol}/\text{g}$ ) and  $b$  is the Langmuir isotherm constant ( $100 \text{ ml}/\mu\text{mol}$ ).

To determine the constants in the Langmuir isotherm, equation 4-3 was linearized by plotting  $C_e/q_e$  against  $C_e$ . The fitting of the experimental data to the linearized Langmuir adsorption model is shown in Figure 4-13. The comparison between the experimental data and the simulated adsorption isotherms of  $\text{Ni}^{2+}$  onto the hydrothermally converted material is presented in Figure 4-14. The error bars in this figure represent the uncertainties accompanying the simulated and experimentally calculated  $q_e$  values and were displayed in order to assess the manner in which potential experimental errors affect the fitting of experimental data to the isotherm, as it was simulated by the Langmuir model.

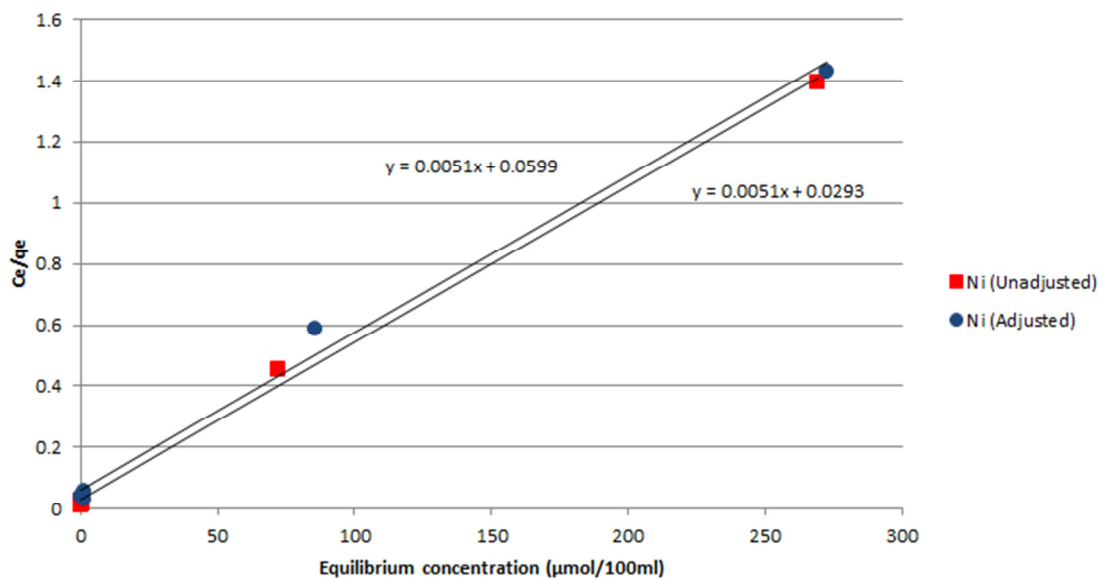


**Figure 4-13 Experimental data fitting with linearized Langmuir adsorption model [249].**

$Q_0$  and  $b$  values for the pH adjusted and unadjusted samples were estimated based on the slope and intercept of the linearized plots and are presented in Table 4-9.

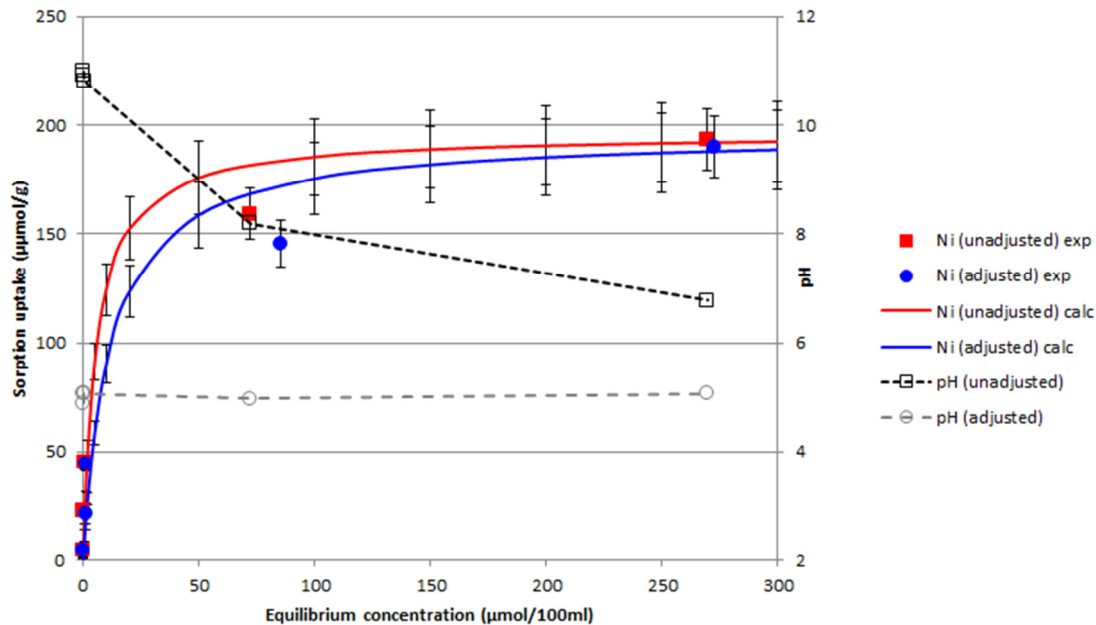


**Figure 4-14 Comparison of experimental data and simulated adsorption isotherms of  $\text{Ni}^{2+}$  onto the hydrothermally converted material according to Langmuir adsorption model [249].**

Based on the high regression coefficients values ( $R^2 > 0.99$ ) and the satisfactory proximity between the experimental equilibrium curves and the ones predicted by the Langmuir model, for both the tested adsorbent-adsorbate solutions, it could be inferred that Langmuir equation adequately describes the adsorption of  $\text{Ni}^{2+}$  onto the hydrothermally converted material.

The estimated adsorption capacities ( $Q_0$ ) of the samples prior and after pH readjustment were found to be equal to  $196.08 \mu\text{mol}$  of  $\text{Ni}^{2+}$  /g of sorbent or  $11.51 \text{ mg}$  of  $\text{Ni}^{2+}$ /g of sorbent.

As already mentioned, the calculation of  $Q_0$  is made based on the slopes of the linearized Langmuir equation plots which were found to be the same for both of the investigated cases. The same value of  $Q_0$  characterizing both pH adjusted and unadjusted adsorbent-adsorbate solutions should be attributed to the limited number of experimental data available. If more experimental data points were available it is more likely that a notable difference between

the  $Q_0$  values characterizing the adsorbent-adsorbate system prior and after pH readjustment would be observed. Based on the obtained experimental results, the particular difference should be expected to be in favor of the pH unadjusted adsorbent-adsorbate solution. However, as has been clearly shown by the equilibrium adsorption isotherms of  $Ni^{2+}$  on the hydrothermally converted material (Figure 4-12), the  $q_e$  values ascribed to both of the investigated solutions are remarkably close to each other and therefore, not a significant difference between the  $Q_0$  values of the tested adsorption systems should be anticipated.

The essential characteristics of Langmuir isotherm can be expressed in terms of a dimensionless constant separation factor, namely  $R_L$  that predicts the affinity between the adsorbate and the adsorbent and is expressed by the following equation:

$$R_L = \frac{1}{1 + bC_0} \quad (4-4)$$

where  $C_0$  is the initial concentration of  $Ni^{2+}$  in the solution ( $\mu\text{mol}/100\text{ml}$ ).

The value of separation parameter indicates the shape of the isotherm and provides useful information about the nature of adsorption. According to literature,  $R_L$  values ranging between 0 and 1 indicate favorable adsorption, values above 1 characterize unfavorable adsorption and  $R_L$  values equal to 0 indicate irreversible adsorption [251, 254]. When  $R_L$  is found equal to 1 the type of Langmuir isotherm is linear [251, 254].

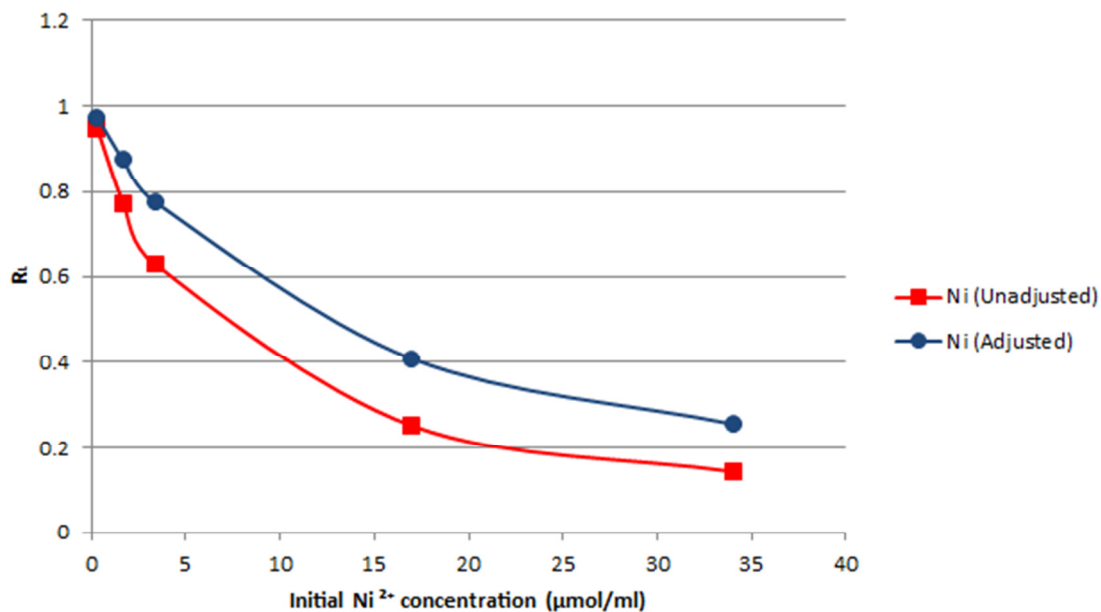


**Figure 4-15 Variation of separation factor ( $R_L$ ) as a function of initial  $Ni^{2+}$  ion concentration (adsorbent dosage = 1g, shaking time = 24 hours, shaking speed = 160 rpm,  $T = 20\text{ }^{\circ}C$ ,  $pH = 5$ ).**

The values of  $R_L$  further confirm the validity of the particular model. In fact, the  $R_L$  values for  $Ni^{2+}$  adsorption by the synthesized material in pH adjusted and unadjusted solutions ranged between 0.97 and 0.26 and between 0.94 and 0.14, respectively, for initial  $Ni^{2+}$  concentrations of 2 - 200 mg/L. These values range between 0 and 1, indicating favorable adsorption of  $Ni^{2+}$  onto the hydrothermally converted material.

Moreover, the fact that in both cases the  $R_L$  values decreased as the  $C_0$  values increased (Figure 4-15) reaffirms the fact that the removal of  $Ni^{2+}$  onto the synthesized material is less favorable at high concentrations of the metal in the solution.

#### 4.4.3.2. Freundlich adsorption model

Freundlich isotherm is not constrained by the assumptions made in the Langmuir model. Instead, it is an empirical relationship describing the physical adsorption process that can be applied to adsorbents with heterogeneous surfaces [253]. The adsorption sites distributed all over the adsorbent's surface, are characterized by different affinity for the adsorbate, whereas the adsorbed material forms more than one layers on the surface of the adsorbent [253].

Freundlich model is mathematically expressed as:

$$q_e = K_f \cdot C_e^{1/n} \quad (4-5)$$

where  $K_f$  and  $n$  are the Freundlich isotherm constants, corresponding to adsorption capacity and adsorption intensity, respectively.

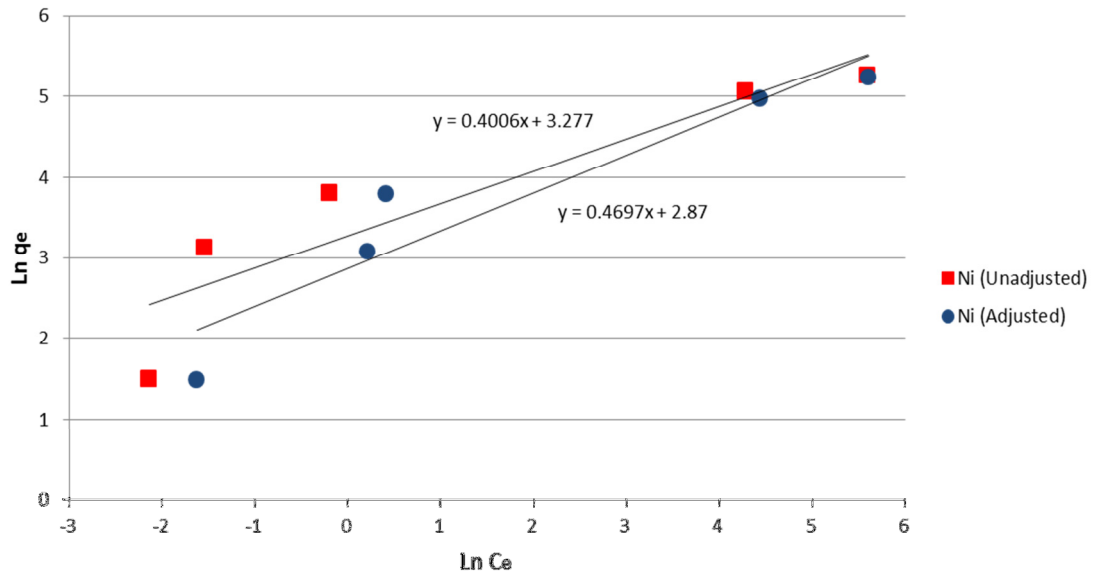


**Figure 4-16 Experimental data fitting with linearized Freundlich adsorption model [249].**

To determine the Freundlich parameters, namely  $K_f$  and  $n$ , Equation 4-5 can be linearized by plotting  $\ln q_e$  against  $\ln C_e$ . The fitting of the experimental data to the linearized Freundlich adsorption model is shown in Figure 4-16.

The comparison between the experimental data and the simulated adsorption isotherms of  $\text{Ni}^{2+}$  onto the hydrothermally converted material is presented in Figure 4-17. The error bars in this figure represent the uncertainties accompanying both the the simulated  $q_e$  values and the  $q_e$  values calculated based on the experimental results, and were displayed in order to assess the manner in which potential experimental errors affect the fitting of experimental data to the isotherm, as it was simulated using the Freundlich model.

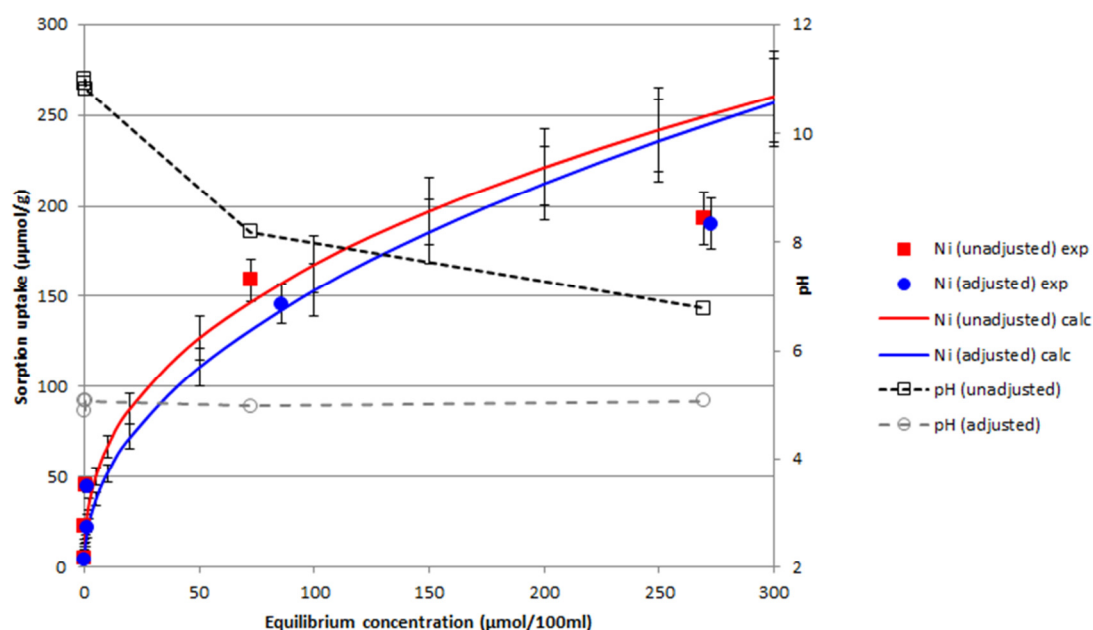


**Figure 4-17 Comparison of experimental data and simulated adsorption isotherms of Ni<sup>2+</sup> onto the hydrothermally converted material according to Freundlich adsorption model [249].**

The values of  $K_f$  and  $n$  were estimated based on the slope and intercept of the linearized plots and are presented in Table 4-9. The  $n$  values of the Freundlich equation calculated for both the pH adjusted and unadjusted adsorbent-adsorbate solutions, were found to be equal to 2.13 and 2.50, respectively. Both these values lie between 1 and 10 and this indicates favorable adsorption of Ni<sup>2+</sup> on the synthesized zeolitic material [253].

Apparently, the Ni<sup>2+</sup> uptakes achieved by the pH adjusted adsorbent-adsorbate solutions were somewhat lower than those attained by the unadjusted ones for equilibrium concentrations ranging between 0 and 300 µmol/100ml.

Judging by the correlation coefficients ( $R^2$ ) and the proximity between the experimental equilibrium curves and the ones predicted by the particular model, the isotherm data of both the adsorbent-adsorbate solutions are fitting the Freundlich equation more poorly compared to the Langmuir model.

#### 4.4.3.3. Temkin adsorption model

Temkin model assumes that the adsorption heat of all the molecules of the layer is linearly decreased with coverage due to the adsorbent-adsorbate

interactions, whereas the binding energies are uniformly distributed. Temkin model is expressed by the following equation:

$$q_e = \frac{R \cdot T}{b_T} \cdot \ln(K_0 \cdot C_e) \quad (4-6)$$

where R is the universal gas constant (8.314 J/mol/K), T is the absolute temperature (K),  $b_T$  is the Temkin constant related to heat of sorption (J/mol) and  $K_0$  is the Temkin isotherm equilibrium binding constant (100ml/ $\mu$ mol).

To determine the coefficients describing the Temkin isotherm, Equation 4-6 was linearized by plotting  $q_e$  against  $\ln C_e$ . The fitting of the experimental data to the linearized Temkin adsorption model is shown in Figure 4-18.

The comparison between the experimental data and the simulated adsorption isotherms of  $\text{Ni}^{2+}$  onto the zeolitic material is presented in Figure 4-19. The error bars in this figure represent the uncertainties accompanying both the the simulated  $q_e$  values and the  $q_e$  values calculated based on the experimental results, and were displayed in order to assess the manner in which potential experimental errors affect the fitting of experimental data to the isotherm, as it was simulated using the Temkin model.

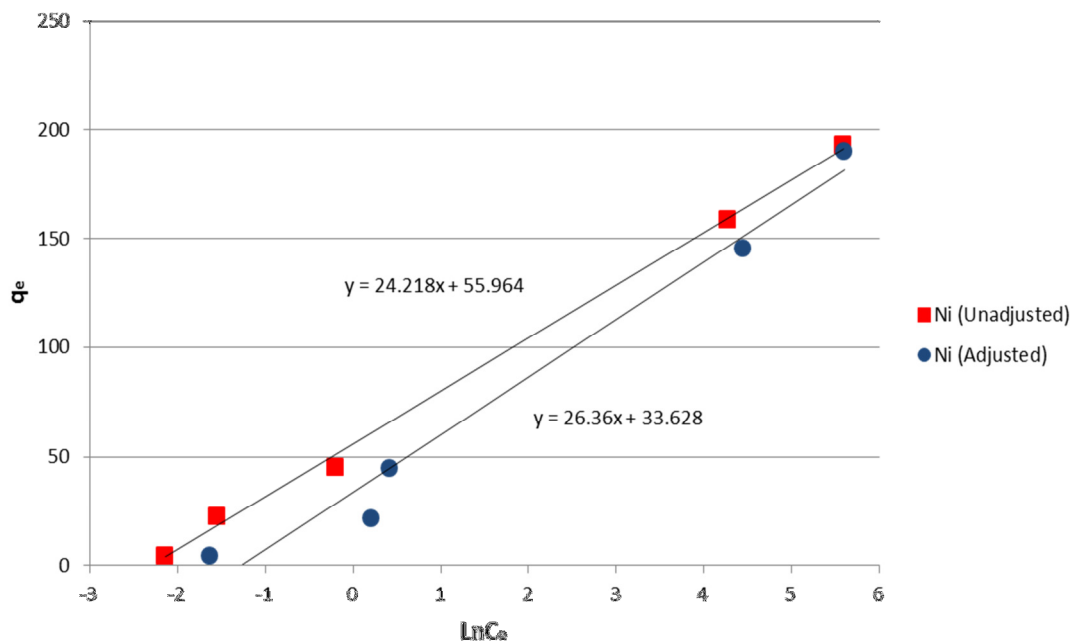


**Figure 4-18 Experimental data fitting with linearized Temkin adsorption model [249].**

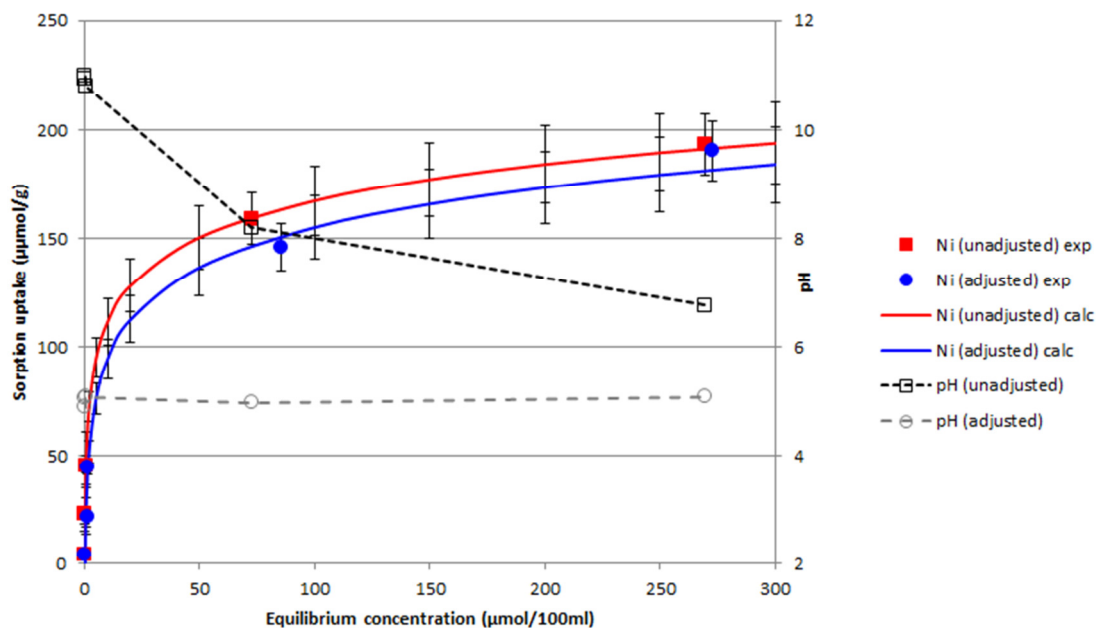


**Figure 4-19 Comparison of experimental data and simulated adsorption isotherms of  $\text{Ni}^{2+}$  onto the hydrothermally converted material according to Temkin adsorption model [249].**

From the proximity of the experimental equilibrium sorption uptakes with the equilibrium curves predicted by Temkin model as it is exhibited by the graph shown in Figure 4-18 and the high correlation coefficients ( $R^2 > 0.97$ ), it is clear that Temkin model satisfactorily describes the adsorption isotherms of  $\text{Ni}^{2+}$  onto the synthesized zeolitic material.

The values of  $K_0$  and  $b_T$  for the pH adjusted and unadjusted samples were estimated based on the slope and intercept of the linearized plots and are presented in Table 4-9.

The very low values of  $b_T$  (92.41 and 100.58  $\text{J mol}^{-1}$  for the pH adjusted and unadjusted adsorbent-adsorbate solution, respectively) signify a rather weak ionic interaction between the metal and the investigated adsorbent and a possible involvement of physical adsorption in the process [254]. Finally, the positive values of  $b_T$ , indicate that metal ions adsorption onto the hydrothermally converted material was exothermic [255].

**Table 4-9 Adsorption isotherm parameters for the Ni<sup>2+</sup> adsorption onto the zeolitic material [249].**

	Linear Equations	Coefficients	Unadjusted	Adjusted
<b>Langmuir Equation</b>	$\frac{C_e}{q_e} = \frac{C_e}{Q_m} + \frac{1}{k \cdot Q_m}$	$Q_m$ ( $\mu\text{mol/g}$ )	196.08	196.08
		$b$ ( $100\text{ml}/\mu\text{mol}$ )	0.174	0.0851
		$R^2$	0.9972	0.9933
<b>Freundlich Equation</b>	$\ln(q_e) = \ln(K_f) + \frac{1}{n} \cdot \ln(C_e)$	$n$	2.50	2.13
		$K_f$ ( $\mu\text{mol/g}$ )	26.50	17.64
		$R^2$	0.840	0.893
<b>Temkin Equation</b>	$q_e = \frac{R \cdot T}{b_T} \ln(K_0) + \frac{R \cdot T}{b_T} \ln(C_e)$	$b_T$ ( $\text{J/mol}$ )	100.58	92.41
		$K_0$ ( $100\text{ml}/\mu\text{mol}$ )	9.97	3.58
		$R^2$	0.998	0.978

#### 4.4.4 Results analysis

The estimated adsorption capacity ( $Q_m$ ) of the investigated zeolitic material prior and after pH readjustment was equal to 11.51 mg/L. A satisfactory value compared to others reported in literature describing the adsorption capacity of various adsorbents towards Ni<sup>2+</sup> (Table B-1 (Appendix B)), but significantly lower than those characterizing the Ni<sup>2+</sup> adsorption capacity of other synthetic zeolites (Table 4-10).

The latter observation has several explanations. First of all, the hydrothermally converted material synthesized in this work was not a pure zeolite. In fact the dominating phase in the composition of the finally synthesized material was tobermorite (70 %), and analcime was present in lower amounts (30 %). As already mentioned, tobermorite has been reported to act as a sorbent through ion exchange mechanism. No study on the adsorption of nickel on tobermorite was found in literature. However, based on comparisons made between the adsorption capacities of synthetic zeolites and synthetic tobermorite towards other heavy metals (e.g. Cd<sup>2+</sup> and Pb<sup>2+</sup>) [256, 259-262], it can be implied that the heavy metal removal ability of tobermorite is notably lower than that of synthetic zeolites. Therefore, it is

logical for the material formed in this work to exhibit lower  $Q_m$  values than pure synthetic zeolites.

Furthermore, although the specific surface area of the herein synthesized material was significantly enhanced compared to that of the original material (BF slag), in relation to the specific surface areas attained in other studies and ranged between 242.04 and 550  $m^2/g$ , it is notably lower (Table 4-10). The comparatively low specific surface area values characterizing the formed material should be attributed to the significant presence of tobermorite in its composition, a phase that is known for its limited specific surface area. Apparently, the lower specific surface area of the formed material limited its  $Ni^{2+}$  adsorption capacity and led to lower  $Q_m$  values.

**Table 4-10 Adsorption capacities, best fitting model and specific surface areas of different synthetic zeolites towards  $Ni^{2+}$**

Type of synthetic zeolite	Best fitting model	Maximum adsorption $Q_m$ (mg/g)	Specific surface area ( $m^2/g$ )	Reference
NaP1	Langmuir model	20.1	27.7	Alvarez-Ayuso et al. [256]
Cancrinite-type zeolite	Langmuir model	89.9	278.9	Qiu and Zheng [242]
Zeolite-like titanosilicate compounds	Langmuir model	113	-	Deesaen et al. [257]
Zeolite-A	Langmuir model	65.66	-	Wassel et al. [258]
Zeolite A	Langmuir/Freundlich /Temkin model	121.9	550	Jamil and Youssef [259]
Analcime	Langmuir/Freundlich /Temkin model	110.2	482.225	Jamil and Youssef [259]
Zeolite X	Langmuir/Freundlich model	79.2	242.04	Wang et al. [260]
<b>Tobermorite -Analcime</b>	<b>Langmuir/Temkin model</b>	<b>11.51</b>	<b>95.23</b>	<b>This study</b>

Finally, the adsorbent-adsorbate solution pH may have also influenced the finally reported adsorption capacity of the synthetic zeolites. As already discussed, at pH values above 5.5, nickel precipitates as  $Ni(OH)_2$  and if the solution's pH is not monitored and readjusted to around 5.5 regularly, this precipitation will be considered as adsorption capacity of the investigated

material. In all of the studies reviewed in this section, the initial pH of the adsorbent-adsorbate solution was adjusted to around 5.5, in order to avoid such biased measurements, but only Qiu and Zheng [242] reported a regular pH monitoring and readjustment to the initial value. However, based on the results of this work and those of Qiu and Zheng [242] who reported Ni<sup>2+</sup> adsorption capacities close to those attributed to the other synthetic zeolites herein reviewed, the absence of a pH control system in the most of the discussed works is not expected to have caused a significant overestimation of the tested materials ability to remove Ni<sup>2+</sup> from aquatic environments.

In Table 4-10, the isotherm models that better described each one of the reviewed adsorption processes, are also reported. According to the findings, Langmuir model seems to be the one that better describes the adsorption of Ni<sup>2+</sup> onto the synthetic zeolites surface. This in combination with the way that zeolites have been reported to act as sorbents and the findings of Chiang et al. [219] and Qiu and Zheng [242], who reported that the ion exchange mechanism is better described by the Langmuir isotherm, suggests that ion exchange is the prevailing mechanism of Ni<sup>2+</sup> adsorption onto synthetic zeolites. Supplementary adsorption mechanisms such as chemi- or physisorption may also occur.

In this work both Langmuir and Temkin isotherms were found to satisfactorily describe the adsorption process. Based on the way that tobermorite and analcime have been found to act as sorbents and the Temkin model coefficients reported before, it could be inferred that apart from cation exchange that was probably the dominant adsorption mechanism of the investigated adsorption process, physisorption must also have been involved to some extent.

## 4.5. Conclusions

The aim of this work was the reproduction of analcime from BF slag following the route originally proposed by Chiang et al. [43], according to which the storage of CO<sub>2</sub> in a stable and benign mineral form is achieved, while valuable minerals (PCC and zeolites) are produced and potential residues are eliminated.

In an effort to improve the extent of calcium leaching that was proved to be the process step that determined the type of the formed zeolite, a more porous material was selected for investigation. In particular, instead of using GBF slag, the use of a different type of BF slag, characterized by higher porosity, namely PBF slag, was preferred. However, the grinding of the slag prior to experimentation probably destroyed its large pores and decreased the porosity of the actually tested material, to levels even below the porosity of GBF slag. This, in combination with the higher amounts of calcium present in the composition of GBF slag in respect with PBF slag, led to the extraction of remarkably lower amounts of calcium from the latter when applying the acetic acid-to-calcium molar ratio (2:1) that according to literature has been proved to be the most efficient for the formation of high amounts of analcime [43].

Although two different NaOH solution concentrations, namely 0.5 M and 2 M, were tested for the hydrothermal conversion of the acetic acid residues, only the higher one was proved to be capable of forming minerals from the acetic acid treated material. The post extraction solid residues were not efficiently washed after their separation from the leachate solution and calcium acetate particles were left in the samples that were subsequently subjected to hydrothermal conversion. Under these circumstances, the NaOH solution of 0.5 M was incapable of increasing the attenuated, due to the presence of the acetates, pH and produce mineral phases.

In the contrary, despite the limited level of calcium extraction achieved and the presence of calcium acetate in the samples as a result of inadequate washing, the hydrothermal conversion of PBF slag in NaOH solution of increased concentration (2 M) led to the formation of notable amounts of analcime and tobermorite.

Judging by the actual ability of the hydrothermally converted material to adsorb  $\text{Ni}^{2+}$  from water, as determined by the maximum monolayer adsorption capacity ( $Q_m$ ) (11.51 mg/g) of the newly formed material towards  $\text{Ni}^{2+}$  that was calculated based on Langmuir equation, this product can potentially be used in wastewater treatment or environmental remediation applications.

The amount of  $\text{Ni}^{2+}$  adsorption attributable to each of the phases composing the hydrothermally activated material (analcime and tobermorite) was not determined. However, both of these phases have been found to be of notable heavy metal adsorption capacity [259, 263-266] and the involvement of both of them in the adsorption of  $\text{Ni}^{2+}$  from the contaminated solutions should be considered as certain.

Regarding the characterization of the investigated adsorption process, the higher regression coefficients ( $R^2 > 0.97$ ), as well as the higher proximity between the experimental data and the simulated theoretical isotherm curves obtained by Langmuir and Temkin isotherms, indicate better description of the investigated adsorption process by the particular models, compared to the Freundlich one. Based on this but also on other characteristics of the process that are analytically discussed in previous sections of this chapter, the adsorption of  $\text{Ni}^{2+}$  ions onto the converted material should be described through an ion exchange mechanism. Moreover, based on the values of the coefficients characterizing the applied models, the adsorption process could also be described as exothermic, whereas physisorption was, probably, also involved.

## 5. CONCLUSIONS AND FUTURE WORK

The valorization of iron- and steel-making slags through processes incorporating mineral carbonation, in order to achieve the formation of products with commercial value and the parallel sequestration of sufficient amounts of CO<sub>2</sub>, was the aim of this project.

From the several types of iron- and steel-making slags, only two of them were found with appealing characteristics for the requirements of this research. By introducing a new index, namely CWR the direct comparison between the carbonation conversions achieved by different experimental studies became possible. Judging by the CWR values and the production amounts characterizing each type of the particular slags, BF and BOF slag were selected for investigation.

Generally, the research gave promising results regarding the coupling of carbonation with supplementary processes as a manner to sequester sufficient amounts of CO<sub>2</sub> while forming value-added products of potential marketability. Nonetheless, several parts of the herein presented methodologies were found requiring further upgrading, something that will be the target of future works. In the following sections, the outcomes of the particular research are gathered, the deficiencies of the studied technologies are specified, ways to improve their efficiency are discussed and additional work required is highlighted.

### 5.1. Valorization of BOF slag

#### 5.1.1. Concluding remarks

With the greater part of BOF slag going for landfilling or utilized in low end applications, it is clear that new valorization ways for the particular type of steel-making slag are required. The granulation and granulation-carbonation treatments using water or alkali-solution (NaOH+Na<sub>2</sub>SiO<sub>3</sub>, 50:50) as binders, were examined and evaluated as potential efficient manners to accomplish the simultaneous sequestration of sufficient amounts of CO<sub>2</sub> and production of aggregates for construction applications.

Alkali-activation was proved to facilitate the achievement of the aforementioned goals. In fact, the use of sodium solution as the binder during granulation or granulation-carbonation treatments of the slag resulted in the production of granules characterized by ACVs close to the ones attributed to natural aggregates, and notable amounts of stored CO<sub>2</sub>. More specifically, the single granulation and the combined treatment of alkali-activated BOF slag employing a W/S ratio of 0.12 and 0.14, respectively, resulted in the production of granules with the highest ACVs in the study. In particular the combined treatment of the alkali activated BOF slag (W/S = 0.12, 60 minutes), caused the sequestration of notable amounts of CO<sub>2</sub> (40 g/kg steel slag), which were found to be the highest achieved in the study, and also resulted in significant particle size enlargement with respect to the particle size of the starting material.

Nonetheless, the environmental behavior of the synthesized materials was rather problematic, at least according to the legislation applied in Italy. In particular, the leaching behavior assessment of the crushed and uncrushed granules produced after the most of the tested treatments resulted in pH values above the regulatory limit that was set at 12 by the Italian principles. In fact, only one treatment (granulation-carbonation, using water as the liquid agent, carried out for 60 minutes) resulted in the production of granules which in their uncrushed state, resulted in eluates with pH values lower than 12 (11.87). Moreover, although the most of the treatments were found to comply with Italian legislation regarding the release levels of regulated elements, the leaching assessment of uncrushed granules resulting from the combined granulation-carbonation of alkali activated BOF slag and that of the crushed granules produced after 60 minutes of the combined granulation-carbonation of alkali activated BOF slag employing a W/S ratio of 0.14 L/kg, revealed high mobility of Cr and V, at levels above the Italian limits. Apparently, the environmental behavior of the granules produced after the aforementioned processes requires further improvement.

### 5.1.2. Future work

Since the investigated reuse of BOF slag is as a partial aggregate replacement in civil engineering applications, the actual mechanical and environmental behavior of the formed granules in such applications should be examined. To this end, representative mortar specimens that will be used for compressive strength and environmental behavior testing will be prepared. These specimens will actually be cement mortars, composed by aggregates, cement and water, all used at specific mix ratios. Two types of such specimens should be formed, one that would represent the reference specimen, and should be prepared using a natural aggregate (e.g. quartz sand) and cement as binder, and another in which the natural aggregates would be partially replaced by the formed granules. Different specimens of the latter type of mortars, in which different ratios of natural aggregates/synthesized granules would be applied, should also be prepared in order to discover the most suitable for its compressive strength performance, such ratio. The formation of these mortars, as well as the testing of their compressive strength should be performed following a standard process (e.g. EN 196-1, ASTM C109). The binder/aggregate and the water/binder mass ratios at which the mortar specimens are prepared, as well as the type of the compressive strength testing and thereupon, the equipment that should be used for it, will be dictated by the standard process that will be followed.

In any case, after the compressive strength testing, a crushed mortar sample will be obtained. To discover the leaching behavior of the mortar specimens, the crushed samples resulting from the compressive strength tests should be subjected to leaching tests following the EN-12457-2 standard process. This standard process is proposed, since it is the one already used in the assessment of the environmental behavior of the synthesized granules. Other standard processes, suitable for the assessment of the leaching behavior of the crushed mortar samples, could also be applied. The resulting eluate will be filtered and the retrieved filtrate will then be subjected to ICP-OES analysis for the determination of its content in major and regulated elements.

Another aspect that would be interesting to assess is the performance of the particular experimental set-up using carbonating gases with lower concentrations of CO<sub>2</sub>. To this end, the granulation-carbonation tests described in this work will be performed again using the same experimental apparatus only this time, synthetically prepared carbonating gases with different volumetric CO<sub>2</sub> concentrations (e.g. 10%, 40% and 100%) will be introduced to the granulator. By investigating the direct treatment of gases with diluted CO<sub>2</sub>, the possibility of treating CO<sub>2</sub> flows as they are originally emitted by the industry, without prior capturing and CO<sub>2</sub> separation, will be evaluated, and thereupon the potential of sequestering satisfactory amounts of CO<sub>2</sub> in a simplified and less costly method, will be assessed. Nevertheless, based on the already exerted results regarding the levels of CO<sub>2</sub> uptake achieved by the granules formed using pure CO<sub>2</sub>, it is not likely for carbonating gases with lower CO<sub>2</sub> concentrations to achieve the sequestration of satisfactory amounts of CO<sub>2</sub>. However, it would be interesting to see the way that CO<sub>2</sub> concentration affects the other qualities of the formed granules, such as their particle size, their compressive strength or their leaching behavior.

The possibility of the examined methodology to get scaled up should also be explored. To achieve that, the lab-scale tests described in this work, should be performed using a pilot-scale reactor. A suitable for the purposes of this study such reactor is a pilot-scale rotary kiln unit available at ENEA's infrastructures in Rome, Italy. The particular unit is a 9.2 kW steel rotary drum reactor of cylindrical shape that rotates between two fixed flanges positioned at its ends. Its length is 1.55 m and its diameter is 9.4 cm (inner diameter = 8 cm). Its maximum temperature is 1600 °C, it has an inclination ability of up to 7 ° from the horizontal, whereas its highest mixing speed is 8 rpm. In these tests considerably higher amounts of BOF slag could be used, whereas the selection of the tested temperatures and L/S ratios should be made according to the herein exerted lab-scale granulation-carbonation results. Following the same procedures as in the lab scale tests, the CO<sub>2</sub> uptakes, the size, the compressive strength, as well as the leaching behavior of the granules synthesized in the pilot-scale reactor will be estimated. The results achieved

by lab and pilot-scale tests will be compared and the potential of the investigated process to get scaled up will be evaluated.

Finally, the economic and environmental sustainability of the proposed BOF slag treatments for the production of secondary aggregates should also be assessed. The production of sodium hydroxide that is used in this process, as a constituent of the alkaline activation solution, has a notable impact to the environment. In order to minimize the negative environmental impact of the proposed processes and improve their economic feasibility, the alkali activation of the treated material, using other solutions, preferably coming from waste streams, will also be investigated.

## **5.2. Valorization of BF slag**

### **5.2.1. Concluding remarks**

Contrarily to BOF slag that is in pressing need for new valorization routes, BF slag is already commercially exploited to a large extent in construction business, mainly as a replacement of traditional PC in concrete mixtures. In an effort to introduce an alternative valorization method for the particular iron-making byproduct, Chiang et al. [43] proposed an innovative technology according to which through the production of two (instead of one) value added products (PCC and zeolites) and the parallel sequestration of CO<sub>2</sub>, higher value could be generated from the material. The reproducibility of zeolitic phases through the hydrothermal conversion of the solid residues resulting from the calcium extraction step of the indirect carbonation of PBF slag, following the particular process but using an inherently more porous type of BF slag (PBFS instead of GBFS), was investigated in this part of the research. To this end, acetic acid of a specific concentration (2 M) was employed for the extraction of calcium from the material, whereas NaOH solutions of different compositions (0.5 and 2 M) were used for the hydrothermal conversion process. Furthermore, the evaluation of the synthesized material as efficient heavy metal adsorbent in aquatic environments was also performed.

Unfortunately, in contrary to what was expected, the use of PBFS instead of GBFS was proved less favorable for the calcium extraction process. In fact, due to the lower content of calcium characterizing PBFS in regards with GBFS and the crushing of PBFS prior to experimentation that caused the shattering of its large pores, the amount of calcium released to the acetic acid solution from the PBFS was found to be remarkably lower than the one leached from GBFS.

Moreover, the poor washing of the calcium extraction solids allowed the presence of calcium (in the form of acetates) in the composition of the samples that were subjected to hydrothermal conversion for the production of zeolites. The occurrence of calcite acetates in the particular samples inhibited the activation of the material and the formation of crystal phases when the lower concentration of NaOH solution (0.5 M) was used and promoted the formation of the undesirable phase of tobermorite over that of analcime when NaOH solution of 2 M was employed for the hydrothermal conversion process.

Nevertheless, despite the porosity destruction of PBFS and the inadequate washing of the calcium extraction residues from residual soluble acetates, the formation of a remarkable amount of analcime (30 wt%) in the finally produced material was achieved.

The synthesized material, mainly composed by analcime and tobermorite, exhibited satisfactory performance as adsorbent of  $\text{Ni}^{2+}$  from synthetically contaminated solutions. Thereupon, it could be inferred that the particular material can be used as  $\text{Ni}^{2+}$  adsorbent in wastewater treatment or environmental remediation applications.

However, the presence of tobermorite in its composition at such high amounts does not fit the requirements of the originally proposed methodology [43], according to which the calcium content of the slag should be exploited in the formation of high purity PCC and therefore tobermorite is an undesirable phase of the hydrothermal conversion process, whose content in the activated material should be negligible, if not zero.

Nevertheless, the notable occurrence of analcime in the composition of the hydrothermally converted material, even under the above described unfavorable for its formation conditions, implies that if the washing step of the process was properly conducted, the formation of a material with significantly higher amounts of analcime and remarkably limited presence of tobermorite would be achieved.

### **5.2.2. Future Work**

Apparently, the repetition of the experiment securing the proper washing of the solid residues resulting from the calcium extraction step of the process is required, in order to discover whether the occurrence of analcime in the finally formed material will be remarkably increased and the presence of tobermorite will be significantly constrained, as expected.

In this work, only a preliminary assessment of the finally synthesized material's ability to adsorb heavy metals was conducted. Further research regarding different aspects of the material's heavy metal adsorption capacity should be carried out. In particular, the adsorption capacity of the hydrothermally converted material towards more heavy metals should be evaluated, the effects of more parameters (e.g. temperature, sorbents particle size and sorbent dosage) on the adsorption process should be assessed, the adsorption's kinetic study should be conducted and the adsorption competition between different heavy metals should be researched.

The evaluation of the sorbent's adsorption capacity towards more heavy metals will be attempted performing the same equilibrium adsorption experiments that were conducted in the present study, only instead of  $\text{Ni}^{2+}$ , other heavy metals, such as  $\text{Cu}^{2+}$ ,  $\text{Pb}^{2+}$  or  $\text{Cd}^{2+}$ , will be used as models for investigation. As in this work, different initial concentrations of the investigated heavy metals will be tested. In that stage, it is important to make sure that for each concentration tested, the different metals should be present in the contaminated solutions in equimolar amounts. As in the herein described experiments, for the conduction of the experiments, 1 g of the hydrothermally converted material will be dispersed in 100 ml of the synthetically contaminated solutions and the mixtures will then be agitated under the same

conditions (for 24 hours, at 160 rpm and 20 °C). The resulting slurry will be subjected to centrifugation in order for the solids to be separated from the solution and finally the resulting supernatant will be subjected to ICP-OES analysis for its content in the investigated metal. The ICP-OES analysis is indicatively mentioned. Other methods for the determination of the investigated metal's content in the supernatant, such as Atomic Absorption Spectroscopy (AAS), could also be used.

Apart from the influence of the initial heavy metal concentration that, for the case of Ni<sup>2+</sup>, was examined in this work, the effects of other experimental parameters like contact time, initial pH value, temperature, sorbent dosage and sorbent particle size on the efficiency of the adsorption process, will also be assessed. To this end, batch adsorption experiments will be carried out. During these tests, different values of the aforementioned experimental parameters will be applied. It should be noted that the effect of each one of the tested parameters on the adsorption process should be evaluated while holding all the other parameters fixed. After the end of prescribed contact times, the solutions will be subjected to centrifugation and the resulting supernatant will be analysed for its content in the investigated heavy metal, using ICP-OES. Based on these concentrations, the manner in which the investigated parameters affect the adsorption process will be discovered.

For the assessment of both sorption kinetics and competition for adsorption sites, multi- element solutions of varying initial concentrations will be prepared. For each concentration tested, the solution should contain the same amounts of the different heavy metals selected for investigation. A specific amount of the synthesized adsorbent will then be dispersed to the different solutions and the mixture will be agitated at a certain speed (e.g. 160 rpm) over a specific period (e.g. 5 days). At the end of the prescribed contact time, the resulting slurry will be syringe filtered in order to remove the solids from the solution and the latter will be subjected to ICP-OES analysis to determine its content in the investigated heavy metals. Based on their amount in the solution, the affinity of the adsorbent to each of the examined metals will be evaluated.

To assess the kinetics of the process, samples of the same multi-element solutions will be withdrawn from them, at intermediate time intervals. These samples will be syringe filtered and the resulting solutions will be analysed for their content in the investigated metals, using ICP-OES. Based on the amount of the investigated heavy metals in the samples taken from the solution at different time intervals, the kinetics of the adsorption process will be determined.

The economic and environmental feasibility of the process should also be assessed. The impact of hydrothermal activation using sodium hydroxide solution to the environment is not negligible and thereupon different alkaline solutions which affect the environment in considerably less extent should be examined.

Finally, based on the high amounts of amorphous silica that were present in the composition of the calcium extraction residues, apart from the formation of zeolites, the particular solids could also be tested as a partial replacement of PC in concrete mixtures.

PC is an indispensable ingredient of concrete mixtures. However, it is also the largest contributor to embodied greenhouse gas emissions and energy in concrete. Indicatively, it has been estimated that about 927 kg of CO<sub>2</sub> are emitted for every 1000 kg of PC produced in the USA [287]. In order to create a more environmental friendly type of concrete, while preserving, if not improving, its strength and durability, and to mitigate the costs related to its production, different materials have been proposed to partially replace PC in the concrete mix [288-298]. Such materials are called pozzolans.

Pozzolans are characterized by a silicate-based composition that enables them to react with the calcium hydroxide that is produced during the hydration of PC. The particular phase comprises approximately 25 % of the hydrated PC and does not contribute to the concrete's strength or durability. Its consumption by the pozzolanic substitutes leads to the production of additional calcium-hydroxide-silicate (C-S-H) gel, which is the main source of concrete's strength.

As already mentioned, a large part of BF slag production is utilized as PC replacement in concrete mixtures. In fact, among the numerous materials that have been tested for their efficiency as potential pozzolans, BF slag is the one that presents a composition that is closer to that of PC. This is why the particular material is suitable to substitute much larger quantities of PC than the other pozzolans. In fact, BF slag can replace up to 50 % of PC in a concrete mixture (1:1, by mass), whereas this percentage can reach even 80 % if special applications of concrete are required (e.g. mass concrete) [299].

Several studies have focused on the use of BF slag as a partial PC substitution material and the way the concrete's compressive strength is affected [300-304]. According to them, one of the basic disadvantages of concrete mixtures containing BF slag as partial substitute of PC cement is the slow strength development that leads to low compressive strength of the concrete at the early stages. In particular, it has been concluded that the strength development of this type of concrete is considerably slower under the standard curing conditions at normal temperatures (20 °C), than the strength development of concrete incorporating only PC, due to the slower rate of hydration of cement containing BF slag.

If instead of using fresh BF slag, a material resulting from the subjecting of the slag to a calcium extraction process was employed, extra amorphous silica would be available to react with the calcium hydroxide generated from the hydration of PC, potentially increasing the speed of this reaction and enhancing the early stage strength of the concrete.

To assess the potential of the particular hypothesis to improve the early stage strength of concrete mixtures incorporating slag cement, BF slag will be firstly subjected to a calcium extraction process and will subsequently be tested for its pozzolanic activity. The proposed methodology will be investigated as a parallel process to that of PCC formation from BF slag, towards the zero-waste valorization of the particular byproduct. Based on the findings of the present study, the most efficient way to selectively extract calcium is by subjecting BF slag to two cycles of calcium extraction using  $\text{CH}_3\text{COOH}$  solution of certain concentration (2 M), as the extraction agent. This process

will be followed in this case, as well. After the end of mixing, the slurry will be vacuum filtered in order to obtain the filter cake which will be thoroughly washed using ultra-pure water, to remove any potential residual leaching solution from it. To retrieve the final product (modified BF slag), the washed material will be oven dried at 105 °C, for 24 hours.

The pozzolanic activity of a material can be determined by applying several tests. In this case, the pozzolanic activity of the formed material will be assessed by using two different testing procedures: the saturated lime test [305-307] and a variation of the electrical conductivity test [308]. For the conduction of both tests, a saturated lime solution should be synthesized. After its preparation, the samples will be prepared by adding a certain amount of the modified BF slag (1 g) to a specific volume (75 ml) of the saturated lime solution in plastic bottles. Apart from the samples prepared using the modified BF slag, a reference sample incorporating the as received BF slag, will also be prepared. The mixtures will be stirred under certain conditions, for different periods (0, 1, 7, and 28 days).

For the needs of the saturated lime solution tests, after the end of each period the samples will be syringe filtered. The content of calcium in both the saturated lime solution and the filtered solutions will be determined by using ICP-OES. The quantity of the lime fixed by the tested materials will be the difference between the content of calcium in the saturated lime solution and the one in the filtered solutions.

For the requirements of the electrical conductivity tests, the conductivity of the saturated lime solution and that of the treated samples will be measured using an electrical conductivity meter. Generally, increased pozzolanic activity leads to electrical conductivity decrease. Accordingly, compared to the saturated lime solution, the electrical conductivity of the treated samples should be reduced. By comparing the electrical conductivity of the tested samples with that of the saturated lime solution the pozzolanic activity of the tested materials will be determined.

Apparently, the different pozzolanic activity testing procedures will determine the efficiency of the proposed mechanism as a method to accelerate the

pozzolanic reactions in concrete mixtures containing slag cement, in different ways. In particular, the saturated lime solution tests will assess the process efficiency by comparing the fixed amounts of calcium achieved by the samples including the as received BF slag, with those of the samples prepared using the modified BF slag, after each treatment period tested. According to this testing procedure, the proposed mechanism will be proved promising, in case that, especially for the shorter reaction periods (0, 1, and 7 days), the amount of calcium fixed by the samples of the modified BF slag, is higher than that of the samples prepared using the as received BF slag.

On the other hand, the electrical conductivity tests will assess the efficiency of the process by comparing the level of electrical conductivity decrease achieved by the samples including the as received BF slag, with that achieved by the samples prepared using the modified one. In case that, especially for the shorter treatment periods (0, 1 and 7 days), the electrical conductivity of the samples incorporating the modified BF slag is lower than the electrical conductivity measured for the samples including the as received BF slag, the proposed methodology could be judged as promising.

## REFERENCES

- [1] Georgakopoulos, E., Santos, R.M., Chiang, Y.W., Manovic, V. (2016), Influence of process parameters on carbonation rate and conversion of steelmaking slags – Introduction of the ‘carbonation weathering rate’, *Greenhouse Gas Science and Technology*, vol. 6, no. 4, pp. 470-491.
- [2] Tans, P. and Keeling R (2016), Trends in Atmospheric Carbon Dioxide, NOAA/ESRL, available at: <http://www.esrl.noaa.gov/gmd/ccgg/trends> (accessed on October 17, 2016).
- [3] National Oceanic and Atmospheric Administration (2016), Climate at a Glance, NOAA, available at: <http://www.ncdc.noaa.gov/cag/time-series/global> (accessed on August 22, 2016).
- [4] Sherwood, S.C., Bony, S. and Dufresne J.L. (2014), “Spread in modelclimate sensitivity traced to atmospheric convective mixing”, *Nature*, vol. 505, pp. 37–42.
- [5] European Commission, Climate Action, Paris Agreement (2016), available at: <http://ec.europa.eu/clima/policies/international/negotiations/future/indexen.htm> (accessed on August 21, 2016).
- [6] Goff, F. and Lackner K.S. (1998), “Carbon dioxide sequestering using ultramafic rocks”, *Environmental Geosciences*, vol. 5, no. 3, pp. 89–101.
- [7] Kirchofer, A., Becker, A., Brandt, A. and Wilcox, J. (2013), “CO<sub>2</sub> mitigation potential of mineral carbonation with industrial alkalinity sources in the United States”, *Environmental Science and Technology*, vol. 47, no. 13, pp. 7548–7554.
- [8] Central Intelligence Agency (CIA) (2013), “The World Factbook 2013-14”, *Washington, United States*.
- [9] International Energy Agency (IEA) (2013), “Technology roadmap: Carbon capture and storage”, IEA, Paris, France.
- [10] Bodor, M., Santos, R.M., Van Gerven, T. and Vlad, M. (2013), “Recent developments and perspectives on the treatment of industrial wastes by

mineral carbonation - a review”, *Central European Journal of Engineering*, vol. 3, no. 4, pp. 566–584.

[11] Santos, R.M., Mertens, G., Salman, M., Cizer, Ö. and Van Gerven, T. (2013), “Comparative study of ageing, heat treatment and accelerated carbonation for stabilization of municipal solid waste incineration bottom ash in view of reducing regulated heavy metal/metalloid leaching”, *Journal of Environmental management*, vol. 128, pp. 807–821.

[12] Bodor, M., Santos, R.M., Cristea, G. and Van Gerven, T. (2016), “Laboratory investigation of carbonated BOF slag used as partial replacement of natural aggregate in cement mortars”, *Cement and Concrete Composites*, vol. 65, pp. 55-66.

[13] Costa, G., Baciocchi, R., Poletini, A., Pomi, R., Hills, C.D. and Carey, P.J. (2007), “Current status and perspectives of accelerated carbonation processes on municipal waste combustion residues”, *Environmental Monitoring and Assessment*, vol. 135, no. 1-3, pp. 55–75.

[14] Hasanbeigi, A., Arens, M. and Price, L. (2013), *Emerging Energy-efficiency and Carbon Dioxide Emission-reduction Technologies for the Iron and Steel Industry*, Ernest Orlando Lawrence Berkeley National Laboratory, USA.

[15] Carpenter, A. (2012), *CO<sub>2</sub> abatement in the iron and steel industry, Profiles*, International Energy Agency (IEA) Clean Coal Centre, London, UK.

[16] Proctor, D.M., Fehling, K.A., Shay, E.C., Wittenborn, J.L., Green, J.J., Avent, C., Bingham, R.T., Connolly, M., Lee, B., Shepker, T.O. and Zak, M.A. (2000), “Physical and Chemical Characteristics of Blast Furnace, Basic Oxygen Furnace, and Electric Arc Furnace Steel Industry Slags”, *Environmental Science and Technology*, vol. 34, no. 8, pp. 1576–1582.

[17] Motz, H. and Geiseler, J. (2001), “Products of steel slags an opportunity to save natural resources”, *Waste Management*, vol. 21, no. 3, pp. 285–293.

[18] Shen, H. and Forsberg E. (2003), “An overview of recovery of metals from slags”, *Waste Management*, vol. 23, no. 10, pp. 933–949.

- [19] Johnson, D.C. (2000), "Accelerated carbonation of waste calcium silicate materials", *SCI Lecture Papers Series*, vol. 108, pp. 1–10.
- [20] Tai, C.I., Su, C.Y., Chen, Y.T., Shih, S.M. and Chien, W.C. (2008), "Carbonation of natural rock and steel slag using supercritical carbon dioxide", 11th European Meeting on Supercritical Fluids, International Society for Advancement of Supercritical Fluids (ISASF), 4–7 May 2008, Barcelona, Spain.
- [21] Huijgen, W.J.J. and Comans, R.N.J. (2005), Carbon dioxide sequestration by mineral carbonation, Literature review update 2003-2004, ECN-C-05-022, available at: <http://www.ecn.nl/docs/library/report/2005/c05022.pdf> (accessed on May 11, 2016).
- [22] Eloneva, S., Teir, S., Salminen, J., Fogelholm, C.J. and Zerenhoven, R. (2007), "Fixation of CO<sub>2</sub> by carbonating calcium derived from blast furnace slag", *Energy*, vol. 33, no. 9, pp. 1461–1467.
- [23] Stollarof, J.K., Lowry, G.V. and Keith, D.W. (2005), "Using CaO- and MgO-rich industrial waste streams for carbon sequestration", *Energy Conversion and Management*, vol. 46, no. 5, pp. 687–699.
- [24] Van Oss, H. (2016), *Iron and Steel Slag*, U.S. Geological Survey, Mineral Commodities Summaries, U.S. Geological Survey, Reston, Virginia, USA.
- [25] Böhmer, S., Moser, G., Neubauer, C., Peltoniemi, M., Schachermayer, E., Tesar, M., Walter, B. and Winter, B. (2008), *Aggregate case study, Final report*, Umweltbundesamt, Vienna, Austria.
- [26] Das, B., Prakash, S., Reddy, P. and Misra, V. (2007), "An overview of utilization of slag and sludge from steel industries", *Resources Conservation and Recycling Journal*, vol. 50, no. 1, pp. 40–57.
- [27] Slag Cement Association (2008), Slag Cement in Concrete – Terminology and Specifications, available at: [http://www.slagcement.org/news/pdf/no12\\_specifi\\_terminology.pdf](http://www.slagcement.org/news/pdf/no12_specifi_terminology.pdf) (accessed on May 13, 2016).

- [28] Zeghichi, L. (2006), "The effect of replacement of natural aggregates by slag products on the strength of concrete", *Asian Journal of Civil Engineering*, vol. 7, no. 1, pp. 27-35.
- [29] Menéndez, G., Bonavetti, V. and Irassar, E.F. (2003), "Strength development of ternary blended cement with limestone filler and blast-furnace slag", *Cement and Concrete Composites*, vol. 25, no. 1, pp. 61–67.
- [30] Pal, S.C., Mukherjee, A. and Pathak, S.R. (2003), "Investigation of hydraulic activity of ground granulated blast furnace slag in concrete", *Cement and Concrete Research*, vol. 33, no. 9, pp. 1481–1486.
- [31] Shoaib, M.M., Ahmed, S.A. and Balaha, M.M. (2001), "Effect of fire and cooling mode on the properties of slag mortars", *Cement and Concrete Research*, vol. 31, no. 11, pp. 1533–1538.
- [32] Shi, C. and Qian, J. (2000), "High performance cementing materials from industrial slags – a review", *Resources Conservation and Recycling Journal*, vol. 29, no. 3, pp. 195–207.
- [33] ASTM D 422-63:1998, *Standard Test Method for Particle-Size Analysis of Soils* (1998).
- [34] British Standard 12457-2-2002, *Characterisation of waste - Leaching - Compliance test for leaching of granular waste materials and sludges - Part 2: One stage batch test at a liquid to solid ratio of 10 L/kg for materials with particle size below 4 mm (without or with size reduction)* (2002).
- [35] British Standard 812-110:1990, *Testing aggregates – part 110: Methods for determination of aggregate crushing value (ACV)*. ISBN 0 580 18825 6 (1990).
- [36] Huijgen, W.J.J., Witkamp, G.J. and Comans, R.N.J. (2005), "Mineral CO<sub>2</sub> sequestration by steel slag carbonation", *Environmental Science and Technology*, vol. 39, no. 24, pp. 9676–9682.

- [37] Chang, E.E., Chen, C.H., Chen, Y.H., Pan, S.Y. and Chiang, P.C. (2011), "Performance evaluation for carbonation of steel-making slags in a slurry reactor", *Journal of Hazardous Materials*, vol. 186, no. 1, pp. 558–564.
- [38] Santos, R.M., Ling, D., Sarvaramini, A., Guo, M., Elsen, J., Larachi, F., Beaudoin, G., Blanpain, B. and Van Gerven, T. (2012), "Stabilization of basic oxygen furnace slag by hot-stage carbonation treatment", *Chemical Engineering Journal*, vol. 203, pp. 239–250.
- [39] Chang, E.E., Pan, S.Y., Chen, Y.H., Tan, C.S. and Chiang, P.C. (2012), "Accelerated carbonation of steelmaking slags in a high-gravity rotating packed bed", *Journal of Hazardous Materials*, vol. 227–228, pp. 97–106.
- [40] Chen, C.C., Chen, C.S., Jhan, J.Y. and Ko, M.S. (2016), "The improve of accelerated carbonation on engineering properties of basic oxygen furnace slag", *Key Engineering Materials*, vol. 709, pp. 42-45.
- [41] Morone, M., Costa, G., Polettini, A., Pomi, R. and Baciocchi, R. (2014), "Valorization of steel slag by a combined carbonation and granulation treatment", *Minerals Engineering*, vol. 59, pp. 82-90.
- [42] Pacheco-Torgal, F., Castro-Gomes, J. and Jalali, S. (2008), "Alkali-activated binders: a review. Part 2. About materials and binders manufacture", *Construction and Building Materials*, vol. 22, no. 7, pp. 1315–1322.
- [43] Chiang, Y.W., Santos, R.M., Elsen, J., Meesschaert, B., Martens, J.A. and Van Gerven, T. (2014), "Towards zero-waste mineral carbon sequestration via two-way valorization of ironmaking slag", *Chemical Engineering Journal*, vol. 249, pp. 260-269.
- [44] De Crom, K., Chiang, Y.W., Van Gerven, T. and Santos, R.M. (2015), "Purification of slag-derived leachate and selective carbonation for high-quality precipitated calcium carbonate synthesis", *Chemical Engineering Research and Design*, vol. 104, pp. 180-190.
- [45] Taylor, M. (2012), "The current and future state of CCS and its deployment around the world", *Greenhouse Gases Science and Technology*, vol. 2, no. 6, pp. 399–401.

- [46] Johnsson, F. (2011), "Perspectives on CO<sub>2</sub> capture and storage", *Greenhouse Gases Science and Technology*, vol. 1, no. 2, pp. 119–133.
- [47] Petroleum Technology Research Centre (2014), *What Happens When CO<sub>2</sub> is Stored Underground? Q&A from the IEAGHG Weyburn-Midale CO<sub>2</sub> Monitoring and Storage Project*, Global Carbon Capture and Storage Institute Limited, Melbourne, Australia.
- [48] Zhang, D. and Song, J. (2014), "Mechanisms for geological carbon sequestration", in *Mechanics for the World: Proceedings of the 23rd International Congress of Theoretical and Applied Mechanics, Procedia IUTAM*, vol. 10, pp. 319–327.
- [49] Benson, S.M. and Cole, D.R. (2008), "CO<sub>2</sub> Sequestration in Deep Sedimentary Formations", *Elements*, vol. 4, pp. 325-331.
- [50] Lackner, K. (2003), "A guide to CO<sub>2</sub> sequestration", *Science*, vol. 300, no. 5626, pp. 1677–1678.
- [51] Prigiobbe, V., Poletini, A. and Baciocchi, R. (2009), "Gas-solid carbonation kinetics of air pollution control residues for CO<sub>2</sub> storage", *Chemical Engineering Journal*, vol. 148, no. 2-3, pp. 270-278.
- [52] Winkler, E.M. (1966), "Important agents of weathering for building and monumental stone", *Engineering Geology*, vol. 1, no. 5, pp. 381–400.
- [53] Seifritz, W. (1990), "CO<sub>2</sub> disposal by means of silicates", *Nature*, vol. 345, no. 6275, pp. 486.
- [54] Santos, R.M., Verbeeck, W., Knops, P., Rijnsburger, K., Pontikes, Y. and Van Gerven, T. (2013), "Integrated mineral carbonation reactor technology for sustainable carbon dioxide sequestration: 'CO<sub>2</sub> Energy Reactor'", in *GHGT-11 Proceedings of the 11th International Conference on Greenhouse Gas Control Technologies*, 18-22 November 2012, Kyoto, Japan, *Energy Procedia*, vol. 37, pp. 5884–5891.

- [55] Moazzem, S., Rasul, M.G. and Khan, M.M.K. (2013), "Energy recovery opportunities from mineral carbonation process in coal fired power plant", *Applied Thermal Engineering*, vol. 51, no. 1-2, pp. 281–291.
- [56] Haszeldine, R.S. (2006), 'Deep geological CO<sub>2</sub> storage: principles reviewed, and prospecting for bio-energy disposal site', *Mitigation and Adaptation Strategies for Global Change*, vol. 11, no. 2, pp. 369–393.
- [57] Bruant, R.G., Guswa, A.J., Celia, M.A. and Peters, C.A. (2002), "Safe Storage of CO<sub>2</sub> in Deep Saline Aquifers", *Environmental Science and Technology*, vol. 36, no. 11, pp. 240A-245A.
- [58] Jenkins, C.R., Cook, P.J., Ennis-King, J., Undershultz, J., Boreham, C., Dance, T., de Caritat, P., Etheridge, D.M., Freifeld, B.M., Hortle, A., Kirste, D. Paterson, L., Pevzner, R., Schacht, U., Sharma, S., Stalker, L. and Urosevic, M. (2012), "Safe storage and effective monitoring of CO<sub>2</sub> in depleted gas fields", *Proceedings of the National Academy of Science of the United States of America*, vol. 109, no. 2, pp. E35-41.
- [59] White, C.M., Strazisar, B.R., Granite, E.J., Hoffman, J.S. and Pennline, H.W. (2003), "Separation and capture of CO<sub>2</sub> from large stationary sources and sequestration in geological formations—Coalbeds and deep saline aquifers", *Journal of the Air and Waste Management Association*, vol. 53, no. 6, pp. 645-715.
- [60] Lackner, K.S., Butt, D.P. and Wendt, C.H. (1997), "Progress on binding CO<sub>2</sub> in mineral substrates", Proceedings of the Third International Conference on Carbon Dioxide Removal, *Energy Conversion and Management*, vol. 38, pp. S259–S264.
- [61] Sanna, A., Uibu, M., Caramanna, G., Kuusik, R. and Maroto-Valer, M.M. (2014), "A review of mineral carbonation technologies to sequester CO<sub>2</sub>", *Chemical Society Reviews*, vol. 43, pp. 8049-8080.
- [62] Monkman, S. and Shao, Y. (2006), "Assessing the carbonation behavior of cementitious materials", *Journal of Materials in Civil Engineering*, vol. 18, no. 6, pp. 768–776.

- [63] Baciocchi, R., Costa, G., Di Bartolomeo, E., Poletini, A. and Pomi, R. (2011), "Wet versus slurry carbonation of EAF steel slag", *Greenhouse Gases Science and Technology*, vol. 1, no. 4, pp. 312–319.
- [64] Santos, R.M. and Van Gerven, T. (2011), "Process intensification routes for mineral carbonation", *Greenhouse Gases Science and Technology*, vol. 1, no. 4, pp. 287–293.
- [65] Baciocchi, R., Costa, G., Di Bartolomeo, E., Poletini, A. and Pomi, R. (2010), "Carbonation of stainless steel slag as a process for CO<sub>2</sub> storage and slag valorization", *Waste and Biomass Valorization*, vol. 1, no. 4, pp. 467–477.
- [66] Santos, R.M., Van Bouwel, J., Vandeveld, E., Mertens, G., Elsen, J. and Van Gerven, T. (2013), "Accelerated mineral carbonation of stainless steel slags for CO<sub>2</sub> storage and waste valorization: Effect of process parameters on geochemical properties", *International Journal of Greenhouse Gas and Control*, vol. 17, pp. 32–45.
- [67] Luo, F.L. and Ye, H. (2013), *Renewable energy systems - Advanced conversion technologies and applications*, CRC Press, Taylor and Francis group, Florida, USA.
- [68] Kultermann, E. and Spence, W.P. (2016), *Construction materials, methods, and techniques-Building for a sustainable future*, 4<sup>th</sup> ed, CENGAGE Learning, Virginia, USA.
- [69] McIntyre, J. and Blaine, F.C. (1920), *The Making, Shaping and Treating of Steel*, 2<sup>nd</sup> ed, Carnegie Steel Company, Pittsburgh, USA.
- [70] Ramesh, S. (2012), *Applied welding engineering: Processes, codes and standards*, 1<sup>st</sup> ed, Elsevier, Massachusetts, USA.
- [71] International iron metallic association (IIMA) (2016), Basic Oxygen Furnace, available at: <http://metallics.org.uk/basic-oxygen-furnace/> (accessed on June 19, 2016).
- [72] Jones, J.A.T. (2016), Making Steel, how it is made, processes: Electric Arc Furnace Steelmaking, available at: [http://www.steel.org/en/Making%](http://www.steel.org/en/Making%20Steel)

[20Steel/How%20Its%20Made/Processes/Processes%20Info/Electric%20Arc%20Furnace%20Steelmaking.aspx](http://www.steel.org/en/Making%20Steel/How%20Its%20Made/Processes/Processes%20Info/Electric%20Arc%20Furnace%20Steelmaking.aspx) (accessed on July 15, 2016).

[73] Jones, J. (1997), Understanding electric arc furnace operations, The EPRI center for materials production, available at: <http://infohouse.p2ric.org/ref/10/09047.pdf> (accessed on July 25, 2016).

[74] Praxair (2016), Improving quality and productivity with AOD, available at: <http://www.praxair.com/-/media/documents/specification-sheets-and-brochures/industries/metal-production/p10018.pdf> (accessed on July 25, 2016).

[75] Song, H.S., Byun, S.M., Min, D.I., Yoon, S.K. and Ahn, S.Y. (1992), "Optimization of the AOD Process at POSCO", *Proceedings of the 1<sup>st</sup> International Chromium steel and Alloys Congress, Cape Town, Johannesburg, SAIMM*, vol. 2, pp. 89-95.

[76] Kozak, B. and Dzierzawski, J. (2016), Making Steel, how it is made, processes: Continuous Casting of Steel: Basic Principles, available at: <http://www.steel.org/en/Making%20Steel/How%20Its%20Made/Processes/Processes%20Info/Continuous%20Casting%20of%20Steel%20-%20Basic%20Principles.aspx> (accessed on July 25, 2016).

[77] Worldsteel association (2016), Fact Sheet-Energy use in the steel industry, available at: [https://www.worldsteel.org/.../factenergy\\_2016.pdf](https://www.worldsteel.org/.../factenergy_2016.pdf) (accessed on July 24, 2016).

[78] Emery, J. (1992), *Mineral Aggregate Conservation Reuse and Recycling*, Geotechnical Engineering Limited, Ontario, Canada.

[79] van Oss, H.G. and Padovani, A.C. (2003), "Cement manufacture and the environment part II: environmental challenges and opportunities", *Journal of Industrial Ecology*, vol. 7, no. 1, pp. 93-126.

[80] Branca, T.A. and Colla, V. (2012), "Possible uses of steelmaking slag in agriculture: an overview", Achilias, D. S. (Ed.), in: *Material recycling — Trends and Perspectives*, In Tech, Rijeka, Croatia.

- [81] Bapat, J.D. (2012), *Mineral Admixtures in Cement and Concrete*, CRC Press, Taylor and Francis Group, Boca Raton, Florida, USA.
- [82] Yildirim, I.Z. and Prezzi, M. (2011), “Chemical, Mineralogical, and Morphological Properties of Steel Slag”, *Advances in Civil Engineering*, vol. 2011, pp. 1-13.
- [83] Juckes, L. M. (2003), “The volume stability of modern steelmaking slags”, *Mineral Processing and Extractive Metallurgy*, vol. 112, no. 3, pp. 177–197.
- [84] Mahieux, P.Y., Aubert, J.-E. and Escadeillas, G. (2009), “Utilization of weathered basic oxygen furnace slag in the production of hydraulic road binders”, *Construction and Building Materials*, vol. 23, no. 2, pp. 742-747.
- [85] Waligora, J., Bulteel, D., Degrugilliers, P., Damidot, P., Potdevin, J.L. and Measson, M. (2010), “Chemical and mineralogical characterization of LD converter steel slags: a multi-analytical techniques approach”, *Material Characterization*, vol. 61, no. 1, pp. 39-48.
- [86] Euroslag & Eurofer (2012), *Position paper on the status of ferrous slag, complying with the Waste Framework Directive (Articles 5 / 6) and the REACH regulation*, Germany.
- [87] Luxán, M.P., Sotolongo, R., Dorrego, F., and Herrero, E. (2000), “Characteristics of the slags produced in the fusion of scrap steel by electric arc furnace”, *Cement and Concrete Research*, vol. 30, no. 4, pp. 517–519.
- [88] Manso, J.M., Polanco, J.A., Losañez, M. and González, J.J. (2006), “Durability of concrete made with EAF slag as aggregate”, *Cement and Concrete Composites*, vol. 28, no. 6, pp. 528–534.
- [89] Tossavainen, M., Engstrom, F., Yang, Q., Menad, N., Lidstrom Larsson, M. and Bjorkman, B. (2007), “Characteristics of steel slag under different cooling conditions”, in Wascon 2006 6th International Conference: Developments in the re-use of mineral waste, *Waste management*, vol. 27, no. 10, pp. 1335-1344.

- [90] Tsakiridis, P.E., Papadimitriou, G.D., Tsivilis, S. and Koroneos, C. (2008), "Utilization of steel slag for Portland cement clinker production", *Journal of Hazardous Materials*, vol. 152, no. 2, pp. 805-811.
- [91] Pellegrino, C. and Gaddo, V. (2009), "Mechanical and durability characteristics of concrete containing EAF slag as aggregate", *Cement and Concrete Composites*, vol. 31, no. 9, pp. 663-671.
- [92] Pellegrino, C. and Faleschini, F. (2013), "Experimental behavior of reinforced concrete beams with electric arc furnace slag as recycled aggregate", *Materials Journal*, vol. 110, no. 2, pp. 197-206.
- [93] Sekaran, A., Palaniswamy, M. and Balaraju, S. (2015), "A study on suitability of EAF oxidizing slag in concrete: an eco-friendly and sustainable replacement for natural coarse aggregate", *The Scientific World Journal*, vol. 2015, pp. 1-8.
- [94] Beh, C.L., Chuah, L., Choong, T.S.Y., Kamarudzaman, M.Z.B. and Abdan, K. (2010), "Adsorption study of electric arc furnace slag for the removal of manganese from solution", *American Journal of Applied Sciences*, vol. 7, no. 4, pp. 442-446.
- [95] Chen, X., Hou, W.H., Song, G.L. and Wang, Q.H. (2011), "Adsorption of Cu, Cd, Zn and Pb ions from aqueous solutions by electric arc furnace slag and the effects of pH and grain size", *Chemical and Biochemical Engineering Quarterly Journal*, vol. 25, no. 1, pp. 105-114.
- [96] Song, G., Wu, Y., Chen, X., Hou, W. and Wang, Q. (2014), "Adsorption performance of heavy metal ions between EAF steel slag and common mineral adsorbents", *Desalination and Water Treatment*, vol. 52, no. 37-39, pp. 7125-7132.
- [97] Qian, G.R., Sun, D.D., Tay, J.H. and Lai, Z.Y. (2002), "Hydrothermal reaction and autoclave stability of Mg bearing RO phase in steel slag", *British Ceramic Transactions*, vol. 101, no. 4, pp. 159-164.

- [98] Qian, G., Sun, D.D., Tay, J.H., Lai, Z. and Xu, G. (2002), "Autoclave properties of kirschsteinite-based steel slag", *Cement and Concrete Research*, vol. 32, no. 9, pp. 1377–1382.
- [99] Shen, H., Forssberg, E. and Nordström, U. (2004), "Physicochemical and mineralogical properties of stainless steel slags oriented to metal recovery, Resources", *Conservation and Recycling*, vol. 40, no. 3, pp. 245–271.
- [100] Ramachandran, V.S. and Sereda, P.J. Feldman, R.F. (1964), "Mechanism of hydration of calcium oxide", *Nature*, vol. 201, pp. 288–299.
- [101] Crawford, C.B. and Burn, K.N. (1969), "Building damage from expansive steel slag backfill", *Journal of the Soil Mechanics and Foundations Division*, vol. 95, no. SM6, pp. 1325–1334.
- [102] Verhasselt, A. and Choquet, F. (1989), "Steel slags as unbound aggregate in road construction: problems and recommendations", *Proceedings of the 3<sup>rd</sup> International Symposium on Unbound Aggregates in Roads, University of Nottingham, April 11-13*, Butterworths and Company Publishers Limited, pp. 204–211, .
- [103] Motz, H. and Geiseler, J. (2001), "Products of steel slags an opportunity to save natural resources", *Waste Management*, vol. 21, no. 3, pp. 285–293.
- [104] Yang, Q., Engström, F., Tossavainen, M. and Adolfsson, D. (2005), "Treatments of AOD slag to Enhance Recycling and Resource Conservation", *Securing the Future, International Conference on Mining and the Environment, Metals and Energy Recovery, June 27-July 1 2005, Skellefteå, Sweden*.
- [105] Guzzon, M., Mapelli, C., Memoli, F. and Marcozzi, M. (2007), "Recycling of ladle slag in the EAF: improvement of the foaming behaviour and decrease of the environmental impact", *Revue de Métallurgie*, vol. 104, no. 4, pp. 171-178.
- [106] Kim, Y.J., Nettleship, I. and Kriven, W.M. (1992), "Phase Transformations in Dicalcium Silicate: II, TEM Studies of Crystallography,

Microstructure, and Mechanisms”, *Journal of the American Ceramic Society*, vol. 75, no. 9, pp. 2407-2419.

[107] Durinck, D., Engström, F., Arnout, S., Heulens, J., Jones, P.T., Björkman, B., Blanpain, B. and Wollants, P. (2008), “Hot stage processing of metallurgical slags”, *Resources, Conservation and Recycling*, vol. 52, no. 10, pp. 1121-1131.

[108] Salman, M., Cizer, Ö., Pontikes, Y., Santos, R.M., Snellings, R., Vandewalle, L., Blanpain, B. and Van Balen, K. (2014), “Effect of accelerated carbonation on AOD stainless steel slag for its valorisation as a CO<sub>2</sub>-sequestering construction material”, *Chemical Engineering Journal*, vol. 246, pp. 39-52.

[109] Rastovčan-Mioč, A., Sofilić, T. and Mioč, B. (2009), Application of electric arc furnace slag. In: Grilec, K. and Marič, G. (ed.), Proceedings matrib Vela luka, island Korčula, Hrvatska 24–26. lipnja. Hrvatsko društvo za materijale i tribologiju, Zagreb, 436–444.

[110] The International Stainless Steel Forum (ISSF) (2016), Media Release: “Stainless steel production for 2015 was 41.5 million metric tons”, Brussels, Belgium (released on 14/4/2016).

[111] Chang, E.E., Pan, S.Y., Chen, Y.H., Chu, H.W., Wang, C.F. and Chiang, P.C. (2011), “CO<sub>2</sub> sequestration by carbonation of steelmaking slags in an autoclave reactor”, *Journal of Hazardous Materials*, vol. 195, pp. 107–114.

[112] Chang, E.E., Chiu, A.C., Pan, S.Y., Chen, Y.H., Tan, C.S. and Chiang, P.C. (2013), “Carbonation of basic oxygen furnace slag with metalworking wastewater in a slurry reactor”, *International Journal Greenhouse Gas Control*, vol. 12, pp. 382–389.

[113] van Zomeren, A., van der Laan, S.R., Kobesen, H.B.A., Huijgen, W.J.J. and Comans, R.N. (2011), “Changes in mineralogical and leaching properties of converter steel slag resulting from accelerated carbonation at low CO<sub>2</sub> pressure”, *Waste Management*, vol. 31, no. 11, pp. 2236–2244.

- [114] Poletini, A., Pomi, R. and Stramazzo, A. (2015), "Carbon sequestration via steel slag accelerated carbonation: the influence of operating conditions on process evolution and yield", *Proceedings of the 5th International Conference on Accelerated Carbonation for Environmental and Material Engineering (ACEME)*, 21–24 June 2015, New York, USA.
- [115] Baciocchi, R., Costa, G., Poletini, A., Pomi, R., Stramazzo, A. and Zingaretti, D. (2015), "Accelerated carbonation of steel slags using CO<sub>2</sub> diluted sources: CO<sub>2</sub> uptakes and energy requirements", *Proceedings of the 5th International Conference on Accelerated Carbonation for Environmental and Material Engineering (ACEME)*, 21–24 June 2015, New York, USA.
- [116] Baciocchi, R., Costa, G., Poletini, A. and Pomi, R. (2009), "Influence of particle size on the carbonation of stainless steel slag for CO<sub>2</sub> storage", in *Proceedings of the 9th International Conference on Greenhouse Gas Control Technologies (GHGT-9)*, 16–20 November 2008, Washington DC, USA, *Energy Procedia*, vol. 1, no. 1, pp. 4859–4866.
- [117] Johnson, D.C., McLeod, C.L., Carey, P.J. and Hills, C.D. (2003), "Solidification of stainless steel slag by accelerated carbonation", *Environmental Technology*, vol. 24, no. 6, pp. 671–678.
- [118] Vandeveld E (2010), *Mineral carbonation of stainless steel slag*, Master's Thesis, KU Leuven, Leuven, Belgium.
- [119] Santos, R.M., François, D., Mertens, G., Elsen, J. and Van Gerven T. (2013), "Ultrasound-intensified mineral carbonation", *Applied Thermal Engineering*, vol. 57, no. 1–2, pp. 154–163.
- [120] Van Bouwel, J. (2012), *Intensified aqueous mineral carbonation of alkaline industrial residues for CO<sub>2</sub> storage and waste remediation: effect of process parameters on carbonation conversion, leaching behavior and mineralogy*, Master's Thesis, KU Leuven, Leuven, Belgium.
- [121] Chang, J., Fang, Y. and Shang, X. (2016), "The role of  $\beta$ -C<sub>2</sub>S and  $\gamma$ -C<sub>2</sub>S in carbon capture and strength development", *Materials and Structures*, vol. 49, no. 10, pp. 4417–4424.

- [122] Cappai, G., De Giudici, G., Medas, D., Muntoni, A., Nieddu, A., Orrù, G. and Piredda, M. (2015), "Carbon dioxide sequestration by accelerated carbonation of Waelz slag", *Proceedings of the 5th International Conference on Accelerated Carbonation for Environmental and Material Engineering (ACEME), 21–24 June 2015, New York, USA.*
- [123] Bodor, M., Santos, R.M., Kriskova, L., Elsen, J., Vlad, M. and Van Gerven, T. (2013), "Susceptibility of mineral phases of steel slags towards carbonation: Mineralogical, morphological and chemical assessment", *European Journal of Mineralogy*, vol. 25, no. 4, pp. 533–549.
- [124] Tinke, A.P., Carnicer, A., Govoreanu, R., Scheltjens, G., Lauwerysen, L., Mertens, N., Vanhoutte, K. and Brewster, M.E. (2008), "Particle shape and orientation in laser diffraction and static image analysis size distribution analysis of micrometer sized rectangular particles", *Powder Technology*, vol. 186, no. 2, pp. 154–167.
- [125] Santos, R.M. (2012), *Sustainable materialization of residues from thermal processes into carbon sinks*, PhD Thesis, KU Leuven, Leuven, Belgium.
- [126] Eloneva, S., Mannisto, P., Said, A., Fogelholm, C.J. and Zevenhoven R. (2011), "Ammonium salt-based steelmaking slag carbonation: Precipitation of CaCO<sub>3</sub> and ammonia losses assessment", *Greenhouse Gases Science and Technology*, vol. 1, no. 4, pp. 305-311.
- [127] Mun, M. and Cho, H. (2013), "Mineral carbonation for carbon sequestration with industrial waste", in GHGT-11 Proceedings of the 11th International Conference on Greenhouse Gas Control Technologies, 18-22 November 2012, Kyoto, Japan, *Energy procedia*, vol. 37, pp. 6999–7005.
- [128] Santos, R.M., Chiang, Y.W., Elsen, J. and Van Gerven, T. (2014), "Distinguishing between carbonate and non-carbonate precipitates from the carbonation of calcium-containing organic acid leachates", *Hydrometallurgy*, vol. 147-148, pp. 90-94.

- [129] Monkman, S., Shao, Y. and Shi, C. (2009), "Carbonated ladle slag fines for carbon uptake and sand substitute", *Journal of Materials in Civil Engineering*, vol. 21, no. 11, pp. 657-665.
- [130] Morone, M., Cizer, O., Costa, G. and Baciocchi, R. (2015), "Investigation of the effects of alkali activation and CO<sub>2</sub> curing on BOF steel slag", *Proceedings of the 5th International Conference on Accelerated Carbonation for Environmental and Material Engineering (ACEME), 21–24 June 2015*, New York, USA.
- [131] Quaghebeur, M., Nielsen, P., Horckmans, L. and Van Mechelen, D. (2015), "Accelerated carbonation of steel slag compacts: development of high-strength construction materials", *Frontiers in Energy Research*, vol. 3, no. 52, pp. 1-12.
- [132] Eloneva, S., Teir, S., Salminen, J., Fogelholm, C.J. and Zevenhoven, R. (2008b), "Steel converter slag as a raw material for precipitation of pure calcium carbonate", *Industrial and Engineering Chemistry Research*, vol. 47, no.18, pp. 7104–7111.
- [133] Sun, Y., Yao, M.S., Zhang, J.P. and Yang, G. (2011), "Indirect CO<sub>2</sub> mineral sequestration by steelmaking slag with NH<sub>4</sub>Cl as leaching solution", *Chemical Engineering Journal*, vol. 173, no. 2, pp. 437–445.
- [134] Mattila, H.P., Grigaliūnaitė, I., Said, A., Fogelholm, C.J. and Zevenhoven, R. (2012), "Production of papermaking grade calcium carbonate from steelmaking slag-product quality and development of a larger scale process", *Proceedings of SCANMET IV, International Conference on Process Development in Iron and Steelmaking, 10-13 June 2012*, Luleå, Sweden.
- [135] Chang, E.E., Chen, T.L., Pan, S.Y., Chen, Y.H. and Chiang, P.C. (2013), "Kinetic modeling on CO<sub>2</sub> capture using basic oxygen furnace slag coupled with cold-rolling wastewater in a rotating packed bed", *Journal of Hazardous Materials*, vol. 260, pp. 937-946.
- [136] Morone, M., Costa, G., Georgakopoulos, E., Cizer, Ö., Manovic, V., Baciocchi, R. (2016), Granulation-carbonation treatment of alkali activated

steel slag for secondary aggregates production, Waste and Biomass Valorization.

[137] Euroslag (2012), Statistics, available at: <http://www.euroslag.org/products/statistics/2012/> (accessed on March 23, 2016).

[138] European Commission (2015), Proposal for a Directive Of The European Parliament And Of The Council amending Directive 2008/98/EC on waste Brussels, 2.12.2015 COM (2015) 595 final 2015/0275 (COD).

[139] Shen, D.-H., Wu, C.-M. and Du, J.-C. (2009), "Laboratory investigation of Basic Oxygen Furnace slag for substitution of aggregate in porous asphalt mixture", *Construction and Building Materials*, vol. 23, no. 1, pp. 453-461.

[140] Herrmann, I., Andreas, L., Diener, S. and Lind, L. (2010), "Steel slag used in landfill cover liners: laboratory and field tests", *Waste Management and Research*, vol. 28, no. 12, pp. 1114-1121.

[141] Wang, G., Wang, Y. and Gao, Z. (2010), "Use of steel slag as a granular material: volume expansion prediction and usability criteria", *Journal of Hazardous Materials*, vol. 184, no. 1–3, pp. 555-560.

[142] Italian Ministerial Decree 186/2006 (2006): Regolamento recante modifiche al decreto ministeriale 5 febbraio 1998 Individuazione dei rifiuti non pericolosi sottoposti alle procedure semplificate di recupero, ai sensi degli articoli 31 e 33 del decreto legislativo 5 febbraio 1997, n. 22. Gazzetta Ufficiale 19 maggio 2006, n. 115 (in italian).

[143] Baciocchi, R., Costa, G., Poletini, A. and Pomi, R. (2015), "Effects of thin-film accelerated carbonation on steel slag leaching", *Journal of Hazardous Materials*, vol. 286, pp. 369-378.

[144] Huijgen, W.J. and Comans, R.N. (2006), "Carbonation of steel slag for CO<sub>2</sub> sequestration: leaching of products and reaction mechanisms", *Environmental Science and Technology*, vol. 40, no. 8, pp. 2790-2796.

- [145] Lange, L.C., Hills, C.D. and Poole, A.B. (1996), "The influence of mix parameters and binder choice on the carbonation of cement solidified wastes", *Waste Management*, vol. 16, no. 8, pp. 749-756.
- [146] Fernandez Bertos, M., Li, X., Simons, J.R., Hills, C.D. and Corey, P.J. (2004), "Investigation of accelerated carbonation for the stabilization of MSW incinerator ashes and the sequestration of CO<sub>2</sub>", *Green Chemistry*, vol. 6, no. 8, pp. 428-436.
- [147] Chen, Q., Johnson, D.C. Zhu, L., Yuan, M. and Hills, C.D. (2007), "Accelerated carbonation and leaching behavior of the slag from iron and steel making industry", *Journal of University of Science and Technology Beijing, Mineral, Metallurgy, Material*, vol. 14, no. 4, pp. 297-301.
- [148] Solanki, H.K., Basuri, T., Thakkar, J.H. and Patel, C.A. (2010), "Recent advantages in granulation technology", *International Journal of Pharmaceutical Sciences Review and Research*, vol. 5, no. 3, pp. 48-54.
- [149] Shanmugam, S. (2015), "Granulation techniques and technologies: recent progresses", *Bioimpacts*, vol. 5, no. 1, pp. 55-63.
- [150] Litster, J. and Ennis, B. (2004), *The science and engineering of granulation processes*, Springer Netherlands, Netherlands.
- [151] Tousey, M.D. (2002), The granulation process 101 Basic technologies for tablet making, available at: <http://techceuticals.com/wp-content/uploads/2016/07/Article-The-Granulation-Process.pdf> (accessed on April 3rd, 2016)
- [152] Herting, M.G. and Kleinebudde, P. (2007), "Roll compaction/dry granulation: Effect of raw material particle size on granule and tablet properties", *International Journal of Pharmaceutics*, vol. 338, no. 1-2, pp. 110-118.
- [153] Iveson, S.M., Litster, J.D., Hapgood, K. and Ennis, B.J. (2001), "Nucleation, growth and breakage phenomena in agitated wet granulation processes: a review", *Powder Technology*, vol. 117, no. 1-2, pp. 3-39.

- [154] am Ende, D.J. (Ed.) (2011), *Chemical engineering in the pharmaceutical industry: R&D to manufacturing*, John Wiley and Sons, Inc. Publications, Hoboken, New Jersey, USA.
- [155] Tardos, G.I, Irfan Khan, M. and Mort, P.R. (1997), “Critical parameters and limiting conditions in binder granulation of fine powder”, *Powder Technology*, vol. 94, no. 3, pp. 245–258.
- [156] Ennis, B.J. and Litster, J.D. (1997), “Particle enlargement”, Green, D.W., Perry, R.H. (eds)., in: *Perry’s Chemical Engineer’s Handbook*, 7<sup>th</sup> ed, McGraw Hill, New York, USA.
- [157] Sochon, R.P.J. and Salman, A.D. (2010), “Particle growth and agglomeration processes”, Pohorecki, R., Bridgwater, J., Molzahn, M., Gani, R. and Gallegos, C. (eds), in: *Chemical engineering and chemical process technology, Unit operations – Fluids and solids*, 2, Eolss Publishers Co. Ltd., United Kingdom.
- [158] Iveson, S.M. and Litster, J.D. (1998), “Fundamental studies of granule consolidation Part 2: Quantifying the effects of particle and binder properties”, *Powder Technology*, vol. 99, no. 3, pp. 243-250.
- [159] Gunning, P.J., Hills, C.D. and Carey, P.J. (2009), “Production of lightweight aggregate from industrial waste and carbon dioxide”, *Waste Management*, vol. 29, no. 10, pp. 2722-2728.
- [160] Song, S., Sohn, D., Jennings, H.M. and Mason, T.O. (2000), “Hydration of alkali-activated ground granulated blast furnace slag”, *Journal of Materials Science*, vol. 35, no. 1, pp. 249-257.
- [161] Rashad, A.M. (2013), “A comprehensive overview about the influence of different additives on the properties of alkali-activated slag—A guide for Civil Engineer”, *Construction and Building Materials*, vol. 47, pp. 29-55.
- [162] Krizan, D. and Zivanovic, B. (2002), “Effects of dosage and modulus of water glass on early hydration of alkali–slag cements”, *Cement and Concrete Research*, vol. 32, no. 8, pp. 1181-1188.

- [163] Shi, C. and Day, R.L. (1996), "Some factors affecting early hydration of alkali-slag cements", *Cement and Concrete Research*, vol. 26, no. 3, pp. 439-447.
- [164] Shi, C. and Day, R.L. (1996), "Selectivity of alkaline activators for the activation of slags", *Cement Concrete Aggregates*, vol. 18, no. 1, pp. 8-14.
- [165] Pacheco-Torgal, F., Castro-Gomes, J. and Jalali, S. (2008), "Alkali-activated binders: A review: Part 1. Historical background, terminology, reaction mechanisms and hydration products", *Construction and Building Materials*, vol. 22, no. 7, pp. 1305–1314.
- [166] Palomo, A., Grutzeck, M.W. and Blanco, M.T. (1999), "Alkali-activated fly ashes: A cement for the future", *Cement and Concrete Research*, vol. 29, no. 8, pp. 1323–1329.
- [167] Salman, M., Cizer, Ö., Pontikes, Y., Vandewalle, L., Blanpain, B. and Van Balen, K. (2014), "Effect of curing temperatures on the alkali activation of crystalline continuous casting stainless steel slag", *Construction and Building Materials*, vol. 71, pp. 308–316.
- [168] Kriskova, L., Pontikes, Y., Zhang, F., Cizer, Ö., Jones, P. T., Van Balen, K. and Blanpain, B. (2014), "Influence of mechanical and chemical activation on the hydraulic properties of gamma dicalcium silicate", *Cement and Concrete Research*, vol. 55, pp. 59–68.
- [169] Baciocchi, R., Costa, G., Di Gianfilippo, M., Poletti, A., Pomi, R. and Stramazzo, A. (2015), "Thin-film versus slurry-phase carbonation of steel slag: CO<sub>2</sub> uptake and effects on mineralogy", *Journal of Hazardous Materials*, vol. 283, pp. 302–313.
- [170] Adetayo, A.A., Litster, J.D. and Desai, M. (1993), "The effect of process parameters on drum granulation of fertilizers with broad size distribution", *Chemical Engineering Science*, vol. 48, no. 23, pp. 3951-3961.
- [171] Mackaplow, M.B., Rosen, L.A. and Michaels, J.N. (2000), "Effect of primary particle size on granule growth and endpoint determination in high-shear wet granulation", *Powder Technology*, vol. 108, no. 1, pp. 32–45.

- [172] Keningley, S.T., Knight, P.C. and Marson, A.D. (1997), "An investigation into the effects of binder viscosity on agglomeration behavior", *Powder Technology*, vol. 91, no. 2, pp. 95-103.
- [173] Hoornaert, F., Wauters, P.A.L., Meesters, G.M.H., Pratsinis, S.E. and Scarlett, B. (1998), "Agglomeration behaviour of powders in a Lodige mixer granulator", *Powder Technology*, vol. 96, no. 2, pp. 116-128.
- [174] Badawy, S.I.F., Narang, A.S., LaMarche, K., Subramanian, G. and Varia, S.A. (2012), "Mechanistic basis for the effects of process parameters on quality attributes in high shear wet granulation", *International Journal of Pharmaceutics*, vol. 439, no. 1-2, pp. 324– 333.
- [175] Kokubo, H. and Sunada, H. (1996), "Effect of process variables on the properties and binder distribution of granules prepared by a high-speed mixer", *Chemical and Pharmaceutical Bulletin*, vol. 44, no. 8, pp. 1546-1549.
- [176] Ranjbarian, S. and Farhadi, F. (2013), "Experimental studies on the effects of process parameters on granule properties in a conical high shear granulator", *Iranian Journal of Chemistry and Chemical Engineering*, vol. 32, no. 3, pp. 115-125.
- [177] Knight, P.C. (1993), "An investigation of the kinetics of granulation using a high shear mixer", *Powder Technology*, vol. 77, no. 2, pp. 159-169.
- [178] Mills, P.J.T., Seville, J.P.K., Knight, P.C. and Adams, M.J. (2000), "The effect of binder viscosity on particle agglomeration in a low shear mixer/agglomerator", *Powder Technology*, vol. 113, no. 1-2, pp. 140–147.
- [179] Bock, T.K. and Kraas, U. (2001), "Experience with the Diosna mini-granulator and assessment of process scalability", *European Journal of Pharmaceutics and Biopharmaceutics*, vol. 52, no. 3, pp. 297–303.
- [180] Pathare, P.B., Bas, N., Fitzpatrick, J.J., Cronin, K. and Byrne, E.P. (2011), "Effect of high shear granulation process parameters on the production of granola cereal aggregates", *Biosystems Engineering*, vol. 110, no. 4, pp. 473-481.

- [181] Suzuki, T., Kikuchi, H., Yamamura, S., Terada, K. and Yamamoto, K. (2001), "The change in characteristics of microcrystalline cellulose during wet granulation using a high-shear mixer", *Journal of Pharmacy and Pharmacology*, vol. 53, no. 5, pp. 609-616.
- [182] Harvard University, A Summary of Error Propagation, available at: [http://ipl.physics.harvard.edu/wpuploads/2013/03/PS3\\_Error\\_Propagation\\_sp13.pdf](http://ipl.physics.harvard.edu/wpuploads/2013/03/PS3_Error_Propagation_sp13.pdf) (as accessed on March 17<sup>th</sup>, 2017)
- [183] Worldsteel Association (2016), World steel in figures 2016, Worldsteel Association, Brussels, Belgium.
- [184] Gluba, T. (2002), "The effect of wetting conditions on the strength of granules", *Physicochemical Problems of Mineral Processing*, vol. 36, pp. 233-242.
- [185] Rahmanian, N., Naji, A. and Ghadiri, M. (2011), "Effects of process parameters on granules properties produced in a high shear granulator", *Chemical Engineering Research and Design*, vol. 89, no. 5, pp. 512-518.
- [186] Cornelis, G., Johnson, A., Van Gerven, T. and Vandecasteele, C. (2008), "Leaching mechanisms of oxyanionic metalloids and metal species in alkaline solid wastes: A review", *Applied Geochemistry*, vol. 23, no. 5, pp. 955–976.
- [187] Worldatlas (2016), Cost of electricity by country, available at: <http://www.worldatlas.com/articles/electricity-rates-around-the-world.html> (accessed on March 12<sup>th</sup>, 2017).
- [188] Fischer Scientific (2017), Shop products, available at: <https://www.fishersci.com/us/en/catalog/search/products/sodiumhydroxide> (accessed on March 15<sup>th</sup>, 2017)
- [189] Sigma Aldrich (2017), Sodium silicate solution, available at: <http://www.sigmaaldrich.com/catalog/product/sigma/> (accessed on March 15<sup>th</sup>, 2017).

- [190] Garbarino E. and Blengini G.A. (2013), “The economics of construction and demolition waste (C and DW) management facilities”, Pacheco-Torgal, F., Tam, V.W.Y., Labrincha, J.A., Ding, Y., de Brito, J. (eds)., in: Handbook of recycled concrete and demolition waste, 7th ed, Woodhead Publishing, Cambridge, UK.
- [191] Zhang, C., Qiao, Q., Appel, E. and Huang B. (2012), “Discriminating sources of anthropogenic heavy metals in urban street dusts using magnetic and chemical methods”, *Journal of Geochemical Exploration*, vol. 119-120, pp. 60-75.
- [192] Hu, Y., , Liu, X., Bai, J., Shih, K., Zeng, E.Y. and Cheng, H. (2013), “Assessing heavy metal pollution in the surface soils of a region that had undergone three decades of intense industrialization and urbanization”, *Environmental Science and Pollution Research*, vol. 20, pp. 6150-6159.
- [193] Duffus, J.H. (2002), ““Heavy metals” - A meaningless term? (IUPAC Technical Report)”, *Pure and Applied Chemistry*, vol. 74, no. 5, pp. 793-807.
- [194] Singh, R., Gautam, N., Mishra, A. and Gupta, R. (2011), “Heavy metals and living systems: An overview”, *Indian Journal of Pharmacology*, vol. 43, no. 3, pp. 246-253.
- [195] Tchounwou, P.B., Yedjou, C.G., Patlolla, A.K. and Sutton, D.J. (2012), “Heavy Metals Toxicity and the Environment”, *Molecular, Clinical and Environmental Toxicology, Experientia Supplementum*, vol. 101, pp. 133–164.
- [196] Mizuta, K., Matsumoto, T., Hatate, Y., Nishihara, K. and Nakanishi, T. (2004), “Removal of nitrate-nitrogen from drinking water using bamboo powder charcoal”, *Bioresource Technology*, vol. 95, no. 3, pp. 255-257.
- [197] Kumar, P.S., Ramalingam, S., Kirupha, S.D., Murugesan, A., Vidhyadevi, T. and Sivanesan, S. (2011), “Adsorption behavior of nickel(II) onto cashew nut shell: Equilibrium, thermodynamics, kinetics, mechanism and process design”, *Chemical Engineering Journal*, vol. 167, no. 1, pp. 122–131.
- [198] Al-Degs, Y.S., El-Barghouthi, M.I., El-Sheikh, A.H. and Walker, G.M. (2008), “Effect of solution pH, ionic strength, and temperature on adsorption

behavior of reactive dyes on activated carbon”, *Dyes and Pigments*, vol. 77, no. 1, pp. 16-23.

[199] Gupta, V.K., Jain, C.K. Ali, I., Sharma, M. and Saini, V.K. (2003), “Removal of cadmium and nickel from wastewater using bagasse fly ash—a sugar industry waste”, *Water Research*, vol. 37, no. 16, pp. 4038–4044.

[200] Malkoc, E. and Nuhoglu, Y. (2005), “Investigations of nickel(II) removal from aqueous solutions using tea factory waste”, *Journal of Hazardous Materials*, vol. 127, no. 1-3, pp. 120–128.

[201] Hasar, H. (2003), “Adsorption of nickel(II) from aqueous solution onto activated carbon prepared from almond husk”, *Journal of Hazardous Materials*, vol. 97, no. 1-3, pp. 49–57.

[202] Boujelben, N., Bouzid, J. and Elouear, Z. (2009), “Adsorption of nickel and copper onto natural iron oxide-coated sand from aqueous solutions: Study in single and binary systems”, *Journal of Hazardous Materials*, vol. 163, no. 1, pp. 376–382.

[203] Popuri, S.R., Vijaya, Y., Boddu, V.M. and Abburi, K. (2009), “Adsorptive removal of copper and nickel ions from water using chitosan coated PVC beads”, *Bioresource Technology*, vol. 100, no. 1, pp. 194–199.

[204] Ewecharoen, A., Thiravetyan, P. and Nakbanpote, W. (2008), “Comparison of nickel adsorption from electroplating rinse water by coir pith and modified coir pith”, *Chemical Engineering Journal*, vol. 137, no. 2, pp. 181–188.

[205] Gunay, A., Arslankaya, E. and Tosun, I. (2007), “Lead removal from aqueous solution by natural and pretreated clinoptilolite: Adsorption equilibrium and kinetics”, *Journal of Hazardous Materials*, vol. 146, no. 1-2, pp. 362-371.

[206] Malik, P.K. (2003), “Use of activated carbons prepared from sawdust and rice-husk for adsorption of acid dyes: a case study of Acid Yellow 36”, *Dyes and Pigments*, vol. 56, no. 3, pp. 239–249.

- [207] Ghaedi, M., Golestani Nasab, A., Khodadoust, S., Rajabi, M. and Azizian, S. (2014), "Application of activated carbon as adsorbents for efficient removal of methylene blue: Kinetics and equilibrium study", *Journal of Industrial and Engineering Chemistry*, vol. 20, no. 4, pp. 2317–2324.
- [208] Singh, T.S. and Pant, K.K. (2004), "Equilibrium, kinetics and thermodynamic studies for adsorption of As(III) on activated alumina", *Separation and Purification Technology*, vol. 36, no. 2, pp. 139-147.
- [209] Bishnoi, N.R., Bajaj, M., Sharma, N. and Gupta A. (2004), "Adsorption of Cr(VI) on activated rice husk carbon and activated alumina", *Bioresource Technology*, vol. 91, no. 3, pp. 305–307.
- [210] Wang, S. and Peng, Y. (2010), "Natural zeolites as effective adsorbents in water and wastewater treatment", *Chemical Engineering Journal*, vol. 156, no. 1, pp. 11–24.
- [211] Chutia, P., Kato, S., Kojima, T. and Satokawa, S. (2009), "Arsenic adsorption from aqueous solution on synthetic zeolites", *Journal of Hazardous Materials*, vol. 162, no. 1, pp. 440–447.
- [212] Puanggam, M. and Unob, F. (2008), "Preparation and use of chemically modified MCM-41 and silica gel as selective adsorbents for Hg(II) ions", *Journal of Hazardous Materials*, vol. 154, no. 1-3, pp. 578–587.
- [213] Shevade, S. and Ford, R.G. (2004), "Use of synthetic zeolites for arsenate removal from pollutant water", *Water Research*, vol. 38, no. 14-15, pp. 3197-3204.
- [214] Erdem, E., Karapinar, N. and Donat, R. (2004), "The removal of heavy metal cations by natural zeolites", *Journal of Colloid and Interface Science*, vol. 280, no. 2, pp. 309-314.
- [215] Ruggieri, F., Marín, V., Gimeno, D., Fernandez-Turiel, J.L., García-Valles, M. and Gutierrez, L. (2008), "Application of zeolitic volcanic rocks for arsenic removal from water", *Engineering Geology*, vol. 101, no. 3-4, pp. 245-250.

- [216] Terdkiatburana, T., Wang. S. and Tadé, M.O. (2009), “Adsorption of heavy metal ions by natural and synthesized zeolites for wastewater treatment”, *International Journal of Environment and Waste Management*, vol. 3, no. 3-4, pp. 327-335.
- [217] Gholikandi, G.B., Baneshi, M.M., Dehghanifard, E., Salehi, S. and Yari, A.R. (2010), “Natural Zeolites Application as Sustainable Adsorbent for Heavy Metals Removal from Drinking Water”, *Iranian Journal of Toxicology*, vol. 3, no. 3, pp. 302-310.
- [218] Shoumkova, A. (2011), “Zeolites for water and wastewater treatment: An overview”, *2011 Research Bulletin of the Australian Institute of High Energetic Materials*, 2, 10-70.
- [219] Chiang, Y.W., Ghyselbrecht, K., Santos, R.M., Meesschaert, B. and Martens, J.A. (2012), “Synthesis of zeolitic-type adsorbent material from municipal solid waste incinerator bottom ash and its application in heavy metal adsorption”, *Catalysis Today*, vol. 190, no. 1, pp. 23-30.
- [220] Davis, R.J. (2003), “New perspectives on basic zeolites as catalysts and catalyst supports”, *Journal of Catalysis*, vol. 216, no. 1-2, pp. 396–405.
- [221] Primo A. and Garcia, H. (2014), “Zeolites as catalysts in oil refining”, *Chemical Society Reviews*, vol. 43, pp. 7548-7561.
- [222] Vaiana, R., luele, T. and Gallelli, V. (2013), “Warm Mix asphalt with synthetic zeolite: A laboratory study on mixes workability”, *International Journal of Pavement Research and Technology*, vol. 6, no. 5, pp. 562-569.
- [223] Handayani, A.T., Setiaji, B.H. and Prabandiyani, S. (2015), “The Use of Natural Zeolite as an Additive in Warm Mix Asphalt with Polymer Modified Asphalt Binder”, *International Journal of Engineering Research in Africa*, vol. 15, pp. 35-46.
- [224] Jana, D. (2007), “A new look to an old pozzolan, clinoptilolite – a 654 promising pozzolan in concrete”, *Proceedings of the 29th ICMA conference on cement microscopy, 21-24 May 2007, Quebec City, Canada*.

- [225] Valipour, M., Pargar, F., Shekarchi, M. and Khani, S. (2013), "Comparing a natural pozzolan, zeolite, to metakaolin and silica fume in terms of their effect on the durability characteristics of concrete: A laboratory study", *Construction and Building Materials*, vol. 41, pp. 879-888.
- [226] Tomasevic-Canovic, M. (2005), "Purification of natural zeolite-clinoptilolite for medical application-Extraction of lead", *Journal of the Serbian Chemical Society*, vol. 70, no. 11, pp. 1335-1345.
- [227] Andronescu, E., Grigore, F., Tardei, C. and Stefan, E. (2006), "Natural zeolites with medical applications-preliminary preparation and characterization", *Revista medico-chirurgicala a Societatii de Medici si Naturalisti din Iasi*, vol. 110, no. 1, pp. 236-241.
- [228] Rhee, P., Brown, C., Martin, M., Salim, A., Plurad, D., Green, D., Chambers, L., Demetriades, D., Velmahos, G. and Alam, H. (2008), "QuikClot use in trauma for hemorrhage control: case series of 103 documented uses", *The Journal of Trauma*, vol. 64, no. 4, pp. 1093-1099.
- [229] Mumpton, F.A. (1985), "Using zeolites in agriculture", Elfring C. (ed.), in: *Innovative Biological Technologies for Lesser Developed Countries*, Congress of the United States, Office of Technology Assessment, Washington, DC, USA.
- [230] Mumpton, F.A. (1999), "La roca magica: Uses of natural zeolites in agriculture and industry", *Proceedings of the National Academy of Science of the United States of America*, vol. 96, no. 7, pp. 3463-3470.
- [231] Ramesh, K., Reddy, D.D., Biswas, A.K. and Rao, A.S. (2011), "Zeolites and their potential uses in agriculture", *Advances in Agronomy*, vol. 113, pp. 215-236.
- [232] Ruen-ngam, D., Rungsuk, D., Apiratikul, R. and Pavasant, P. (2009), "Zeolite formation from coal fly ash and its adsorption potential", *Journal of the Air & Waste Management Association*, vol. 59, no. 10, pp. 1140-1147.
- [233] Jha, V.K., Nagae, M., Matsuda, M. and Miyake, M. (2009), "Zeolite formation from coal fly ash and heavy metal ion removal characteristics of

thus-obtained Zeolite X in multi-metal systems”, *Journal of Environmental Management*, vol. 90, no. 8, pp. 2507-2514.

[234] Fan, Y., Zhang, F.S., Zhu, J. and Liu, Z. (2008), “Effective utilization of waste ash from MSW and coal co-combustion power plant—Zeolite synthesis”, *Journal of Hazardous Materials*, vol. 153, no. 1-2, pp. 382-388.

[235] Rios, C.A. and Williams, C.D. (2008), “Synthesis of zeolitic materials from natural clinker: A new alternative for recycling coal combustion by-products”, *Fuel*, vol. 87, no. 12, pp. 2482-2492.

[236] Basaldella, E.I., Kikot, A. and Pereira, E. (1990), “Synthesis of zeolites from mechanically activated kaolin clays”, *Reactivity of Solids*, vol. 8, no. 1-2, pp. 169-177.

[237] Murat, M., Amokrane, A., Bastide, J.P. and Montanaro, L. (1992), “Synthesis of Zeolites from thermally activated kaolinite. Some observations on nucleation and growth”, *Clay Minerals*, vol. 27, pp. 119-130.

[238] Miao, Q., Zhou, Z., Yang, J., Lu, J., Yan, S. and Wang, J. (2009), “Synthesis of NaA zeolite from kaolin source”, *Frontiers of Chemical Engineering in China*, vol. 3, no. 1, pp. 8-11.

[239] Kuwahara, Y., Ohmichi, T., Kamegawa, T., Mori, K. and Yamashita, H. (2010), “A novel conversion process from waste slag: synthesis of a hydrotalcite-like compound and zeolite from blast furnace slag and evaluation of adsorption capacities”, *Journal of Materials Chemistry*, vol. 20, no. 1, pp. 5052-5062.

[240] Murakami, T., Sugano, Y., Narushima, T., Iguchi, Y. and Ouchi, C. (2011), “Recovery of calcium from BF slag and synthesis of zeolite A using its residue”, *ISIJ International*, vol. 51, no. 6, pp. 901-905.

[241] Sugano, Y., Sahara, R., Murakami, T., Narushima, T., Iguchi, Y. and Ouchi, C. (2005), “Hydrothermal synthesis of zeolite A using blast furnace slag”, *ISIJ International*, vol. 45, no. 6, pp. 937-945.

- [242] Qiu, W. and Zheng, Y. (2009) "Removal of lead, copper, nickel, cobalt, and zinc from water by a cancrinite-type zeolite synthesized from fly ash", *Chemical Engineering Journal*, vol. 145, no.3, pp. 483–488.
- [243] Teir, S., Eloneva, S., Fogelholm, C.-J. and Zevenhoven, R. (2007), "Dissolution of steelmaking slags in acetic acid for precipitated calcium carbonate production", in ECOS 05 18th International Conference on Efficiency, Cost, Optimization, Simulation, and Environmental Impact of Energy Systems — ECOS 05, *Energy*, vol. 32, no. 4, pp. 528-539.
- [244] Tsutsumi, T., Nishimoto, S., Kameshima, Y. and Miyake, M. (2014), "Hydrothermal preparation of tobermorite from blast furnace slag for Cs<sup>+</sup> and Sr<sup>2+</sup> sorption", *Journal of Hazardous Materials*, vol. 266, pp. 174-181.
- [245] Komarneni, S. (1985), "Heavy metal removal from aqueous solutions by tobermorites and zeolites", *Nuclear and Chemical Waste Management*, vol. 5, no. 4, pp. 247-250.
- [246] Bingham, E. and Cohrssen, B. (2012), *Patty's Toxicology*, 6<sup>th</sup> ed., John Wiley & Sons, Hoboken.
- [247] Bonfils, B., Julcour-Lebigue, C., Guyot, F., Bodéan, F., Chiquet, P. and Bourgeois, F. (2012), "Comprehensive analysis of direct aqueous mineral carbonation using dissolution enhancing organic additives", *International Journal of Greenhouse Gas Control*, vol. 9, pp. 334-346.
- [248] Eloneva, S., Teir, S., Revitzer, H., Salminen, J., Said, A., Fogelholm, C.J. and Zevenhoven, R. (2009), "Reduction of CO<sub>2</sub> emissions from steel plants by using steelmaking slags for production of marketable calcium carbonate", *Steel Research International*, vol. 80, no. 6, pp. 415-421.
- [249] Georgakopoulos, E., Santos R.M., Chiang, Y.W., Manovic, V., (2017) "Two-way valorization of blast furnace slag: synthesis of precipitated calcium carbonate and zeolitic heavy metal adsorbent", *Journal of Visualized Experiments*, vol. 120, e55062.

- [250] Chiang, Y.W., Santos, R.M., Ghyselbrecht, K., Cappuyens, V., Martens, J.A., Swennen, R., Van Gerven, T. and Meesschaert, B. (2012), "Strategic selection of an optimal sorbent mixture for in-situ remediation of heavy metal contaminated sediments: Framework and case study", *Journal of Environmental Management*, vol. 105, pp. 1-11.
- [251] McKay, G., Blair, H.S. and Gardiner, J.R. (1982), "Adsorption of dyes on chitin. I. Equilibrium studies", *Journal of Applied Polymer Science*, vol. 27, no. 8, pp. 3043-3057.
- [252] Ho, Y.S., Porter, J.F. and McKay, G. (2002), "Equilibrium isotherm studies for the sorption of divalent metal ions onto peat: copper, nickel and lead single component systems", *Water, Air, and Soil Pollution*, vol. 141, pp. 1-33.
- [253] Kadirvelu, K., and Namasivayam, C. (2000), "Agricultural by-product as metal adsorbent: Sorption of lead (II) from aqueous solution onto coirpith carbon", *Environmental Technology*, vol. 21, no. 10, pp.1091-1097.
- [254] Kiran, B. and Kaushik, A. (2008), "Chromium binding capacity of *Lyngbya putealis* exopolysaccharides", *Biochemical Engineering Journal*, vol. 38, no. 1, pp. 47-54.
- [255] Wang, Y., Huang, L. and Lau, R. (2016), "Conversion of municipal solid waste incineration bottom ash to sorbent material for pollutants removal from water", *Journal of the Taiwan Institute of Chemical Engineers*, vol. 60, pp. 275-286.
- [256] Alvarez-Ayuso, E., Garcia-Sanchez, A. and Querol, X. (2003) "Purification of metal electroplating waste waters using zeolites", *Water Research*, vol. 37, pp. 4855–4862.
- [257] Deesaen, P., Opaprakasit P., Manyam, J., Egashira, R. and Sreearunothai P. (2015), "Effect of synthesis time and crystallinity on the Ni (II) sorption performance of zeolite-like compounds", *Proceedings of The IRES 7th International Conference, 16th August 2015*, Kuala Lumpur, Malaysia.

- [258] Wassel, M.A., Shehata, H.A, Youssef, H.F., Elzaref, A.S. and Fahmy, A. (2015), "Nickel ions adsorption by prepared zeolite-A: examination of process parameters, kinetics and isotherms", *International Journal of Innovative Science, Engineering & Technology*, vol. 3, no. 7, pp. 2348 – 7968.
- [259] Jamil, T.S. and Youssef, H.F. (2016), "Microwave synthesis of zeolites from Egyptian kaolin: Evaluation of heavy metals removal", *Separation Science and Technology*, vol. 51, no. 18, pp. 2876-2886.
- [260] Wang, H., Wang, X., Xu, Z. and Zhang, M. (2016), "Synthetic zeolite from coal bottom ash and its application in cadmium and nickel removal from acidic wastewater", *Desalination and Water Treatment*, vol. 57, no. 2016, pp. 26089–26100.
- [261] Qi, H., Du, H., and Yin, C. (2011), "Experimental Research on Adsorption of Cadmium with Synthetic Tobermorite from Wastewater", *Advanced Materials Research*, vol. 160-162, pp. 1038-1043.
- [262] Qi, H., Du, H., Liang, S-P., and Yin, C. (2010) "Study on adsorption of  $Pb^{2+}$  by synthetic tobermorite", *Proceedings of the 2010 International Conference on Mechanic Automation and Control Engineering*, 26-28<sup>th</sup> June 2010, Wuhan, China.
- [263] Šiaučiūnas, R., Vaiciukyniene, D. and Ivanauskas, R. (2002), "Elimination of heavy metals from water by modified tobermorite", *Environmental Research, Engineering and Management*, vol. 3, no. 21, pp. 61-66.
- [264] Luo, F., Wei, C., Xue, B., Wang, S. and Jiang, Y. (2013), "Dynamic hydrothermal synthesis of Al-substituted 11 Å tobermorite from solid waste fly ash residue-extracted  $Al_2O_3$ ", *Research on Chemical Intermediates*, vol. 39, no. 2, pp. 693–705.
- [265] Rachkova, N.G. and Shuktomova, I.I. (2010), "Sorption of U(VI) and Ra from aqueous solutions with analcime-containing rock", *Radiochemistry*, vol. 52, no. 1, pp. 76-80.

- [266] Hegazy, E.Z., Hamdy, I. and Abo El Enin, R.M.M. (2010), "Preparation and characterization of Ti and V modified analcime from local kaolin", *Applied Clay Science*, vol. 49, no. 3, pp. 149-155.
- [267] Kumar, P. and Dara, S.S. (1981), "Binding heavy metal ions with polymerized onion skin", *Journal of Polymer Science, Part A: Polymer Chemistry*, vol. 19, no. 2, pp. 397-402.
- [268] Suemitsu, R., Venishi, R., Akashi, I. and Nakana, M. (1986), "The use of dyestuff-treated rice hulls for removal of heavy metals from waste water", *Journal of Applied Polymer Science*, vol. 31, no. 1, pp. 75–83.
- [269] Okieimen, F.E. and Onyekpa, V.U. (1989), "Removal of heavy metal ions in aqueous solutions with melon (*Citrullus Rulgaris*) seed husk", *Biological Waste*, vol. 29, no.1, pp. 11–16.
- [270] Vishwakarma, P.P., Yadava, K.P. and Singh, V.N. (1989), "Nickel (II) removal from aqueous solutions by adsorption on fly-ash", *Pertanika*, vol. 12, no. 3, pp. 357–366.
- [271] Allen, H.E. and Minear, R.A. (1989), "Metallic ions", M.J. Suess (ed.), *Examination of Water for Pollution Control, Physical Chemical and Radiological Examinations*, vol. 2, Pergamon, Oxford.
- [272] Hawash, S., Farash, J.Y. and El-Geundi, M.S. (1992), "Investigation of nickel ion removal by means of activated clay adsorption", *Adsorption Science and Technology*, vol. 9, no. 4, pp. 244-257.
- [273] Viraraghavan, T. and Drohamraju, M.M. (1993), "Removal of copper, nickel and zinc from wastewater by adsorption using feat", *Journal of Environmental Science and Health. Part A: Environmental Science and Engineering and Toxicology*, vol. 28, no. 6, pp. 1261-1276.
- [274] Marshall, W.E., Champagne, E.T. and Evans, W.J. (1993), "Use of rice milling byproducts (hulls and bran) to remove metal ions from aqueous solution", *Journal of Environmental Science and Health. Part A: Environmental Science and Engineering and Toxicology*, vol. 28, no. 9, pp. 1977-1992.

- [275] Zouboulis A.I. and Kydros, K.A. (1993), "Use of red mud for toxic metals removal: The case of nickel", *Journal of Chemical Technology and Biotechnology*, vol. 58, no. 1, pp. 95–101.
- [276] Namasivayam, C. and Ranganathan K. (1994), "Recycling of 'waste' FE(III)/CR(III) hydroxide for the removal of nickel from wastewater: Adsorption and equilibrium studies", *Waste Management*, vol. 14, no. 8, pp. 709-716.
- [277] Hawash, S., El-Abd, H., El-Geundi, M.S., Nassar, M.M. and Farah, J.Y. (1992), "Useful adsorption equilibriums by means of natural clay", *Adsorption Science & Technology*, vol. 9, no. 4, pp. 231-243.
- [278] Periasamy, K. and Namasivayam, C. (1995), "Removal of nickel(II) from aqueous solution and nickel plating industry wastewater using an agricultural waste: Peanut hulls", *Waste management*, vol. 15, no. 1, pp. 63-68.
- [279] Dimitrova, S.V. (1996), "Metal sorption on blast furnace slag", *Water Research*, vol. 30, no. 1, pp. 228-232.
- [280] Singh, D. and Rawat, N.S. (1997), "Adsorption of heavy metals on treated and untreated low grade bituminous coal", *Indian Journal of Chemical Technology*, vol. 4, no. 1, pp. 39-41.
- [281] Kapoor, A. and Viraraghavan, T. (1998), "Biosorption of heavy metals on *Aspergillus niger*: Effect of pretreatment", *Bioresource Technology*, vol. 63, no. 2, pp. 109-113.
- [282] K. Kadirvelu, K., Thamaraiselvi, K. and Namasivayam, C. (2001), "Adsorption of nickel(II) from aqueous solution onto activated carbon prepared from coir pith", *Separation and Purification Technology*, vol. 24, pp. 497–505.
- [283] Yavuz, O., Altunkaynak, Y. and Guzel, F. (2003), "Removal of copper, nickel, cobalt and manganese from aqueous solution by kaolinite", *Water Research*, vol. 37, no. 4, pp. 948-952.
- [284] Kandah, M.I. and Meunier, J.L. (2007), "Removal of nickel ions from water by multi-walled carbon nanotubes", *Journal of Hazardous Materials*, vol. 146, no. 1-2, pp. 283–288.

- [285] Kumar, P.S. and Kirthika, K. (2009), "Equilibrium and kinetic study of adsorption of nickel from aqueous solution onto bael tree leaf powder", *Journal of Engineering Science and Technology*, vol. 4, no. 4, pp. 351 – 363.
- [286] Srivastava, V., Weng, C.H., Singh, V.K. and Sharma, Y.C. (2011), "Adsorption of Nickel Ions from Aqueous Solutions by Nano Alumina: Kinetic, Mass Transfer, and Equilibrium Studies", *Journal of Chemical and Engineering Data*, vol. 56, no. 4, pp. 1414–1422.
- [287] Marceau, M.L., Nisbet, M.A. and Van Geem, M.G. (2006), *Life Cycle Inventory of Portland Cement Manufacture*, Portland Cement Association, Skokie, Illinois, USA.
- [288] Barger, G.S., Hill, R.L. and Ramme, B.W. (2003), *Use of Fly Ash in Concrete*, American Concrete Institute, Farmington Hills, Miami, USA.
- [289] Oner, A., Akyuz, S. and Yildiz, R. (2005), "An experimental study on strength development of concrete containing fly ash and optimum usage of fly ash in concrete", *Cement and Concrete Research*, vol. 35, no. 6, pp. 1165–1171.
- [290] Siddique, R. (2004), "Performance characteristics of high-volume Class F fly ash concrete", *Cement and Concrete Research*, vol. 34, no. 3, pp. 487–493.
- [291] Berryman, C., Zhu, J., Jensen, W. and Tadros, M. (2005), "High-percentage replacement of cement with fly ash for reinforced concrete pipe", *Cement and Concrete Research*, vol. 35, no. 6, pp. 1088–1091.
- [292] Mazloom, M., Ramezani pour, A.A. and Brooks, J.J. (2004), "Effect of silica fume on mechanical properties of high-strength concrete", *Cement and Concrete Composites*, vol. 26, no.4, pp. 347–357.
- [293] Almusallam, A.A., Beshr, H., Maslehuddin, M. and Al-Amoudi, O.S.B. (2004), "Effect of silica fume on the mechanical properties of low quality coarse aggregate concrete", *Cement and Concrete Composites*, vol. 26, no. 7, pp. 891–900.

- [294] Siddique, R. (2011), "Utilization of silica fume in concrete: Review of hardened properties", *Resources, Conservation and Recycling*, vol. 55, no. 11, pp. 923–932.
- [295] Thomas, M.D.A., Hooton, D., Cail, K., Smith, B., De Wal, J. and Kazanis, K. (2010), "Field trials of concrete produced with Portland limestone cement", *Concrete International*, vol. 32, no. 1, pp. 35–41.
- [296] Senhadji, Y., Escadeillas, G., Mouli, M., Khelafi, H. and Benosman (2014), "Influence of natural pozzolan, silica fume and limestone fine on strength, acid resistance and microstructure of mortar", *Powder Technology*, vol. 254, pp. 314–323.
- [297] Bhimani, P. and Vyas, C.M. (2013), "Performance of Concrete with China Clay (Kaolin) Waste", *International Journal of Latest Trends in Engineering and Technology*, vol. 2, no. 3, pp. 49-54.
- [298] Amin, N. (2012), "Use of clay as a cement replacement in mortar and its chemical activation to reduce the cost and emission of greenhouse gases", *Construction and Building Materials*, vol. 34, pp. 381–384.
- [299] Prusinski, J.R., Marceau, M.L and Van Geem, M.G. (2004), "Life cycle inventory of slag cement concrete", *Proceedings of the 8<sup>th</sup> CANMET/ACI International Conference on Fly Ash, Silica Fume, Slag and Natural Pozzolans in Concrete – Supplemental Papers*, American Concrete Institute, Farmington Hills, Michigan, USA.
- [300] Yatagai, A., Nito, N., Koibuchi, K., Miyazawa, S., Yokomuro, T. and Sakai, E. (2013), "Properties of concrete with blast-furnace slag cement Made from clinker with adjusted mineral composition", *Proceedings of the 3rd International Conference on Sustainable Construction Materials and Technologies*, Kyoto, Japan.
- [301] Dubey, A., Chandak, R. and Yadav, R.K. (2012), "Effect of blast furnace slag powder on compressive strength of concrete", *International Journal of Scientific & Engineering Research*, vol. 3, no. 8, pp. 1-5.

- [302] Oner, M., Erdogdu, K. and Gunlu, A. (2003), "Effect of components fineness on strength of blast furnace slag cement", *Cement and Concrete Research*, vol. 33, no. 4, pp. 463-469.
- [303] Chidiac, S.E. and Panesar, D.K. (2008), "Evolution of mechanical properties of concrete containing ground granulated blast furnace slag and effects on the scaling resistance test at 28 days", *Cement and Concrete Composites*, vol. 30, no. 2, pp. 63-71.
- [304] Barnett, S.J., Soutsos, M.N., Millard, S.G. and Bungey, J.H. (2006), "Strength development of mortars containing ground granulated blast-furnace slag: Effect of curing temperature and determination of apparent activation energies", *Cement and Concrete Research*, vol. 36, no. 3, pp. 434-440.
- [305] Donatello, S., Tyrer, M., Cheeseman, C.R. (2010), "Comparison of test methods to assess pozzolanic activity", *Cement & Concrete Composites*, vol. 32, no. 2, pp. 121-127.
- [306] Garcia, R., Vigil de la Villa, R., Vegas, I., Frias, M., Sanchez de Rojas, M.I. (2008), "The pozzolanic properties of paper sludge waste", *Construction and Building Materials*, vol. 22, no. 7, pp. 1484-1490.
- [307] Frias, M., Villar-Cocina, E., Valencia-Morales, E. (2007), "Characterisation of sugar cane straw waste as pozzolanic material for construction: calcining temperature and kinetic parameters", *Waste Management*, vol. 27, no. 4, pp. 533–538.
- [308] McCarter, W.J, Tran, D. (1996), "Monitoring pozzolanic activity by direct activation with calcium hydroxide", *Construction and Building Materials*, vol. 10, no. 3, pp. 179-184.



## APPENDIX A: LITERATURE REVIEW ON THE CARBONATION OF IRON- AND STEEL-MAKING SLAGS

Table A-1: Types of slags and reactors, and carbonation routes used in various carbonation studies [1]

Reference	Slag Type	Reactor Type	Carbonation Route
Huijgen et al. [36]	BOF	Autoclave Reactor	Slurry Carbonation
Chang et al. [37]	BOF	Column Slurry Reactor	Slurry Carbonation
Van Zomeren [113]	BOF	Column Reactor	Wet/Slurry Carbonation
Santos et al. [38]	BOF	TGA Reaction: crucible Pressurized Basket Reactor Atmospheric Furnace	Dry Carbonation
Chang et al. [39]	BOF	High-Gravity Rotating Packed Bed (RPB)	Slurry Carbonation
Chang et al. [112]	BOF	Column Slurry Reactor	Slurry Carbonation
Polettini et al. [114]	BOF	Pressurized Stainless Steel Reactor	Slurry Carbonation
Baciocchi et al. [115]	BOF	Pressurized Stainless Steel Reactor	Wet/Slurry Carbonation
Tai et al. [20]	BOF	Stirred High-Pressure Batch Reactor	Slurry Carbonation
Johnson et al. [117]	SS	Pressurized Sealed Chamber	Mold Carbonation
Baciocchi et al. [116]	SS	Pressurized Stainless Steel Reactor	Wet Carbonation
Baciocchi et al. [65]	EAF, AOD	Pressurized Stainless Steel Reactor	Wet Carbonation
Baciocchi et al. [63]	EAF	Pressurized Stainless Steel Reactor	Slurry Carbonation
Vandevelde [118]	AOD,CC	Pressurized Incubator Chamber	Wet Carbonation
Santos et al. [64]	AOD,CC	Common Glass Beaker	Slurry Carbonation
Van Bouwel [120]	AOD,CC	Autoclave Reactor	Slurry Carbonation
Santos et al. [66]	AOD, CC	Thin Film Reaction: Incubator Slurry Reaction: Autoclave Reactor	Thin Film Reaction: Wet Carbonation Slurry Reaction: Slurry Carbonation
Chang et al. [111]	BF	Autoclave Reactor	Slurry Carbonation
Cappai et al. [122]	Waelz	Pressurized Batch Reactor	Wet/Slurry Carbonation

**Table A-2 Summary of process conditions and their general enhancement effects on carbonation conversion extent (indicated by the slope of arrows) of several slag carbonation studies [1]**

Reference	Slag Type	Temperature	Reaction time	CO <sub>2</sub> Pressure	L/S ratio	Slurry volume	Particle size	Steam addition	Stirring rate	CO <sub>2</sub> Flow Rate	Highest CO <sub>2</sub> conversion (%) achieved
Huijgen et al. [36]	BOF	(between 25 °C - 200 °C) → (for T >200 °C) ←	→	(0-9 bar) → (>9 bar) No clear effect	Highest conversion presented: L/S=2kg/kg . For values lower or higher the conversion extent gets lower	—	←	—	(0 - 500rpm) → (500-1500rpm) ↔ (1500-2000rpm) →	—	<b>74 %</b> (after 30 min, particle size=38µm, T=100 °C, P <sub>CO<sub>2</sub></sub> =19 bar, 500 rpm, and L/S= 10kg / kg)
Chang et al. [37]	BOF	(30 °C- 60 °C) → (60 °C - 80 °C) ←	(for the first 60 minutes) → (60min-240min) ↔	Steady (1.013 bar)	Steady (10 mL/g)	—	Steady (< 44 µm)	—	—	←	<b>68 %</b> (after 60 min, T=70 °C, particle size <44µm, P <sub>CO<sub>2</sub></sub> = 1.013 bar, L/S= 10 mL/g, flow rate=0.1 L/min)
van Zomeren [113]	BOF	(L/S: 2 L/kg) (up to 90 °C) → (L/S: 0.1 L/kg) ←	→	—	→	—	Steady (2 - 3.3 mm)	—	—	Steady (400mL /min)	<b>4.7%</b> (after ~60 hours, T=90 °C, particle size: 2- 3.3mm, P <sub>CO<sub>2</sub></sub> =0.2 bar, L/S=2 L/kg, flow rate=0.4 L/min)

Reference	Slag Type	Temperature	Reaction time	CO <sub>2</sub> Pressure	L/S ratio	Slurry volume	Particle size	Steam addition	Stirring rate	CO <sub>2</sub> Flow Rate	Highest CO <sub>2</sub> conversion (%) achieved
Santos et al. [38]	BOF (Pressurized Basket Reactor Carbonation)	(more important for lower pCO <sub>2</sub> )	(for 725 °C and 800 °C) Sharp CO <sub>2</sub> uptake improvement for the initial 7.5 min. (for 575 °C and 600 °C) Gradual uptake improvement with time.	(at 350 °C) ↗ (at 500 °C) Very slight improvement (at 650 °C) ↔	—	—	↖	(more significant in percentage for BOF <sub>1</sub> ) ↗ (greater uptakes achieved by BOF <sub>2</sub> )	—	—	~36 % (for BOF <sub>2</sub> , after 30 min, T=650 °C, particle size <0.08 mm, at total pressure=20 bar)
Chang et al. [39]	BOF	(from 25 °C – 65 °C) ↗	(For the first 6 to 7 min) ↗ (10min-30min) ↔	Steady (1 bar)	Steady (20 mL/g)	Steady (1.575 L)	Steady (< 88 μm)	—	(500-1000rpm) ↗ (1000-1250rpm) ↖	(for the first 15 min and flow rate <1.2m L/min) ↗ (after 15 min) ↔	93.5 % (after 30 min, at T=65 °C, particle size=62μm, P <sub>CO<sub>2</sub></sub> =1 bar, L/S=20mL/g, flow rate=1.2 L/min)

(Table A-2 continued)

Reference	Slag Type	Temperature	Reaction time	CO <sub>2</sub> Pressure	L/S ratio	Slurry volume	Particle size	Steam addition	Stirring rate	CO <sub>2</sub> Flow Rate	Highest CO <sub>2</sub> conversion (%) achieved
Chang et al. [112]	BOF	—	(for the first 10 min) ↗ (after 10 min) ↔	Steady (1.013 bar)	Highest conversion presented: <b>L/S=20mL/g</b> . For values lower or higher than that the conversion extent gets lower.	(300mL- 350 mL) ↗ (>350 mL- 450 mL) ↘	Steady (<44 μm)	—	—	Highest conversion presented: <b>flow rate=1 L/min</b> . For values less or more than that the conversion extent gets lower.	<b>89.4 %</b> (for CRW/BOF slag system after 2h, at T=25 °C, particle size<44 μm, P <sub>CO<sub>2</sub></sub> = 1.013 bar, flow rate=1L/min, L/S=20mL/g)
Polettini et al. [114]	BOF	↗	—	(for CO <sub>2</sub> conc. of 10% and 40% and especially for total pressures <6 bar) ↗ (for CO <sub>2</sub> conc.=100% the effect is less significant)	Steady (5 L/kg)	—	Steady (63-100μm)	—	—	—	<b>53.6%</b> (after 4h, at T=100 °C, particle size=63-100 μm, P <sub>CO<sub>2</sub></sub> =5 bar, L/S= 5 L/kg, CO <sub>2</sub> Concentration =40%)

(Table A-2 continued)

Reference	Slag Type	Temperature	Reaction time	CO <sub>2</sub> Pressure	L/S ratio	Slurry volume	Particle size	Steam addition	Stirring rate	CO <sub>2</sub> Flow Rate	Highest CO <sub>2</sub> conversion (%) achieved
Tai et al. [20]	BOF	(100 °C – 150 °C) ↗ (150 °C - 200 °C) ↖	(from 0 -1 hour) ↗ (from 1 – 3 hours) ↔	Steady (80 bar)	Steady (9 L/kg)	Steady (20 mL)	Ranging between 63 – 90 μm	—	Steady (500 rpm)	—	<b>65 %</b> (after 1h, T=150 °C, particle size between 63 and 90μm P <sub>CO<sub>2</sub></sub> =80 bar, rotating speed of 500 rpm)
Baciocchi et al. [116]	SS	↗	↗	No clear Effect	< 0.4 L/kg ↗ > 0.4 L/kg ↖	—	↖	—	—	—	<b>27.15 %</b> (after 8 h, for 40 °C, particle size <0.105mm, P <sub>CO<sub>2</sub></sub> =3 bar, L/S=0.4 L/kg)

(Table A-2 continued)

Reference	Slag Type	Temperature	Reaction time	CO <sub>2</sub> Pressure	L/S ratio	Slurry volume	Particle size	Steam addition	Stirring rate	CO <sub>2</sub> Flow Rate	Highest CO <sub>2</sub> conversion (%) achieved
Baciocchi et al. [65]	EAF	Steady (50 °C)	↗	(reaction time < 1 hour) At 1 bar, 30% less CO <sub>2</sub> uptake than at higher pressures (3 and 10 bar) (reaction time > 1 hour) ↔	Steady (0.4 L/kg)	—	↖	—	—	—	<b>49.1 %</b> (after 24h, T=50 °C, part. size < 150 μm, P <sub>CO<sub>2</sub></sub> =0.3 bar, L/S=0.4 L/kg)
	AOD	Steady (50 °C)	↗	↗	Steady (0.4 L/kg)	—	↖	—	—	—	<b>69.9 %</b> (after 24h T=50 °C, P <sub>CO<sub>2</sub></sub> =10 bar, L/S=0.4 L/kg)

(Table A-2 continued)

Reference	Slag Type	Temperature	Reaction time	CO <sub>2</sub> Pressure	L/S ratio	Slurry volume	Particle size	Steam addition	Stirring rate	CO <sub>2</sub> Flow Rate	Highest CO <sub>2</sub> conversion (%) achieved
Baciocchi et al. [63]	EAF (wet)	Steady (50 °C)	↗	(reaction time < 1 hour) At 1 bar, 30% less CO <sub>2</sub> uptake than at higher pressures (3 and 10 bar) (reaction time > 1hour) ↔	Steady (0.4 L/kg)	—	<150 μm	—	—	—	<b>49.1%</b> (after 24h, T=50 °C, part. size<150 μm, P <sub>CO<sub>2</sub></sub> =3 bar, L/S=0.4 L/kg.)
	EAF (slurry)	(Until 2 hours and up to 150 °C) ↗	(P <sub>CO<sub>2</sub></sub> = 10 bar and T = 100 °C) ↗	No clear effect	Steady (10 L/kg)	—	<150 μm	—	Steady (500 rpm)	—	<b>38 %</b> (after 4h, T=100 °C, particle size<150μm, P <sub>CO<sub>2</sub></sub> =10 bar)

(Table A-2 continued)

Reference	Slag Type	Temperature	Reaction time	CO <sub>2</sub> Pressure	L/S ratio	Slurry volume	Particle size	Steam addition	Stirring rate	CO <sub>2</sub> Flow Rate	Highest CO <sub>2</sub> conversion (%) achieved
Vandeveldt [118]	AOD	(carbonation at 30 °C was higher than that at 50 °C )	(steeper during the first 6 hours)  (total duration 7 days)	Steady (1 bar)	(6 hours) (<0.2 L/kg) (>0.2 L/kg) (24 hours) (< 0.5 L/kg)	—	—	—	—	—	<b>32%</b> (after 6 days, T=30 °C, L/S=0.2 L/kg, CO <sub>2</sub> =20%)
	CC	Steady (30 °C)	(total duration 24 hours)	—	—	—	(>25.3 μm) (<25.3 μm)	—	—	—	<b>45%</b> (after 6 days, T=30 °C, L/S=0.25 L/kg, CO <sub>2</sub> =20%)

(Table A-2 continued)

Reference	Slag Type	Temperature	Reaction time	CO <sub>2</sub> Pressure	L/S ratio	Slurry volume	Particle size	Steam addition	Stirring rate	CO <sub>2</sub> Flow Rate	Highest CO <sub>2</sub> conversion (%) achieved
Santos et al. [64]	AOD	Steady (50 °C)	(Steeper during the first 30 minutes) ↗ (Maximal uptake after 240 minutes)	—	Steady (1 L/10g)	—	Ranging between 63 and 200 μm	—	Steady (340 rpm)	Steady (0.24 L/min)	<b>30.5%</b> (after 4 hours, T=50 °C, particle size=60-200μm, L/S=100, no sonication) <b>48.5%</b> (under the same conditions, with sonication)
	CC	Steady (50 °C)	(Steeper during the first 30 minutes) ↗ (Maximal uptake after 240 minutes)	—	Steady (1 L/10g)	—	Ranging between 63 and 200 μm	—	Steady (340 rpm)	Steady (0.24 L/min)	<b>61.6%</b> (after 4 hours, T=50 °C, particle size=60-200μm, L/S=100, no sonication) <b>73.2%</b> (under the same conditions, with sonication)

(Table A-2 continued)

Reference	Slag Type	Temperature	Reaction time	CO <sub>2</sub> Pressure	L/S ratio	Slurry volume	Particle size	Steam addition	Stirring rate	CO <sub>2</sub> Flow Rate	Highest CO <sub>2</sub> conversion (%) achieved
Van Bouwel [120]	AOD	(<60 °C) ↗ (60 °C-90 °C) ↖ (90 °C -180 °C) ↗	(Steeper during the first minutes) ↗	(the initial conversion is low and becomes higher after 12 bar) ↗	(L/S<8L/kg) ↔ (L/S>8L/kg) ↖	—	Steady (46.1 μm)	—	Steady (1000rpm)	—	<b>63%</b> (after 1 hour, T=90 °C, particle size=46.1 μm, P <sub>CO2</sub> =30bar and L/S=16)
	CC	(<60 °C) ↗ (>60 °C) ↔	(Steeper during the first minutes) ↗	(2bar-12 bar) ↗ (12 bar-20 bar) ↖ (>20 bar) ↔	(L/S<8L/kg) ↗ (L/S>8L/kg) ↖	—	Steady (39.3 μm)	—	Steady (1000rpm)	—	<b>76%</b> (after 1 hour, T=90 °C, particle size=39.3 μm, P <sub>CO2</sub> =30bar, L/S ratio=16)

(Table A-2 continued)

Reference	Slag Type	Temperature	Reaction time	CO <sub>2</sub> Pressure	L/S ratio	Slurry volume	Particle size	Steam addition	Stirring rate	CO <sub>2</sub> Flow Rate	Highest CO <sub>2</sub> conversion (%) achieved
Santos et al. [66]	AOD	<p>(from 30 °C – 60 °C)</p> <p>(from 60 °C -90 °C)</p> <p>(from 90 °C -120°C)</p> <p>(&gt;120 °C)</p> <p>(Higher conversion achieved at 120 °C)</p>	<p>(Very sharp increase for the first minute of reaction)</p>	<p>(until 15 bar)</p> <p>(&gt;15 bar)</p> <p>(slight decrease)</p>	<p>(L/S&lt;8L/kg)</p> <p>(slight increase)</p> <p>(L/S&gt;8L/kg)</p>	<p>thin film carbonation experiments:</p> <p>Steady (133.3 mL)</p>	46.1 μm	—	Steady (1000rpm)	—	<p><b>24.2%</b></p> <p>(after 144 hours, thin film carbonation, T= 30 °C, particle size=46.1 μm, P<sub>CO2</sub>=0.2 atm, and L/S=25wt%)</p> <p><b>44%</b></p> <p>(after 60mins, slurry carbonation, T=90 °C, particle size=46.1 μm P<sub>CO2</sub>=15 bar, and S/L=62.5g/L)</p>
	CC	<p>(from 30 °C-90 °C)</p> <p>(from 90 °C-120°C)</p> <p>(&gt;120 °C)</p> <p>(Higher conversion achieved at 90 °C)</p>	<p>(Very sharp increase for the first minute of reaction)</p>	<p>(until 9 bar)</p> <p>(9 bar-12 bar)</p> <p>(&gt;12 bar)</p>	<p>(L/S&lt;16L/kg)</p> <p>(L/S&gt;16L/kg)</p>	<p>slurry carbonation experiments:</p> <p>Ranging between 820 mL and 1L</p>	39.3 μm	—	Steady (1000rpm)	—	<p><b>37%</b></p> <p>(after 144 hours, T=30 °C. particle size=39.3 μm, P<sub>CO2</sub>=0.2atm, and L/S= 25wt%)</p> <p><b>57%</b></p> <p>(after 60 mins, slurry carbonation at T=90 °C, particle size=39.3 μm P<sub>CO2</sub>=30 bar, and S/L=62.5g/L)</p>

(Table A-2 continued)

Reference	Slag Type	Temperature	Reaction time	CO <sub>2</sub> Pressure	L/S ratio	Slurry volume	Particle size	Steam addition	Stirring rate	CO <sub>2</sub> Flow Rate	Highest CO <sub>2</sub> conversion (%) achieved
Chang et al. [111]	BF	(for P <sub>CO<sub>2</sub></sub> =48.3 bar, from 40 °C – 100 °C)									68.3 % (after 12 h, at T=160 °C, particle size <44 μm, P <sub>CO<sub>2</sub></sub> =48 bar L/S ratio=10mL/g)
		(for P <sub>CO<sub>2</sub></sub> =48.3bar, from 100 °C – 160 °C)	(until 60 min)	Conversion under 89.6 bar was slightly lower than the conversion under 48.3 bar	(Until 10 mL/g)		Steady (<44 μm)				
		(for P <sub>CO<sub>2</sub></sub> =89.6bar, from 40 °C – 160 °C)	(after 60 min)		(10-20 mL/g)						
					(>20 mL/g)						
Cappai et al. [122]	Waelz slag	Steady (25 °C)					Steady (<4 mm)				18.3 % (after 240h, at T=25 °C, particle size < 4 mm, P <sub>CO<sub>2</sub></sub> =20 bar, L/S ratio=1mL/g)

(Table A-2 End)

Legend: The arrows indicate **increase** ( ↗ ) or **decrease** ( ↘ ) of the carbonation extent **in relation to the increase** (unless otherwise stated) of the **examined parameter**. This symbol ( ↔ ) is used when **no alteration** of the carbonation extent is observed with increasing of the examined parameter's value. Whenever no clear effect of the alterations of the parameters is observed in the carbonation extent, it is clearly mentioned "**No clear effect**". When the effect of a parameter is not tested in an experiment or there is no information about this parameter, this symbol ( — ) is used.

**Table A-3 Summary of slag and process parameters from different carbonation studies and the resulting calculated Carbonation Weathering Rate (CWR) [1]**

Reference	Type of Slag	Particle diameter ( $\mu\text{m}$ )	$r_x(\mu\text{m})$	Conversion, C% (%)	$t_{carb}(\mu\text{m})$	Reaction time, $T_{react}$ (min)	CWR ( $\mu\text{m}/\text{min}$ )
Huijgen et al. [36]	BOF	38	19	74	6.87	30	0.229
Chang et al. [37]	BOF	44	22	68	6.95	60	0.116
Van Zomeren [113]	BOF	2000-3300	1000-1650	4.67	16.95 – 27.97	3600	0.004 – 0.007
Santos et al. [38]	BOF	80	40	36	5.53	30	0.184
Chang et al. [39]	BOF	62	31	93.5	18.54	30	0.618
Chang et al. [112]	BOF	44	22	89.4	11.59	120	0.097
Polettini et al. [114]	BOF	63-100	31.5-50	53.6	7.11 – 11.29	240	0.030 – 0.047
Tai et al. [20]	BOF	63-90	31.5-45	65	9.30 – 13.29	60	0.155 – 0.221
Baciocchi et al. [116]	SS	105	52.5	27.2	5.26	480	0.011
Baciocchi et al. [63]	EAF(wet)	150	75	34.3	9.80	1440	0.007
	EAF(slurry)	150	75	25.4	7.00	240	0.029
Baciocchi et al. [65]	AOD	150	75	69.9	50.73	1440	0.017

Reference	Type of Slag	Particle diameter ( $\mu\text{m}$ )	$r_x(\mu\text{m})$	Conversion, C% (%)	$t_{carb}(\mu\text{m})$	Reaction time, $t_{react}(\text{min})$	CWR ( $\mu\text{m}/\text{min}$ )
Vandeveld [118]	AOD	38.7	19.35	32	2.33	8640	0.00027
	CC	40.7	20.35	45	3.67	8640	0.00043
	AOD(mechanical)	60-230	30-115	30.5	3.43 – 13.14	240	0.0143 – 0.0547
Santos et al. [64]	CC(mechanical)	60-230	30-115	61.6	8.20 – 31.41	240	0.0341 – 0.1309
	AOD(sonication)	60-230	30-115	48.5	5.95 – 22.82	240	0.025 – 0.095
	CC(sonication)	60-230	30-115	73.2	10.66 – 40.86	240	0.044 – 0.170
Van Bouwel [120]	AOD	46.1	23.05	63	6.50	60	0.108
	CC	39.3	19.65	76	7.44	60	0.124
Santos et al. [66]	AOD(wet)	46.1	23.05	24.2	2.03	8640	0.000235
	CC(wet)	39.3	19.65	37	2.81	8640	0.000325
	AOD(slurry)	46.1	23.05	44	4.05	60	0.068
	CC(slurry)	39.3	19.65	57	4.82	60	0.080
Chang et al. [111]	BF	44	22	68.3	7.00	720	0.010
Cappai et al. [122]	Waelz	4000	2000	18.3	130.46	14400	0.009

(Table A-3 End)

## APPENDIX B: ADSORPTION CAPACITY OF THE FORMED ZEOLITIC MATERIAL TOWARDS Ni<sup>2+</sup>

Table B-1 Adsorption capacities of different adsorbents towards Ni<sup>2+</sup>

Adsorbent	Q <sub>0</sub> (mg/g)	Reference
Polymerized onion skin	7.55	<i>Kumar &amp; Dara [267]</i>
Rice hull	5.58	<i>Suemitsu et al. [268]</i>
Dye stuff treated rice hull	6.16	<i>Suemitsu et al. [268]</i>
Melon seed husk	5.9	<i>Okieman &amp; Ohyenkpa [269]</i>
Fly ash	0.683	<i>Viswakarma [270]</i>
Chemically treated coal	7.29	<i>Allen &amp; Minear [271]</i>
Clay treated with NaCl	14.54	<i>Hawash et al. [272]</i>
Clay treated with HCl	10.93	<i>Hawash et al. [272]</i>
Sphagnum peat	14.69	<i>Viraraghavan &amp; Drohamraju [273]</i>
Soyabean hull	89.52	<i>Marshall et al. [274]</i>
Cotton seed hulls	46.57	<i>Marshall et al. [274]</i>
NaOH treated rice hull	12.31	<i>Marshall et al. [274]</i>
Red mud	15	<i>Zouboulis &amp; Kydros [275]</i>
Fe(III)/Cr(III) hydroxide	22.94	<i>Namasivayam &amp; Ranganathan [276]</i>
Natural clay	12.5	<i>Hawash et al. [277]</i>
Peanut hull carbon	53.65	<i>Periasamy &amp; Namasivayam [278]</i>
Granular activated carbon	1.49	<i>Periasamy &amp; Namasivayam [278]</i>
Blast furnace slag	55.75	<i>Dimitrova [279]</i>
H <sub>2</sub> O <sub>2</sub> treated coal	8.12	<i>Singh &amp; Rawat [280]</i>
Bituminas coal	6.47	<i>Singh &amp; Rawat [280]</i>
Aspergillus niger	1.1	<i>Kapoor &amp; Viraraghavan [281]</i>
Rhizopus nigricans	1	<i>Kapoor &amp; Viraraghavan [281]</i>
Coirpith carbon	62.5	<i>Kadirvelu et al. [282]</i>
Activated almond husk	30.769	<i>Hasar [201]</i>
Activated almond husk with H <sub>2</sub> SO <sub>4</sub>	37.175	<i>Hasar [201]</i>
Bagasse fly ash	1.12-1.7	<i>Gupta et al. [199]</i>
Kaolinite	1.669	<i>Yavuz et al. [283]</i>
Tea factory waste	15.26	<i>Malkoc &amp; Nuhoglu [200]</i>
Multi-walled carbon nanotubes	18.083	<i>Kandaha &amp; Meunier [284]</i>
Oxidized multi-walled carbon nanotubes	49.261	<i>Kandaha &amp; Meunier [284]</i>
Coir pith	9.5	<i>Ewecharoen et al. [204]</i>
Modified coir pith	38.9	<i>Ewecharoen et al. [204]</i>
Chitosan coated polyvinyl chloride	120.5	<i>Popuri et al. [203]</i>
Natural iron oxide-coated sand	0.9-1.26	<i>Boujelben et al. [202]</i>
Bael tree leaf powder	1.527	<i>Kumar &amp; Kirthika [285]</i>
Nano Alumina	30.82	<i>Srivastava et al. [286]</i>
Cashew nut shell	18.868	<i>Kumar et al. [197]</i>
<b>Hydrothermally activated, Ca-depleted BF slag</b>	<b>11.51</b>	<b>This study</b>

